# Diverse Polyoxometalate Clusters and Bismuth-chloro Derivatives: Synthesis, Characterization, Catalysis and Photo-physical Studies

Thesis
Submitted for the Degree of
**DOCTOR OF PHILOSOPHY**

By

**SRINIVASA RAO AMANCHI**


**School of Chemistry**
**University of Hyderabad**
**Hyderabad 500 046**
**INDIA**

**June 2011**

*With the blessings of Shiridi Sai*

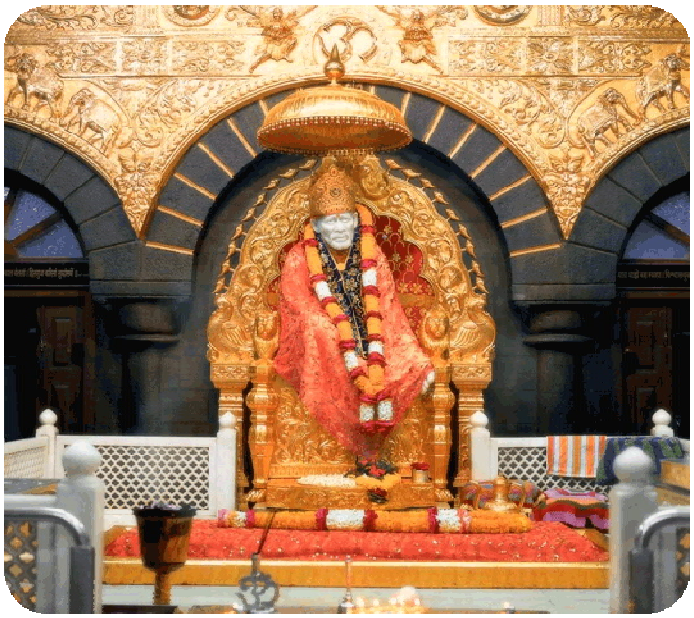

***Dedicated to***
***My beloved parents***
***&***
***teachers***

**Prof. Samar Kumar Das, F.A.Sc**
**School of chemistry**
**University of Hyderabad**
**Gachibowli, Hyderabad-500046, India**
**Work: +91-40-23011007**
**Residence: +91-40-23010536**
**Fax: +91-40-2301246**
**E-mail: skdsc@uohyd.ernet.in**

# CERTIFICATE

Certified that the work contained in the thesis entitled "**Diverse Polyoxometalate Clusters and Bismuth-chloro Derivatives: Synthesis, Characterization, Catalysis and Photo-physical Studies"** has been carried out by Mr. Srinivasa Rao Amanchi under my supervision and the same has not been submitted elsewhere for a degree.

**Prof. Samar K. Das**

**(Supervisor)**

**Dean**

**School of Chemistry**

# Statement

I hereby declare that the matter embodied in the thesis is the result of investigation carried out by me in the School of Chemistry, University of Hyderabad, Hyderabad, India, under the supervision of **Prof. Samar K. Das**.

In keeping with the general practice of reporting scientific observations, due acknowledgements have been made wherever the work described is based on the findings of other investigators. Any omission, which might have occurred by oversight or error, is regretted.

**Srinivasa Rao Amnachi**

University of Hyderabad

June, 2011

## ***Acknowledgements***

I express my deep sense of gratitude and profound thanks to my supervisor **Prof. Samar K. Das** for his inspiring guidance, patience, encouragement, and for the freedom he gave me in carrying out research. His optimistic approach towards every aspect was admirable and inspiring. Throughout my Ph.D tenure, he is always approachable, helpful, friendly and extremely tolerant. I consider my association with him as a rewarding experience in my life.

I take this opportunity to thank Prof. M. V. Rajasekharan, Dean, School of Chemistry for providing us the facilities needed for our research. I extend my sincere thanks to former Deans Prof. D. Basavaiah and Prof. M. Periasamy, and all the faculty members, School of Chemistry for their co-operation on various aspects.

I am deeply indebted to Prof. S. Pal and Prof. K. C. Kumara Swamy for their valuable suggestions to carry out my doctorial work.

I sincerely acknowledged to Sri Rama Chandra Chaitanya Swamiji garu for his heartful blessings, advices and encouragement to go head in the modern society.

I feel proud to say thanks to Dr. T. Arumuganthan, for his encouragement and who made me to initiate my doctorial work and taught me every aspect related to my work.

It is great pleasure to thank my lab seniors Dr. V. Shivaiah, Dr. S. Supriya, Dr. V. Madhu, Dr. Raghavaiah, Dr. C. P. Pradeep, Dr. Prabhakar, and Dr. Tanmay for their help, pleasant company, and cooperation during my Ph.D. tenure. I wish to thank my colleagues and juniors Mr. Ramababu (rams), GDP garu, Mr. Bharat (baru), Mr. Kishore, Ms. Monima, Mrs. Sridevi garu, Mr. Veeranna, and Ms. Paulami for their cooperation, help, and creating cheerful work atmosphere. I thank to project students Mr. T.Vijay Kumar, Murali, Sunil, Narayana, Sivayya, Ms. Upama, V. Sreenivasulu and Danabal working with me and helping to complete my thesis work. I further thank to project students Arti, Nagaraju, Suneetha for their help.

I also thank all the non-teaching staff of the School of Chemistry for their assistance on various occasions. It's my privilege to acknowledge Mr. Shetty and Mr. A. R. Shetty for timely supply of chemicals, Mr. Vara Prasad for all his art with glass blowing, Mr. Satyanarayana, and Mr. Bhaskar Rao for their excellent job with NMR spectra and LC-MS spectra, Mr. Ramana helping in XRD facility, and Ms. Asia Parwez for her tireless effort for collecting IR spectra. The assistance of Dr. Manjunath and Mr. Suresh (EPR) are gratefully appreciated.

I would like to acknowledge Prof. A.V. Prasad Rao, Prof. GNR and Dr. Vani Medam, and all my teachers during my post graduation at Andhra University, Visakhapatnam, and all my teachers in graduation and under graduation studies especially Phaneendra garu, Seetharama Rao garu, Viswanatha Raju garu who created the interest to study well in mathematics, physics and chemistry at Govt. Jr College, Tadepalligudem and D. R. G. Goinka Degree College, Pentapadu for their suggestions, advice and timely guidance regarding to higher studies.

I take this opportunity to thank all my school teachers, especially Venkat Rao garu. Parameswara Rao garu, Bhaskara Rao garu, Raja Rao master for their wonderful teaching, encouragement, kindness, and affection.

I am lucky enough to have the support of Ch. Rajesh, Phaneendra, Narasimham, Kishore (VB Lab), Kalyan, D. K Srinivas, and who have been good friends over the years, for keeping me sane, giving me perspective and who have made the time here more enjoyable. My heartful thanks to 'behind the scenes' people pandu gadu, Kethan, Shilpi and Jwala bayya.

My stay on this campus has been pleasant with the association of many people Ramesh garu, Satish anna, Dr. Ramesh Reddy, Dr. Phani Pavan, Ravi Kumar, Dr. Sivaranjan Reddy, Dr. Aravind, Dr. Jagadish anna Mr. Anjanaylu, Krishna Chari, Naga Raju, Mallesh, NagaRaju (MP lab), Chaitanya, M. Ramu, Ramaraju, Amulya, Sravani, Saikat (Mehta lab) , Dr. Srinivas anna, Ram Suresh, Dr. Venu Srinivas, Dr. Vikram, Vijji, Anand, Santhosh, Balu, Sanjeev, Narayana, Chandrsekhar, Ajay, Pramithi, Bashik, Gupta, Hari, Srinivas, Karunakar, Ramu Yadav, Shesu, Rama Krishna, Venu, Suresh, Madhu, Rama Raju, Ramesh, Nagarjuna, Anish, Sekhar Reddy, Ganesh, Vigensh, Praveen, Dr. Arindam, Dr. Arun Babu, Malakappa, Swami, Dr. Bijju, Dr. Bhargavi, Dr. Bipul, Ranjith, Naba, Palash, Suryanarayana, Rajesh, Ashok, Chandu, Dr. J. P. anna, Dr. Abhijit, Dr. Rajesh, Balaswamy, Dr. Narahari anna,Tirupathi Reddy, Pavan, Yaseen, Dr. Bhuvan anna, Ramesh, Gangadhar, Srinu, Sekhar Reddy, Santosh, Mallikarjun, Guru Braham, , Rajgopal Sr., Rajgopal Jr., Dr. Kishore, Dr. Ramkumar, Dr. Narayana, Dr. Rumpa, Vijayander Reddy, Chary, Bharani, Srinivas Reddy, Ganesh, Srinivas, Raveendra Babu, Vanaja, Naveen, Sandip, Tradib, Sasi, Venky(NMR) exceptionally generous in helping me at various occasions. I also feel happy to stay in NRS hostel with the good company of Palgun(Chairman), Veerraju anna, Mungul, Sifi, Reddana, Dr. Siva Garu and all other friends.

I am happy to acknowledge all my school friends Vineel, Tara, maddu srinu, Rajakumar, Sai, Ramakrishna, Prasad, Nagasiri, Srilakshmi and Sarada for their competitive spirit and memorable moments in Z. P. High School, Kommugudem. Narayana master, Subramanyam sir are specially acknowledged for their valuable suggestions and encouragemen. I thank my family friends Dr. Baskara Rao and Visalakshmi garu for their happiest relations with my family. I specially thanks to Laxman, Sekhar (Nag), Hanumanth, Sai Sankar for their good company throughout my studies.

I am happy to say some cheerful moments in every year night cup when I watch the Suraj's play in the cricket ground especially for his long and dashing sixes. I also feel happy to watch play of Dr. Dinakar anna, Kishore (all-rounder), Srisailam, Achyuth and Kedar.

I am glad to say that I had happy moments in P.G with my friends like Suresh, Gopal, Sanyasnaidu, Srinivas (BARC), R.P, Sridhar, Brahmaji, Govind, Prem Sagar, Suresh garu, Subbarao garu, Rajesh garu, Vijay Kumar, Chakri, Kiran, Basavaiah, Krishnam Raju, Balaji and all other friends.

The unconditional love of my parents and their blessings made me what I am today and I owe everything to them. It is great pleasure to thank my Family for their support and affection throughout my life. I would take this opportunity to thank my sisters, brothers-in-law and their families for their love and support.

I also thank DST funded National Single Crystal X-ray Diffraction Facility, UGC / UPE for providing the basic requirements and CSIR for the financial support.

Acharya Bharadwaja Prabhu is greately acknowledged for introducing the Shirdi Sai Baba in our life and his teachings made us the discipline life. Also sincere thanks to Appa Rao garu and Gayatri garu for their devotional wishes.

I would like to express my deep sense of love and gratitude to Sri Shirdi Sai Baba, who is my source of Inspiration, and who taught me the basic principles of life. I thank him for giving me patience and perseverance to endure the challenges in my life. I am happy to receive his blessings.

**Srinivasa Rao Amanchi**

University of Hyderabad

June-2011

# CONTENTS

# Introduction to Polyoxometalates and Bismuth Based Materials

**Abstract:** The first part of my thesis work mainly deals with the synthesis and structural characterization of inorganic-organic hybrid materials, based on polyoxometalates (e.g., Anderson type heteropolyanion, decavanadate anion etc.) and various organic amines, transition metals and alkali metals as cations. The second part of my thesis includes mostly bismuth chloro derivatives with aromatic amines and 1, 5-benzodiazapine. We also have described the application studies (catalysis) of polyoxometalate compounds in the oxidation reaction of styrene. Electronic absorption- and emission-spectral studies are performed mostly for bismuth-chloroderivatives

## 1. Preface

The development of the useful technologies often hinge on the availability of solid state materials with appropriate physical and chemical properties. Oxygen is not only the most abundant terrestrial element but it is also highly reactive; consequently, oxides exist for all of the elements with the exceptions of radon and the lighter noble gases. The significant contemporary interest in solid state oxides reflects a structural and compositional diversity that endows these materials with a range of physical properties that yield applications in the area of magnetism, conducting polymers, microporous inorganic crystalline zeolite materials, opto-electronics, sorption, catalysis, bio-mineralization, and solar energy conversion. Catalytic applications of polyoxometalate-based materials are extensively useful to develop a new methodology for organic transformations (for example, to synthesize aromatic aldehydes and ketones). Cobalt salt of silico tungstate $\{Co_3[Si_2W_{12}O_{40}]\}$ is a good catalyst for organic oxidation.[1] The thesis work deals with the synthesis, characterization and application studies of 'early-transition metal-oxo-clusters which is termed as polyoxometalates (POMs) clusters' and some bismuth-chloro derivatives by using various aromatic amines. In this chapter, we have discussed briefly about the properties and applications of POMs based solid state materials, and bismuth-chloro derivatives starting from the history of relevance to the present progress.

## 1.2. General Concepts of the Polyoxometalate Chemistry

### 1.2.1. What is Polyoxometalates (POM)?

Polyoxometalate is a large family of metal-oxygen clusters, which are especially formed by the inner transition metals Mo, W, V, Nb and Ta ("addenda atoms"), have been viewed as ideal inorganic building blocks for the design and construction of multi-functional materials.[1a] A large number of potential coordination sites (both terminal and bridging oxygen atoms) from the POM cluster-surfaces are the main source for the multifunctional activity. In general, POM clusters are known in anionic form, and hence appropriate cations are needed for their successful isolation.

The formation of POMs depends on (i) the appropriate relationship of coulombic factors of ionic radius and charge (cationic radius should be within the range of 0.65 – 0.80 Å; for addenda atoms $V^{5+}$ (0.68 Å), $Mo^{6+}$ (0.77 Å), $W^{6+}$ (0.74 Å) whereas for $Cr^{6+}$ (0.58 Å)). (ii) on the accessibility of vacant d orbital for metal–oxygen bonding. That is the reason why the formation of POMs clusters are limited to only above mentioned inner- transition metals and not by other metals.

### 1.2.2. Classification and Types

In a general point of view, POM clusters are classified as (i) Isopolyanions ("IPA"; generic formula: $H_nM_mO_y^{p-}$) (ii) Heteropolyanions[2] ("HPA"; generic formula: $X_xM_mO_y^{q-}$, $x \leq m$) where M are the addenda atoms and X is hetero element, namely, P, S, Si, As, etc. At present, more than 70 different elements including most non-metals and transition metals can function as hetero atom. POM anions can also be classified into three types based on the presence of number of oxygen attached to the addenda atom. The "mono-oxo" ($C_{4v}$) class (or) type I, which have one terminal oxo group in which Lowest Unoccupied Molecular Orbital (LUMO) is approximately non-bonding and metal centered, hence type I class POMs clusters may be reduced reversibly to mixed valence species. Whereas in type II or "cis-dioxo" ($C_{2v}$) class there are two terminal oxo groups[1b], LUMO for the octahedral is strongly anti-bonding with respect to the M = O bonds. Type III anions (which is observed very rarely) have both kinds of M atom sites. The above entire discussion is offered in the Scheme 1.1.

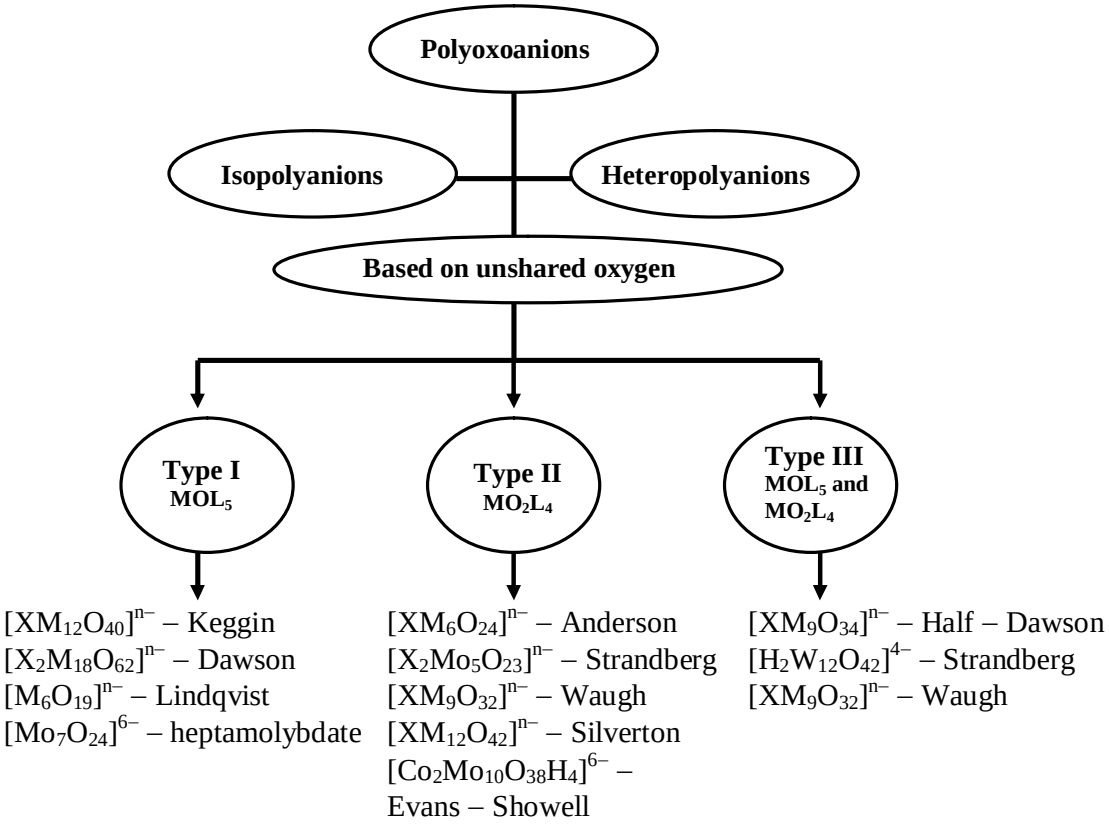


**Scheme 1.1.** Classification of POM anions based on composition and unshared oxygens attached to M atom.

The polyanion structures that contain three or more terminal oxo groups are not observed. A restriction, which has been explained in terms of the strong trans influence of the terminal M–O bonds, facilitates dissociation of the cluster. This restriction is named as "Lipscomb principle".[1b]

### 1.2.3. Historical Background of POMs Anion Chemistry

The first polyoxoanion was reported almost two centuries ago, but that could only be characterized structurally more than 100 years later. Ammonium phosphomolybdate $[NH_4]_3[PMo_{12}O_{40}]. xH_2O$ can be prepared by adding ammonium molybdate and phosphoric acid in aqueous medium, which is one of the earliest metal oxide clusters, synthesized by Berzelius in 1826.[3]

## 1.3. Basic Principles in POMs Cluster Structure, Synthesis and Properties

### 1.3.1 Structure

POM cluster anions are comprised of aggregates of metal–oxygen units where the metal is adopted in the center of a polyhedron and the oxygen ligands define the vertices of this polyhedron. The structure of a POM cluster can be considered to form via a self-assembly process, which involves linking or aggregation of the polyhedra.[4] This involves a series of condensation reactions. Consequently, the overall structure of a polyanion cluster can be represented by a group of polyhedra that have corner- or edge-sharing modes, see figure 1.1 (face sharing is also possible but very rarely seen).

(a)

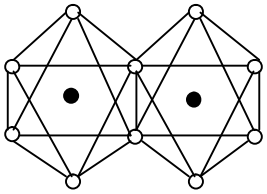

(b)

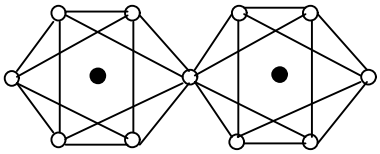

**Fig. 1.1**. The linking modes of two adjacent polyhedra (a) via edge sharing (b) via corner sharing. Black circles represent the inner transition metals Mo, W, and V etc., white circles represent oxygen atoms.

Anderson anion[5a] '$\{Al(OH)_6Mo_6O_{18}\}^{3-}$' can be described as as the $Al(OH)_6$, placed in the centre of the cluster, around which six $MoO_6$ are arranged via Al–O–Mo bridges, so that the total cluster is having negative charge of 3–. Generally, the POMs clusters including Lindqvist[5b], Anderson[5], and Strandberg[5d] anions were well characterized by X-ray crystallography. Some of the POMs structures, which are common in the literature, are shown in Fig. 1.2.

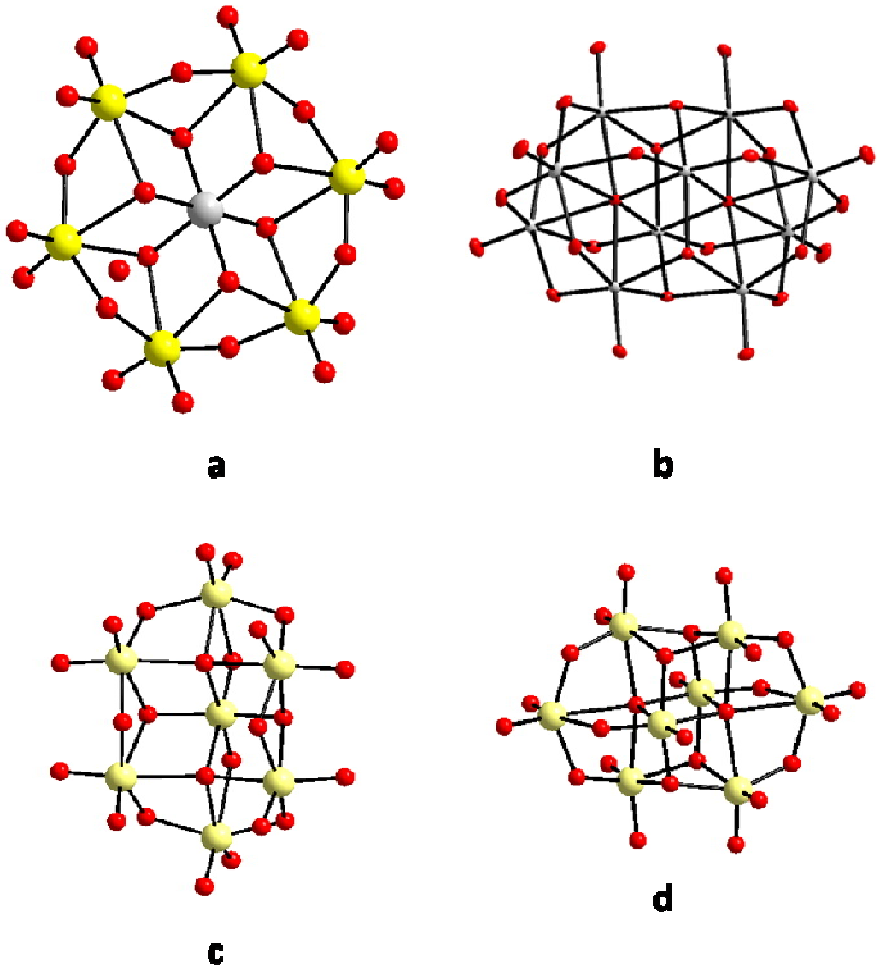


**Fig. 1.2** Some of the POMs structures which are common in literature:
(a) "$\{Al(OH)_6Mo_6O_{18}\}^{3-}$" (b) $\{V_{10}O_{28}\}^{6-}$ (c) $[Mo_7O_{24}]^{6-}$ (d) $[Mo_8O_{24}]^{6-}$. Color code: O, red; V , red, Al, grey: Mo, yellow.

### 1.3.2. Synthesis and Properties

In practice, POMs are most frequently prepared by one-pot proton-induced condensation-dehydration reactions in aqueous medium. The mechanism for the formation of polyoxometalates is still not clear and usually described as self assembly. Therefore it is not possible to design a multi-step sequence for the synthesis of a novel POMs cluster anion. The successful isolation of POMs cluster anion depends on many factors during the course of the reaction, such as, (i) concentration of the reactants (ii) pH of the medium (iii) temperature (iv) solvent (v) sequence of adding reagents (vi) presence of reducing agents/additional ligands etc.,

(a) Synthesis of plenary POMs from aqueous and non-aqueous medium:

The acidification of aqueous solution contains simple oxoanions such as $MoO_4^{2-}$ or $WO_4^{2-}$ resulting in the formation of isopolyanion (IPA) and heteropolyanion (HPA) with necessary added heteroatom. The formation of isopolyanion and heteropolyanion can be described as

$7MoO_4^{2-} + 8H^+ \longrightarrow [Mo_7O_{24}]^{6-} + 4H_2O$ and

$6MoO_4^{2-} + [Al(H_2O)_6]^{3+} + 6H^+ \longrightarrow [Al(OH)_6Mo_6O_{18}]^{3-} + 6H_2O$ respectively.

In non-aqueous solutions, the hexa and decatungstate anions are well characterized. The syntheses of isopolyanions from an organic solution were performed by Jahr and Fuchs.[6] The synthesis was performed by the hydrolysis of the metal esters in the presence of organic bases. The formation of hexatungstate in non-aqueous medium can be described as

$WO(OEt)_4 + NR_4OH + H_2O \longrightarrow [NR_4]_2[W_6O_{19}]$.

(b) Derivative of POMs anions:

Functionalization of POMs anion can be achieved in three possible different ways.

(i) Substituting with transition metal:

The treatment of a base to the heteropoly species can produce defect POMs structure, so-called "lacunary" heteropoly species, wherein one or more addenda atoms have been eliminated from the structure along with the oxygen; those addenda were not sharing with other atoms. Lacunary species are more readily react with a wide variety of octahedral coordinating metal ions to refill the vacant sites. The unshared coordination position of a substituted metal ion is available for coordination of other ligands, so that it produces transition metal ion substituted POMs. For example,

$[A\text{–}\alpha\ SiW_9O_{34}]^{10-} + 3Cu^{2+} \longrightarrow [Cu_3(H_2O)_3(A\text{–}\alpha\ SiW_9O_{34}]^{10-}$

(ii) By the support of Transition Metal Complexes (TMCs) or organic moieties:

Attachment of a transition metal complex (TMC) on the surface of a POM anion using covalent bonds can produce discrete POMs supported transition metal complexes. The covalent attachment of organic groups to POM *via* linkages extends their potential use as pharmaceuticals.[7]

(iii) Multi dimensional inorganic–organic hybrid materials:

The POMs anions (discrete clusters) are suitable building blocks to obtain extended framework type materials. Two adjacent POMs clusters are connected by one or more number of transition metal complexes, in which transition metal complex acts as a linker. Added organic ligand may acts as either a coordinating ligand/template or both. A

'template' can be defined as structure directing ligand during the course of reaction time or acts as space filling agents. The organic ligands, especially the amine templates including $RNH_2$, $R_2NH$, $R_3N$ $R_4N^+$ and diamines either may coordinate to the transition metal or merely acts as counter cation by protonation. Coordination dimension mainly depends on the number of possible coordination sites available in POMs cluster and transition metal complexes. By taking the advantage of the ability of POMs to act as ligands, variety of multidimensional structures including 1D, 2D, and 3D have been synthesized hydrothermally and a significant contribution was made by Jon Zubieta et al.[8] in this particular field of research work, some of these structures are known with open framework containing well defined cavity.[8b] The following Figure 1.3 illustrates the incorporation of POMs in voids present in the multidimensional structure.

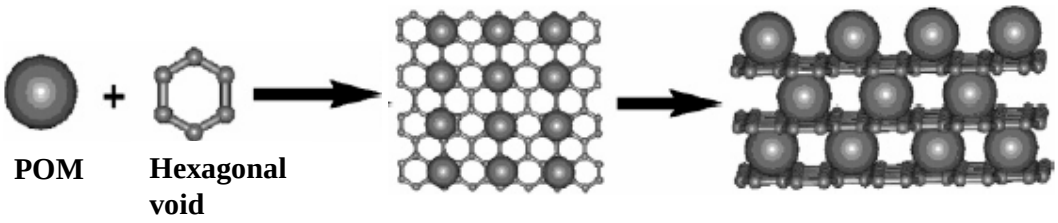


**Fig.1.3.** The incorporation of POMs cluster in the hexagonal voids present in porous multidimensional structure.

## 1.4 Higher Nuclear POM Clusters and Applications

### 1.4.1. Polyoxovanadate

Polyoxovanadate anions are structurally very flexible and the central vanadium atom exists in tetrahedral, trigonal-bipyramidal, square pyramidal and octahedral geometries. In tetrahedral/ trigonal-bipyramidal case, vanadium always found in +5 oxidation state, whereas in square pyramidal and octahedral cases, the central metal atom is either in +4 (or) +5 oxidation state. Square pyramidal geometry is responsible for the formation of cluster shells/ cages in which templates (generally anions, sometime neutral molecules) are accommodated as guest molecules. Higher Nuclear cluster shells/ cages are known from $\{V_{12}\}$ to $\{V_{34}\}$ with various topologies;[9] among these, many exist in mixed valence ($V^{4+}/V^{5+}$) state. Cluster (Host) – templates (Guest) molecules are stabilized by weak forces (in the case of anionic guest weak repulsive force). Fig. 1.4 describes the growth of cluster shells/cages by the effect of the templates. Many

polyoxovanadate cluster shells / cages act as cryptands/clatharate host for neutral, cation or anionic molecules.

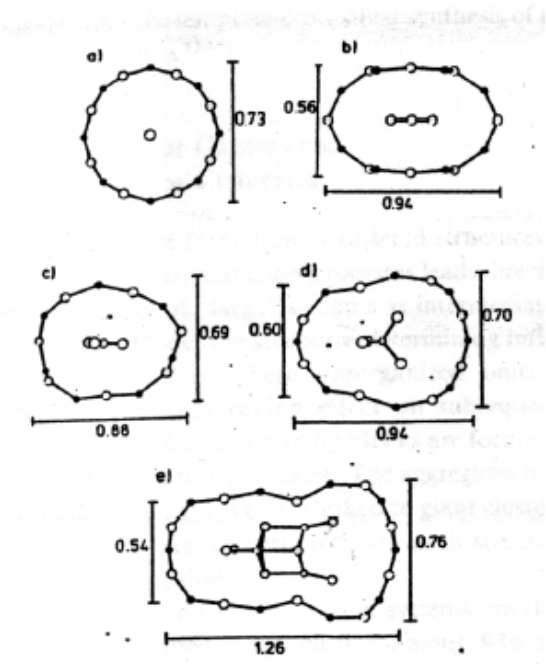


**Fig. 1.4.** Simplified representation of the shape and size (measurements in nm) of the several polyoxovanadate cluster anions: (a) $[H_4V_{18}O_{42}(X)]^{9-}$ (X = Cl, Br, I), (b) $[H_2V_{18}O_{44}(N_3)]^{5-}$, (c) $[HV_{18}O_{44}(NO_3)]^{10-}$, (d) $[HV_{22}O_{54}(ClO_4)]^{6-}$, (e) $[V_{30}O_{74}(\{V_4O_4(O_{term})_4)]^{10-}$ .

### 1.4.1.1. Molecular Magnetism

It is well known that, only two isopolyanions $[V_{10}O_{28}]^{6-(10)}$ and $[V_{12}O_{32}]^{4-(9c)}$ are known in which all the vanadium centers are in +5 oxidation state. Several polyoxovanadates are known in mixed valence (nearly all ratios of $V^{4+}$ to $V^{5+}$ are known) and some of them are known in which all the vanadium centers are in $V^{4+}(d^1)^{9d}$. Especially, the mixed valence ($V^{5+}/V^{4+}$) and reduced (only $V^{4+}$) vanadium clusters show an interesting magnetic behavior. In such a way, fully reduced vanadium clusters (containing only $V^{4+}$) can be viewed as fully magnetic cluster in which S = ½ spins for each $V^{4+}$ and $V^{4+}$ centers are anti-ferromagnetically coupled. Consequently, the intermolecular magnetic interactions are expected to be a maximum which open up a new gateway in molecular magnetism.

**(i) Single Molecule Magnets (SMMs)**

In the context of above discussion, the best known single molecule magnets (SMMs) are $Mn_4$[11a], $Mn_{12}$[11b], $Mn_{16}$[11c], $Mn_{18}$[11d], $Mn_{26}$[11e], $Mn_{30}$[11f], $Fe_4$[11g], $Fe_8$[11h], $Fe_{10}$[11i], $Fe_{19}$[11j], $V_4$[11k], $Co_4$[11L], $Ni_4$[11m], $Ni_{12}$[11n], $Ni_{21}$[11o]. A single molecule magnet can be defined as "a class of molecules exhibiting magnetic properties similar to those observed in conventional bulk magnets, but of molecular origin". A molecule should have two basic requirements to behave as a single molecule magnet. These are (a) high spin ground state (b) high zero field splitting (due to high magnetic anisotropy). The combination of these two properties can lead to an energy barrier and hence the molecular system can be trapped in one of the high spin energy wells at low temperatures. SMMs show applications on high data storage and quantum computation as quantum bits.[12] Recently heteropolyvanadate clusters $K_6[V_{15}As_6O_{42}(H_2O)]$. $8H_2O$ and $(NH_4)_6[V_{14}As_8O_{42}(SO_3)]$, known as (V15) and (V14) respectively, have been shown to exhibit some of the properties of SMM. [9d,9e] A cartoon representation of the spin orientation of V15 molecule is presented in Scheme 1.2. These types of molecules contain a finite number of paramagnetic spin centers and provide an opportunity to study about the magnetic interactions.

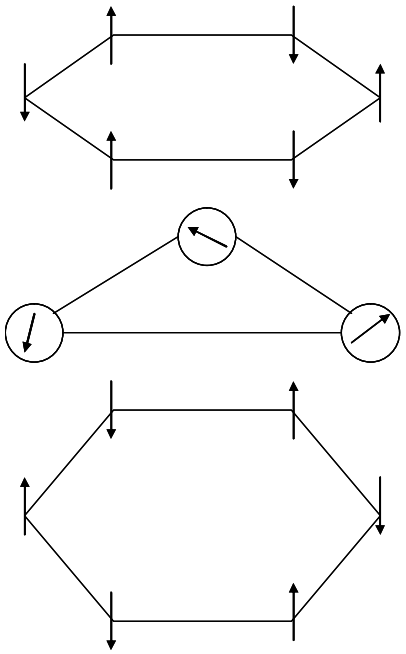

**Scheme 1.2** Spin frustration in magnetic layers of $K_6[V_{15}As_6O_{42}(H_2O)]$

### 1.4.2. Heteropoly Blues and Browns

As we discussed earlier, type I POMs, such as, Keggin, Well-Dawson, and Lindqvist type cluster anion can be reduced to mixed valence heteropoly blues and browns. The reduction of a heteropolyanion to a heteropoly blue or brown involves the reversible addition of one or more electrons. The added electron must be entered into the non-bonding orbital. The availability of non-bonding orbital is possible in only type I POMs, whereas in the type II (two terminal oxygen atoms) metal's d orbital are involved in σ and π bonding. Consequently type II POMs does not undergo reversible reduction to heteropoly blue or brown. The extinction coefficients of reduced "molybdenum blue" or "tungsten blue" are significantly comparable to those of organic dyes. Molybdenum blue solution is instantaneously formed by the reduction of $Mo^{6+}$ to $Mo^{5+}$ in aqueous acidic solution (pH ≤ 3). Reducing agents, such as metals (Cu, Zn, Al etc.,) $B_2H_6$, $NaBH_4$, $N_2H_4$, $NH_2OH$, $H_2S$, $SO_2$, $SO_3^{2-}$, $S_2O_4^{2-}$, $S_2O_3^{2-}$, $SnCl_2$, $MoCl_5$, $MoOCl_5^{2-}$, HCOOH, $C_2H_5OH$, ascorbic acid can be used successfully to generate "molybdenum blue".[1,13] Strong reducing conditions are needed to generate brown species. In the research area of "molybdenum blue", the pioneer contribution has been done by Müller et.al. This group published variety of articles, in which molybdenum higher nuclear clusters are decorated by diverse architectures. The molecular growth of high nuclear molybdenum cluster evolution can be described as follows,

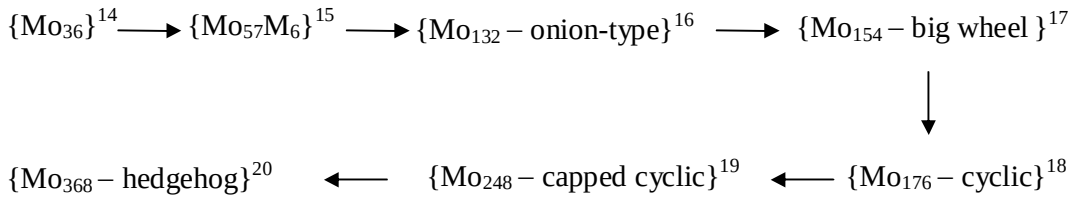


### 1.4.3. POM in Catalysis

The mainstream of POMs applications is found in the area of catalysis. The redox properties of these POMs make them important as catalyst for a number of oxidation and dehydrogenation reactions of organic substrates. The main role of POMs cluster anion in catalysis is in the activation of hydrogen peroxide, alkylhydroperoxide etc. As a result of the activation of peroxides, an inorganic peroxo, hydroperoxo, alkyl peroxo, or acyl peroxo intermediates are formed and those are very reactive species and hence lead to

oxygenation of the organic substrate. Overall literature[21] survey of the activation of hydrogenperoxide by a catalyst is represented in Figure 1.5. The superiority of POMs as

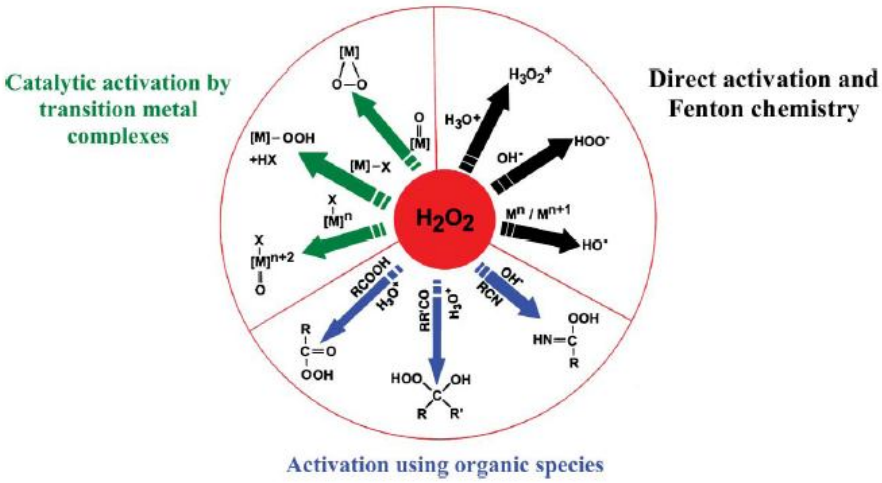


**Fig.1.5** Activation of hydrogen peroxide by a catalytst.

catalysts, when compare to other catalyst, is reflected by their stability towards strong oxygen donors, such as molecular oxygen and hydrogen peroxide. Mostly transition metal substituted POMs clusters or POMs supported transition metal complexes shows applications in catalysis. The literature shows about 85% of the patents and applications of POMs are related with catalysis.[22] There are three different approaches that are available for POM catalysis related literature[23] in which solid heteropolyoxometalates act as catalyst. (Fig. 1.5.)

(a) Surface type: In this approach, heterogeneous catalyst is used and reaction takes place on the solid surface. (Fig. 1.5(a))

(b) Pseudo – liquid Bulk type (I): When the diffusion rate of reactant molecules is faster than the reaction (diffusion considered in the solid lattice rather than in the solid pores) the solid bulk forms a pseudo liquid phase in which catalytic reactions can be performed. (Fig. 1.5(b))

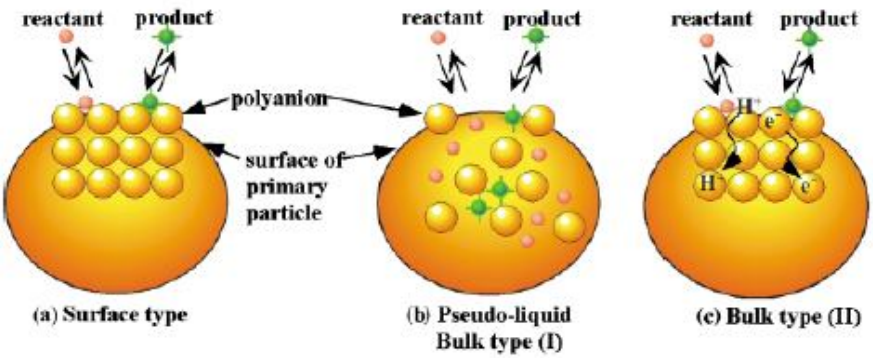


**Fig. 1.5** Depicts the catalytic approach of a solid heteropoly anion: (a) surface type (b) Pseudo-liquid Bulk type (I) (c) Bulk type (II).

(c) Bulk type (II): When the gaseous/liquid phase reactants molecules penetrate in between the solid POMs molecules, the distance between the polyanions increased and reaction takes place inside the bulk solid. The products are released in the gas/liquid phase to the surface of the bulk solid. (Fig. 1.5(c))

The design of the catalyst in oxidation reactions basically depends on three important factors i) the function of the catalyst leads to the selective product (desired product) ii) the usage of the oxidant also plays a key role, it should be green oxidant iii) the catalyst should be stable when the reaction carried out. If the catalyst is in the limit of above regulations, it can be called "The ideal oxidation catalyst" The whole requirements are shown in the following picture.[24]

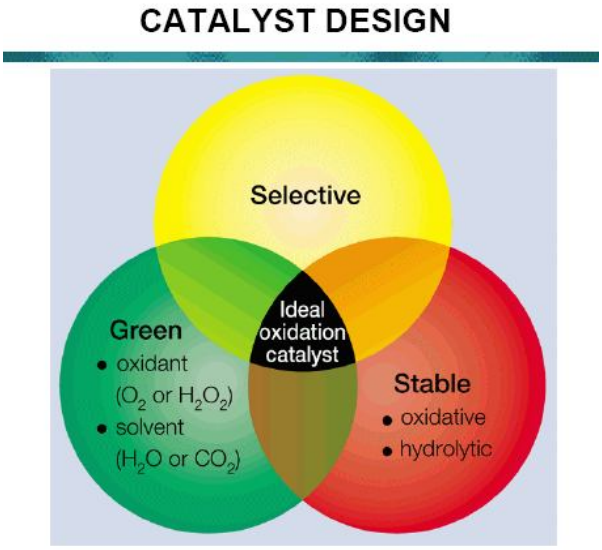


**Fig.1.6.** Three intersecting range must be considered for ideal oxidation catalyst.

### 1.4.4. POM in medicine

Research work on the application of POMs in medicinal field is mainly focused on antitumor and antiviral (including anti HIV) properties. The mechanism for the antitumoral activity of POMs is first proposed by Yamase and his group.[25] They found that revolving around a single electron reduction / oxidation cycle is a key point for antitumoral activity. The reduced form of heptamolybdate, $[Mo_7O_{23}(OH)]^{6-}$ is highly toxic, whereas the oxidized form $[Mo_7O_{24}]^{6-}$ is not toxic. This group also proposed that some domains in tumor cells reduce $[Mo_7O_{24}]^{6-}$ to $[Mo_7O_{23}(OH)]^{6-}$ while other domains deoxidize $[Mo_7O_{23}(OH)]^{6-}$ to $[Mo_7O_{24}]^{6-}$. The first antiviral activity of POMs was reportd in 1971. The inhibition of viral adsorption / fusion as a function of POM structure in a cell-based assay was first studied by Hill et al.[26] This study pointed out the POMs anions $[SiW_{12}O_{40}]^{4-}$, $[BW_{12}O_{40}]^{5-}$ and $[NaSb_9W_{21}O_{86}]^{18-}$ were able to completely inhibit cell fusion in HIV-infected lymphocytes.

The current attention of POMs has been focused on the applications in medicinal chemistry. Particularly this area of interest would be requiring chiral POMs. Since much biological activity is expected to depend on the chiral configuration. Chiral POMs structures are classified in three different classes in the literature. (i) The structure which undergoes rapid racemization via water exchange, partial hydrolysis, or fluxinol behaviour. Some of the relevant examples include $[X_2MO_{21}]^{n-}$ (X = OP, RP, S, Se; M = Mo, W)[27] $[(MeAsO_3)Mo_6O_{18}(H_2O)_6]^{2-}$,[28] $[X^vMo_9O_{31}(H_2O)_3]^{3-}$,[29] $[X_2{}^vMo_{18}O_{62}]^{6-}$,[30] and $[M^{iv}Mo_9O_{32}]^{6-}$ [M = Mn, Ni] [31] (ii) The structure which are non–labile but it is so similar with enantiomer that separation has not been achieved (e.g. $[\beta_2–SiW_{11}O_{39}]^{6-}$, $[\alpha–P_2W_{17}O_{61}]^{10-}$) [32] and their metal substituents $[WM_3(H_2O)_2(XW_9O_{34})_2]^{12-}$ [M = X = Zn, Co] [33] and (iii) the structure which are non-labile but enantiomer can be separated (e.g. $[Co_2Mo_{10}O_{38}H_4]^{6-}$, [34] and $[P_2W_{18}O_{79}]^{20-}$)[35]

### 1.4.5. Research in Nuclear Waste

Much research work was carried out on the safe disposal of the long lived radioisotopes, such as, Np–237 etc. The f–block elements are highly oxophilic and always prefer higher coordination number. Besides this, POMs (generally in anionc nature) are nucleophilic consisting of vast number of oxygen on the surface for coordination and most of the time acts as multi-dentate ligand, combination of these two

preferably shows application on nuclear waste treatment process. POMs readily form complexes with tri and tetravalent lanthanides and actinides.[36] A large amount of research has been carried out on $AsW_9$[37] and $P_2W_{17}O_{61}$[38] to use the POMs clusters as coordinating ligand in radioactive waste treatment via sequestration of trans-uranium elements. The outstanding similarity of coordination chemistry in POMs may have great significance in the development of new waste treatment technologies.

### 1.4.6. Supramolecular Interactions in POMs

Supramolecular chemistry can be defined as the interaction between two or more number of molecules which leads to the supramolecular assembly. Supramolecular chemistry deals with non-covalent interactions which are broadly differed from the traditional organic chemistry (where making and breaking of covalent bonds occur to construct desired molecules). When a metal center is a part of the structure, a supramolecular framework can be constructed in two different ways.

(i) Through coordinate covalent bonds by linking metal and organic ligands.[8]

(ii) Through weak non-covalent intermolecular forces such as hydrogen bonding, Van der waals forces, pi-pi interactions, hydrophobic/hydrophilic interactions, ionic forces, etc., Structures are held together by above mentioned weak intermolecular forces, consequently that offers extra stability to the framework. Supramolecular chemistry often used as a tool to develop new functions like high-tech sensors, pharmaceutical therapies etc., that cannot appear from a single molecule. Since POMs are basically oxo-clusters containing many number of oxygen atoms on the cluster surface and also crystallized with significant number of lattice water molecules, the crystal structure often stabilized by O–H···O hydrogen bonding interactions (in case of hybrid compounds C–H···O, N–H···O, C–H···N etc. also included). Basically supramolecular chemistry has been varied by changing the cation.

Recently several reports have come, in the context of supramolecular chemistry, that are based on Anderson anion and decavanadate cluster. These materials can be isolated by using the 1, 10-phenanthraline and 2, 2- bipyridine.[39] A representative supramolecular architecture is presented in the Fig.1.7.

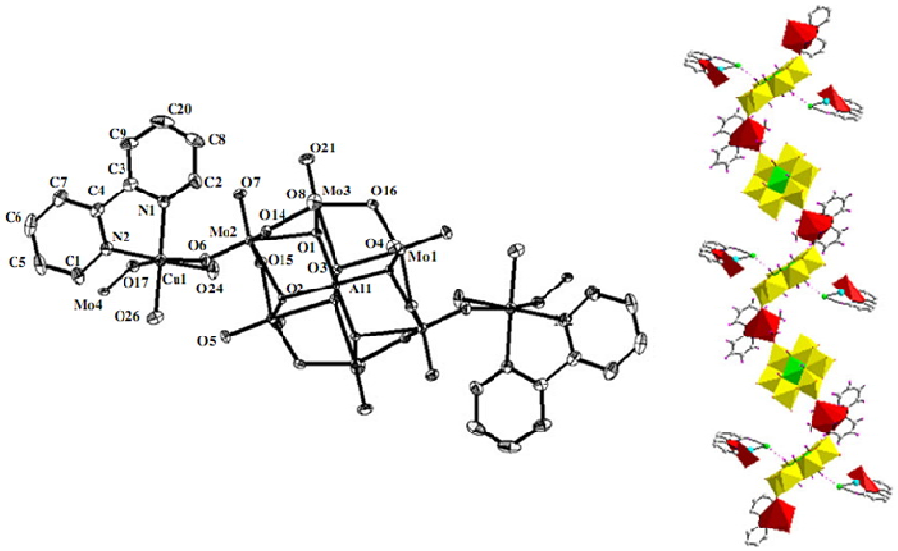


**Figure 1.7** **(**Left) Coordination of an Anderson anion via terminal oxygen atoms on molybdenum to $[Cu(bipy)(H_2O)_2]^{2+}$ complex fragments in compound $[Cu^{II}(2,2'\text{-}bipy)(H_2O)_2Cl][Cu^{II}(2,2'\text{-}bipy)(H_2O)_2Al(OH)_6Mo_6O_{18}]\cdot 4H_2O$. (Right) the structure of $[Cu^{II}(2,2'\text{-}bipy)(H_2O)_2Cl][Cu^{II}(2,2'\text{-}bipy)(H_2O)_2Al(OH)_6Mo_6O_{18}]$ showing a chainlike array of $\{Al(OH)_6Mo_6O_{18}\}^{3-}$ cluster anions interconnected through $\{Cu^{II}(bipy)(H_2O)_2\}^{2+}$ bridging copper complex fragments. Two chloro-copper complexes are hydrogen bonded, alternatively, to only one type of Anderson anion in the chain. The Anderson cluster anion is shown in polyhedral representation.

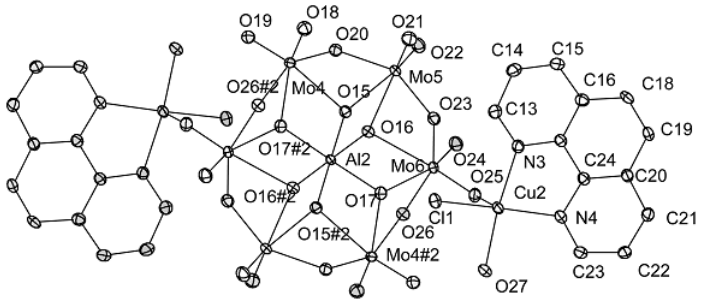


**Fig. 1.8** Thermal ellipsoidal plot of the compound $[Al(OH)_6Mo_6O_{18}\{Cu(phen)(H_2O)_2\}_2]$ with 30% propabibility. The atoms with additional label #2 is related to by the following symmetry operations: #2, –x+3, -y-1, -z+1.

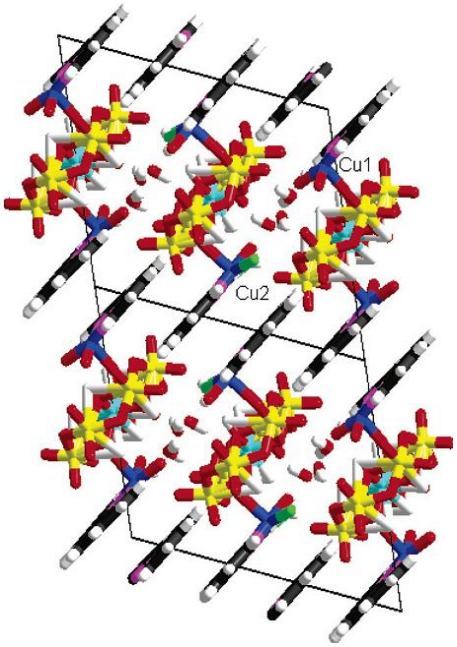


**Fig.1.9** Packing diagram of the $[Al(OH)_6Mo_6O_{18}\{Cu(phen)(H_2O)_2\}_2]$ with wire frame in 4X4 cells.Colorcode: Al, cyan; Mo, yellow O, red; Cu, blue; N, purple; Cl, green; C, dark gray; H, white.

### 1.4.7. Other Applications

Apart from the aforementioned discussion, an intense research work on the applications of POMs is known in the literature such as conductivity,[40] photochromism,[41] corrosion,[42] analytical,[43] gas sensors,[44] fuel cells,[45] wood pulp bleaching,[46] protein precipitating agents,[47] etc.,

## 1.5. Bismuth-chloro Derivatives:

Gabriella Bombieri suggested that halogenobismuthate(III) complex salts may contain an array of variously organized halobismuthate anions since different polynuclear species can be formed through oligomerization by halide bridging.[48] In the majority of the cases the coordination sphere of bismuth appears dominated by the tendency towards hexa coordination with polybismuthate species arising from corner, edge or face sharing $BiX_6$ distorted octahedra. The formation of the anionic sub lattice is clearly determined by the counter cations but the effects of their most evident properties such as charge, size and shape are not exactly predictable but it can be done to some extent.

### 1.5.1. Number of nuclearity in bismuth-chloro derivatives:

From the survey of the literature, $\{BiCl_6\}^{3-}$ is the most common bismuth-chloro derivative as a salt of many organic amines.[49] The nuclearity of bismuth in the chlorobismuthate derivative has been tuned by changing the counter cation for example, its size, charge and shape. Some literature suggested that formation of $\{Bi_2Cl_9\}^{3-}$is possible by using the higher size of the cation like $[(CH_3)_4P]^{1+}$.[50] Very few results are reported for the formation of $\{Bi_2Cl_{10}\}^{4-}$ by using some organic ammonium salts.[51] $\{BiCl_6\}^{3-}$, $\{Bi_2Cl_9\}^{3-}$ and $\{Bi_2Cl_{10}\}^{4-}$ are represented in the Figs. 1.10-1.12

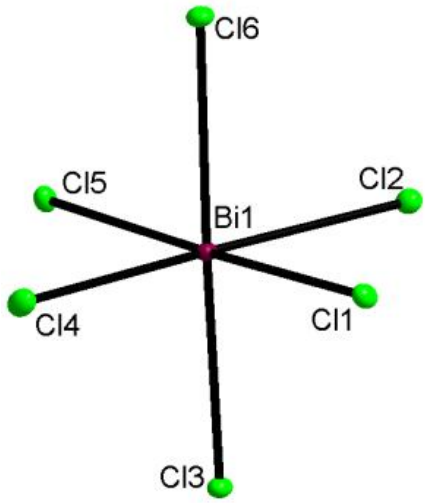


**Fig.1.10** Ball and stick representations of bismuth monomer $[BiCl_6]^{3-}$.

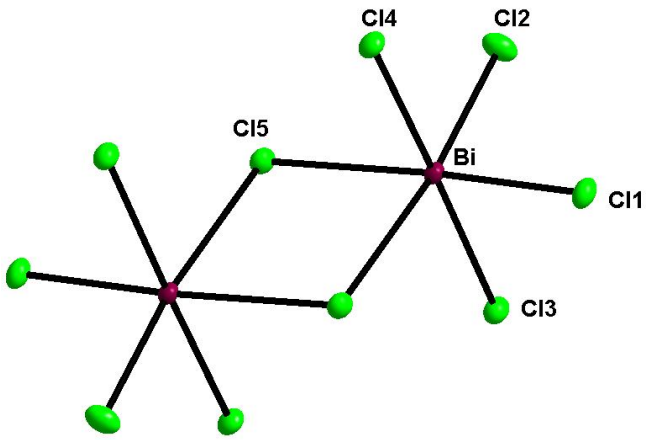


**Fig. 1.11** Ball and stick representations of bismuth dimer $\{Bi_2Cl_{10}\}^{4-}$.

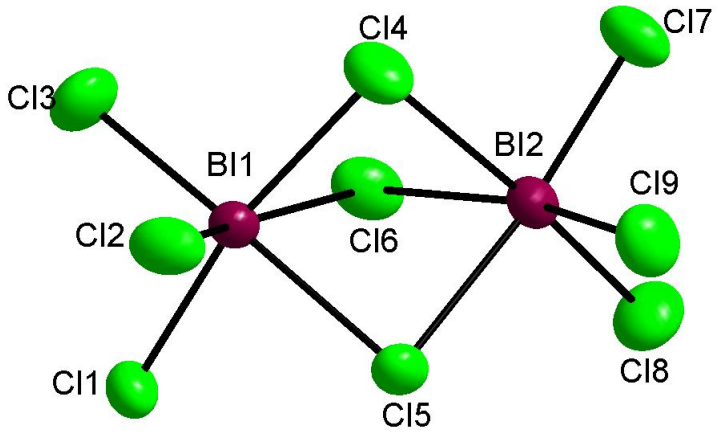


**Fig. 1.12** Ball and stick representations of bismuth dimer $\{Bi_2Cl_9\}^{3-}$

Halogenobismuthates(III) of general formula $R_aM_bX_{(3b+a)}$ (R = alkyl ammonium cations; M = Bi; X = Cl,) are examples of such systems exhibiting diverse properties like ferroic (ferroelastic, ferroelectric) behaviour in commensurate modulated phases.[52] Some representative examples of such species that are characterized in various anionic forms, belong to $R_2Bi_2X_{10}$ and $R^1{}_3BiCl_6$ classes (where R is doubly protonated cation and $R^1$ is mono-protonated cation).

Compounds of general formula $[NH_{4-n}(CH_3)_n]_3M_2X_9$ (where M = Sb, Bi; X = Cl, Br, I; n = 1–4) have been the subject of many investigations due to their fascinating properties. It was postulated that the unusual electric properties of the crystal were governed by the dynamics of the alkylammonium cations.[52a,53] Some of the crystals, particularly those with small alkylammonium cations, reveal the ferroelectricity, e.g. $(CH_3NH_3)_3M_2Br_9$ [54a], $[(CH_3)_2NH_2)]_3Sb_2X_9$ [54b] and $[(CH_3)_3NH]_3Sb_2C1_9$ [55c]. It has turned out that cationic dynamics of these compounds is affected by the type of anionic structure. From the methylammonium subgroup, $(CH_3NH_3)_3M_2X_9$, the chlorine derivatives form one-dimensional double chains of polyanions. [54d]

## 1.5.2. Supramolecular chemistry of bismuth-chloro derivatives:

Basically the supramolecular chemistry has been varied by changing the counter cation because it is noticed that C–H···Cl, N–H···Cl were observed in the reported compounds. One of the compounds, [1,3,5-Tris(4-pyridinium)-2,4,6-triazine][$BiCl_6$]has shown the C–H···Cl, N–H···Cl interactions as shown in Fig. 1.13 leading to the formation of the synthon motif.[55]

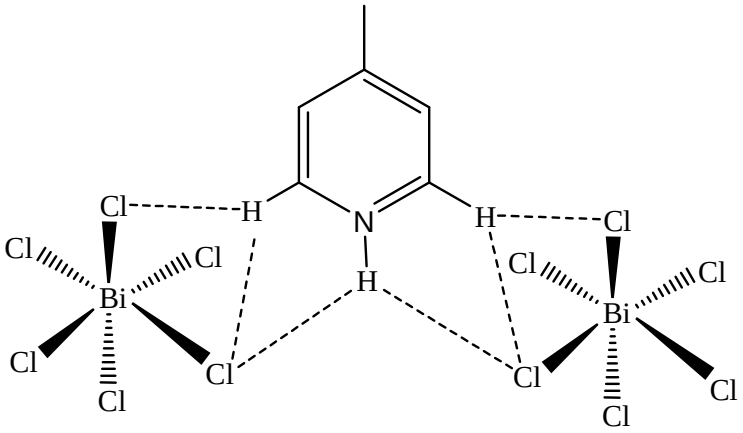


**Fig.1.13** Formation of synthon in the [1,3,5-Tris(3-pyridinium)-2,4,6-triazine][$BiCl_6$].

Thus the compound [1,3,5-tris(4-pyridinium)-2,4,6-triazine][$BiCl_6$] shows the C–H···Cl, N–H···Cl interactions to all the directions, which results in the formation of fascinating network leading to the another synthon motif as shown in the Fig.1.14. Hydrogen bonding is observed around the cation with $BiCl_6$ leading to the formation triangular nerwork.[55]

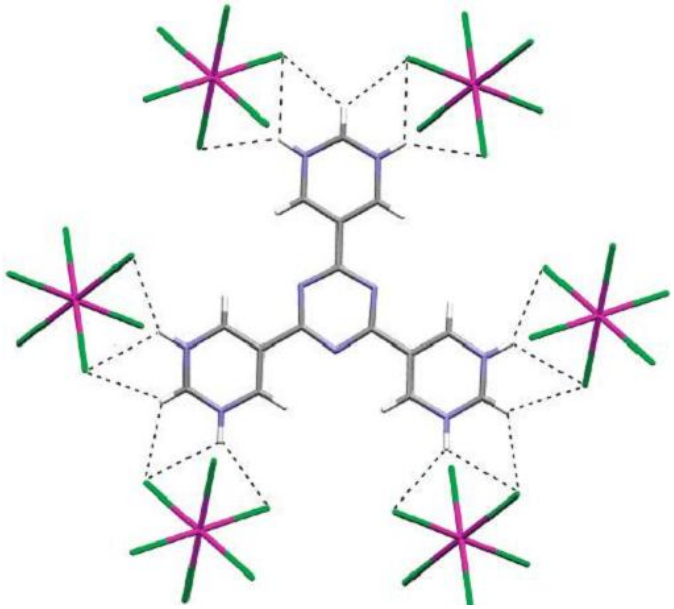

**Fig.1.14** [1,3,5-tris(4-pyridinium)-2,4,6-triazine][BiCl6] shows the C–H···Cl, N–H···Cl interaction around the counter cation with $BiCl_6^{3-}$.

Another important class of the material, [1,3,5-tris(2-pyridinium)-2,4,6-triazine][$BiCl_6$]·$3H_2O$ has received much importance in the supramolecular chemistry because of C–H···Cl, N–H···Cl interactions leading to the formation of similar kind of network as shown in Fig. 1.15.

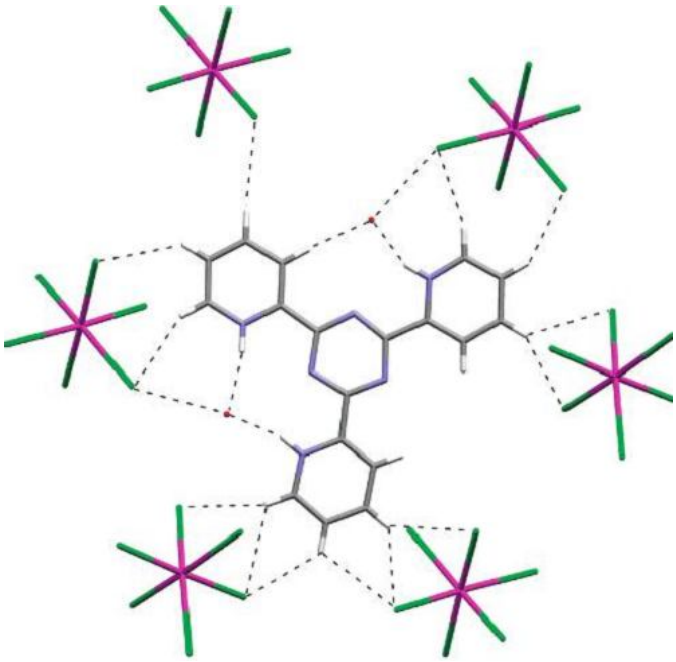

**Fig.1.15.**1,3,5-tris(2-pyridinium)-2,4,6-triazine][$BiCl_6$]·$3H_2O$ shows the C–H···Cl, N–H···Cl between counter cation and $\{BiCl_6\}^{3-}$

### 1.5.3. Applications of the bismuth compounds and its chloro derivatives

Bismuth based materials are receiving considerable attention because of their numerous potential applications including oxidation catalysis,[56a] next generation memory devices,[56b] high Tc superconductors,[56c] high temperature electrolytes,[56d] and nonlinear optical materials.[56e] Bismuth-chloro compounds have lot of applications in the area of semiconductors due to their promising properties like low temperatures anti-ferro or antiferrielectric properties,[57a] ferroelectric property [57b] and ferro elastic properties.[57c]

Moreover, bismuth coordination compounds are highly useful in drug industry. Numerous compounds are reported as anti cancer agent and anti ulcer agent. Bismuthcarboxylates, or their partially hydrolysed derivatives, have long been important compounds for chemotherapy; bismuth subgallate, subcitrate, tartrate and subsalicylate are used to treat syphilis, hypertension, infection as well as gastrointestinal disorders, and

also used in cosmetics to control skin conditions.[58] Bismuth sub salicylate (BSS), colloidal bismuthsubcitrate(CBS) and ranitidine bismuth citrate have been used worldwide as over-the-counter medications for the treatment of diarrhea, dyspepsia, and peptic and duodenal ulcers.

**1.6. Motivation of present Thesis**

Above mentioned discussion presents a general over-view of POMs and their related topics. Since the time, first POMs cluster was discovered, application of POMs as a material is grown step by step. Currently we are in the position to seek out such category of materials with some unique properties. Further work on developing reliable and versatile functional materials with useful properties is essential. The studies on solid state properties of POMs based crystalline materials in new perspectives open up unexplored solid state aspects on their possible applications in the interdisciplinary areas. In general, POMs are in anionic form which can be isolated as crystalline material with appropriate cation and the properties of the same also can be tuned to a large extent. This present work describes POMs based materials synthesis, crystal structures, and their possible studies in application point of view. We have chosen transition metal supported heptamolybdate system for the catalysis studies in the reaction of oxidation of styrene, and particularly we reuse of the catalyst at least for three times. These catalytic studies are extended to catalysis by decvanadate anionic cluster and Anderson anion. By using aminopyridine derivatives as templates, a series of decavanadate and Anderson anionic clusters were isolated and catalytic activity was also studied in the above reactions and results are described in chapters 2, 3 and 4 respectively. In chapters 3 and 4, we have studied the supramolecular interactions among the organic cation and cluster anion using O–H···O, C–H···O and N–H···O interactions. Another important aspect of this thesis is to explore small water clusters (cyclic tetramer and pentamer), that are formed by O–H···O interactions, as described in chapter 3. In chapter 5, synthesis of monomeric bismuth choro derivatives $\{BiCl_6\}^{3-}$ and $\{Bi_2Cl_{10}\}^{4-}$ were described that are stabilized with aminopyridine and bipyridine respectively. Interestingly, one of these compounds exhibits emission property, which has been described by calculating the quantum yield and its quenching property is also studied. Another dimeric bismuth cluster $\{Bi_2Cl_9\}^{3-}$ has been isolated as 1, 5-benzodiazepinium salt, where 1, 5-benzodiazepine is generated *insitu* in the solution starting from ethanon/propanol and opda. The resulting compounds

were studied in terms of supramolecular relevance, as they show weak interactions, such as C–H···Cl with surrounding cations.

### 1.6. References


1. Pope, M. T. *Heteropoly and Isopoly Oxometalates;* Springer-Verlag: Berlin, 1983.
2. (a) Kouffman, G. B.; Vartanian, P. F. *J. Chem. Edu.* **1970**, *47*, 212; (b) Pope, M. T. *Inorg. Chem.* **1972**, *11*, 1973.
3. Berzelius, J. *Pogg. Ann.,* **1826**, *6*, 369.
4. (a) Müller, A.; Kögerler, P.; Kuhlmann, C. *Chem. Commun.* **1999**, 1347. (b) Müller, A.; Kögerler, P.; Bögge, H. *Mol. Self-assembly,* **2000**, *96*, 203.
5. (a) Keggin, J. F. *Proc. Roy. Soc., A.* **1934**, *144*, 75. (b) Lindqvist, I. *Arkiv Kemi.*, **1950**, *2*, 325. (c) Anderson, J. S. *Nature,* **1937**, *140*, 850. (d) Strandberg, R. *Acta Chem. Scand.*, **1973**, *27*, 1004.
6. (a) Jahr, K. F.; Fuchs, J. *Chem. Ber.*, **1963**, *96*, 2457. (b) Fuchs, J.; Jahr, K. F. *Chem. Ber.*, **1963**, *96*, 2460. (c) Fuchs, J.; Jahr, K. F. *Chem. Ber.*, **1963**, *96*, 2472.
7. Rhule, J. T.; Hill, C. L.; Judd, D. A.; Schinazi, R. F. *Chem. Rev.* **1998**, *98*, 327.
8. (a) Burkholder, E.; Golub, V.; P'Connor, C. J.; Zubieta, J. *Inorg. Chem. Commun.*, **2004**, *7*, 363. (b) Soghomonian, V.; Chen, Q.; Haushalter, R. C.; Zubieta, J.; O'Connor, C. J. *Science*, **1993**, *259*, 1596.
9. (a) Barra, A. L.; Gatteschi, D.; Tsukerblatt, B. S.; Doring, J.; Müller, A.; Brunel, L. C. *Inorg. Chem.* **1992**, *31*, 5132. (b) Klemperer, W. G.; Marquart, T. A.; Yaghi, O. M. *Angew. Chem., Int. Ed. Engl.* **1992**, *31*, 49; (c) Day, V. W.; Klemperer, W. G.; Yaghi, O. M. *J. Am. Chem. Soc.* **1989**, *111*, 5959; (d) Barra, A. L.; Gatteschi, D.; Pardi, L.; Müller, A.; Doring, J. *J. Am. Chem. Soc.* **1992**, *114*, 8509; (e) Gatteschi, D.; Pardi, L.; Barra, A. L.; Müller, A.; Doring, J. *Nature*, **1991**, *354*, 463. (f) Müller, A.; Doring, J. *Angew. Chem., Int. Ed. Engl.* **1988**, *27*, 1721. (g) Müller, A.; Krickemeyer, E.; Penk, M.; Rohlfing, R.; Armatage, A.; Bögge, H. *Angew Chem., Int. Ed. Engl.* **1991**, *30*, 1674; (h) Müller, A.; Rohlfing, R.; Doring, J.; Penk, M. *Angew. Chem., Int. Ed. Engl.* **1991**, *30*, 588.
10. Jr, H. T. E. *Inorg. Chem.* **1966**, *5*, 967.
11. (a) Aubin, S. M. J.; Wemple, M. W.; Adams, D. M.; Tsai, H. L.; Christou, G.; Hendrickson, D. N. *J. Am. Chem. Soc.* **1996**, *118*, 7746. (b) Sessoli, R.; Tsai, H.

L; Schake, A. R.; Wang, S.; Vincent, J. B.; Folting, K.; Gatteschi, D.; Christou, G.; Hendrickson, D. N.; *J. Am. Chem. Soc.* **1993**, *115*, 1804; (c) Price, J. P.; Batten, S. R.; Moubaraki, B.; Murray, K. S. *Chem. Commun.* **2002**, 762. (d) Brechin, E. K.; Boskovic, C.; Wernsdorfer, W.; Yoo, J.; Yamaguchi, A.; Sañudo, E. C.; Concolino, T. R.; Rheingold, A. L.; Ishimoto, H.; Hendrickson, D. N.; Christou, G. *J. Am. Chem. Soc.* **2002**, *124*, 9710. (e) Jones, L. F.; Brechin, E. K.; Collison, D.; Harrison, A.; Teat, S. J.; Wernsdorfer, W. *Chem. Commun*. **2002**, 2974. (f) Soler, M.; Wernsdorfer, W.; Folting, K.; Pink, M.; Christou, G.; *J. Am. Chem. Soc.* **2004**, *126*, 2156. (g) Gatteschi, D.; Sessoli, R.; Cornia, A. *Chem. Commun.* **2000**, 725. (h) Delfs, C.; Gatteschi, D.; Pardi, L.; Sessoli, R.; Wieghardt, K.; Hanke, D. *Inorg. Chem.* **1993**, *32*, 3099. (i) Benelli, C.; Cano, J.; Journaux, Y.; Sessoli, R.; Solan, G. A.; Winpenny, R. E. P. *Inorg. Chem*. **2001**, *40*, 188. (j) Goodwin, J. C.; Sessoli, R.; Gatteschi, D.; Wernsdorfer, W.; Powell, A. K.; Heath, S. L. *J. Chem. Soc., Dalton Trans.* **2000**, 1835. (k) Sun, Z.; Grant, C. M.; Castro, S. L.; Hendrickson, D. N.; Christou, G. *Chem. Commun*. **1998**, 721. (l) Yang, E. –Ch.; Hendrickson. D. N.; Wernsdorfer, W.; Nakano, M.; Zakharo, L. N.; Sommer, R. D.; Rheingold, A. L.; Ledezma–Gairaud, M.; Christou, G. *J. Appl. Phys.* **2002**, *91*, 7382. (m) Boskovic, C.; Rusanov, E.; Stoeckli–Evans, H.; Gudel, H. U. *Inorg. Chem. Commun.* **2002**, *5*, 881; (n) Cadiou, C.; Murrie, M.; Paulsen, C.; Villar, V.; Wernsdorfer, W.; Winpenny, R. E. P. *Chem. Commun.* **2001**, 2666. (o) Ochsenbein, S. T.; Murrie, M.; Rusanov, E.; Stoeckli–Evans, H.; Sekine, C.; Gudel, H. U. *Inorg.Chem.* **2002**, *41*, 5133.

12. Leuenberger, M. N.; Loss, D. *Nature*, **2001**, *410*, 789. (b) Hill, S.; Edwards, R. S.; Aliaga-Alcalde, N.; Christou, G. *Science*, **2003**, *302*, 1015. (c) Sessoli, R.; Tsai, H. –L.; Schake, A. R.; Wang, S.; Vincent, J. B.; Folting, K.; Gatteschi, D.; Christou, G.; Hendrickson, D. N. *J. Am. Chem. Soc.*, **1993**, *115*, 1804.
13. Müller, A.; Meyer, J.; Krickemeyer, E.; Diemann, E. *Angew. Chem., Int. Ed.* **1996**, *35*, 1206.
14. Müller, A.; Krickemeyer, E.; Dillinger, S.; Bögge, H.; Plass, W.; Proust, A.; Dloczik, L.; Menke, C.; Meyer, J.; Rohlfing, R. *Z. Anorg. Allg. Chem.* **1994**, *620*, 599.
15. (a) Zhang, S. -W.; Huang, G. -Q.; Shao, M. –C.; Tang, Y. –Q. *J. Chem. Soc., Chem. Commun*, **1993**, 37. (b) Müller, A.; Krickemeyer, E.; Dillinger, S.; Bögge, H.; Proust, A.; Plass, W.; Rohlfing, R. *Naturwissenschaften* **1993**, *80*, 560. (c)

Müller, A.; Bögge, H.; Krickemeyer, E.; Dillinger, S. *Bull. Pol. Acad. Sci., Chem.* **1994**, *42*, 291.

16. Müller, A.; Krickemeyer, E.; Bögge, H.; Schmidtmann, M. F. Peters, *Angew. Chem., Int. Ed.*. **1998**, *37*, 3360.
17. Müller, A.; Krickemeyer, E.; Meyer, J.; Bögge, H.; Peters, F.; Plass, W.; Diemann, E.; Dillinger, S.; Nonnenbruch, F.; Randerath, M.; Menke, C. *Angew. Chem., Int. Ed. Engl.* **1995**, *34*, 2122.
18. Müller, A.; Krickemeyer, E.; Bögge, H.; Schmidtmann, M.; Beugholt, C.; Kögerler, P.; Lu, C. *Angew. Chem., Int. Ed.*. **1998**, *37*, 1220. (b) Jiang, C. C.; Wei, Y. G.; Liu, Q.; Zhang, S. W.; Shao, M. C.; Tang, Y. Q. *Chem. Commun.* **1998**, 1937.
19. Müller, A.; Shah, S. Q. N.; Bögge, H.; Schmidtmann, M. *Nature*, **1999**, *397*, 48.
20. Müller, A.; Beckmann, E.; Bögge, H.; Schmidtmann, M.; Dress, A. *Angew. Chem., Int. Ed*. **2002**, *41*, 1162.
21. Brégeault, J. –M. *J. Chem. Soc., Dalton Trans.*, **2003**, 3289.
22. Katsoulis, D. E. *Chem. Rev.* **1998**, *98*, 359.
23. Misono, M. *Chem. Commun.*, **2001**, 1141.
24. Hill, C. L. *nature*, **1999**, 436.
25. Yamase, T. *Mole. Eng*. **1993**, *3*, 241.
26. Hill, C. L.; Hartnup, M.; Faraj, M.; Weeks, M.; Prosser-Mccartha, C. M.; Brown Jr, R. B.; Kadkhodayan, M.; Sommadossi, J, -P,; Schinazi, R. F. *In Advances in Chemotherapy of AIDS*; Diasio, R. B.; Sommadossi, J. –P. Eds.; Pergamon Press, Inc.: New York, 1990.
27. (a) Strandberg, R. *Acta Chem. Scand.* **1973**, *27*, 1004. (b) Matsumoto, K. Y.; Kato, M.; Sasaki, Y. *Bull. Chem. Soc. Jpn.* **1976**, *49*, 106. (c) Day, V. W.; Fredrich, M. F.; Klemperer, W. G.; Shum, W. *J. Am. Chem. Soc.* **1977**, *99*, 952. (d) Hedman, B. *Acta Chem. Scand.* **1977**, *27*, 3335. (e) Knoth, W. H.; Harlow, R. L. *J. Am. Chem. Soc.* **1981**, *103*, 1865.
28. Matsumoto, K. Y. *Bull. Chem. Soc. Jpn*, **1979**, *52*, 3284.
29. Pope, M. T. *Inorg. Chem.* **1976**, *15*, 2008.
30. Strandberg, R. *Acta Chem. Scand., Ser. A.* **1975**, *29*, 350. (b) D'Amour, H. *Acta Crystallogr., Sect. B.* **1976**, *32*, 729. (c) Garvey, J. F.; Pope, M. T. *Inorg. Chem.* **1978**, *17*, 1115.

31. (a) Tézé, A.; Hervé, G. J. *Inorg. Nucl. Chem.* **1977**, *39*, 999. (b) Tézé, A.; Hervé, G. J. *Inorg. Nucl. Chem.* **1977**, *39*, 2151.

32. Contant, R.; Ciabrini, J. P. *J. Chem. Res.* **1977**, *M*, 2601 (b) Contant, R.; Ciabrni, J. P.; *J. Chem. Res.* **1977**, *S*, 222 (c) Contant, R.; Ciabrini, J. P. *J. Chem. Nucl. Chem.* **1981**, *43*, 1525. (d) Harmalker, S. P. Ph. D Thesis, Georgetown University, 1982. (e) Kozik, M.; baker, L. C. W. *Polyoxometalates: From Platonic Solids to Antiretro Viral Activity*, Pope, M. T.; Müller, A. Eds.; Kluwer Academic Publisher: The Netherlands, 1994. (f) Tourné, C. M.; Tourné, G. F.; Zonnevijlle, F. *J. Chem. Soc., Dalton Trans.* **1991**, 143.

33. (a) Evans Jr., H. T.; Showell, J. S. *J. Am. Chem. Soc.* **1969**, *91*, 6881. (b) Ada, T.; Hidaka, J.; Shimura, R. *Bull. Chem. Soc. Jpn*, **1970**, *43*, 2654.

34. Waugh, J. C. T.; Schoemaker, D. P.; Pauling, L. *Acta Crystallogr*. **1954**, *7*, 438. (b) Baker, L. C. W.; Weakley, T. J. R. *J. Inorg. Nucl. Chem.* **1966**, *28*, 447. (c) Nomiya, K.; Kobayashi, R.; Miwa, M.; *Bull. Chem. Soc. Jpn*, **1983**, *56*, 3505.

35. (a) Fuchs, J.; Palm, R. Z. Z. *Naturforsch., B: Chem. Sci.* **1988**, *43*, 1529. (b) Acerete, R.; Server-Carrió, J. *J. Am. Chem. Soc.* **1990**, *112*, 9386.

36. Yosov, A. B.; Shilov, V. P. *Radiochemistry*, **1999**, *41*, 3.

37. (a) Wassermann, K.; Pope, M. T.; Salmen, M.; Dann, J. N.; Lunk, H. –J. *J. Solid State Chem.* **2000**, *149*, 378. (b) Pope, M. T.; Wei, X.; Wassermann, K.; Dickman, M. H. C. R. *Acad. Sci., Ser. IIc* **1998**, *I*, 297. (c) Wassermann, K.; Dickman, M. H.; Pope, M. T. *Angew. Chem. Int. Ed. Engl.* **1997**, *36*, 1445.

38. (a) Kremlyakova, N. Y.; Novikov, A. P.; Myasoedov, B. F.; Katargin, N. V. *J. Radioanal. Nucl. Chem.*, **1990**, *145*, 183. (b) Molochnikova, N. P.; Frenkel, V. Y.; Myasoedov, B. F. *Radiokhimiya*, **1989**, *31*, 65.

39. a) Shivaiah, V.; Das, S. K. *Inorg. Chem.*, **2005**, *44*, 8846. b) Shivaiah, V.; Nagaraju, M.; Das, S. K. *Inorg.Chem.* **2003,** *42***,** 6604.

40. (a) Peng, J.; Wang, E.; Zhou, Y.; Xing, Y.; Jia, H.; Lin, Y.; Shen, Y. *J. Chem. Soc., Dalton Trans.*, **1998**, 3865.

41. Coué, V.; Dessapt, R.; Bujoli-Doeuff, M.; Evain, M.; Jobic, S. *Inorg. Chem.* **2007**, *46*, 2824.

42. Lomakina, S. V.; Shatova, T. S.; Kazansky, L. P. *Corros. Sci*., **1994**, *36*, 1645. (b) Wu, N.; Wang, S.; Xu, H.; Fang, J. *Yingyong Huaxu*., **1993**, *10*, 5.

43. Svec, V.; Mikulaj, V.; Hazel, R. *J. Radioanal. Nucl. Chem.*, **1996**, *208*, 487.

44. (a) Polak, A.; Young, P.; U. S. Patent 4714482, 1987; *Chem. Abstr.* **1988**, *108*, 95874. (b) Petty-Weeks, S. U.S. Patent 4661211, 1987; *Chem. Abstr.* **1987**, *107*, 69923.

45. Nakamura, O.; Kodama, T.; Ogino, I.; Miyake, Y. Japanese Patent JP 51106694, 1976; *Chem Abstr.* **1976**, *86*, 19085; (b) Nakamura, O.; Kodama, T.; Ogino, I.; Miyake, Y. U. S. Patent 4024036, 1977.

46. Kaneda, T.; Jinnai, K.; Koshizuka, T.; Kimura, A. Japanese Patent JP07082243 A2, 1995, *Chem Abstr.* **1995**, *123*, 82854.

47. Vallance, D. T.; Byrne, D. J.; Winder, A. F. *Clin. Chim. Chim. Acta*. **1994**, *229*, 77. (b) Yeang, H. Y.; Sunderasan, E.; Bahri, A. R. S. *J. Nat. Rubber. Res*. **1994**, *9*, 70.

48. a) Davidovic, R. L.; Buslaev, Y. A. *Coord. Chim.*, **1988**, *14*, 1011. b) Bowmaker, G. A.; Junk, P. C.; Lee, A. M.; Skelton, B. W.; White, A. H. *J. Aust. Chem.* **1998**, *51*, 293. c) Benetollo, F.; Bombieri, G.; Alonzo, G.; Bertazzi, N.; Caslla, G. *J. Chem. Crystallogr.*, **1998**, *28*, 791. d) Alonzo, G.; Benetollo, F.; Bertazzi, N.; Bombieri, G. *J. Chem. Crystallogr.*, **1999**, *29*, 913.

49. Podesta, T. J.; Orpen, A. G. *Cryst. Growth Des.*, **2005**, *5*, 681.

50. a) Jakubas, R.; Bator, G.; Medycki, W.; Piglewski, N.; Decressain, R.; Lefebvre, J.; Franqois, P. *J. Mole. Str.* **1996**, *385*, 145 b) Jakubas, R.; Tomaszewski, P.; Sobczyk, L. *Phys. Status Solidi (a).*, **1989**, *111*, K27.

51 a) Benetollo, F.; Bombieri, G.; Pra, A. D.; Alonzo, G.; Bertazzi, N. *Inorg.Chim. Acta*., **2001**, *319*, 49. b) Bigoli, F.; Lanfranchi, M.; Pellinghelli, M. A. *Inorg. Chim. Acta*, **1984**, *90*, 215.

52 a) Jakubas, R.; Sobczyk, L. *Phase Transit.* **1990**, *20*, 163; b) Sobczyk, L.; Jakubas, R.; Zaleski, J. *Pol. J. Chem.*, **1997**, *71*, 265; c) Mróz, B.; Tuszyński, J. A.; Kiefte, H.; Clouter, M. J.; Jakubas, R.; Sept. D. *Phys.Rev.* **1997**, B58, 14261. d) Kawai, T.; Takao, E.; Shimanuki, S.; Iwata, M.; Miyashita, A.; Ishibashi, Y. *J. Phys. Soc. Japan*., **1999**, *68*, 2848. e) Hashimoto, M.; Hashimoto, S.; Terao, H.; Kuma, M.; Niki, H.; Ino H. *Z. Naturf.*, **2002,** *a55*, 167. f) Wojtaś, M.; Bator, G.; Jakubas, R.; Zaleski, J.; Kosturek, B.; Baran, J. *J. Solid State Chem*., **2003**, *173*, 425. g) Gutbier, V. A.; Müller, M. *Z. Anorg. Allg. Chem.*,**1923**, *128*, 137.

53. a) Vama, V.; Bhattarcharjee, R.; Vasan, H. N.; Rao, C.N.R. *Spectrochim. Acta.*, **1992**, *48A*, 1631. b) Ishihara, H.; Watanabe, K.; lwata, A.; Yamada, K.; Kinoshita,

Y.; Okuda, T.; Krishnan, V. G.; Dou, S.; Weiss, A. *Z. Natuf-forsch.*, **1992**, *47a*, 65.

54. a) Jakubas, R.; Krzewska, U.; Bator, G.; Sobczyk, L.; *Ferro-electrics*., **1988,** *77*, 129. b) Jakubas, R.; Sobczyk, L.; Matuszewski, J.; *Ferro-electrics*., **1987**, *80*,339. c) Jakubas, R.; Czapla, Z.; Galewski, Z.; Sobczyk, L. *Ferro-electrics* Lett., **1988**, *5*, 69. d) Kihara, K.; Sudo, T. *Acta Cryst.*, **1974**, *B30*, 1088.

55. a) Podesta, T. J.; Orpen, A. G. *Cryst. Growth Des.*, **2005**, *5*, 681.

56 a) Shido, T.; Okita, G.; Asakura, K.; Iwasawa, Y. *J. Phys. Chem.*, **2000,** *B104*, 12263. b) Scott, J. F.; Alexe, M.; Zakharov, N. D.; Pignolet, A.; Curran, C.; Hesse, D. *Integrated Ferroelectrics.*, **1998**, *12*, 1; c) Scott, J. F. *Inte-grated Ferroelectrics.*, **2000**, *31*, 139. d) Maeda, H. *Materia*, **2001**, *40*, 947. e) Maeda, H.; Tanaka, Y.; Fukuyama, M.; Asano, T. *Jpn J. Appl. Phys*., **1988**, *27*; L209. (f) Zha, S.; Cheng, J.; Lieu, Y.; Lieu, X.; Meng, G. *Solid-StateIonics*., **2003,** *156*, 197. (g) Abraham, F.; Bovin, J.-C.; Mair-aisse, G.; Nowogrocki, G. *Solid-StateIonics.*, **1990**, *934*, 40. h) Arbosa, M. C.; Frejlich, J. *Trends in Optics and Photonics.*, **2003**, *87*, 8731. i) Ando, M.; Kamata, K.; Ota, K.; Audebert, P.; Delidet, J-F.; Nakaya, K.; Delellis, J.; *Jpn Kokai Tokkyo, Koho* **2003**, 12.

57. a) Zaleski, J.; Jakubas, R.; Sobczyk, L.; Mróz, J. *Ferro-electrics.*, **1990**, *103*, 83. b) Jakubas, R.; Czapla, Z.; Galewski, Z.; Sobczyk, L.; Zogał, O. J.; Lis, T. *Phys. Status Solidi a*., **1986**, *93*, 449. c) Kallel, A.; Bats, J. *Acta Crystallogr.* **1985**, *C51*, 1022. d) Lazarini, F. *Acta Crystallogr.* **1977**, *B33*, 2686.

58 Briand, G. G.; Burford, N. *Chem. Rev.*, **1999**, *99*, 2601.

**********

# Oxidation of Styrene to Benzaldehyde Using Transition Metal Complexes Supported by Heptamolybdate anion

**Abstract:** Oxidation of styrene is carried out by using heptamolybdate supported transition metal ($Co^{2+}$, $Zn^{2+}$ ) complexes, $[2\text{-ampH}]_4[Co(H_2O)_5Mo_7O_{24}]\cdot 9H_2O$ (**1**), $[3\text{-ampH}]_4[\{Co(H_2O)_5\}Mo_7O_{24}]\cdot 9H_2O$ (**2**), $[2\text{-ampH}]_4[\{Zn(2\text{-ampy})(H_2O)_4\}Mo_7O_{24}]\cdot 4H_2O$ (**3**), $[3\text{-ampH}]_4[\{Zn(3\text{-ampy})(H_2O)_4\}Mo_7O_{24}]\cdot 4H_2O$ (**4**) as catalyst and $H_2O_2$ as an oxidant at 80 $^0$C. The leaching study was carried out to check the quality of catalyst and it was reused for three times with good percentage of conversion. For the first two catalysts (compounds **1** and **2**), the major product obtained is benzaldehyde and benzoic acid is the major product for next two catalysts (compounds **3** and **4**). Quality of catalysts was analyzed by IR- , UV-spectroscopy and powder X-ray crystallography.

## 2.1. Introduction

Since last few decades, mainstream of POMs applications is found in the area of catalysis[1] besides their applications in the field of materials science,[2] medicine,[3] and magneto chemistry.[4] The redox properties of these POMs make them promising materials as good catalysts for a number of oxidation and dehydrogenation reactions of organic substrates. The main role of POM-cluster anion in catalysis is in the activation of the oxidant, e.g., hydrogen peroxide, alkylhydroperoxide etc. As a result of the activation of peroxides, an inorganic peroxo, hydroperoxo, alkyl peroxo, or acyl peroxo intermediates are formed and those are very reactive species leading to oxygenation of the organic substrate.

In the similar way, oxidation of olefins to aldehyde or ketone is currently fascinating in industrial chemistry. This can be divided into three categories: 1) the cleavage of the C=C bond by using the surface of the metal oxide like osmium or molybdenum oxides with the stoichiometric amount.[5] 2) The ozonolysis of olefin leading to the formation of keto functional group.[5c,6] 3) Olefin oxidation by using hydrogen peroxide resulting in the formation of C=O functional group.[7] At present era important problems in the oxidation reactions are mainly wastage of the materials and usage of the highly expensive materials. In order to overcome all these problems, we have chosen

hydrogen peroxide as a green oxidizing agent because, in this case, water is a side product, which is benign to our environment. And it is a very attractive oxidant for liquid phase reactions.[8] It can oxidize the organic compounds with an efficiency of 47 % (active oxidant= 47%) and it is very cheap (< 0.7 US $ $Kg^{-1}$). It is essential to mention that $H_2O_2$ is an ideal and waste free oxidant if it is used without organic substrates and toxic materials. Safety reasons are not required very much for its storage.[9] Moreover $H_2O_2$ is used in the large scale reactions to synthesize the caprolactame (Sumitomo Chemical Co.)[10] and propylene oxidation (BASF and Dow Chemical Co.).[11]

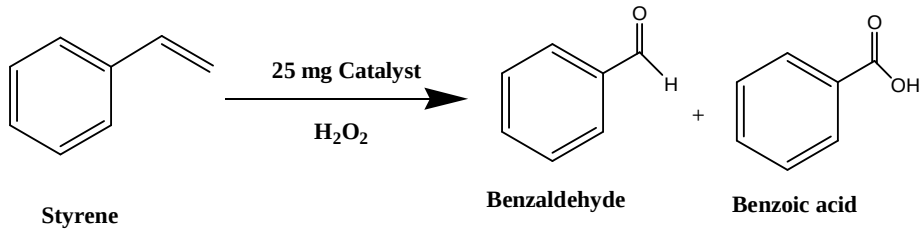


**Scheme 2.1** Oxidation of styrene leads to benzaldehyde and benzoic acid by using the transition metal complexes supported by heptamolybdate as catalyst.

In this regard, polyoxometalates are well known to act as catalyst for oxidation of olefins and alcohols[12]. Due to availability of duel oxidation states of metal ion, it offers the catalytic behavior in the oxidation of alcohols and olefins to simple functional groups like aldehyde or ketone. Such properties are tuned by changing the counter cation of the polyoxoanions for example, $Co_3[Si_2W_{12}O_{40}]$ is a good catalyst in oxidation of alcohols, whereas, other salts of Keggin $[Si_2W_{12}O_{40}]^{6-}$ is not that much efficient catalyst for alcohol oxidation.[13] In the present study, we have examined the catalytic applications of conversion of styrene to benzaldehyde / benzoic acid by four transition metal complexes supported by polyoxometalates (**1-4**). We have reported here that catalysts are efficient to reuse for three times with similar percentage of conversion.

## 2.2. Experimental Section:

### 2.2.1 Materials:

$[2\text{-ampH}]_4[Co(H_2O)_5Mo_7O_{24}]\cdot 9H_2O$ (**1**), $[3\text{-ampH}]_4[\{Co(H_2O)_5\}Mo_7O_{24}]\cdot 9H_2O$ (**2**), $[3\text{-ampH}]_4[\{Zn(3\text{-ampy})(H_2O)_4\}Mo_7O_{24}]\cdot 4H_2O$ (**3**), $[3\text{-ampH}]_4[\{Co(3\text{-ampy})(H_2O)_4\}Mo_7O_{24}]\cdot 4H_2O$ (**4**) are synthesized according literature procedure[14]. Styrene and $H_2O_2$ (30%) are purchased from Hi-Chem.

### 2.2.2 Physical Measurements:

Micro analytical (C, H, N) data were obtained with a FLASH EA 1112 Series CHNS Analyzer. Infrared (IR) spectra were recorded on KBr pellets with a JASCO FT/IR-5300 spectrometer in the region of 400–4000 $cm^{-1}$. Electronic absorption spectra were recorded on a Cary 100 Bio UV–Vis spectrophotometer. G.C. analysis was performed on GCMS equipped with ZB-1column (30 m x 0.25mm, pressure= 20.0 k Pa, detector= EI, 300 $^oC$) with helium gas as carrier.

## 2.3. Results and Discussions:

### 2.3.1 Catalysis:

The oxidation of styrene with 30% of $H_2O_2$, catalyzed by four synthesized materials (**1-4**), produces benzaldehyde/ benzoic acid as the major products and the minor products are styrene oxide and acetophenone. The advantages of these catalysts lie in the fact that they are recycled in the same oxidation for at least three times with similar percentage of conversion. The complete results of the styrene oxidation by using four catalysts are shown in Table 2.1. As shown in the table, all the four compounds are good catalysts in the oxidation of styrene. When the same oxidation is performed with ammonium heptamolybdate as a catalyst (instead of compounds **1-4**), we found only 5% conversion. On the other hand, the title compounds results in a good percentage (>99) of conversion under similar condition.

Comparing the IR spectra of pure catalyst **1** and regenerated catalyst **1** suggests that there is no structural change in the catalyst even after several cycles. Infra red spectra of both parent **1** and regenerated **1** are shown in the Fig. 2.1 and Fig 2.2 respectively. Solid state UV spectroscopy of the pure catalyst and regenerated catalyst also suggest that

catalyst does not leach after completion of the reaction as shown in Fig. 2.3 and Fig 2.4 respectively. Powder-XRD studies of parent **1** and regenerated **1** also suggest that catalyst is not destroyed after the catalysis as shown in Fig 2.3 and Fig 2.4 respectively. We have carried out the same reaction by varying the amount of the catalyst and amount of hydrogen peroxide (oxidant), the observations have been shown in the Table 2.2.

| **Catalyst** | **Conversion (%)** | **Selectivity(%)** | | | | |
|---|---|---|---|---|---|---|
| | | **Benzaldehyde** | **Epoxide** | **Benzyl alcohol** | **Benzoic acid** | **Acetophenone** |
| **1*** | **99.3** | **76** | – | – | **24** | – |
| **2*** | **96** | **76** | **3** | **5** | **15** | **1** |
| **3†** | **100** | **16** | **0** | **6** | **58** | **20** |
| **4†** | **100** | **15** | **3.8** | **1.2** | **69** | **11** |

**Table 2.1** Oxidation of styrene by using the four catalysts (**1**–**4**)

Nate: 25 mg of the catalyst at 80 ºC and time is 24 h; *1:2 ratio and† 1:3 ratio of styrene and $H_2O_2$

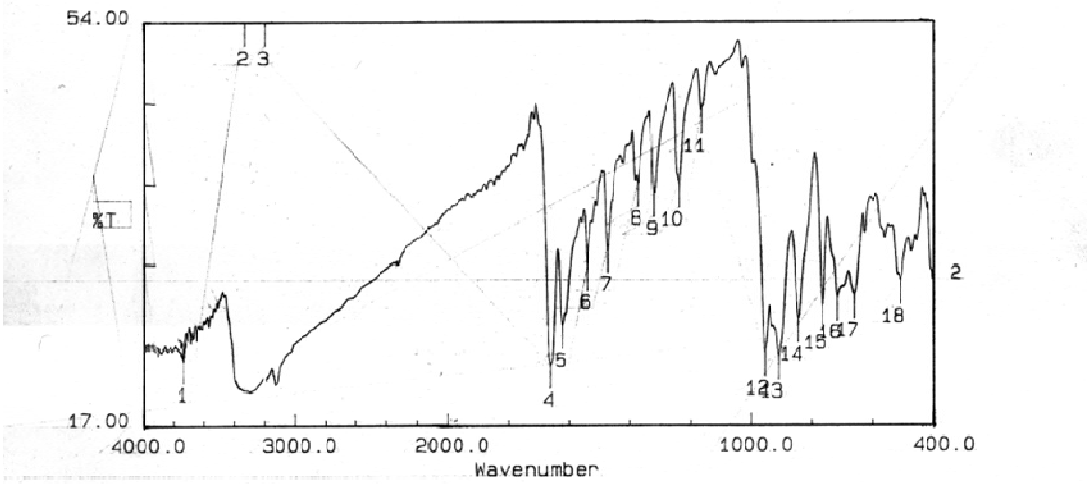


Condition

upper 54.00 lower 17.00 depth 2.00

Peak table

| | | | | | | | |
|---|---|---|---|---|---|---|---|
| 1: | 3736.45 ( 23.2) | 2: | 3335.22 ( 20.0) | 3: | 3198.26 ( 19.2) | 4: | 1662.79 ( 22.7) |
| 5: | 1622.28 ( 26.3) | 6: | 1541.26 ( 31.6) | 7: | 1473.75 ( 33.3) | 8: | 1373.44 ( 39.3) |
| 9: | 1319.43 ( 38.4) | 10: | 1236.48 ( 39.3) | 11: | 1163.18 ( 46.0) | 12: | 954.85 ( 23.7) |
| 13: | 908.55 ( 23.4) | 14: | 842.97 ( 26.8) | 15: | 763.88 ( 27.9) | 16: | 715.66 ( 28.8) |
| 17: | 657.79 ( 29.0) | 18: | 507.32 ( 30.3) | | | | |

**Fig.2.1** Infra Red spectroscopy of catalyst **1**

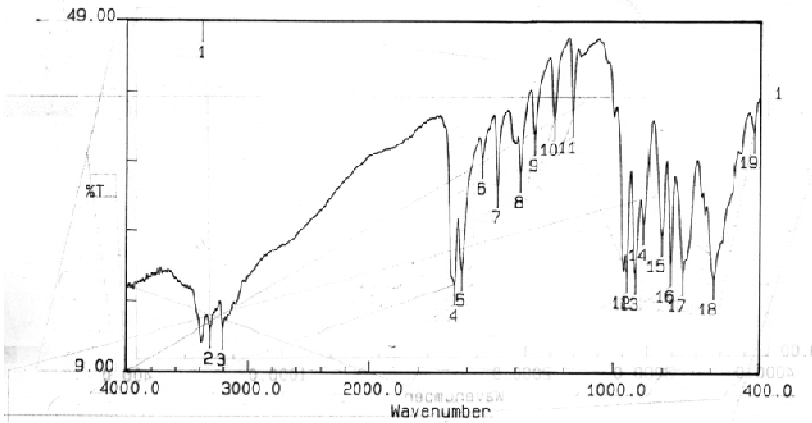


Condition

upper 49.00 lower 9.00 depth 2.00

Peak table

| | | | | | | | |
|---|---|---|---|---|---|---|---|
| 1: | 3387.31 ( 12.4) | 2: | 3315.93 ( 14.0) | 3: | 3209.84 ( 13.9) | 4: | 1653.14 ( 19.0) |
| 5: | 1624.21 ( 20.6) | 6: | 1539.33 ( 33.4) | 7: | 1477.61 ( 30.2) | 8: | 1383.09 ( 31.9) |
| 9: | 1323.29 ( 36.1) | 10: | 1240.34 ( 38.0) | 11: | 1165.11 ( 38.2) | 12: | 943.29 ( 20.4) |
| 13: | 908.55 ( 20.3) | 14: | 875.76 ( 26.0) | 15: | 802.46 ( 24.7) | 16: | 765.81 ( 21.2) |
| 17: | 715.66 ( 20.2) | 18: | 586.34 ( 19.8) | 19: | 422.45 ( 36.5) | | |

**Fig.2.2** Infra Red spectroscopy of regenerated catalyst **1**

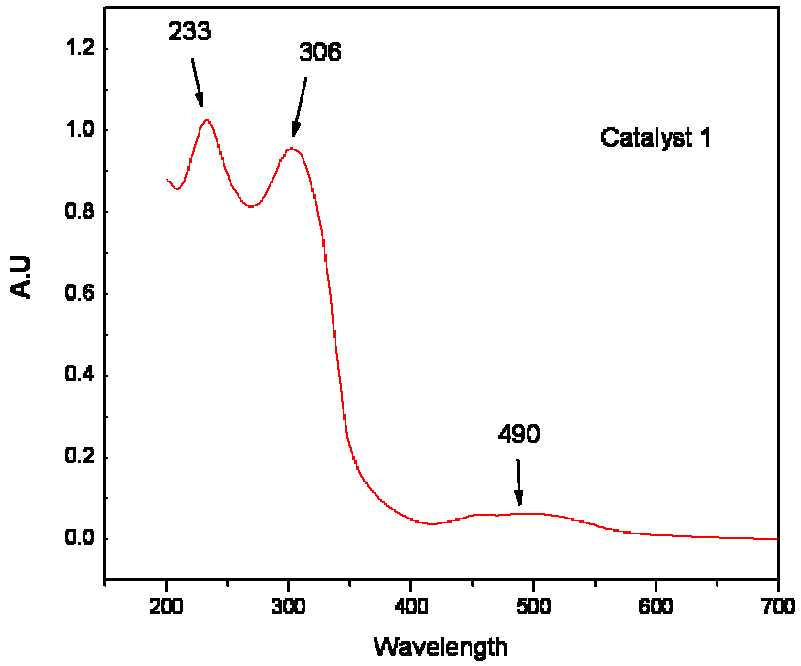


**Fig. 2.3** Diffuse reflectance spectra of catalyst **1.**

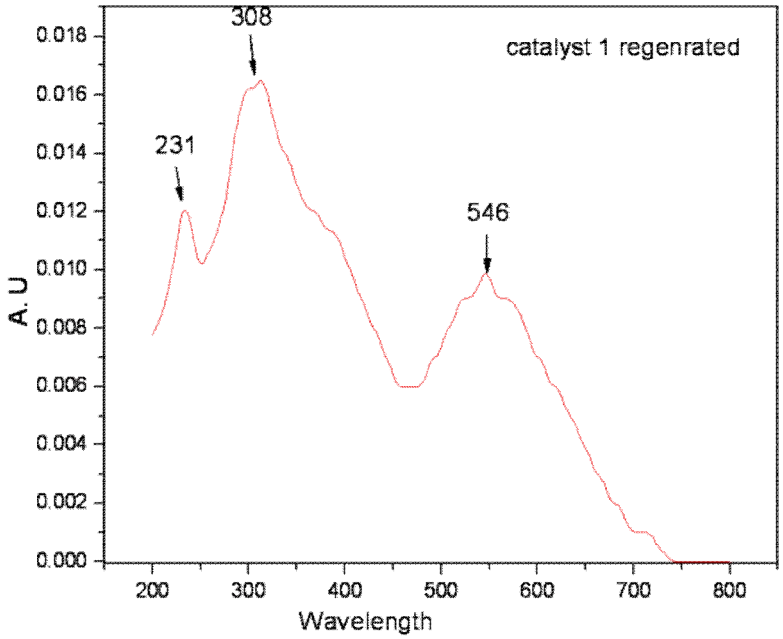


**Fig. 2.4** Diffuse reflectance spectra of regenerated catalyst **1**

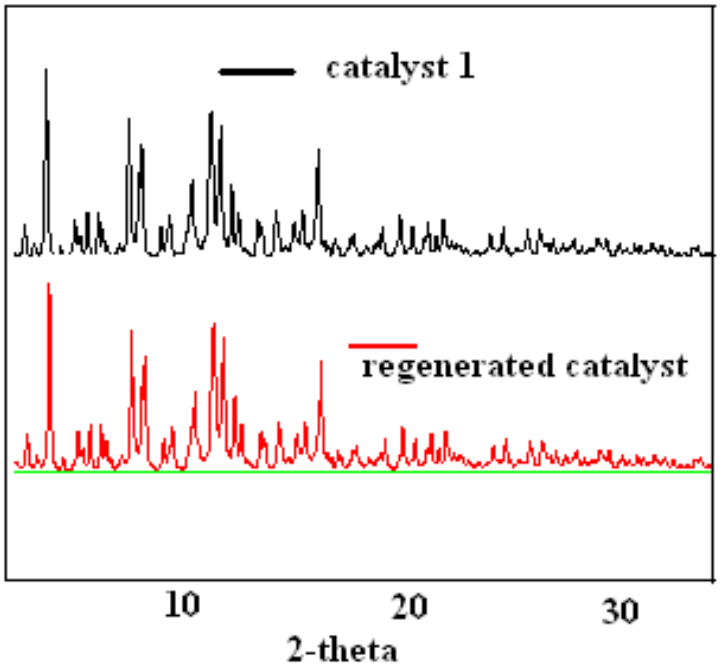


**Fig. 2.5** Powder XRD pattern of catalyst **1** and regenerated catalyst **1**

As shown in Table 2.2, increasing the conc. $H_2O_2$ increases the percentage of conversion increases but the conversion of benzaldehyde is decreased. This is because the additional hydrogen peroxide oxidizes the generated benzaldehyde further to benzoic acid. So the conversion of benzoic acid increases with increase in conc. of $H_2O_2$. In all the cases, benzaldehyde is the product with major selectivity especially under the condition of 1:2 ratio of styrene and hydrogenperoxide; other products are epoxide, and benzophenone with minor selectivity. We have run several reactions for styrene oxidation with catalyst **1** under various conditions and finally one condition was optimized with 1:2 ratio of styrene and hydrogen peroxide at 80 ºC for 24 h for the maximum selectivity of benzaldehyde.

**Table 2.2** The results for the reaction of oxidation of styrene by varying the conc. of $H_2O_2$ (Condition : Time = 24 h; Temperature = 80 ºC)

| Reaction Condition (Sty:$H_2O_2$) | Percentage of Conversion | Selectivity (%) | | | | |
|---|---|---|---|---|---|---|
| | | Benzaldehyde | Epoxide | Benzyl alcohol | Benzoic acid | Acetophenone |
| 1:1 | 36 | 88 | 2 | - | 10 | - |
| 1:2 | 96 | 76 | - | - | 24 | - |
| 1:3 | 99.3 | 53 | 3.5 | - | 31 | 12.5 |

Important observation is that after 2 h reaction, the color of the reaction mixture became yellow; subsequently this color disappears (after 10 h) and finally the reaction mixture became bluish in color. This may be due to the change in oxidation state of molybdenum while going the reaction. In fact the catalyst is not soluble in any solvent, either in the starting substrates or hydrogen peroxide but it is completely soluble in reaction mixture (after addition of substrates and hydrogen peroxide). As already mentioned, the percentage of conversion increases with increasing the amount of the catalyst **1** (Fig. 2.6). In the similar way, selectivity of benzaldehyde as we increase the amount of catalyst as shown in Fig. 2.7. The observation with second catalyst follows identical fashion for the same conversion.

**Table 2.3** Results of percentage of conversion by varying the amount of catalyst **1** for oxidation of styrene.*

| Amount of Catalyst 1 | Percentage of Conversion | Selectivity (%) | | | | |
|---|---|---|---|---|---|---|
| | | Benzaldehyde | Epoxide | Benzyl alcohol | Benzoic acid | Acetophenone |
| 5mg | 74 | 56.6 | 3 | 4.4 | 28 | 8 |
| 10mg | 91 | 61.6 | 1 | 2 | 27 | 8.4 |
| 15mg | 98 | 65.4 | 4.6 | 3.8 | 18 | 8.2 |
| 20mg | 99 | 71 | 1.6 | 3.4 | 18 | 6 |
| 25mg | 99.6 | 76 | 0 | 0 | 24 | 0 |

*Condition: 1 mmol of styrene and 2 mmol of $H_2O_2$ at 80 ºC for 24 h.

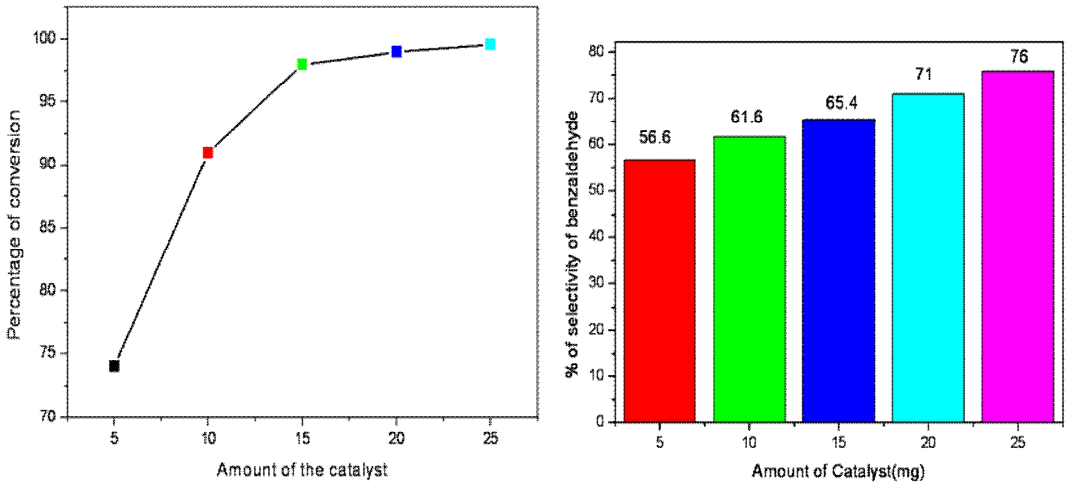


**Fig.2.6** (Left) Graphical view of percentage of conversion in the reaction of oxidation of styrene with amount of catalyst. **(**Right) Selectivity (%) of benzaldehyde by changing the amount of catalyst

**Catalysis of $[3\text{-ampH}]_4[\{Co(H_2O)_5\}Mo_7O_{24}]\cdot 9H_2O$ (2)** : Optimized condition has been preferred a reaction with 1:2 ratio of styrene and hydrogen peroxide because the benzaldehyde is formed as a major product. We are able to reuse this catalyst for three times without destroying the catalyst and percentage of conversion is similar in all the cases. From the IR spectroscopy, diffused UV-spectroscopy and powder XRD pattern it is confirmed that catalyst is not leaching after completion of the reaction at least for three times (See Fig. 2.7 to Fig.2.11).

As increasing the amount of hydrogen peroxide from 1 mmol to 3 mmol with respect to styrene, 99 % of conversion was found in the reaction corresponding to 1:3 ratio of styrene and $H_2O_2$, but the formation of benzaldehyde is reduced because the excess of hydrogen peroxide oxidizes some amount of benzaldehyde leading the formation of benzoic acid. So the selectivity (%) for benzoic acid is increased from first condition to third condition. Increasing the amount of catalyst leads to increment in the percentage of conversion and selectivity of benzaldehyde, as observed for catalyst **1.**

**Table 2.4** Results of percentage of conversion by varying the amount of catalyst **2** for oxidation of styrene. ( 25 mg of catalyst at 80 ºC for 24 h time)

| Ratio of styrene and $H_2O_2$ | Percentage of Conversion | Selectivity | | | | |
|---|---|---|---|---|---|---|
| | | Benzaldehyde | Epoxide | Benzyl alcohol | Benzoic acid | Acetophenone |
| 1:1 | 40 | 50 | 0 | 6 | 15 | 29 |
| 1:2 | 96 | 76 | 3 | 5 | 15 | 1 |
| 1:3 | 99 | 62.3 | 1.3 | 2.4 | 25 | 9 |

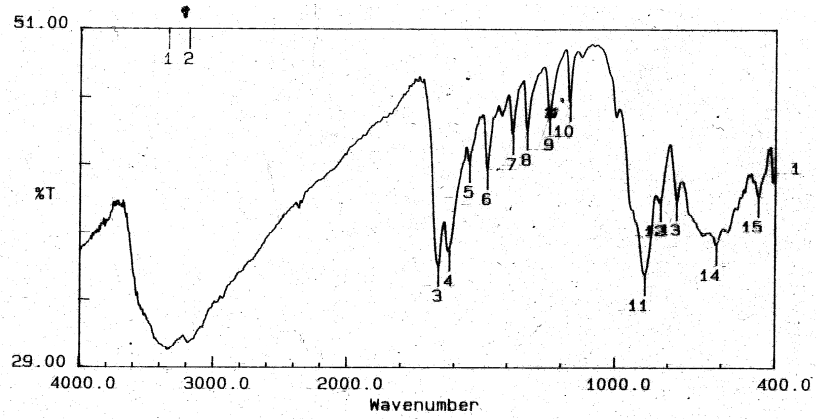


Condition
upper 51.00 lower 29.00 depth 2.00
Peak table

| | | | | | | | |
|---|---|---|---|---|---|---|---|
| 1: | 3341.01 ( 30.1) | 2: | 3182.83 ( 30.7) | 3: | 1658.93 ( 35.6) | 4: | 1618.42 ( 36.6) |
| 5: | 1543.19 ( 42.4) | 6: | 1475.68 ( 42.0) | 7: | 1381.16 ( 44.2) | 8: | 1327.14 ( 44.5) |
| 9: | 1244.20 ( 45.5) | 10: | 1168.97 ( 46.3) | 11: | 887.34 ( 35.1) | 12: | 827.54 ( 40.0) |
| 13: | 767.74 ( 40.0) | 14: | 619.21 ( 37.0) | 15: | 462.96 ( 40.2) | | |

**Fig. 2.7** IR spectroscopy of neat catalyst **2** (compound **2**)

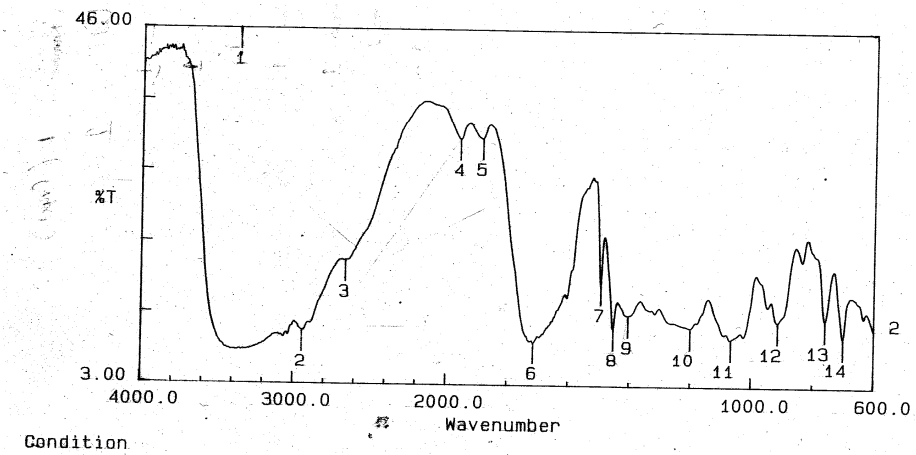


Condition
upper 46.00 lower 3.00 depth 2.00
Peak table

| | | | | | | | |
|---|---|---|---|---|---|---|---|
| 1: | 3371.87 ( 7.1) | 2: | 2941.71 ( 9.5) | 3: | 2662.01 ( 18.0) | 4: | 1959.85 ( 32.8) |
| 5: | 1884.62 ( 32.8) | 6: | 1714.87 ( 8.3) | 7: | 1494.97 ( 15.4) | 8: | 1452.53 ( 10.0) |
| 9: | 1404.30 ( 11.6) | 10: | 1201.76 ( 10.2) | 11: | 1068.66 ( 8.8) | 12: | 914.34 ( 11.0) |
| 13: | 760.02 ( 11.2) | 14: | 702.15 ( 9.1) | | | | |

**Fig. 2.8** IR spectroscopy of regenerated catalyst **2** (compound **2**)

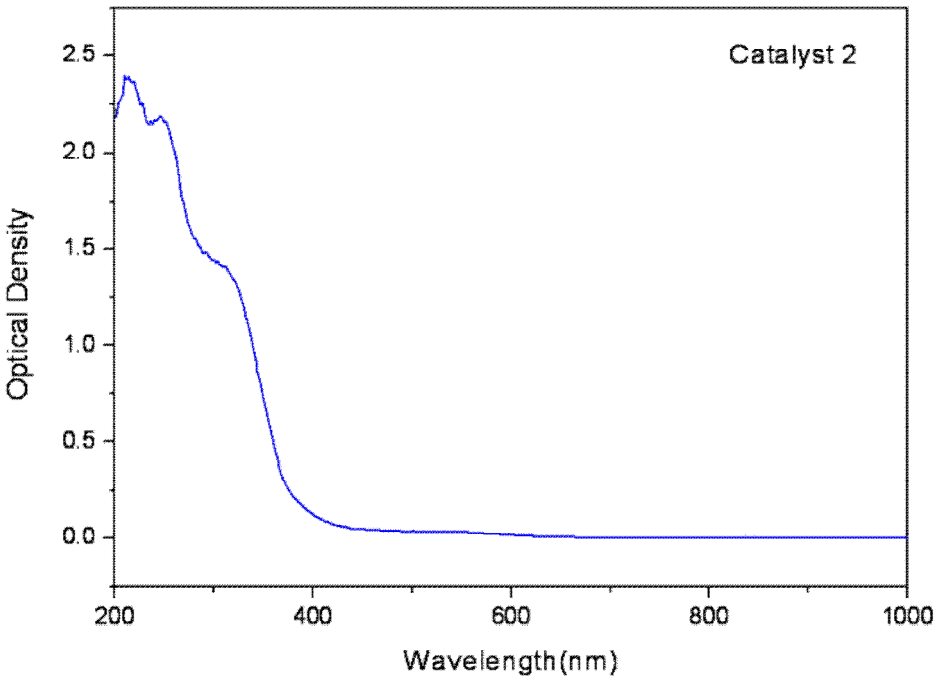


**Fig 2.9** Diffuse reflectance spectra of pure catalyst **2.**

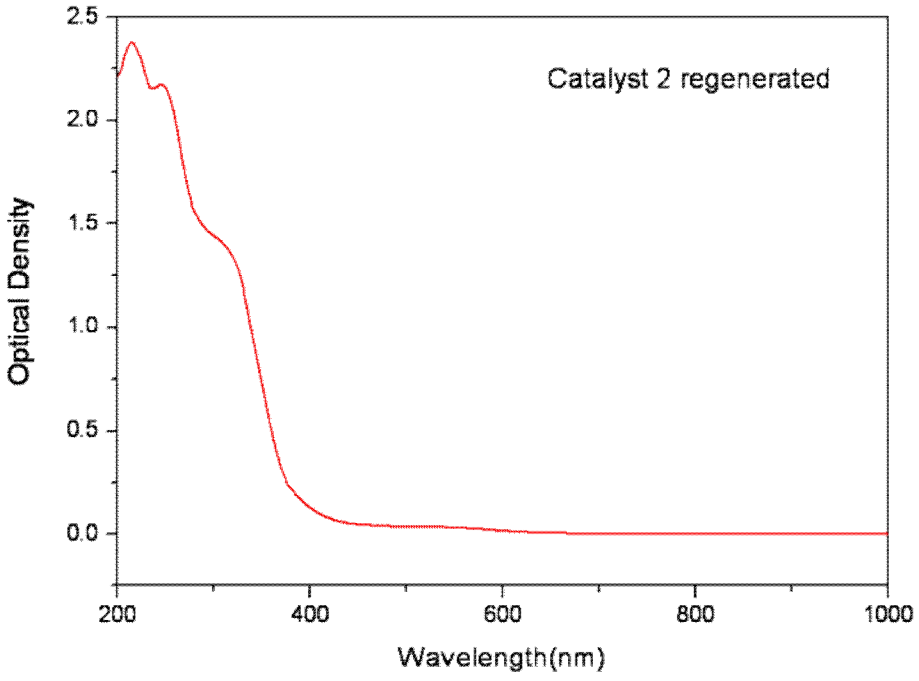


**Fig 2.10** Diffuse reflectance spectra of regenerated catalyst **2.**

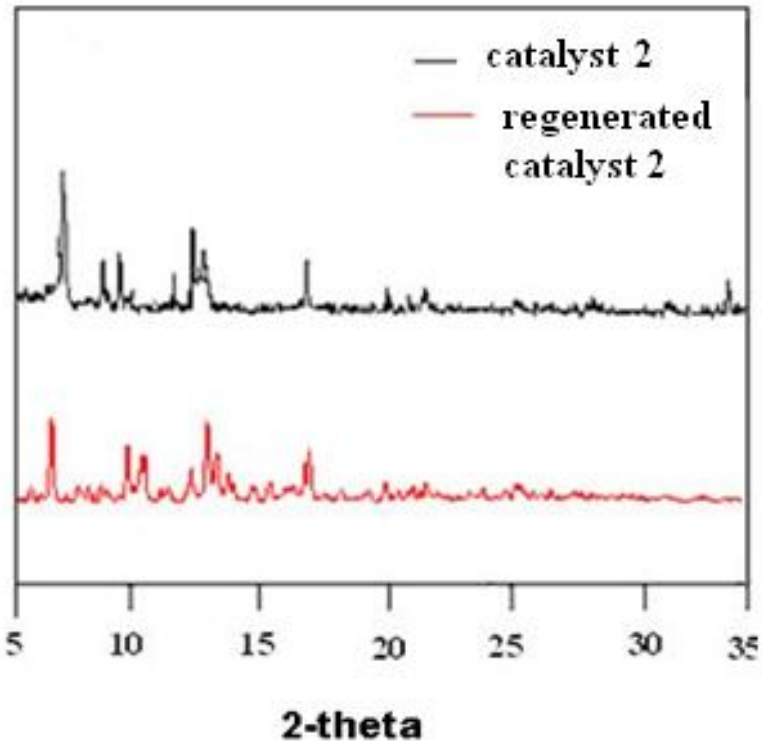


**Fig 2.11** P-XRD of pure catalyst **2** and regenerated catalyst **2 .**

**Catalysis of $[2\text{-ampH}]_4[\{Zn(2\text{-ampy})(H_2O)_4\}Mo_7O_{24}]\cdot 4H_2O$ (3):**

Compound **3** also shows the good catalytic activity in the reaction of oxidation of styrene with various products like benzaldehyde, benzoic acid, acetophenone. In this case benzoic acid is formed with major selectivity (%). Increasing the amount of hydrogen peroxide, percentage of conversion also increases and finally the reaction with 1:3 mole ratio of styrene and hydrogen peroxide is taken as the optimized condition. The results are tabulated in Table 2.5.

By changing the concentration of hydrogen peroxide from 1 mmol to 3 mmol with respect to styrene, the formation of benzoic acid increases because $H_2O_2$ oxidizes the generated benzaldehyde to benzoic acid. At the moment of condition of 1:3 ratio of styrene and $H_2O_2$ both percentage of conversion and formation of benzoic acid reached the maximum. Thus this condition is taken as optimized condition to oxidize the styrene.

**Table 2.5** The results for the variation of amount of $H_2O_2$ in the reaction of styrene oxidation with catalyst **3**

Catalyst **3**

| Ratio of styrene and $H_2O_2$ | Percentage of Conversion | Selectivity(%) | | | | |
|---|---|---|---|---|---|---|
| | | Benzaldehyde | Epoxide | Benzyl alcohol | Benzoic acid | Acetophenone |
| 1:1 | 70 | 32.8 | 4.2 | 6 | 25 | 32 |
| 1:2 | 99.7 | 14.5 | 0 | 4.5 | 56 | 25 |
| 1:3 | 99.9 | 16 | 0 | 6 | 58 | 20 |

In the similar fashion, catalyst **3** was reused for three times. This remains intact (not destroyed) even after three cycles, as confirmed by IR spectroscopy and powder x-ray diffractormeter patterns. (Figs 2.12 and 2.14 respectively).

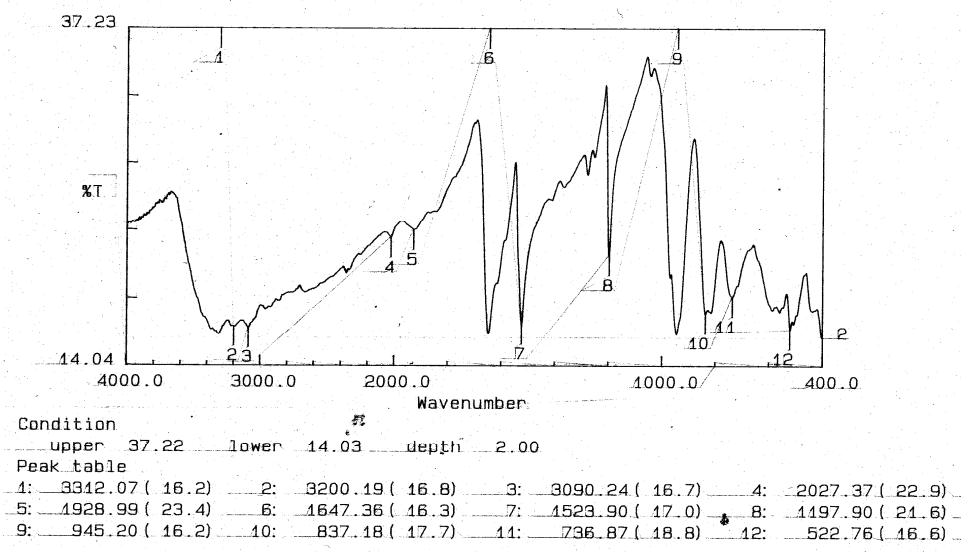


**Fig. 2.12** IR spectra of neat catalyst **3** (compound **3**)

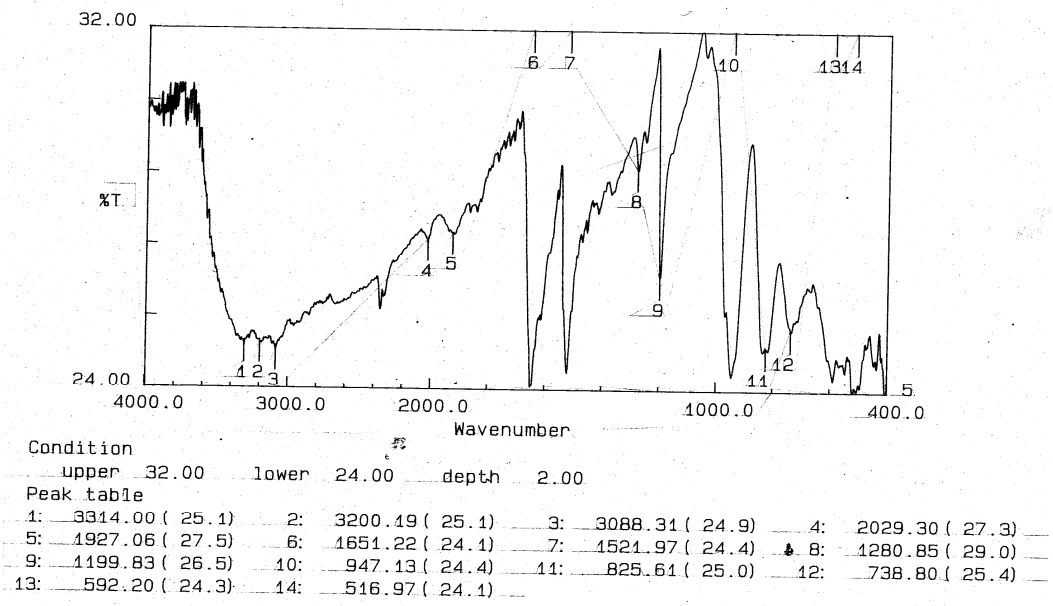


**Fig. 2.13** IR spectra of regenerated catalyst **3** (compound **3**)

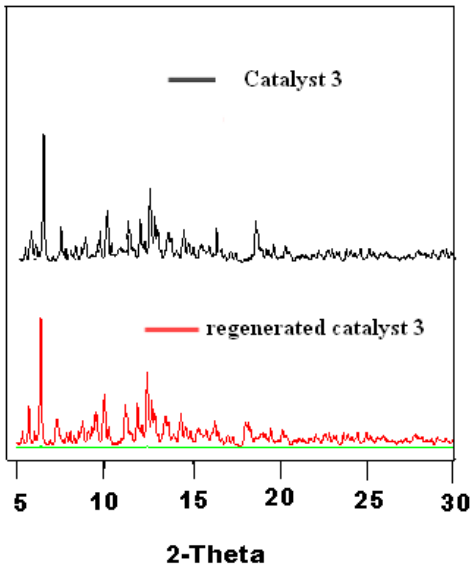


**Fig 2.14** Powder XRD pattern of pure catalyst **3** and regenerated catalyst **3 .**

**Catalysis of $[3\text{-ampH}]_4[\{Zn(3\text{-ampy})(H_2O)_4\}Mo_7O_{24}]\cdot 4H_2O$ (4):**

The catalytic activity of the compound $[3\text{-ampH}]_4[\{Zn(3\text{-ampy})(H_2O)_4\}Mo_7O_{24}]\cdot 4H_2O$ (**4**) towards the oxidation of styrene by using the hydrogen peroxide as an oxidizing agent leads to again the formation of benzaldehyde, acetophenone and benzoic acid. But major selective (%) product is benzoic acid at 1:3 mole ratio of styrene and hydrogen peroxide besides 99% of conversion. So this condition is being considered as optimized condition for this conversion at 80 ºC. In this condition, benzaldehyde is generated with 72 % selectivity; the reason might be the case that reaction has been quenched by the formation of benzyl alcohol. In the case of second condition (1:2 of styrene and $H_2O_2$), the generated benzyl alcohol completely oxidizes to benzoic acid. The third condition (1:3 of styrene and $H_2O_2$) reveals that the percentage of selectivity of benzoic acid has reached maximum value because $H_2O_2$ completely oxidizes to benzoic acid. As usual, the effect of the amount of catalyst is same as shown in the case of compound **3** under the similar condition. More over, the catalyst can be recycled three times for the reaction; the purity of catalyst was analyzed by IR spectroscopy and powder x-ray diffraction as shown in Figs. 2.16 to 2.18.

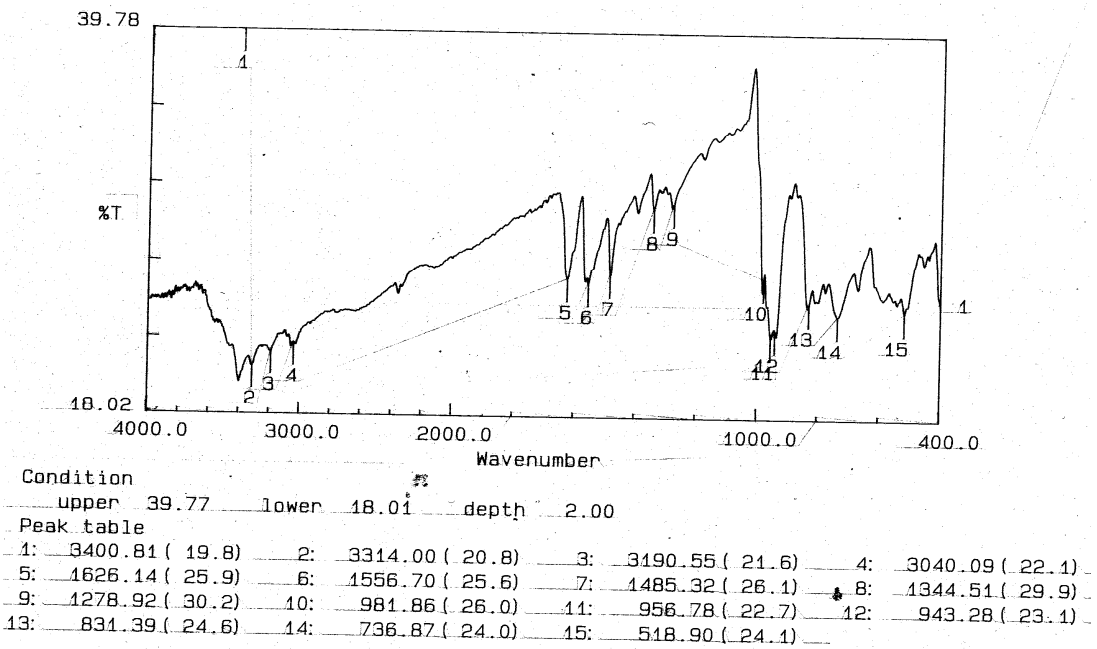


**Fig.2.16** IR spectra of fresh catalyst **4** (compound **4**)

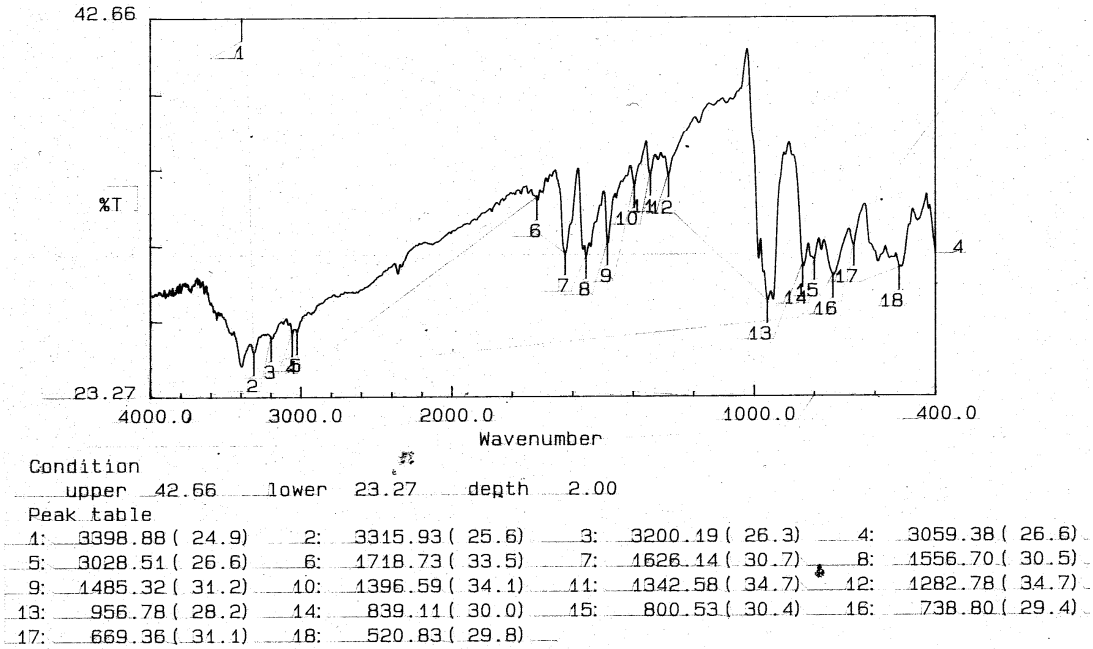


Condition
upper 42.66 lower 23.27 depth 2.00
Peak table

| | | | | | | | |
|---|---|---|---|---|---|---|---|
| 1: | 3398.88 ( 24.9) | 2: | 3315.93 ( 25.6) | 3: | 3200.19 ( 26.3) | 4: | 3059.38 ( 26.6) |
| 5: | 3028.51 ( 26.6) | 6: | 1718.73 ( 33.5) | 7: | 1626.14 ( 30.7) | 8: | 1556.70 ( 30.5) |
| 9: | 1485.32 ( 31.2) | 10: | 1396.59 ( 34.1) | 11: | 1342.58 ( 34.7) | 12: | 1282.78 ( 34.7) |
| 13: | 956.78 ( 28.2) | 14: | 839.11 ( 30.0) | 15: | 800.53 ( 30.4) | 16: | 738.80 ( 29.4) |
| 17: | 669.36 ( 31.1) | 18: | 520.83 ( 29.8) | | | | |

**Fig.2.17** IR spectra of regenerated catalyst **4** (compound **4**)

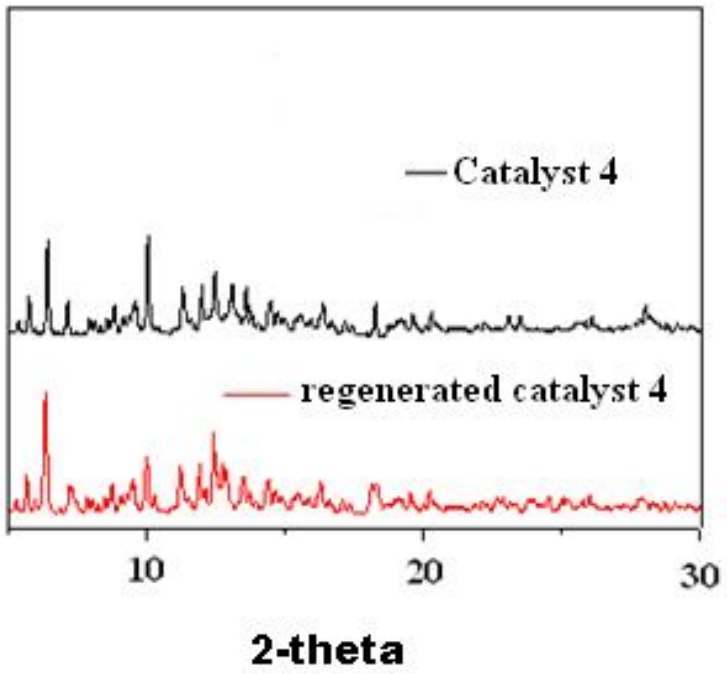


**Fig.2.18** Powder XRD patterns of catalyst **4** regenerated catalyst **4** (compound **4**)

### 2.3.2 Leaching property of the catalyst:

All the catalysts (**1-4**) are regenerated and reused for minimum of three times with similar percentage of conversion. It reveals that catalyst is not losing its catalytic activity even after three cycles in the above said reaction, which is explained based on infrared spectroscopy, solid state UV-visible spectroscopy and powder X-ray crystallography as shown in the Figs 2.1 to 2.11 for catalyst **1**, **2**, **3** and **4**.

### 2.3.3 GC-MS calculations:

The oxidation of styrene[16] is analyzed by Gas Chromatography-Mass Spectral studies. After completion of the reaction, DCM is added to the reaction mixture and then extracted the organic layer with DCM solvent. And then 0.8 μLt. of the reaction mixture was injected into the column, and then it entered the programmed oven (injector temperature: 200 $^{\circ}$C and detector temperature: 250 ºC, ramping temperature: 2.5 ºC).

The percentage-conversion of the substrate and the percentage-selectivity of the products in the reaction are calculated as shown below.[15]

Percentage of conversion = {[Initial mol % –final mol %] / initial mol %}X 100.

Percentage of selectivity = [Product mol % / Substrate mol %] X 100.

## 2.4 Conclusion:

In conclusion, we have demonstrated the catalytic activity of transition metal complexes supported by heptamolybdate anion in the oxidation of styrene by using $H_2O_2$ as an oxidant. All the catalysts are reused for three times with similar percentage of conversion. And the leaching of the catalyst has been checked and studied by infrared spectroscopy, solid state UV-visible spectroscopy and powder X-ray diffraction studies. We have demonstrated the variation of benzaldehyde formation with varying concentration of $H_2O_2$ and varied amount of the catalyst. The percentage of conversion was determined by GC-MS.

**2.5 References:**


1. a) Ben-Daniel, R.; Weiner, L.; Neumann, R.; *J. Am.Chem.Soc.* **1980**, *124*, 8788. b) Hayashi, T.; Kishida, A.; Mizuno, N. *Chemm. Commun*. **2000,** 381. c) Karcz, R.; Pamin, K.; Połtowicz, J.; Haber, J. *Catal. Lett*. **2009**, *132*,159. d) Zhao, W.; Zhang, Y.; Ma, B.; Ding, Y.; Qiu, W. *Catal. Commun*. **2010**, *11*, 527. e) Arumuganthan, T.; Rao, S. A.; Kumar, T. V.; Das. S. K. *J. Chem. Sci*., **2008**, *120*, 95.

2. (a) Pope, M. T. *Compr. Coord. Chem. II* **2004**, *4*, 635.(b) Hill, C. L. *Compr. Coord. Chem.II* **2004**, *4*, 679. (c) Pope, M. T.; Müller, A. *Angew. Chem., Int. Ed*. **1991**, *30*,34.(d) Hill, C. L.; Prosser-McCartha, C. M. *Coord. Chem. Rev*. **1995**, *143*,407.(e) Hill, C. L. *Chem. Rev*. **1998**, 98,1.(f) Izumi, Y.; Urabe, K.; Onaka, M. *Zeolites, Clay and Heteropolyacid in Organic Reactions*; Kodansha:Tokyo,**1992**. (g) Khan, M. I.; Yohannes, E.; Doedens, R. J. *Inorg. Chem*. **2003**, *42*, 3125.(h) Pope, M. T. *Heteropoly and Isopoly Oxometalates;* Springer-Verlag:Berlin,1983.

3. a) Yamase, T. *Mole. Eng*. **1993**, *3*, 241. b) Hill, C. L.; Hartnup, M.; Faraj, M.; Weeks, M.; Prosser-Mccartha, C. M.; Jr, R. B. B.; Kadkhodayan, M.; Sommadossi, J, -P.; Schinazi, R. F. *In Advances in Chemotherapy of AIDS*; Diasio, R. B.; Sommadossi, J. –P.; Eds.; Pergamon Press, Inc.: New York, 1990.

4. (a) *Molecular Electronics Devices I;* Carter, F. L.,Ed.; Dekker: New York, 1982; p.1987.(b) *Topical issue on polyoxometalates*: Hill, C. L. *Chem. Rev*. **1998**, *98*, 1. (c) *Polyoxometalate Chemistry for Nano- Composite Design*; Yamase, T.; Pope, M. T.; Eds.; *Nano structure Science and Technology*, Kluwer Academic/ Plenum Publishing: New York, 2002.(d) *Polyoxomatalates: From Platonic Solids to Anti-Retroviral Activity*; Pope, M. T.; Müller, A.; Eds.; Kluwer: Dordrecht, The Netherlands, 1993.(e) Pope, M. T. *Comp. Coord. Chem*. II **2003**, *4*, 635.(f) *Polyoxometalate Molecular Science*; Borrås-Almenar, J. J.; Coronado, E.; Müller, A.; Pope, M. T.; Eds.; Kluwer: Dordrecht, The Netherlands, 2003.(g) Chen, L.; Jiang, F.; Lin, Z.; Zhou,Y.; Yue, C.; Hong, M. *J. Am. Chem. Soc.* **2005**, *127*, 8588.(h) Zarembowitch, J.; Kahn, O. *New. J. Chem*. **1991**, *15*,181. h) Arumuganathan, T.; Das. S. K.; *Inorg. Chem.* **2009,** *48*, 496.

5. a) Pappo, R.; Jr, D. S. A.; Lemieux, R. U.; Johnson, W. S. *J. Org. Chem.* **1956**, *21*, 478. b) Carlsen, P. H. J.; Katsuki, T.; Martin, V. S.; Sharpless, K. B. *J. Org. Chem.* **1981**, *46*, 3936. c) B. S. Michael, *Organic Synthesis*, (second Ed) McGraw- Hill, New York, 2002.

6. Bailey, P. S. *Chem. Rev.* **1958**, *58*, 925.

7. a) Sheldon, R. A.; Kochi, J. K. *Metal-Catalyzed Oxidations of Organic Compounds*, Academic Press, New York, 1981. b) D. T. Sawyer, *Oxygen Chemistry*, Oxford University Press, New York, 1991.

8. a) Jones, C. W. *Applications of Hydrogen Peroxide and Derivatives*, Royal Society of Chemistry, Cambridge, 1999; (b) *Catalytic Oxidations with Hydrogen Peroxide as Oxidant*, ed. Strukul, G. Kluwer Academic, Dordrecht, The Netherlands, 1992.

9. For the international regulations, see: Regulations Concerning the International Carriage of Dangerous Goods by Rail (RID); European Agreement Concerning the International Carriage of Dangerous Goods by Road (ADR); International Maritime Dangerous Goods Code (IMDG Code); International Civil Aviation Organization Technical Instructions for the Safe Transport of Dangerous Goods by Air (ICAOTI); International Air Transport Association Dangerous Goods Regulation (IATA DGR).

10. Sumitomo Chemical News Release, 2000, Oct. 11; http://www.sumitomo-chem.co.jp/english/e1newsrelease/pdf/20001011e.pdf.

11. Dow Products and Businesses News, 2002, Aug. 1; http://www.dow. com/dow_news/prodbus/2002/20020801a.htm

12. a) Noyori, R.; Aokib, M.; Sato, K. *Chem.Commun.* **2003**, 1977. b) Neumann, R.; Gara, M. *J. Am. Chem. Soc.* **1995**, *117*, 5066. c) Xinrong, L.; Jinyu, X.; Huizhang, L.; Bin, Y.; Songlin, J.; Gaoyanga, X. *J. Mol. Catal. Chemical,* **2000**, *A161*, 163. d) Patel, K.; Tripuramallu, B. K.; Patel, A. *Eur. J. Inorg. Chem.* **2011**, 1871. e) Shringapuri, P.; Patel. A. *Inorg. Chem. Acta.* **2010,** *362*, 3796. f) Patel, K.; Shringarpure, P. ; Patel, A. ; *Trans. Met. Chem.* **2011**, *36*, 171.

13. Hill. C. L.; *Mol. Eng.* **1993**, *3* 263.

14. a) Li, T.; Lü, J.; Gao, S.; Cao, R. ; *Inorg. Chem. Commun.* **2008**, *10*, 1342. b) Arumuganthan, T.; Rao, A. S.; Das, S. K. *Cryst. growth and Design*, **2010**, *10*, 4272.

15. a) Karasek, F. W., Ray E. C. *Basic Gas Chromatography–Mass Spectrometry: Principles & Techniques. Amsterdam:* Elsevier, 1988. b) Hites, R. A.; Biemann, B. *Analytical Chemistry*, **1968**, *40* 1217. c) Hites, R. A.; Biemann, B. *Analytical Chemistry,* **1970**, *40*, 850.

16. For standard optimized catalytic reaction for catalyst **1**or **2**: 1 mmol of styrene and 2 mmol of $H_2O_2$ are taken into the 25 ml of round bottom flask, which was already added 25 mg of catalyst **1** or **2** and stirred for 24 h at 80 ºC, the reaction was quenched with DCM after time period. When the mixture came to room temperature organic layer was extracted in DCM and catalyst was completely came to water layer. Few amount of the organic layer is used for GC-MS analysis. For catalyst **3** or **4**, 1:3 ratio of styrene and $H_2O_2$ were taken as the similar procedure for catalyst **1** or **2.**

# Polyoxovanadate Based Materials: Synthesis, Structural Characterization and Catalysis

**ABSTRACT:-** In this chapter we have described the synthesis, characterization and supramolecular chemistry of $[Co(H_2O)_6][Na_4(H_2O)_{23}]\{V_{10}O_{28}\}\cdot 4H_2O$ (**1**), $[Zn(H_2O)_6][Na_3(H_2O)_{14}]\{HV_{10}O_{28}\}\cdot 10H_2O$ (**2**), $[HMATAH]_2\{H_4V_{10}O_{28}\}\cdot 8H_2O$ **(3)**, $[HMTAH]_2\{(H_2O)_4Zn_2V_{10}O_{28}\}\cdot 2H_2O$ (**4**), $[Co(3\text{-amp})(H_2O)_5]_2[3\text{-ampH}]_2\{V_{10}O_{28}\}\cdot 4H_2O$ (**5**), $[4\text{-ampH}]_5[Na(H_2O)_6]\{V_{10}O_{28}\}\cdot 4H_2O$ (**6**), $[4\text{-ampH}]_{10}[Co(H_2O)_6]\{V_{10}O_{28}\}_2\cdot 10H_2O$ (**7**), $[4\text{-ampH}]_{10}[Zn(H_2O)_6]\{V_{10}O_{28}\}_2\cdot 10H_2O$ (**8**) and $[3\text{-ampH}]_6[V_{10}O_{28}]\cdot 2H_2O$ (**9**). In some of their crystal structures, non-covalent interactions among the lattice water molecules led to the formation of cyclic water tetramer and pentamer. All the compounds (**1–9**) are synthesized at an ambient temperature and are characterized by single crystal X-ray crystallography. They are additionally characterized by elemental analyses and infra-red spectral studies. Catalytic applications of all these materials (**1–9**) are studied in the oxidation of styrene to benzaldehyde successfully. Percentages of conversions are analyzed by GC-MS.

## 3.1 Introduction

The modern chemical research on polyoxometalates (POMs) based solid state materials fascinates synthetic chemists because of their potential applications in diverse research areas, such as, catalysis,[1] electrical conductivity, medicinal chemistry, and materials science.[2] Among these, the area of polyoxovanadates (henceforth, POVs) based materials has received special attention due to not only their diverse topologies, structural and electronic properties but also their fascinating versatile industrial applications, e.g., catalysis and materials applications.[3]Among POVs, decavanadate cluster anion is a versatile POM cluster anion, which is constructed by ten edge-shared $VO_6$ octahedra with $D_{2h}$ symmetry operation as shown in Scheme **3.1**. Eight terminals, fourteen doubly bridged ($\mu^2$), four triply bridged ($\mu^3$) and two hexa bridged ($\mu^6$) oxygen atoms exist within this cluster. Thus it has six negative charges (6–). Formation of the decavanadate anionic cluster can be recognized by IR spectroscopy, in which its characteristic peaks are 990 $cm^{-1}$ and 1000 $cm^{-1}$. This cluster can be isolated by using various cations e.g., transition metal cations, alkali metal cations, lanthanide ions and protonated organic amine cations for

charge compensation. Several heptamolybdates and decavanadate based compounds are reported by using various organic cations including transition metals, alkali metals and their supramolecular architectures are also described clearly.[4,5] Choosing of a cation plays a vital role for tuning the property of the decavanadate cluster. The relevant reports are described with several kinds of polyoxometalates other than decavanadates, such as, $[Mo_7O_{24}]^{6-}$ and $[Si_2W_{12}O_{40}]^{6-}$; their properties are tuned by changing the cations. For example, ammonium salt of heptamolybdate $[Mo_7O_{24}]^{6-}$ shows the antitumor activity and cobalt salt of silicotungstate $\{Co_3[Si_2W_{12}O_{40}]\}$ is a good catalyst in oxidation reactions.[1] Even though, there are copious reports on the crystal structures of POM supported metal complexes and hybrid materials[6] their catalytic applications remain largely unexplored.[7] Pioneering works on catalytic activities of POMs, substituted POMs and POM supported

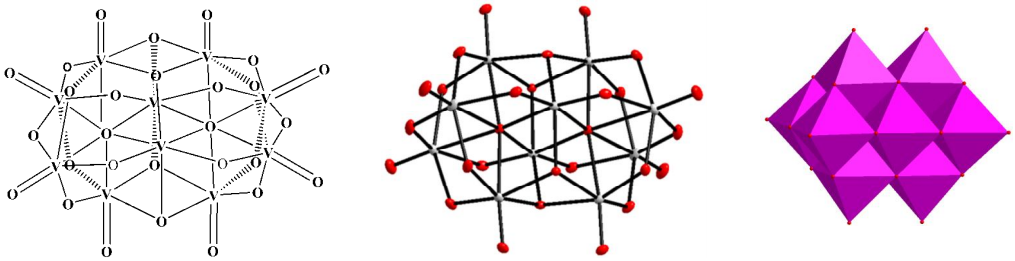

**Scheme 3.1** Decavanadate $\{V_{10}O_{28}^{6-}\}$ anionic cluster

transition metal complexes and alkali metal complexes towards organic transformations of industrial importance, has been well-established by Neumann and his group.[8] Cronin group has also made contribution in this area.[9] In this context, it is important to mention that the selective oxidation of olefines to respective ketone or epoxide is a central conversion in organic synthesis.[10] In the earlier years, the selective oxidation was carried out by several oxidizing agents, such as, hypervalent iodines.[11] Since then numerous methods have been developed for this important oxidation, that are, however, associated with several disadvantages. These include severe environmental problems due to the wastage of solvents, reagents and generation of unwanted side products. In recent years, seeking environmentally benign (green chemistry) methods for the same oxidation have been realized and numerous publications have appeared in this direction. The molecular oxygen ($O_2$) is a green, universal oxidant and several catalytic systems (for example, CuCl.phen,[12a] $H_5PV_2Mo_{10}O_{40}$,[12b-d] PdLn,[12e-g] M-TEMPO,[12h-i] bimetallic systems: Os-Cu and Mo-Cu,[12j-l] ruthenium based catalysts: Ru-biomimetic-coupled systems, Ru-

hydroxyapatite, $RuCl_2(p\text{-cymene})_2/Cs_2CO_3$, $RuO_2$ and perruthenate,[12m-q] Pt and Pt/Bi catalyst,[12r-t] Manganese oxide molecular sieves,[12u] and $V_2O_5$[12v]), that use molecular oxygen as an oxidant for the conversion of olefins to their corresponding ketones, have successfully been developed. The various aspects of the usage of molecular oxygen (as an oxidant) have been reviewed by Sheldon *et.al* in their recent article.[13] Some demerits of the usage of molecular oxygen ($O_2$) are also to be considered seriously, for example, (i) in many cases only one of the two oxygen atoms from the molecular oxygen ($O_2$) is used for the oxidation and hence stoichiometric amount of co-reductant also to be needed, (ii) it is difficult to control the reaction and sometime it leads to the combustion/blast. By taking into account all these, we found another green oxidant 'hydrogen peroxide' as oxygen source. It contains 47.1% of active oxygen (wt %) which is significantly higher than the other common oxidizing agents such as $HNO_3$ (25.0%), tBuOOH (17.8%), and $NaIO_4$ (29.9%) etc. and furthermore, it is prominently easy to handle and gives only water as the by-product. The catalysis, mediated by vanadium clusters, have drawn much attention because vanadium compounds are in general very active and thus room temperature or low temperature (0 ºC) is sufficient to get the successful reaction. We are interested to study the catalytic activities of decavanadate based compounds, that are obtained by altering several cations, e.g., organic cations or transition metal ions or alkali metal ions, toward the oxidation reaction of styrene. In the present chapter, we describe syntheses and structural characterizations of $[Co(H_2O)_6][Na_4(H_2O)_{23}]\{V_{10}O_{28}\}\cdot 4H_2O$ (**1**), $[Zn(H_2O)_6][Na_3(H_2O)_{14}]\{HV_{10}O_{28}\}\cdot 10H_2O$ (**2**), $[HMATAH]_2\{H_4V_{10}O_{28}\}\cdot 4H_2O$ (**3**), $[HMTAH]_2\{(H_2O)_4Zn_2V_{10}O_{28}\}\cdot 2H_2O$ (**4**), $[Co(3\text{-amp})(H_2O)_5]_2[3\text{-ampH}]_2\{V_{10}O_{28}\}\cdot 4H_2O$ (**5**), $[4\text{-ampH}]_5[Na(H_2O)_6]\{V_{10}O_{28}\}\cdot 4H_2O$ (**6**), $[4\text{-ampH}]_{10}[Co(H_2O)_6]\{V_{10}O_{28}\}_2\cdot 10H_2O$ (**7**), $[4\text{-ampH}]_{10}[Zn(H_2O)_6]\{V_{10}O_{28}\}_2\cdot 10H_2O$ (**8**) and $[3\text{-ampH}]_6[V_{10}O_{28}]\cdot 2H_2O$ (**9**) and their supramolecular chemistry emphasizing C–H···O, O–H···O and O···O weak interactions. Finally the catalysis of styrene oxidation, mediated by these nine compounds, is described.

## 3.2 Experimental Section

### 3.2.1 Materials

Sodium metavanadate is received from SISCO Laboratory. The distilled water was used throughout the experiments. 2-Aminopyridine, 3-aminopyridine, 4-aminopyridine and hexamine (hexamethylenetetramine) are received from CHEMLABS. $Zn(NO_3)\cdot 6H_2O$

and $Co(NO_3)\cdot 6H_2O$ are used as received from S.D Fine and FINAR respectively. Styrene and 30% $H_2O_2$ were received from Hi Chem and used without further purification.

**3.2.2 Physical Measurements.**

Micro analytical (C, H, N) data were obtained with a FLASH EA 1112 Series CHNS Analyzer. Infrared (IR) spectra were recorded on KBr pellets with a JASCO FT/IR-5300 spectrometer in the region of 400–4000 $cm^{-1}$. G.C. analysis was performed on GCMS equipped with ZB-1column (30 m x 0.25mm, pressure= 20.0 k Pa, detector= EI, 300 $^oC$) with helium gas as carrier.

**3.2.3 Experimental section.**

**Synthesis of $[Co(H_2O)_6][Na_4(H_2O)_{23}]\{V_{10}O_{28}\}\cdot 4H_2O$ (1):**

Sodium metavanadate (1 g, 4.13 mmol) was dissolved in 100 mL of water and its pH was adjusted to 10.0 by dil. HCl. In a separate beaker, the metal salt, $Co(NO_3)_2\cdot 6H_2O$ (0.5 g, 1.7 mmol) was dissolved in 20 mL of water. This reaction mixture of metal salt was added drop wise to the sodium vanadate solution with stirring. The resulting reaction mixture was stirred for 5 h (during stirring, the formation of precipitate / turbidity was dissolved by heating the reaction mixture at 70–80 ºC in three to four slots). The reaction mixture was then filtered and kept in open beaker for crystallization without any disturbance at room temperature. After one week, orange colored crystals formed, were filtered, washed with plenty of water and finally dried at room temperature. One of the single crystals, suitable for X-ray diffraction study, was selected and characterized structurally. The product obtained with Yield: 1.23 g. Anal. Calcd. (%) for $CoNa_4V_{10}O_{61}H_{66}$:.C, 0.00; H, 3.90; N, 0.00. Found: C, 0.07; H, 3.79; N, 0.00. IR (KBr pellet): ($\nu/cm^{-1}$) 3329, 3171, 1658, 1622, 1541, 1475, 1383, 1327, 1244, 1168, 991, 889, 829, 765, 617.

**Synthesis of $[Zn(H_2O)_6][Na_3(H_2O)_{16}]\{HV_{10}O_{28}\}\cdot 10H_2O$(2):**

Sodium metavanadate (1 g, 4.13 mmol) was dissolved in 100 mL of water and its pH was adjusted to 10.0 by dil. HCl. In a separate beaker, the metal salt $Zn(NO_3)_2\cdot 6H_2O$ (0.5 g, 1.68 mmol) was dissolved in 20 mL of water. This reaction mixture of metal salt was added drop wise to the sodium vanadate solution with stirring. The resulting reaction mixture was stirred for 5 h (during stirring, the formation of precipitate / turbidity was dissolved by heating the reaction mixture at 70–80 $^oC$ in three to four slots). The reaction mixture was then filtered and kept in open beaker for crystallization without any disturbance at room temperature. After one week, orange colored crystals formed, were

filtered, washed with plenty of water and finally dried at room temperature. One of the single crystals, suitable for X-ray diffraction study, was selected and characterized structurally. The product obtained with Yield: 0.35 g. Anal. Calcd. (%) for $H_{65}O_{60}ZnNa_3$: C, 0.00; H, 5.65; N, 0.00. Found: C, 0.09; H, 5.71; N 0.10. IR (KBr pellet): ($\nu/cm^{-1}$) 3337, 3229, 3057, 2085, 1614, 1560, 1485, 1398, 1327, 1332, 1280, 1072,922, 885, 829, 679, 584.

**Synthesis of $[HMATAH]_2\{H_4V_{10}O_{28}\}\cdot 8H_2O$ (3)**

Sodium metavanadate (1 g, 4.13 mmol) was dissolved in 100 mL of water and its pH was adjusted to 3.0 by dil. HCl. In a separate beaker, hexamine (0.25 g, 1.7 mmol) is dissolved in 20 mL of water. This reaction mixture of hexamine was added drop wise to the sodium vanadate solution with stirring. The resulting reaction mixture was stirred for 5hrs (during stirring, the formation of precipitate / turbidity was dissolved by heating the reaction mixture at 70–80 $^oC$ in three to four slots). The reaction mixture was then filtered and kept in open beaker for crystallization without any disturbance at room temperature. After one week, orange colored crystals formed, were filtered, washed with plenty of water and finally dried at room temperature. One of the single crystals, suitable for X-ray diffraction study, was selected and characterized structurally. The product obtained with yield, 0.65 g. Anal. Calcd. (%) for $V_{10}O_{36}C_{12}N_8H_{46}$: C, 10.385; H, 3.34; N, 8.07. Found, C, 10.885; H, 3.94; N, 8.87. IR (KBr pellet): ($\nu/cm^{-1}$): 3440, 3356, 3056, 2045, 1657, 1567, 1456, 1387, 1338, 1178, 1078, 967, 884, 856, 629, 581.

**Synthesis of $[HMTAH]_2\{(H_2O)_4Zn_2V_{10}O_{28}\}\cdot 2H_2O$ (4)**

Sodium metavanadate (1 g, 4.13 mmol) was dissolved in 100 mL of water and its pH was adjusted to 3.0 by dil. HCl. In a separate beaker, the $Zn(NO_3)_2\cdot 6H_2O$ and hexamine ( 0.25 g, 1.68 mmol) were dissolved in 20 mL of water. This reaction mixture was added drop wise to the sodium vanadate solution with stirring. The resulting reaction mixture was stirred for 5 h (during stirring, the formation of precipitate / turbidity was dissolved by heating the reaction mixture at 70–80 $^oC$ in three to four slots). The reaction mixture was then filtered and kept in open beaker for crystallization without any disturbance at room temperature. After one week, orange colored crystals formed, were filtered, washed with plenty of water and finally dried at room temperature. One of the single crystals, suitable for X-ray diffraction study, was selected and characterized structurally. The product obtained with Yield: 0.27 g. Anal. Calcd. (%) for $Zn_2V_{10}O_{34}C_{12}N_8H_{38}$: C, 9.74; H, 2.59; N, 7.57. Found: C, 10.01; H, 278; N, 7.89. IR (KBr

pellet): (ν/$cm^{-1}$) 3420, 3310, 3190, 3078, 2918, 1647, 1614, 1570, 1464, 1386, 1313, 1230, 1182, 1086, 920, 883, 605.

**Synthesis of $[Co(3\text{-}amp)(H_2O)_5]_2[3\text{-}ampH]_2\{V_{10}O_{28}\}\cdot 4H_2O$ (5)**:

Sodium metavanadate (1 g, 4.13 mmol) was dissolved in 100 mL of water and its pH was adjusted to 3.0 by dil. HCl. In a separate beaker, the $Co(NO_3)_2\cdot 6H_2O$ (0.5 g, 1.7 mmol) and 3-aminopyridine (0.25 g, 1.68 mmol) were dissolved in 20 mL of water. This reaction mixture was added drop wise to the sodium vanadate solution with stirring. The resulting reaction mixture was stirred for 5 h (during stirring, the formation of precipitate / turbidity was dissolved by heating the reaction mixture at 70–80 $^oC$ in three to four slots). The reaction mixture was then filtered and kept in open beaker for crystallization without any disturbance at room temperature. After one week, orange colored crystals formed, were filtered, washed with plenty of water and finally dried at room temperature. One of the single crystals, suitable for X-ray diffraction study, was selected and characterized structurally. The product obtained with yield: 0.27 g. Anal. Calcd. (%) for $Co_2V_{10}O_{42}C_{20}N_8H_{54}$: C, 14.081; H, 3.19; N, 6.56. Found: C, 14.21; H, 3.23; N, 6.89. IR (KBr Pellet): (ν/$cm^{-1}$): 3456, 3322, 3170, 2998, 2978, 1654, 1625, 1567, 1469, 1398, 1267, 1156, 1076, 937, 896, 608.

**Synthesis of $[4\text{-}ampH]_5[Na(H_2O)_6]\{V_{10}O_{28}\}\cdot 4H_2O$ (6):**

Sodium metavanadate (1 g, 4.13 mmol) was dissolved in 100 mL of water and its pH was adjusted to 6.0 by dil. HCl. In a separate beaker, the 4-aminopyridine (0.25 g, 1.70 mmol) were dissolved in 20 mL of water. This reaction mixture was added drop wise to the sodium vanadate solution with stirring. The resulting reaction mixture was stirred for 5 h (during stirring, the formation of precipitate / turbidity was dissolved by heating the reaction mixture at 70–80 ºC in three to four slots). The reaction mixture was then filtered and kept in open beaker for crystallization without any disturbance at room temperature. After one week, orange colored crystals formed, were filtered, washed with plenty of water and finally dried at room temperature. One of the single crystals, suitable for X-ray diffraction study, was selected and characterized structurally. The product obtained with Yield: 0.47 g. Anal. Calcd (%) for $V_{10}NaO_{38}C_{25}N_{10}H_{55}$: C, 18.35; H, 3.88; N, 8.56.Found: C, 18.15; H 3.99; N, 8.55. IR (KBr Pellet): (ν/$cm^{-1}$): 3467, 3335, 3178, 2929, 1684, 1629, 1547, 1498, 1339, 1235, 1178, 1007, 967, 849, 619.

**Synthesis of $[4\text{-ampH}]_{10}[Co(H_2O)_6]\{V_{10}O_{28}\}_2\cdot 10H_2O$ (7):**

Sodium metavanadate (1 g, 4.13 mmol) was dissolved in 100 mL of water and its pH was adjusted to 3.0 by dil. HCl. In a separate beaker, the $Co(NO_3)_2\cdot 6H_2O$ (0.5 g, 1.7 mmol) and 4-aminopyridine ( 0.25 g, 1.68 mmol) were dissolved in 20 mL of water. This reaction mixture was added drop wise to the sodium vanadate solution with stirring. The resulting reaction mixture was stirred for 5 h (during stirring, the formation of precipitate / turbidity was dissolved by heating the reaction mixture at 70–80 $^0$C in three to four slots). The reaction mixture was then filtered and kept in open beaker for crystallization without any disturbance at room temperature. After one week, orange colored crystals formed, were filtered, washed with plenty of water and finally dried at room temperature. One of the single crystals, suitable for X-ray diffraction study, was selected and characterized structurally. The product obtained with Yield: 1.87 g. Anal. Calcd. (%) for $V_{20}CoO_{72}C_{50}N_{20}H_{102}$: C,18.69; H, 3.19; N, 8.72. Found: C, 18.55; H, 3.79; N, 8.43. IR (KBr pellet) ($\nu$/cm$^{-1}$): 3427, 3345, 3196, 2822, 1690, 1645, 1556, 1489, 1338, 1268, 1189, 1039, 979, 890, 650.

**Synthesis of $[4\text{-ampH}]_{10}[Zn(H_2O)_6]\{V_{10}O_{28}\}_2\cdot 10H_2O$ (8):**

Sodium metavanadate (1 g, 4.13 mmol) was dissolved in 100 mL of water and its pH was adjusted to 3.0 by dil. HCl. In a separate beaker, the $Zn(NO_3)_2\cdot 6H_2O$ (0.5 g, 1.7 mmol and 4-aminopyridine (0.25 g, 2.6 mmol) were dissolved in 20 mL of water. This reaction mixture was added drop wise to the sodium vanadate solution with stirring. The resulting reaction mixture was stirred for 5h (during stirring, the formation of precipitate / turbidity was dissolved by heating the reaction mixture at 70–80 ºC in three to four slots). The reaction mixture was then filtered and kept in open beaker for crystallization without any disturbance at room temperature. After one week, orange colored crystals formed, were filtered, washed with plenty of water and finally dried at room temperature. One of the single crystals, suitable for X-ray diffraction study, was selected and characterized structurally. The product obtained with Yield: 1.47 g. Anal. Calcd (%) for $V_{20}ZnO_{72}C_{50}N_{20}H_{102}$: C, 18.65; H, 3.19; N, 8.7. Found: C, 18.32; H, 3.45; N, 8.63. IR (KBr pellet) ($\nu$/cm$^{-1}$): 3445, 3385, 3187, 2842, 1677, 1649, 1537, 1424, 1373, 1229, 1175, 1038, 929, 885, 643.

**Synthesis of $[3\text{-ampH}]_6[V_{10}O_{28}]\cdot 2H_2O$ (9):**

Sodium meta-vanadate (1.00 g, 0.82 mmol ) was dissolved in 50 ml of hot deionized water and its pH was adjusted to 2.00 by adding dil. HCl; to this solution were added 20 ml of aqueous solution of $Zn(NO_3)_2 \cdot 5H_2O$ (0.5 g, 1.8 mmol ) and 3-Amino pyridine (0.3 g, 2.9 mmol ). The reaction mixture was then stirred for 5 h and little turbidity, appeared, was removed by filtration. The resulting filtrate was kept for crystallization at room temperature. Block-type orange colored-crystals were found in the solution after 10 days. Yield: 0.46 g. Analysis: Calc. (%) for $C_{30}H_{46}N_{12}O_{30}V_{10}$: C, 23.04; H, 2.96; N, 10.74%. Found: C, 23.10; H, 2.89; N, 10.95%. IR (KBr pellet): 3335, 3229, 3057, 2085, 1624, 1560, 1485, 1398, 1332, 1280, 1072, 968, 885, 829, 679, 584 $cm^{-1}$.

**3.2.4. X-ray Data Collection and Structure Determination**

Data were measured on a Bruker SMART APEX CCD area detector system [λ(Mo Kα) = 0.71073 Å], graphite monochromator, 2400 frames were recorded with an ω scan width of 0.3°, each for 8 second, a crystal detector distance of 60 mm, and a collimator of 0.5mm. The data were reduced using SAINTPLUS,[14a] the structures were solved using SHELXS-97,[14b] and refined using SHELXL-97.[14c] All non hydrogen atoms were refined anisotropically. We tried to locate the hydrogen atom of solvent water molecules for compound **2** & **3** through differential Fourier maps, but couldn't succeed. A summary of the crystallographic data and structure determination parameters for **1–3** are provided in Table 3.1, for **4**–**6**, they are given in Table 3.6, and for compounds **7-9**, they are provided in Table 3.10. Bond lengths and angles for decavanadate anionic cluster for **1** (as it is common cluster for all compounds) are provided in the Table 3.12; they are in good agreement with reported bond distances and angles for decavanadate cluster,[15] $[V_{10}O_{28}]^{6-}$.

**3.3 Results and discussion**

**3.3.1 Synthesis**

The synthetic method for all the title compounds is simple one pot wet fashion reaction at room temperature and their isolations are dependent on pH of the concerned solution. Formation of the cluster is feasible at pH 2–9 in the solution, where pH of the solution is maintained by adding dil. HCl. Here, we have isolated nine ion pair compounds by altering the various cations and simultaneously pH condition. The formation of decavanadate cluster anion can be explained by protonation of vanadate anion followed by the series of condensation reactions. As expected, the IR spectroscopy of all the compounds revealed the presence of decavanadate anionic cluster in title compounds.

$$10VO_3^- + 4H^+ \longrightarrow [V_{10}O_{28}]^{6-} + 2H_2O$$

The generated decavanadate anionic cluster $[V_{10}O_{28}]^{6-}$ has been obtained with various cations (transition metal complexes, alkali metal complexes and protonated amino pyridine derivatives) leading to the isolation of title compounds (**1-9**), which show the diverse supramolecular properties as well as the good catalytic behavior as described in the present chapter. Even though few results are reported by Ramanan group and other groups, concerning to decavanadate cluster, but our compounds are novel materials from earlier literature.[16]

### 3.3.2 Crystallographic studies

**Crystal structure of $[Co(H_2O)_6][Na_4(H_2O)_{23}]\{V_{10}O_{28}\}\cdot 4H_2O$ (1):**

Asymmetric unit of the $[Co(H_2O)_6][Na_4(H_2O)_{14}]\{V_{10}O_{28}\}\cdot 4H_2O$ (**1**) reveals the presence of half of the decavanadate cluster, which supports the sodium aqua complex. A cobalt tri-aqua complex exists to act as the cation; the relevant ORTEP diagram is shown in the Fig. 3.1 (left). In the full molecule of the $[Co(H_2O)_6][Na_4(H_2O)_{23}]\{V_{10}O_{28}\}\cdot 4H_2O$ (**1**), the alkali metal cluster is $[Na_4(H_2O)_{23}]^{4+}$ in which one of the sodium atoms is coordinated to oxide of the decavanadate cluster so that the total moiety consists of –2 charge, which is compensated by the presence of $[Co(H_2O)_6]^{2+}$ as shown in Fig. 3.1 (right). Each sodium ion in $[Na_4(H_2O)_{23}]^{4+}$ is octahedrally coordinated. The formation of this alkali metal cluster can be described by six sodium ions, out of which four exist with half occupancies and two have full occupancies [two Na1 (50% occupancy), two Na2 ( 50% occupancy) and two Na3 (100 % occupancy)]. Five of these (two Na2 + two Na3 +1Na) are interconnected by bridged water ligands resulting in the formation of $Na_{3.5}(H_2O)_{19}$ cluster, which coordinates to the $[V_{10}O_{28}]^{6-}$ cluster through Na1 *via* coordinate covalent bond. The other Na1 [in the form of $Na(H_2O)_4$] ion is linked to the same cluster and other adjacent cluster through coordinated covalent bonds. The situation is shown in Fig. 3.2 (right). This type of sodium-water cluster is not very common in POV chemistry. We believe that, the pH 10 of the concerned synthesis mixture is important in forming this $[Na_4(H_2O)_{23}]^{4+}$ cluster. In the crystal of **1**, an interesting two- dimensional coordination polymer is observed, the formation of which can be described by the sodium water chains that are constructed alternatively by $[Na_{2.5}(H_2O)_{12}]^{2.5+}$ and $[Na_{0.5}(H_2O)_4]^{0.5+}$. These chains are then connected by $[V_{10}O_{28}]^{6-}$ clusters through coordinate covalent bonds between $[V_{10}O_{28}]^{6-}$ and $[Na_{0.5}(H_2O)_4]^{0.5+}$ resulting in the formation of a two-dimensional net (see Scheme and Fig 3.2). The hydrogen bonding situation around each moiety of

$[Co(H_2O)_6][Na_4(H_2O)_{23}]\{V_{10}O_{28}\}\cdot 4H_2O$ (**1**) can be described by O–H···O interactions as shown in Fig. 3.3(d-f). The relevant crystallographic data is available in Table 3.1 and hydrogen bonding distances and angles are shown in Table 3.2 including symmetry operations.

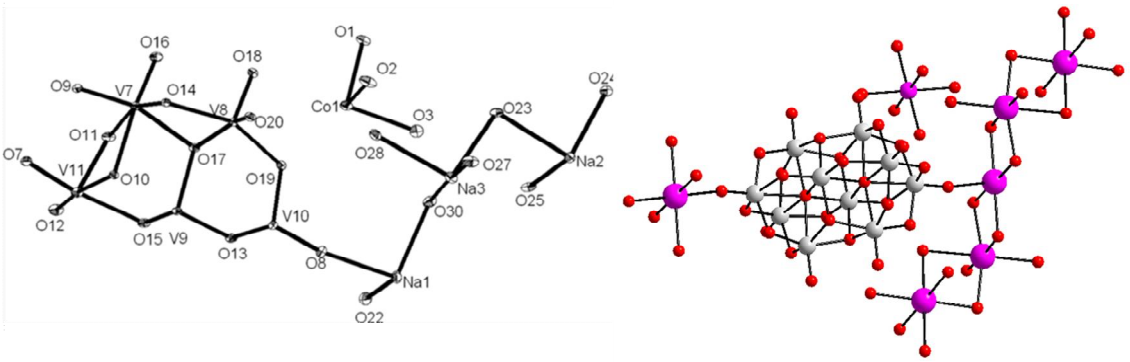


**Fig. 3.1 (Left)** ORTEP diagram of the asymmetric unit of $[Co(H_2O)_6][Na_4(H_2O)_{23}]\{V_{10}O_{28}\}\cdot 4H_2O$ (**1**) with 30% probability (hydrogen atoms are omitted for clarity). (**Right**) Ball and stick representation of the $[Co(H_2O)_6][Na_4(H_2O)_{23}]\{V_{10}O_{28}\}\cdot 4H_2O$ (**1**), color codes: Co, cyan; Na, blue; O, red; V, light grey.

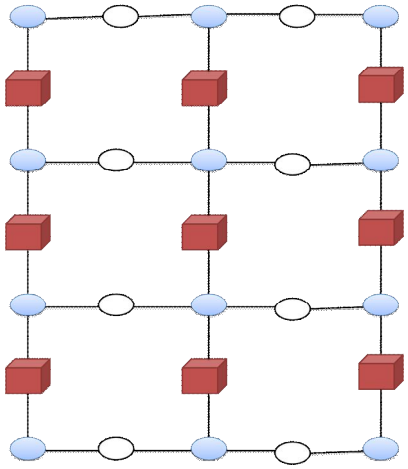

**Scheme 3.2** 2-Dimensional network established in the coordination polymer of $[Co(H_2O)_6][Na_4(H_2O)_{23}]\{V_{10}O_{28}\}\cdot 4H_2O$ (**1**). Color code: red box shows decavanadate, white circle shows $[Na_{2.5}(H_2O)_{12}]$, sky-blue circle corresponds to sodium.

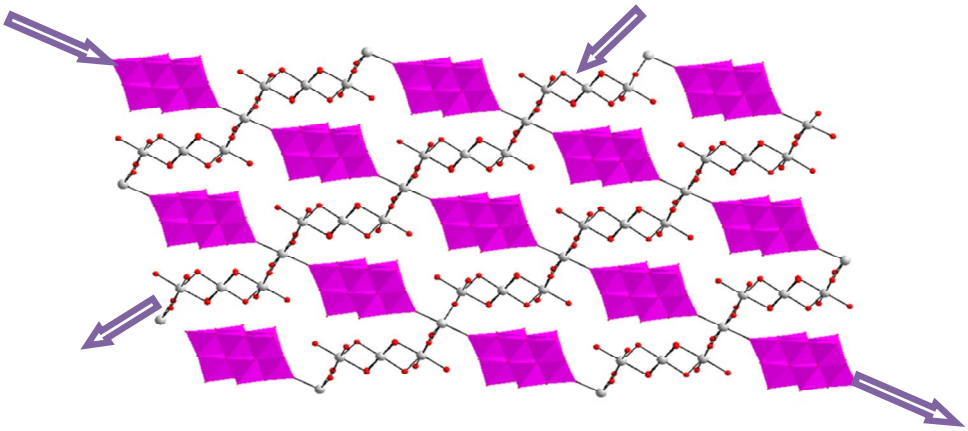

**Fig. 3.2** Picture of 2-dimensional coordination polymer of $[Co(H_2O)_6][Na_4(H_2O)_{23}]\{V_{10}O_{28}\}\cdot 4H_2O$ (**1**), (1-direction) decavanadate chain and (2-direction) sodium aqua chain. color codes: Na, grey; O, red; magenta polyhedra, decavanadate.

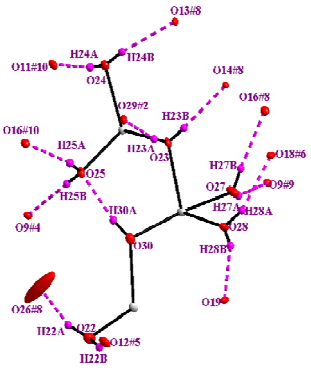


**Fig.3.3a**

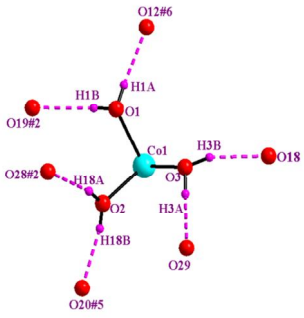


**Fig.3.3b**

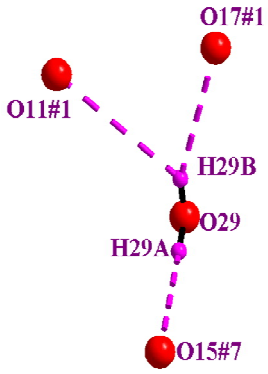


**Fig.3.3c**

**Fig.3.3** Hydrogen bonding situation around {Na}, {Co} and water motifs of $[Co(H_2O)_6][Na_4(H_2O)_{14}]\{V_{10}O_{28}\}\cdot 4H_2O$ (**1**), Color codes: Na, grey, Co, green; O, red, H, purple. symmetry codes: Symmetry codes: #1, -x+2, -y+1, -z+1; #2, -x+1, -y+1, -z; #3, -x+1, -y, -z-1, #4 -x+1, -y, -z; #5 x-1, y, z; #6 -x+2, -y+1, -z; #7 -x+1, -y+1, -z+1, #8 x, y, z-1; #9, -x+2, -y, -z; #10 x-1, y, z-1. Color codes: Co, cyan; Na, blue; O, red; V, light grey.

**Table 3.1** Crystal data and structure refinement for compounds **1, 2** and **3**.

| Entry | **1** | **2** | **3** |
|---|---|---|---|
| Molecular formula | $CoH_{44}Na_4O_{52}V_{10}$ | $ZnNa_3O_{47}V_{10}$ | $C_{12}H_{24}N_8O_{36}V_{10}$ |
| Formula weight | 1536.64 | 1536.64 | 1365.79 |
| Temperature (K) | 298(2) | 298(2) | 298(2) |
| Wavelength (Å) | 0.71073 | 0.71073 | 0.71073 |
| Crystal system | Triclinic | Triclinic | Monoclinic |
| Space group | *P*-1 | *P*-1 | *P*2(1)/n |
| a (Å) | 8.9888(5) | 18.292(4) | 15.0483(16) |
| b (Å) | 11.2680 (17) | 7.5417 (15) | 16.8434(18) |
| c (Å) | 11.6587(15) | 12.483(3) | 9.0203(10) |
| α (deg) | 105.292(15) | 90.000 | 90.000 |
| β (deg) | 96.305(2) | 101.17(3) | 115.99 (10) |
| γ (deg) | 100.77(3) | 90.000 | 90.000 |
| Volume ($Å^3$) | 1098.4(3) | 1689.5(6) | 2055.0(4) |
| Z | 1 | 1 | 2 |
| ρ ($g\ cm^{-3}$) | 2.323 | 1.856 | 2.207 |
| μ ($mm^{-1}$) | 2.567 | 7.384 | 2.285 |
| F (000) | 761 | 936 | 1500 |
| Crystal size ($mm^3$) | 0.24x0.18x0.14 | 0.24x0.18x0.14 | 0.26x0.16x0.10 |
| Θ range for data collection (º) | 1.84 to 25.95 | 1.13 to 24.99 | 2.02 to 25.00 |
| Reflections collected/unique | 11963/4243 | 15283/5923 | 10824 / 2178 |
| R(int) | 0.0205 | 0.0288 | 0.0193 |
| Data/restraints/parameters | 4243/0/395 | 5923/2 /469 | 3030 /0/ 235 |
| Goodness of fit on $F^2$ | 1.234 | 1.032 | 1.060 |
| Final R indices [ I > 2 sigma(I)] | 0.0430,0.0969 | 0.0351 ,0.0912 | 0.0290 / 0.0724 |
| R indices (all data) | 0.0450/0.0977 | 0.0479, 0.1598 | 0.0350 / 0.0753 |
| Largest diff. Peak and hole ($e.Å^{-3}$) | 1.418/-1.524 | 0.780 / -0.325 | 0.447 /-0.210 |

**Table 3.2** Hydrogen bonds for compound **1** [Å and °].

| D–H···A | d(D–H) | d(H···A) | d(D···A) | <(DHA) |
|---|---|---|---|---|
| O(3)-H(3B)...O(18) | 0.87(8) | 2.00(8) | 2.839(5) | 162(7) |
| O(3)-H(3A)...O(29) | 0.86(7) | 1.87(7) | 2.720(5) | 172(6) |
| O(2)-H(18B)...O(20)#5 | 0.77(7) | 1.93(7) | 2.688(5) | 168(6) |
| O(2)-H(18A)...O(28)#2 | 0.82(6) | 1.97(6) | 2.778(5) | 169(5) |
| O(1)-H(1B)...O(19)#2 | 0.72(7) | 1.98(7) | 2.707(5) | 178(7) |
| O(1)-H(1A)...O(12)#6 | 0.82(7) | 1.95(7) | 2.766(5) | 172(6) |
| O(29)-H(29A)...O(15)#7 | 0.73(7) | 2.07(7) | 2.801(5) | 178(7) |
| O(29)-H(29B)...O(17)#1 | 0.64(7) | 2.27(7) | 2.872(5) | 159(8) |
| O(29)-H(29B)...O(11)#1 | 0.64(7) | 2.64(7) | 3.123(5) | 135(8) |
| O(30)-H(30A)...O(25) | 0.86(6) | 2.03(6) | 2.881(5) | 169(5) |
| O(23)-H(23A)...O(29)#2 | 0.78(5) | 2.11(5) | 2.874(5) | 169(5) |
| O(23)-H(23B)...O(14)#8 | 0.74(6) | 2.06(6) | 2.801(4) | 176(6) |
| O(27)-H(27B)...O(16)#8 | 0.79(7) | 2.07(7) | 2.858(5) | 174(7) |
| O(27)-H(27A)...O(9)#9 | 0.65(8) | 2.55(8) | 3.162(5) | 159(9) |
| O(28)-H(28B)...O(19) | 0.70(6) | 2.23(6) | 2.861(5) | 152(6) |
| O(28)-H(28A)...O(18)#6 | 0.82(7) | 2.03(7) | 2.817(5) | 159(6) |
| O(22)-H(22A)...O(26)#8 | 0.85(6) | 1.95(6) | 2.591(7) | 131(5) |
| O(22)-H(22B)...O(12)#5 | 0.90(8) | 2.07(8) | 2.877(5) | 150(7) |
| O(25)-H(25B)...O(9)#4 | 0.73(7) | 2.00(7) | 2.732(5) | 180(8) |
| O(25)-H(25A)...O(16)#10 | 0.77(6) | 2.16(6) | 2.907(5) | 165(5) |
| O(24)-H(24A)...O(11)#10 | 0.67(6) | 2.23(7) | 2.874(5) | 162(7) |
| O(24)-H(24B)...O(13)#8 | 0.81(6) | 2.22(6) | 3.017(5) | 171(5) |

Symmetry transformations used to generate equivalent atoms:

#1, -x+2,-y+1,-z+1; #2, -x+1,-y+1,-z ; #3, -x+1,-y,-z-1; #4, -x+1,-y,-z; #5, x-1,y,z;

#6, -x+2,-y+1,-z; #7, -x+1,-y+1,-z+1; #8, x,y,z-1; #9, -x+2,-y,-z; #10, x-1,y,z-1;

**Crystal structure of $[Zn(H_2O)_6][Na_3(H_2O)_{14}]\{HV_{10}O_{28}\}\cdot 10H_2O$ (2):**

Asymmetric unit of crystal structure of compound **2** consists of two one-half decavanadate clusters, one tri-sodium aqua-complex $[Na_3(H_2O)_{14}]^{3+}$ and one zinc hexa-aqua complex $[Zn(H_2O)_6]^{2+}$ as shown in Fig. 3.4. Thus the full molecule can be formulated

as $[Zn(H_2O)_6][Na_3(H_2O)_{14}]\{HV_{10}O_{28}\}\cdot 10H_2O$ (**2**), in which decavanadate cluster is singly protonated, and the rest of the charge (–5) is counter balanced by $[Zn(H_2O)_6]^{2+}$ and $[Na_3(H_2O)_{14}]^{3+}$ cations. In the crystal structure, ten lattice water molecules were found and fourteen water molecules are found to be linked with three sodium cations; the coordination of each sodium can be described by octahedral arrangement in which two water molecules bridge between any two sodium cations. Hydrogen atoms could not be located for all the water molecules in the concerned crystal. By taking O···O separation in the range of 2.779 Å to 3.211 Å, supramolecular structure of the compound **2** is described. A supramolecular $(H_2O)_9$ cluster is found to be formed by zinc- and sodium-coordinated water molecules and lattice water molecules. These $(H_2O)_9$ clusters are further linked by $(H_2O)_3$ cluster resulting in the formation of a chain-like arrangement. This situation is described in Fig. 3.5. The supramolecular O···O interactions between decavanadate cluster and water chain (O35···O35) lead to the generation of a 2-dimensional network as shown in Fig. 3.6. And it is described as inclusion of POV cluster in the water chain. Thus we can describe that decavanadate cluster is stabilized in the pool of water.

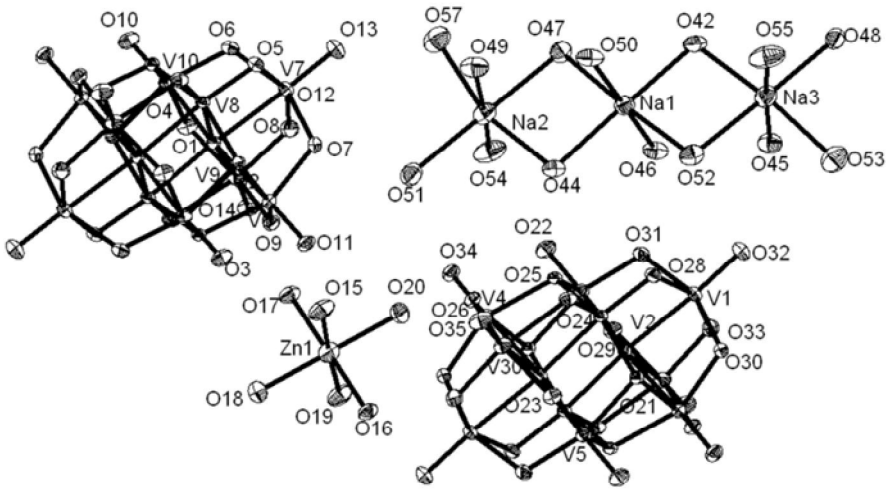


**Fig.3.4** Thermal ellipsoidal diagram of the $[Zn(H_2O)_6][Na_3(H_2O)_{14}]\{HV_{10}O_{28}\}\cdot 10H_2O$ (**2**) with 30% probability (hydrogen atoms and solvent water molecules are omitted for clarity)

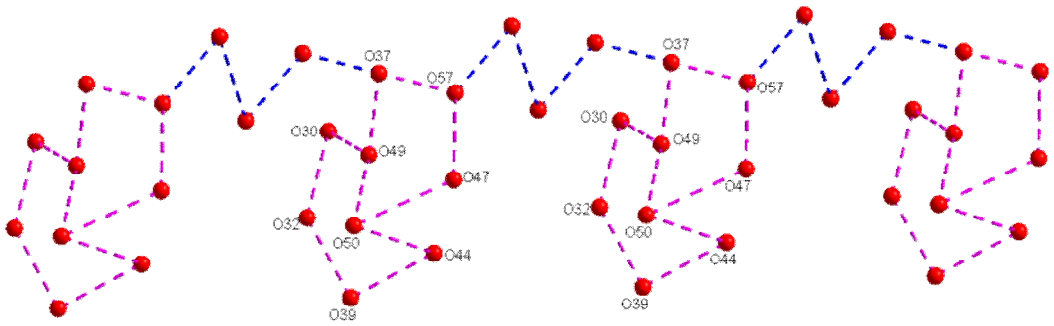


**Fig. 3.5** 1-Dimensional chain is built from water cluster due to O···O interaction among the lattice water molecules of $[Zn(H_2O)_6][Na_3(H_2O)_{14}]\{V_{10}O_{28}\}\cdot 8H_2O$ (**2**). Color codes: O, red.

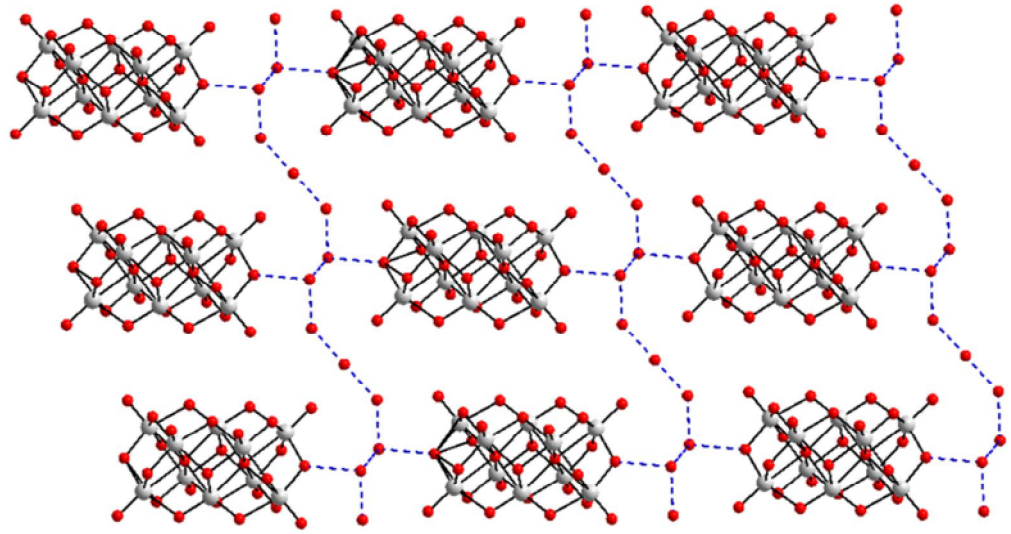

**Fig.3.6** Inclusion of POV anion $[V_{10}O_{28}]^{6-}$ among the water chain led to 2-dimensional chain in $[Zn(H_2O)_6][Na_3(H_2O)_{14}]\{V_{10}O_{28}\}\cdot 8H_2O$ (**2**). Color codes: O, red; V, grey.

**Crystal structure of $[HMATAH]_2\{H_4V_{10}O_{28}\}\cdot 8H_2O$ (3)**

$[HMATAH]_2\{H_4V_{10}O_{28}\}\cdot 8H_2O$ (**3**) is built up of a tetra protonated decavanadate cluster $\{H_4V_{10}O_{28}\}^{2-}$, two molecules of $HMATAH^{1+}$ and eight lattice water molecules as shown in Fig. 3.7. One of the lattice water molecules (O12) is non-covalantely interacted with another three symmetry related O12 water molecules to generate a square-like cyclic water tetramer, from which each corner oxygen atom is hydrogen bonded to O11 lattice water molecules (all four O11 are symmetry related) resulting in the formation of $(H_2O)_8$ cluster as shown in Fig. 3. Each of the corner water molecules (O12) is again non-covalently interacted with O4 and O10 atoms of decavanadate cluster with O···O

separations of 3.144 Å and 3.197 Å respectively leads to a 2-dimensional network as shown in Fig. 3.9. This is also described as availability of decavanadate anionic cluster in water lake. The cationic part of the molecule ($HMATAH^{1+}$) shows C–H···O interactions and the hydrogen bonding environment around the $HMATAH^{1+}$ is shown in the Fig. 3.10 including symmetry operations. The relevant hydrogen bonding distances and angles are given in Table 3.3.

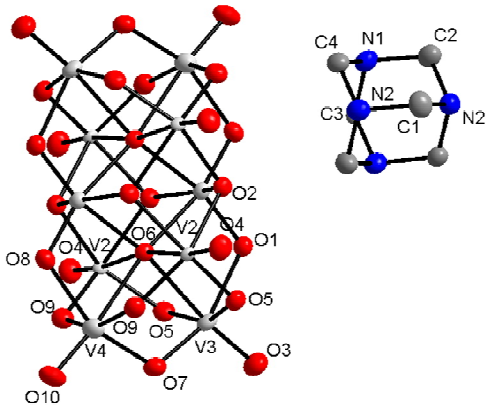


**Fig.3.7** Thermal ellipsoidal diagram of the $[HMATAH]_2\{H_4V_{10}O_{28}\}\cdot 8H_2O$ (**3**) with 30% probability (hydrogen atoms and solvent water molecules are omitted for clarity).color code: V, grey, C, medium grey, N, blue.

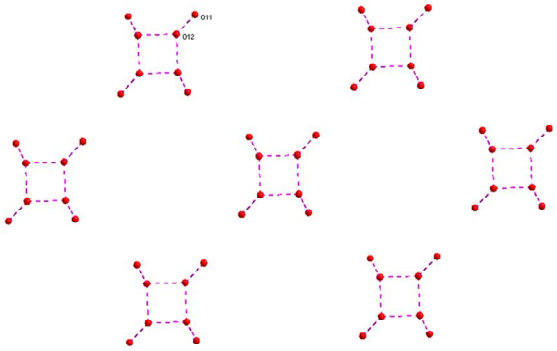

**Fig.3.8**

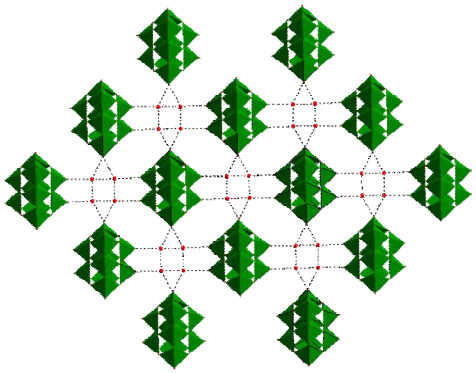

**Fig.3.9**

**Fig.3.8** Arrangement of octamer of water cluster in $[HMATAH]_2\{H_4V_{10}O_{28}\}\cdot 8H_2O$ **(3).** Color code: O, red; **Fig.3.9.** 2-Dimensional network due to O···O interaction between water tetramer and POV in $[HMATAH]_2\{H_4V_{10}O_{28}\}\cdot 8H_2O$ **(3).** Color code: O, red;

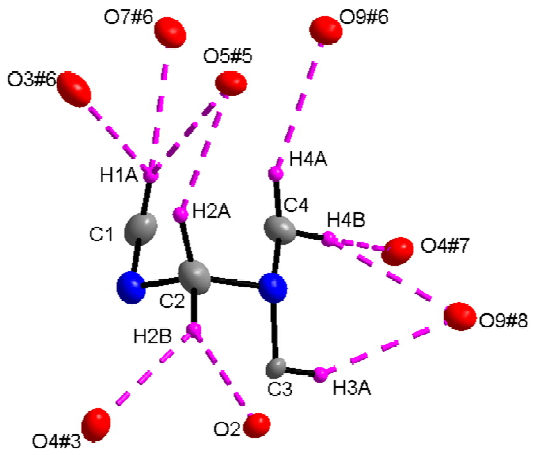


**Fig.3.10** Hydrogen bonding environment around the organic cation $[HMATAH]^{1+}$ for $[HMATAH]_2\{H_4V_{10}O_{28}\}\cdot 8H_2O$ **(3).** Symmetry codes: #1) x, -y, z; #2) -x, -y, -z+1; #3) -x, y, -z+1; #4) -x, y, -z, #5) -x+1/2, -y+1/2, -z+1; #6) -x+1/2, y+1/2, -z+1; #7) x, y, z-1, #8) x, -y, z-1. Color codes: O, red; C, grey; H, Purple.

**Table 3.3** Hydrogen bonds and angles for compound **3** [Å and º.].

| D–H···A | d(D–H) | d(H···A) | d(D···A) | <(DHA) |
|---|---|---|---|---|
| C(2)-H(2A)...O(5)#5 | 1.13(10) | 2.45(10) | 3.453(10) | 147(7) |
| C(1)-H(1A)...O(5)#5 | 1.11(10) | 3.07(10) | 4.093(5) | 153(7) |
| C(1)-H(1A)...O(3)#6 | 1.11(10) | 2.70(10) | 3.603(10) | 138(6) |
| C(1)-H(1A)...O(7)#6 | 1.11(10) | 2.45(10) | 3.431(9) | 146(7) |
| C(4)-H(4A)...O(9)#6 | 0.99(13) | 2.61(13) | 3.540(9) | 155(10) |
| C(4)-H(4B)...O(4)#7 | 0.96(10) | 2.56(10) | 3.408(10) | 147(7) |
| C(4)-H(4B)...O(9)#8 | 0.96(10) | 2.61(10) | 3.453(11) | 146(7) |
| C(3)-H(3A)...O(9)#8 | 0.86(7) | 2.66(8) | 3.426(7) | 148(7) |
| C(2)-H(2B)...O(4)#3 | 1.14(9) | 2.52(9) | 3.450(10) | 138(6) |
| C(2)-H(2B)...O(2) | 1.14(9) | 2.45(9) | 3.502(10) | 153(6) |

Symmetry transformations used to generate equivalent atoms:
#1, x,-y,z; #2, -x,-y,-z+1; #3, -x,y,-z+1; #4, -x,y,-z; #5, -x+1/2,-y+1/2,-z+1; #6, -x+1/2,y+1/2, -z+1; #7 x,y,z-1; #8 x,-y,z-1.

**Crystal structure of $[HMATAH]_2\{(H_2O)_4Zn_2V_{10}O_{28}\}\cdot 2H_2O$ (4)**

A two-dimensional coordination polymer has been synthesized starting from sodium metavanadate, zinc nitrate and hexamine at pH–2.0 in a simple wet synthesis. It has been formulated as $[HMATAH]_2\{(H_2O)_4Zn_2V_{10}O_{28}\}\cdot 2H_2O$ (**4**) from the crystal structure of compound **4** as shown in Fig. 3.11. $[HMATAH]_2\{(H_2O)_4Zn_2V_{10}O_{28}\}\cdot 2H_2O$ (**4**) crystallizes in monoclinic system with space group of *P*2(1)/c. In the crystal structure, decavanadate moiety is functionalized by a Zinc aqua complex, in which Zn1 is coordinated to two terminal oxo groups (O7 and O8) of both sides of decavanadate anion and such repetitive coordination among zinc and decavanadate species results in the formation of 2-dimensional coordination polymer as presented in Fig. 3.12**.** Hydrogen bonding environment around $HMATAH^+$ moiety due to C–H···O interactions is shown in the Fig. 3.13. Hydrogen bond distances and angles are presented in Table 3.4.

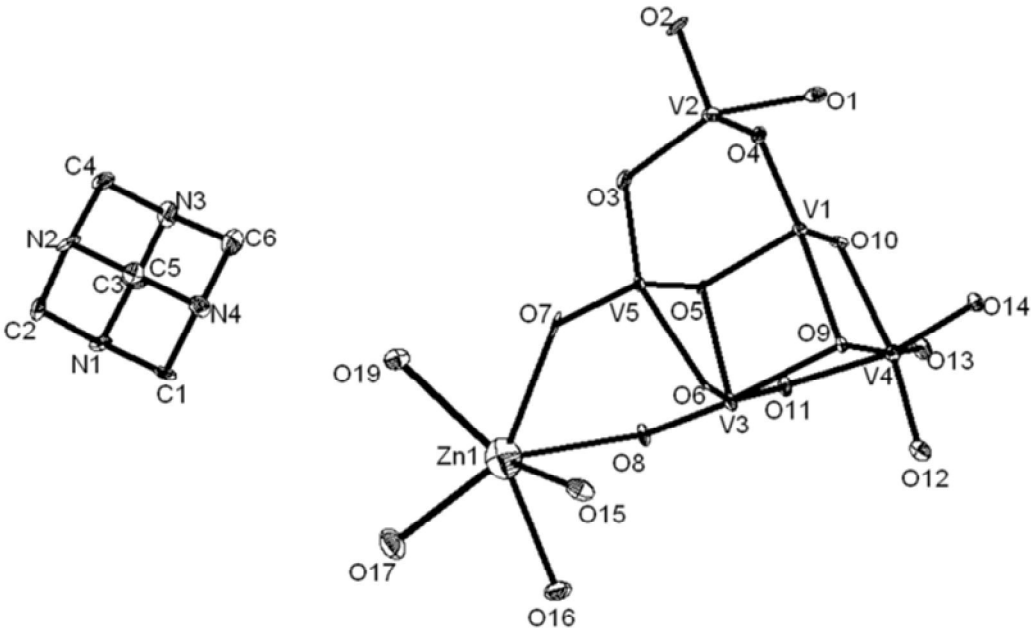


**Fig. 3.11** Thermal ellipsoidal diagram of $[HMATAH]_2\{(H_2O)_4Zn_2V_{10}O_{28}\}\cdot 2H_2O$ (**4**) with 30% probability (hydrogen atoms and solvent water molecules are omitted for clarity).

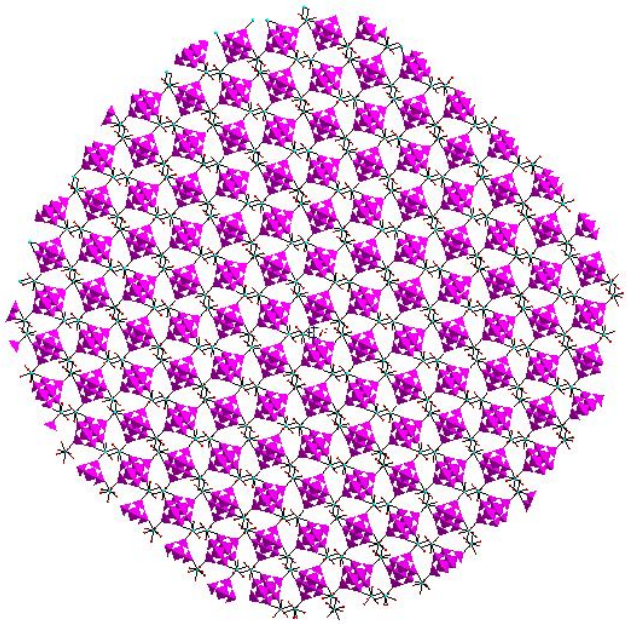

**Fig.3.12** The picture of two-dimensional coordination polymer of $[HMATAH]_2\{(H_2O)_4Zn_2V_{10}O_{28}\}\cdot 2H_2O$ (**4**). Color codes: V–O polyhedra, purple; Zn, Cyan; O, red.

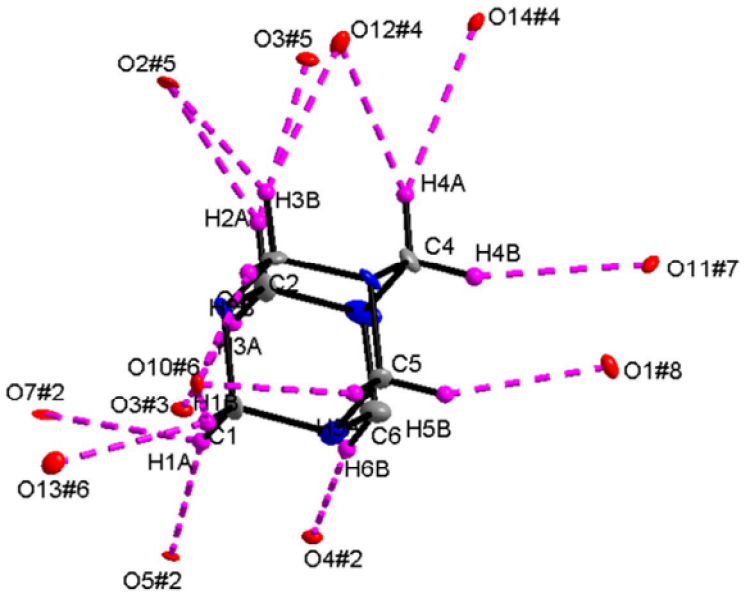


**Fig. 3.13** Hydrogen bonding environment around the organic cation $[HMATAH]^{1+}$ for $[(HMATAH]_2\{(H_2O)_4Zn_2V_{10}O_{28}\}\cdot 2H_2O$ (**4**). Symmetry codes: #1, -x+1,-y+1,-z; #2, x,-y+3/2,z+1/2; #3, x,-y+3/2,z-1/2; #4, x+1,-y+3/2,z+3/2; #5, -x+2,y+1/2,-z+3/2; #6, x, y, z+1, #7 x+1, y, z+1; #8, -x+2,-y+1,-z+1. Color codes: O, red; C, grey; H, Purple.

**Table 3.4** Hydrogen bonds and angles for compound **4** [Å and º].

| D-H···A | d(D-H) | d(H···A) | d(D···A) | <(DHA) |
|---|---|---|---|---|
| C(4)-H(4A)...O(14)#4 | 0.97 | 2.81 | 3.705(16) | 153.8 |
| C(4)-H(4A)...O(12)#4 | 0.97 | 2.60 | 3.418(16) | 141.6 |
| C(3)-H(3B)...O(3)#5 | 0.97 | 2.53 | 3.450(16) | 157.8 |
| C(2)-H(2A)...O(12)#4 | 0.97 | 2.46 | 3.319(16) | 147.1 |
| C(2)-H(2B)...O(10)#6 | 0.97 | 2.40 | 3.286(17) | 151.7 |
| C(5)-H(5A)...O(10)#6 | 0.97 | 2.68 | 3.495(18) | 141.5 |
| C(1)-H(1B)...O(10)#6 | 0.97 | 2.51 | 3.358(16) | 146.3 |
| C(1)-H(1B)...O(13)#6 | 0.97 | 2.51 | 3.297(17) | 138.6 |
| C(1)-H(1A)...O(5)#2 | 0.97 | 2.45 | 3.381(16) | 160.0 |
| C(1)-H(1A)...O(7)#2 | 0.97 | 2.77 | 3.528(17) | 136.0 |
| C(3)-H(3A)...O(3)#2 | 0.97 | 2.31 | 3.273(16) | 170.1 |
| C(6)-H(6B)...O(4)#2 | 0.97 | 2.56 | 3.501(17) | 164.6 |
| C(2)-H(2A)...O(2)#5 | 0.97 | 2.45 | 3.263(16) | 140.7 |
| C(3)-H(3B)...O(2)#5 | 0.97 | 2.72 | 3.453(17) | 132.8 |
| C(4)-H(4B)...O(11)#7 | 0.97 | 2.62 | 3.542(17) | 159.5 |
| C(5)-H(5B)...O(1)#8 | 0.97 | 2.45 | 3.359(17) | 156.7 |

Symmetry transformations used to generate equivalent atoms:
#1, -x+1,-y+1,-z; #2, x,-y+3/2,z+1/2; #3, x,-y+3/2,z-1/2; #4, x+1,-y+3/2,z+3/2;

#5, -x+2,y+1/2,-z+3/2; #6, x,y,z+1; #7, x+1,y,z+1; #8, -x+2,-y+1,-z+1;

**Description of crystal structure of $[Co(3\text{-amp})(H_2O)_5]_2[3\text{-ampH}]_2\{V_{10}O_{28}\}\cdot 4H_2O$ (5)**

A discrete inorganic-organic hybrid material $[Co(3\text{-amp})(H_2O)_5]_2[3\text{-ampH}]_2\{V_{10}O_{28}\}\cdot 4H_2O$ (**5**) containing a cobalt complex, a decavanadate cluster anion, aminopyridinium cation and lattice water molecules, has been isolated with 3-aminopyridine in an aqueous media at pH 10 in an pot synthesis. Crystal system is confined with triclinic *P*-1 space group. The asymmetric unit of compound **5**, as shown in Fig.3.14**,** reveals the presence of half of the decavanadate anionic cluster, one molecule of protonated 3-aminopyridine $[3\text{-ampH}]^+$ and cobalt complex $\{Co(3\text{-amp})(H_2O)_5^{2+}\}$. In the crystal structure, a three-dimensional network has been built due to C–H···O interactions between the cationic part and decavanadate anionic cluster as shown in Fig. 3.15. Apart from columbic interaction between cation and anionic species, non-covalent interactions are also responsible for stability of the compound **5**. Hydrogen bonding situation around the each species, labeled as {N1N2}, {N3N4} and water, is shown in Fig. 3.16 and their hydrogen bonding distances and angles are shown in Table 3.5 including symmetry operations. We found weak π–π interactions among the molecules of 3-aminopyridine (see Fig. 3.17) which results in the formation of 2-dimensional network for compound **5.**

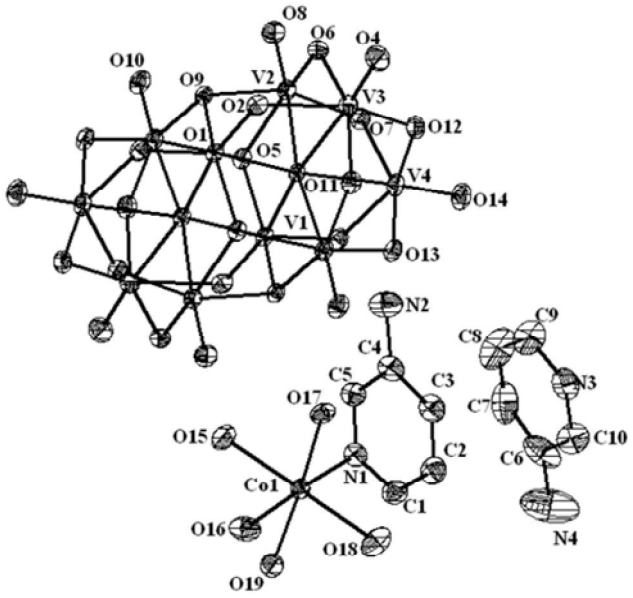


**Fig**.**3.14** Thermal Ellipsoidal diagram of $[Co(3\text{-amp})(H_2O)_5]_2[3\text{-ampH}]_2\{V_{10}O_{28}\}\cdot 6H_2O$ (**5**) with 30% probability (Hydrogen atoms are omitted for clarity).

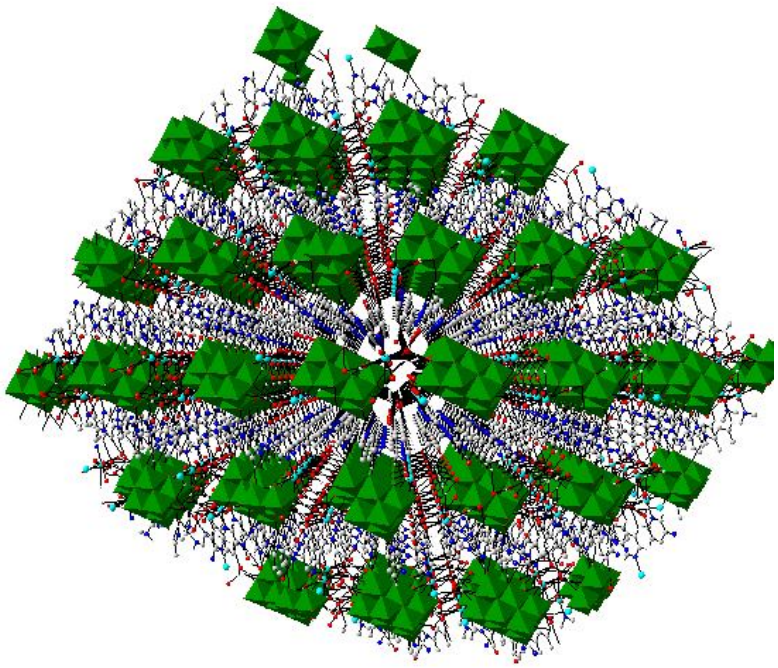

**Fig**.**3.15** 3-Dimensional framework has been generated due to C–H···O interactions between cation and decavanadate anion in the crystal of compound **5**, perspective view. Color codes: Co, Cyan; O, red; Na, blue; C, medium grey; N, blue; V, light grey; H, Purple.

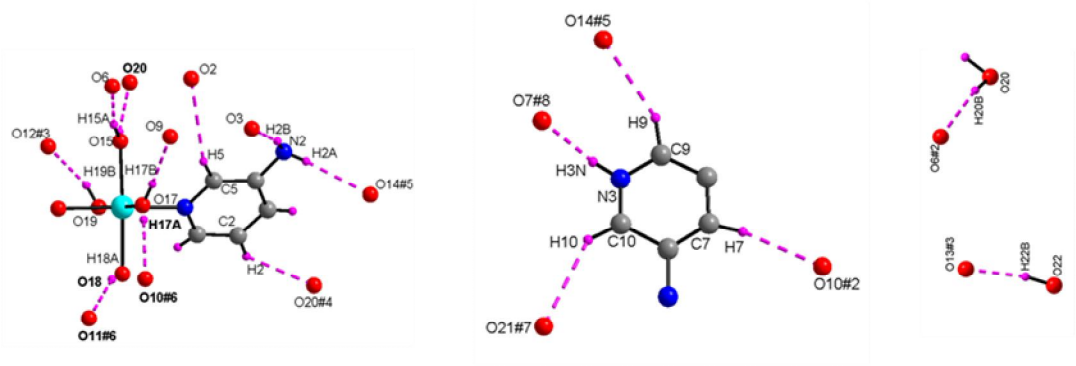


**Fig. 3.16** Hydrogen bonding environment around {N1N2}, {N3N4}, water moieties for compound **5**. Symmetry codes. #1, -x+1,-y+2,-z+2; #2, -x+1,-y+1,-z+2; #3, x,y-1,z; #4, -x+1,-y+1,-z+1; #5, -x+1,-y+2,-z+1; #6, -x+2,-y+2,-z+2; #7, -x+2,-y+1,-z+1; #8, x,y,z-1. Color codes: O, red; C, grey; H, Purple.

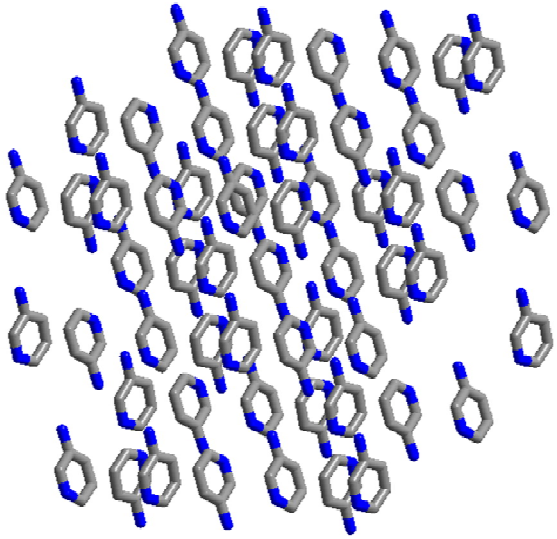

**Fig**. **3.17** Arrangement of 3-aminopyridine molecules due to π–π interactions of [Co(3-amp)$(H_2O)_5]_2$[3-ampH]$_2${$V_{10}O_{28}$}·$6H_2O$ (**5**) (Hydrogen atoms are omitted for clarity) Color codes: blue; C, medium grey; N, blue.

**Table 3.5** Hydrogen bonds and angles for compound **5** [Å and °]

| D–H···A | d(D–H) | d(H···A) | d(D···A) | <(DHA) |
|---|---|---|---|---|
| O(20)-H(20B)...O(6)#2 | 0.86(9) | 2.01(9) | 2.846(6) | 164(8) |
| O(22)-H(22B)...O(13)#3 | 0.92(8) | 1.85(8) | 2.767(5) | 171(7) |
| O(19)-H(19B)...O(12)#3 | 0.80(8) | 1.93(8) | 2.705(5) | 162(8) |
| C(2)-H(2)...O(20)#4 | 0.93(8) | 2.53(8) | 3.272(8) | 138(6) |
| N(2)-H(2A)...O(14)#5 | 0.82(8) | 2.27(8) | 3.056(8) | 162(7) |
| O(17)-H(17B)...O(9) | 0.82(7) | 1.95(7) | 2.750(5) | 166(6) |
| N(2)-H(2B)...O(3) | 0.66(8) | 2.37(8) | 2.991(7) | 157(8) |
| O(17)-H(17B)...O(9) | 0.82(7) | 1.95(7) | 2.750(5) | 166(6) |
| O(15)-H(15B)...O(20) | 0.59(6) | 2.24(6) | 2.804(8) | 163(8) |
| O(15)-H(15A)...O(6) | 0.91(10) | 1.92(10) | 2.816(5) | 169(8) |
| O(18)-H(18A)...O(11)#6 | 0.54(8) | 2.13(8) | 2.650(5) | 160(12) |
| O(17)-H(17A)...O(10)#6 | 0.56(6) | 2.26(6) | 2.811(6) | 174(9) |
| O(17)-H(17B)...O(9) | 0.82(7) | 1.95(7) | 2.750(5) | 166(6) |
| C(7)-H(7)...O(10)#6 | 0.96(9) | 2.37(9) | 3.307(8) | 166(7) |
| C(7)-H(7)...O(8)#6 | 0.96(9) | 2.88(8) | 3.301(8) | 108(6) |
| C(10)-H(10)...O(21)#7 | 1.01(6) | 2.88(7) | 3.745(13) | 144(5) |
| N(3)-H(3N)...O(7)#8 | 0.90(12) | 1.77(12) | 2.662(5) | 172(11) |
| C(9)-H(9)...O(14)#5 | 1.04(10) | 2.49(10) | 3.437(9) | 152(7) |

Symmetry transformations used to generate equivalent atoms:
#1 -x+1,-y+2,-z+2; #2 -x+1,-y+1,-z+2; #3 x,y-1,z; #4 -x+1,-y+1,-z+1; #5 -x+1,-y+2,-z+1 #6 -x+2,-y+2,-z+2; #7 -x+2,-y+1,-z+1; #8, x,y,z-1.

**Description of crystal structure of $[4\text{-ampH}]_5[Na(H_2O)_6]\{V_{10}O_{28}\}\cdot 4H_2O$ (6)**

Asymmetric unit of the crystal structure of compound **6** reveals that two halves of decavanadate anionic cluster $[V_{10}O_{28}]^{6-}$ are assembled with the five cation molecules of 4-ampH$^+$ and a sodium hexa-aqua complex. ORTEP diagram of the $[4\text{-ampH}]_5[Na(H_2O)_6]\{V_{10}O_{28}\}\cdot 4H_2O$ (**6**) is shown in the Fig. 3.18. We have found four lattice water molecules in the crystal structure of $[4\text{-ampH}]_5[Na(H_2O)_6]\{V_{10}O_{28}\}\cdot 4H_2O$ (**6**) and a cyclic pentamer is generated among the water molecules (O28, O29, O30, O33, O36) due to O–H···O interaction, as shown in Fig. 3.19, Such water pentamers are connected with sodium hexa-aqua complex on both sides *via* Na–O–H···O (pentamer) resulting in the generation of an architecture like dumbbell shape as presented in Fig. 3.20. The crystallographic data is provided in Table 3.6. Again C–H···O and O–H···O interactions are responsible to study the hydrogen bonding around {N1N2}, {N3N4}, {N5N6}, {N7N8}, {N9N10}, {Na} and water moieties in the crystal structure of **6** as

shown in the Fig.3.21 and hydrogen bond distances and angles are listed in the Table 3.7 including symmetry operations.

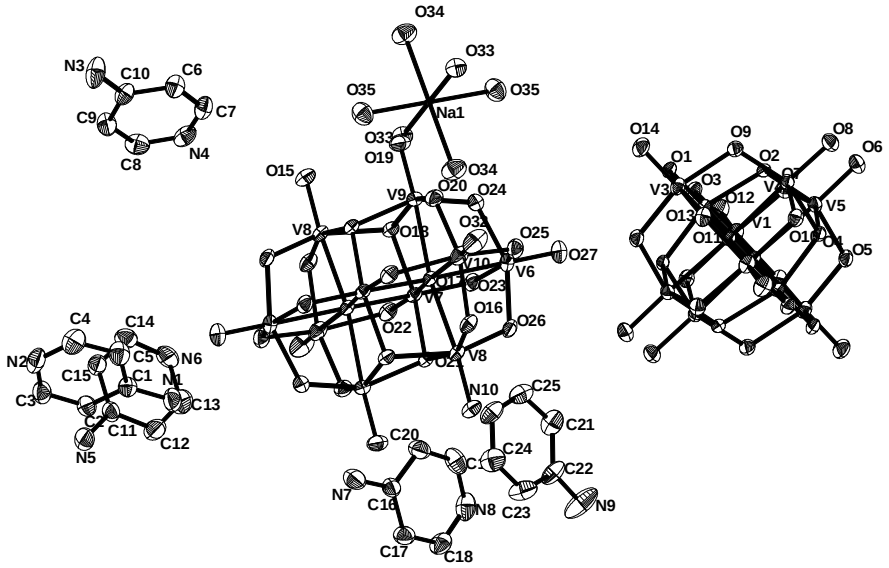


**Fig. 3.18** ORTEP diagram of the [4-ampH]$_5$[Na(H$_2$O)$_6$]{V$_{10}$O$_{28}$}·4H$_2$O (**6**) with 30% probability (Hydrogen atoms and solvent water molecules are omitted for clarity)

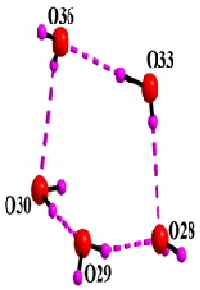


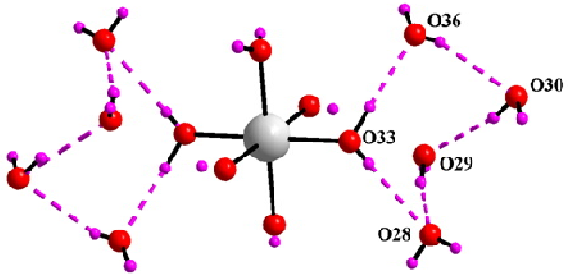


**Fig.3.19** **Fig3.20**

**Fig.3.19** Cyclic water pentamer is generated due to O–H···O interactions in [4-ampH]$_5$[Na(H$_2$O)$_6$]{V$_{10}$O$_{28}$}·4H$_2$O (**6**) **Fig.3.20** Dumbell shape diagram due O–H···O interaction in [4-ampH]$_5$[Na(H$_2$O)$_6$]{V$_{10}$O$_{28}$}·4H$_2$O (**6**).Color codes: O, red; Na, grey; H, Purple;

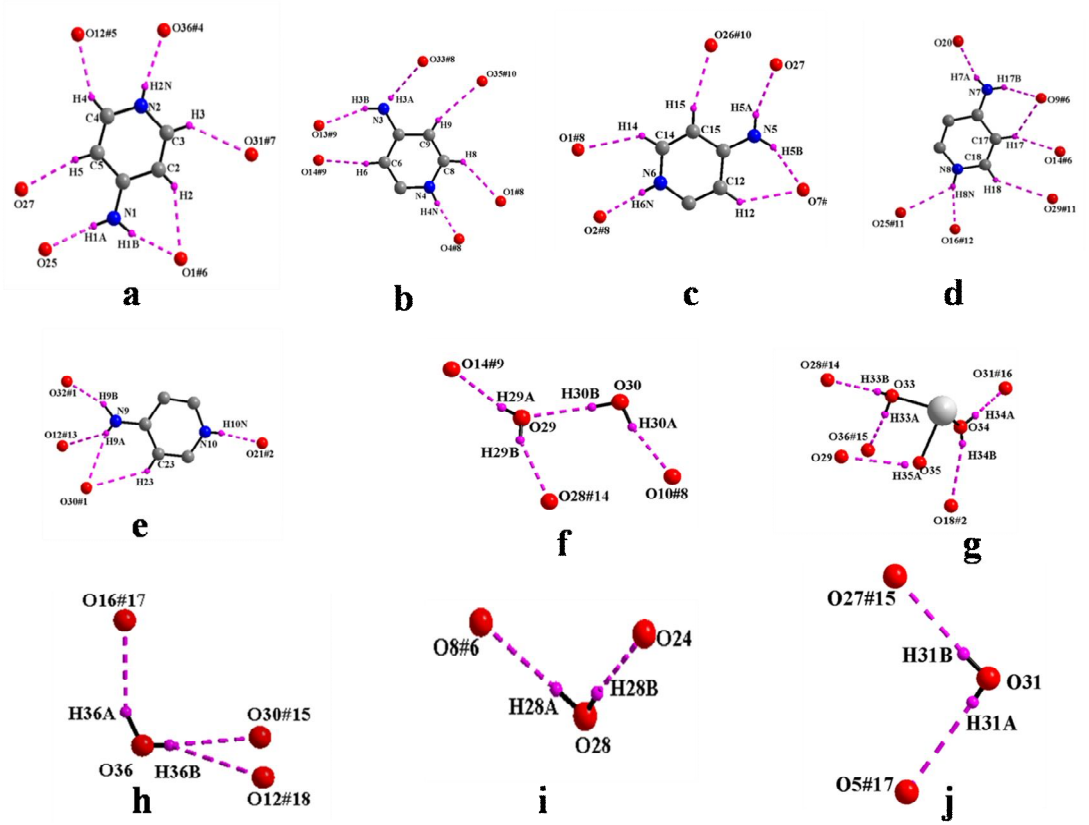


**Fig.3.21** Hydrogen bonding environment around a){N1N2}, b){N3N4},c) ){N5N6},d) {N7N8}, e) {N9N10}, f-j) water moieties for $[4\text{-ampH}]_5[Na(H_2O)_6]\{V_{10}O_{28}\}\cdot 4H_2O$ (**6**). Symmetry codes: #1, -x,-y,-z; #2, -x+1,-y+1,-z; #3, -x,-y+1,-z; #4,x,-y+3/2,z-1/2; #5, x+1,y+1,z; #6, -x+1,y+1/2,-z+1/2; #7, -x+1,y+1/2,-z+3/2; #8, -x,y+1/2,-z+1/2; #9, x,y+1,z; #10, x,-y+3/2,z+1/2; #11, -x+1,y-1/2,-z+1/2; #12, x,-y+1/2,z+1/2; #13, x+1,y,z; #14, x-1,y,z; #15, -x+1,-y+1,-z+1; #16, x,y,z-1; #17, x,y,z+1; #18, x+1,-y+1/2,z+1/2; Color codes: O, red; C, grey; H, Purple;

**Table 3.6** Crystal data and structure refinement for compounds **4, 5** and **6**.

| Entry | **4** | **5** | **6** |
|---|---|---|---|
| Molecular formula | $C_{12}H_{24}N_8O_{38}V_{10}Zn_2$ | $C_{20}H_3Co_2N_8O_4V_{10}$ | $C_{50}H_{100}N_{20}NaO_{72}V_{20}$ |
| Formula weight | 1528.53 | 1721.84 | 3175.29 |
| Temperature (K) | 298(2) | 298(2) | 298(2) |
| Wavelength (Å) | 0.71073 | 0.71073 | 0.71073 |
| Crystal system | Monoclinic | Triclinic | Monoclinic |
| Space group | P21/c | P-1 | P21/c |
| a (Å) | 10.5993(17) | 10.5180(16) | 13.1158(10) |
| b (Å) | 16.4355(18) | 11.9208(18) | 20.0118(16) |
| c (Å) | 13.865(3) | 12.711(2) | 20.1107(16) |
| α (deg) | 90.00 | 97.818(2) | 90.000 |
| β (deg) | 120.191(13) | 107.937(2) | 95.680(3) |
| γ (deg) | 90.00 | 100.240(2) | 90.000 |
| Volume ($Å^3$) | 2087.7(6) | 1460.8(4) | 5251.9(7) |
| Z | 2 | 1 | 2 |
| ρ (g $cm^{-3}$) | 2.432 | 1.957 | 2.008 |
| μ ($mm^{-1}$) | 3.378 | 2.181 | 1.808 |
| F (000) | 1492 | 850 | 3174 |
| Crystal size ($mm^3$) | 0.36x0.18x0.14 | 0.46 x0.34x0.20 | 0.36x0.24x0.18 |
| θ range (º) | 2.98 to 25.00 | 2.20 to 25.09 | 1.44 to 26.01 |
| Reflections collected | 9787 | 13958 | 54039 |
| Unique reflections | 3683 | 5139 | 10321 |
| R(int) | 0.0819 | 0.0209 | 0.0318 |
| parameters | 3683/0/316 | 5139 /0/455 | 10321 / 0 / 936 |
| Goodness of fit on $F^2$ | 1.086 | 1.537 | 1.025 |
| $R_1$, $wR_2$ [ I > 2 sigma(I)] | 0.0885, 0.2660 | 0.0465,0.1582 | 0.0355, 0.0962 |
| $R_1$, $wR_2$ (all data) | 0.1387,0.2895 | 0.0479, 0.1598 | 0.0406, 0.0997 |
| Largest diff. Peak and hole (e.$Å^{-3}$) | 1.854, -3.604 | 2.248, -0.840 | 2.108, -0.417 |

**Table 3.7** Hydrogen bonds and angles for compound **6** [Å and º].

| D–H···A | d(D–H) | d(H···A) | d(D···A) | <(DHA) |
|---|---|---|---|---|
| N(2)-H(2N)...O(36)#4 | 0.69(5) | 2.12(5) | 2.801(5) | 167(5) |
| C(4)-H(4)...O(12)#5 | 0.89(5) | 2.33(5) | 3.123(5) | 148(5) |
| C(5)-H(5)...O(27) | 0.87(5) | 2.30(5) | 3.161(5) | 168(5) |
| N(1)-H(1A)...O(25) | 0.79(5) | 2.29(5) | 3.036(4) | 156(5) |
| N(1)-H(1B)...O(6)#6 | 0.88(5) | 2.05(5) | 2.897(4) | 162(4) |
| C(2)-H(2)...O(6)#6 | 0.84(4) | 2.56(4) | 3.245(4) | 140(3) |
| C(3)-H(3)...O(31)#7 | 0.89(4) | 2.62(4) | 3.333(6) | 138(4) |
| N(3)-H(3A)...O(33)#8 | 0.59(5) | 2.65(5) | 3.177(5) | 150(6) |
| N(3)-H(3B)...O(13)#9 | 0.85(4) | 2.36(4) | 3.166(6) | 158(4) |
| C(6)-H(6)...O(14)#9 | 0.87(4) | 2.58(4) | 3.354(4) | 148(3) |
| N(4)-H(4N)...O(4)#8 | 0.79(4) | 1.91(4) | 2.702(4) | 174(4) |
| C(8)-H(8)...O(1)#8 | 0.88(4) | 2.60(4) | 3.264(4) | 133(4) |
| C(9)-H(9)...O(35)#10 | 0.76(4) | 2.75(4) | 3.471(5) | 159(4) |
| C(15)-H(15)...O(26)#10 | 0.85(4) | 2.50(4) | 3.328(4) | 164(4) |
| N(5)-H(5A)...O(27)#10 | 0.79(4) | 2.24(5) | 2.976(4) | 154(4) |
| N(5)-H(5B)...O(7)#6 | 0.87(5) | 2.13(5) | 2.933(4) | 155(4) |
| C(12)-H(12)...O(7)#6 | 0.92(5) | 2.62(5) | 3.336(5) | 135(4) |
| N(6)-H(6N)...O(2)#8 | 0.80(6) | 1.91(6) | 2.685(4) | 163(6) |
| C(14)-H(14)...O(1)#8 | 0.92(4) | 2.64(4) | 3.352(4) | 135(3) |
| N(7)-H(7A)...O(20) | 0.76(4) | 2.12(5) | 2.844(4) | 162(4) |
| N(7)-H(17B)...O(9)#6 | 0.81(5) | 2.31(5) | 3.033(4) | 150(5) |
| C(17)-H(17)...O(9)#6 | 0.93(5) | 2.63(5) | 3.347(4) | 134(4) |
| C(17)-H(17)...O(14)#6 | 0.93(5) | 2.41(5) | 3.268(4) | 154(4) |
| C(18)-H(18)...O(29)#11 | 0.87(4) | 2.76(4) | 3.477(6) | 140(4) |
| N(8)-H(8N)...O(16)#12 | 0.85(5) | 2.05(5) | 2.855(4) | 159(5) |
| N(8)-H(8N)...O(25)#11 | 0.85(5) | 2.70(5) | 3.319(4) | 131(4) |
| N(10)-H(10N)...O(21)#2 | 0.72(5) | 1.97(5) | 2.677(4) | 168(5) |
| C(23)-H(23)...O(30)#11 | 0.91(5) | 2.81(5) | 3.516(5) | 135(4) |
| N(9)-H(9A)...O(30)#11 | 0.65(7) | 2.63(7) | 3.216(9) | 152(9) |
| N(9)-H(9A)...O(12)#13 | 0.65(7) | 2.43(7) | 2.934(5) | 136(9) |
| N(9)-H(9B)...O(32)#11 | 0.93(7) | 2.06(7) | 2.937(5) | 159(5) |
| O(33)-H(33B)...O(28)#14 | 0.63(4) | 2.18(4) | 2.807(4) | 177(5) |
| O(33)-H(33A)...O(36)#15 | 0.88(4) | 1.92(4) | 2.795(4) | 173(3) |

| | | | | |
|---|---|---|---|---|
| O(35)-H(35A)...O(29) | 0.53(4) | 2.32(4) | 2.829(5) | 160(7) |
| O(34)-H(34B)...O(18)#2 | 0.61(6) | 2.41(6) | 2.967(4) | 153(7) |
| O(34)-H(34A)...O(31)#16 | 0.71(5) | 2.13(5) | 2.790(6) | 156(6) |
| O(28)-H(28A)...O(8)#6 | 0.80(5) | 2.11(6) | 2.906(4) | 174(5) |
| O(28)-H(28B)...O(24) | 0.72(5) | 1.97(5) | 2.686(4) | 170(5) |
| O(36)-H(36A)...O(16)#17 | 0.82(5) | 2.06(5) | 2.824(4) | 154(5) |
| O(36)-H(36B)...O(30)#15 | 0.61(6) | 2.27(6) | 2.841(5) | 157(8) |
| O(36)-H(36B)...O(12)#18 | 0.61(6) | 2.82(6) | 3.254(4) | 132(7) |
| O(29)-H(29A)...O(14)#9 | 0.71(5) | 2.04(5) | 2.746(4) | 170(5) |
| O(29)-H(29B)...O(28)#14 | 0.72(5) | 2.15(5) | 2.815(5) | 154(5) |
| O(30)-H(30B)...O(29) | 0.82(6) | 2.06(6) | 2.866(5) | 169(5) |
| O(30)-H(30A)...O(10)#8 | 0.87(5) | 1.98(5) | 2.837(4) | 168(4) |
| O(31)-H(31B)...O(27)#15 | 0.73(6) | 2.17(6) | 2.903(5) | 176(6) |
| O(31)-H(31A)...O(5)#17 | 0.61(5) | 2.37(5) | 2.976(5) | 170(7) |

Symmetry transformations used to generate equivalent atoms:

#1 -x,-y,-z #2 -x+1,-y+1,-z #3 -x,-y+1,-z; #4 x,-y+3/2,z-1/2; #5 x+1,y+1,z; #6, -x+1,y+1/2,-z+1/2; #7, -x+1,y+1/2,-z+3/2; #8, -x,y+1/2,-z+1/2; #9, x,y+1,z; #10, x,-y+3/2,z+1/2; #11, -x+1,y-1/2,-z+1/2; #12, x,-y+1/2,z+1/2; #13, x+1,y,z; #14, x-1,y,z; #15, -x+1,-y+1,-z+1; #16, x,y,z-1; #17, x,y,z+1; #18, x+1,-y+1/2,z+1/2.

**Description of crystal structure of $[4\text{-ampH}]_{10}[Co(H_2O)_6]\{V_{10}O_{28}\}_2\cdot 10H_2O$ (7):**

The full molecule of the compound **7** has two clusters of decavanadate $\{V_{10}O_{28}\}^{6-}$ anion. For the charge compensation, ten molecules of protonated 4-aminopyridine and one unit of cobalt hexa-aqua complex $[Co(H_2O)_6]^{2+}$ are present in the crystal. Besides, ten lattice water molecules are additionally crystallized in the structure. The full molecule of the compound **7** is presented in Fig. 3.22. In the crystal structure, coordinated water molecules and lattice water molecules are non-covalently interacted through hydrogen bonding, generating water tetramer (O30, O39, O35, O31) with O···H distances of 2.01 Å, 1.842 Å and 2.077 Å respectively and each end of the water tetramer (O30 and O31) is linked to cobalt complex, which is shown in the Fig. 3.23. Hydrogen bonding situation around {N1N2}, {N3N4}, {N5N6}, {N7N8}, {N9N10}, {Co} and water in the crystal structure is shown in the Fig.3.24, which is explained based on C–H···O, O–H···O and N–

H···O interactions. Hydrogen bond distances and angles are listed in the Table 3.8 including symmetry operations.

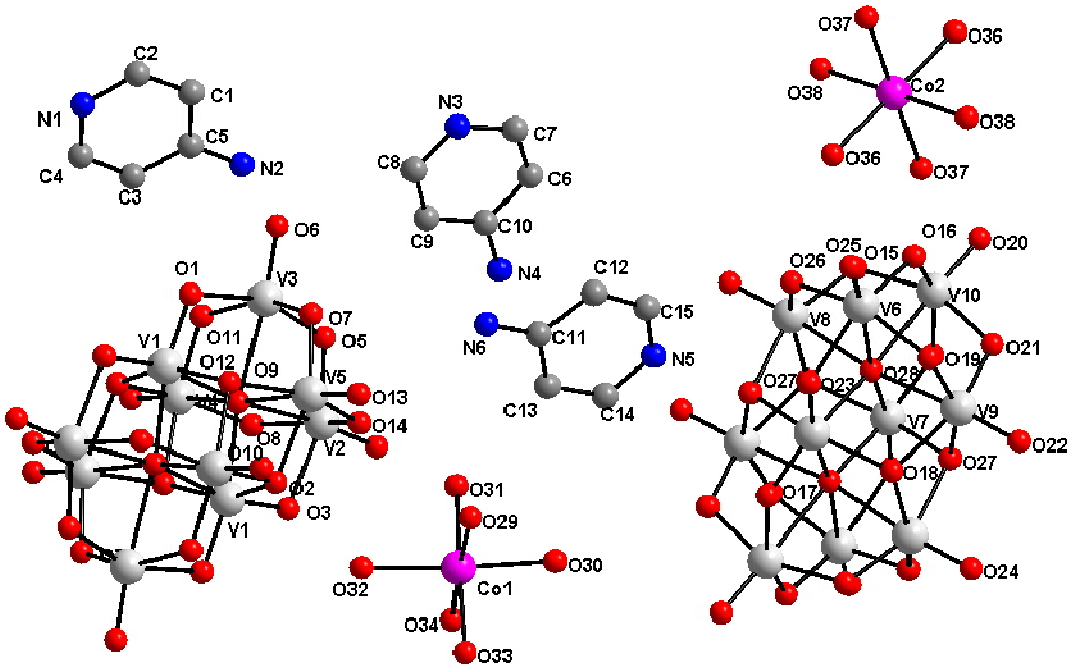


**Fig. 3.22** Ball and stick representation of full molecule of [4-ampH]$_{10}$[Co(H$_2$O)$_6$]{V$_{10}$O$_{28}$}$_2$·10H$_2$O (**7**) (hydrogen atoms and solvent water molecules are omitted for clarity). Color codes: O, red; V, light grey; C, medium grey; Co, purple.

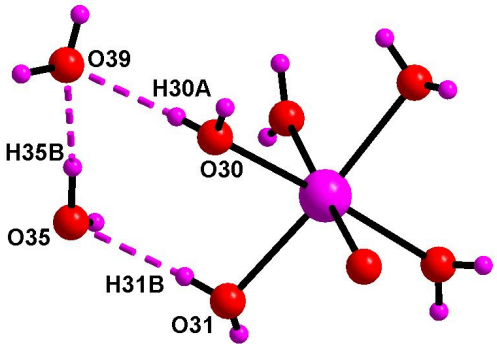


**Fig. 3.23.** Water tetramer is generated due to O–H···O interactions in the crystal of [4-ampH]$_{10}$[Co(H$_2$O)$_6$]{V$_{10}$O$_{28}$}$_2$·10H$_2$O (**7**). Color codes: O, red; Na, grey; H, Purple.

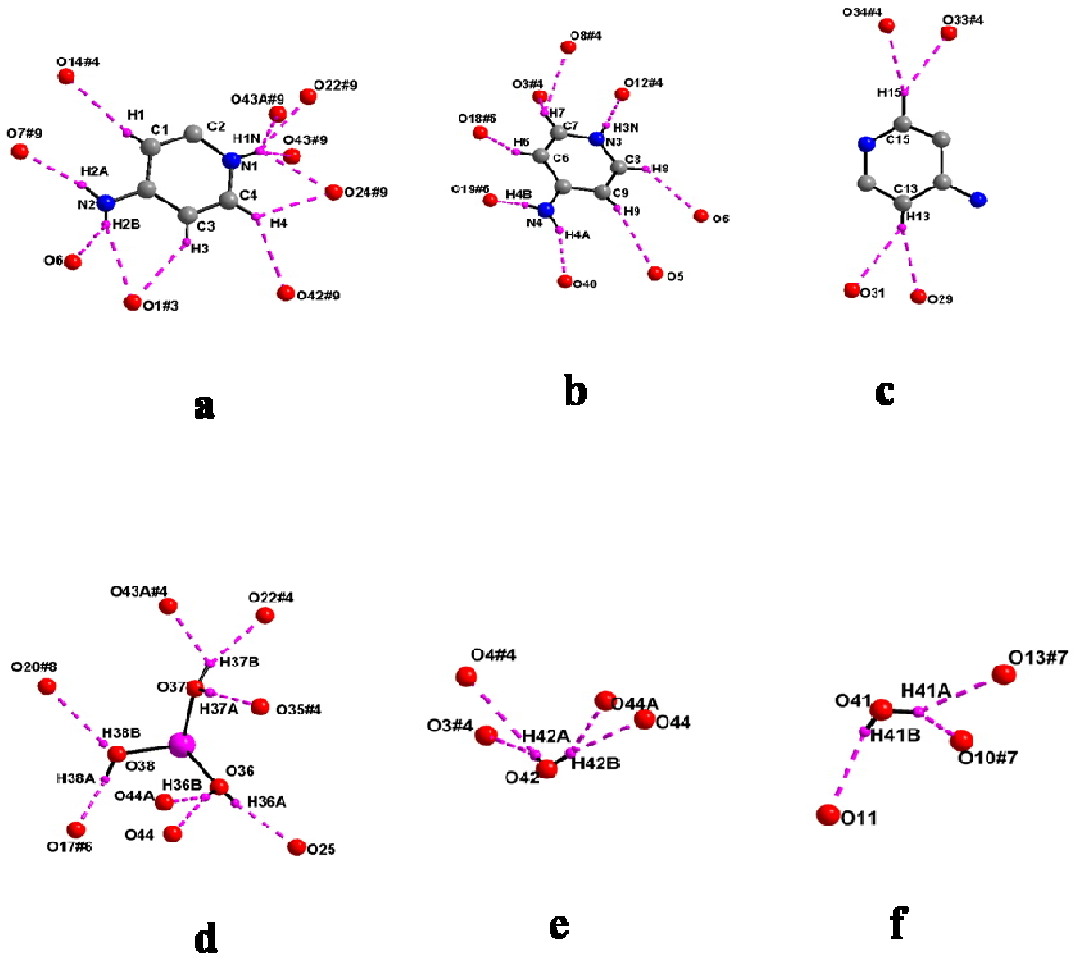


**Fig.3.24.** Hydrogen bonding environment around a){N1N2}, b){N3N4}, c){N5N6},d) {Co}; e-f) water moieties for $[4\text{-ampH}]_{10}[Co(H_2O)_6]\{V_{10}O_{28}\}_2\cdot 10H_2O$ (**7**). Symmetry codes: #1, -x,-y,-z; #2, -x+1,-y+1,-z; #3, -x,-y+1,-z; #4,x,-y+3/2,z-1/2; #5, x+1,y+1,z; #6, -x+1,y+1/2,-z+1/2; #7, -x+1,y+1/2,-z+3/2; #8, -x,y+1/2,-z+1/2; #9, x,y+1,z; #10, x,-y+3/2,z+1/2; #11, -x+1,y-1/2,-z+1/2; #12, x,-y+1/2,z+1/2; #13, x+1,y,z; #14, x-1,y,z; #15, -x+1,-y+1,-z+1; #16, x,y,z-1; #17, x,y,z+1; #18, x+1,-y+1/2,z+1/2; Color codes: O, red; C, grey; H, Purple.

**Table 3.8** Hydrogen bonds and angles for compound **7** [Å and º].

| D-H···A | d(D–H) | d(H···A) | d(D···A) | <(DHA) |
|---|---|---|---|---|
| O(42)-H(42A)···O(3)#4 | 0.58(8) | 2.46(8) | 2.987(6) | 154(10) |
| O(42)-H(42A)···O(4)#4 | 0.58(8) | 2.53(8) | 2.958(6) | 134(10) |
| O(42)-H(42B)···O(44A) | 0.70(8) | 1.83(8) | 2.481(12) | 155(8) |
| O(42)-H(42B)···O(44) | 0.70(8) | 2.17(8) | 2.849(8) | 165(8) |
| O(35)-H(35A)···O(4) | 0.68(7) | 2.89(7) | 3.341(5) | 126(6) |
| O(35)-H(35A)···O(42)#5 | 0.68(7) | 2.25(7) | 2.900(6) | 160(7) |
| O(35)-H(35B)···O(39) | 0.87(6) | 1.84(6) | 2.697(5) | 168(5) |
| O(39)-H(39A)···O(16)#5 | 0.73(6) | 2.03(7) | 2.753(5) | 173(7) |
| O(39)-H(39B)···O(21) | 0.84(7) | 1.88(8) | 2.701(5) | 167(7) |
| O(40)-H(40B)···O(20)#6 | 0.79(8) | 2.34(8) | 2.989(6) | 140(7) |
| O(40)-H(40A)···O(4) | 0.86(8) | 1.93(8) | 2.761(5) | 163(7) |
| O(41)-H(41A)···O(10)#7 | 0.87(7) | 2.23(6) | 2.941(5) | 140(5) |
| O(41)-H(41A)···O(13)#7 | 0.87(7) | 2.12(6) | 2.743(5) | 128(5) |
| O(41)-H(41B)···O(11) | 0.67(8) | 2.09(8) | 2.710(5) | 153(9) |
| O(38)-H(38B)···O(20)#8 | 0.48(8) | 2.32(9) | 2.777(6) | 158(14) |
| O(38)-H(38A)···O(17)#6 | 0.84(7) | 1.86(7) | 2.685(6) | 167(6) |
| O(36)-H(36B)···O(44A) | 0.71(6) | 2.14(6) | 2.812(13) | 160(6) |
| O(36)-H(36B)···O(44) | 0.71(6) | 2.09(6) | 2.788(6) | 171(6) |
| O(36)-H(36A)···O(25) | 0.68(7) | 2.11(7) | 2.754(5) | 158(8) |
| O(37)-H(37A)···O(35)#4 | 0.79(7) | 1.95(8) | 2.722(5) | 165(7) |
| O(37)-H(37B)···O(22)#4 | 0.90(10) | 2.16(10) | 3.030(5) | 163(8) |
| O(37)-H(37B)···O(43A)#4 | 0.90(10) | 2.12(9) | 2.700(12) | 122(7) |
| C(13)-H(13)···O(29) | 0.83(5) | 2.76(5) | 3.416(6) | 137(4) |
| C(13)-H(13)···O(31) | 0.83(5) | 2.73(6) | 3.462(7) | 147(5) |
| C(15)-H(15)···O(33)#4 | 1.07(7) | 2.57(7) | 3.518(8) | 148(5) |
| C(15)-H(15)···O(34)#4 | 1.07(7) | 2.67(7) | 3.526(8) | 136(5) |
| C(6)-H(6)···O(18)#6 | 0.86(7) | 2.54(8) | 3.228(6) | 138(6) |
| N(4)-H(4B)···O(19)#6 | 0.71(6) | 2.39(6) | 2.869(6) | 126(6) |
| N(4)-H(4A)···O(40) | 0.90(9) | 2.05(9) | 2.884(8) | 155(8) |
| C(9)-H(9)···O(5) | 0.82(6) | 2.69(6) | 3.411(6) | 147(5) |
| C(8)-H(8)···O(6) | 0.92(5) | 2.49(5) | 3.192(6) | 134(4) |

| | | | | |
|---|---|---|---|---|
| N(3)-H(3N)···O(12)#4 | 0.83(6) | 1.87(6) | 2.704(5) | 175(6) |
| C(7)-H(7)···O(8)#4 | 0.95(6) | 2.67(6) | 3.392(6) | 134(4) |
| C(7)-H(7)···O(3)#4 | 0.95(6) | 2.63(6) | 3.305(6) | 129(4) |
| C(4)-H(4)···O(42)#9 | 0.92(7) | 2.61(7) | 3.377(7) | 141(5) |
| N(1)-H(1N)···O(43)#9 | 0.87(7) | 2.83(7) | 3.390(7) | 124(5) |
| N(2)-H(2B)···O(1)#3 | 0.75(9) | 2.52(9) | 3.189(6) | 151(9) |
| C(1)-H(1)···O(14)#4 | 0.81(6) | 2.58(6) | 3.331(6) | 155(5) |
| N(2)-H(2A)···O(7)#9 | 0.88(5) | 2.01(6) | 2.875(6) | 171(5) |
| N(2)-H(2B)···O(6) | 0.75(9) | 2.48(9) | 3.094(6) | 141(9) |
| C(3)-H(3)···O(1)#3 | 0.88(6) | 2.48(6) | 3.243(6) | 145(5) |
| C(4)-H(4)···O(24)#9 | 0.92(7) | 2.39(7) | 3.026(6) | 127(5) |
| N(1)-H(1N)···O(24)#9 | 0.87(7) | 2.43(7) | 3.018(6) | 126(5) |
| N(1)-H(1N)···O(22)#9 | 0.87(7) | 2.18(7) | 2.952(6) | 147(6) |
| N(1)-H(1N)···O(43A)#9 | 0.87(7) | 2.88(7) | 3.444(12) | 124(5) |

Symmetry transformations used to generate equivalent atoms:

#1, -x+1, -y+2, -z; #2, -x+2, -y+1, -z #3, -x+1, -y, -z+1 #4, x, y+1, z; #5, x, y-1, z #6 x-1,y,z #7 -x,-y,-z+1 #8 x-1,y+1,z #9 -x+1,-y+1,-z+1.

**Description of crystal structure of $[4\text{-ampH}]_{10}[Zn(H_2O)_6]\{V_{10}O_{28}\}_2\cdot 10H_2O$ (8)**

The crystal structure of $[4\text{-ampH}]_{10}[Zn(H_2O)_6]\{V_{10}O_{28}\}_2\cdot 10H_2O$ **(8)** confined with monoclinic, *P*2(1)/c space group. It consists of two clusters of decavanadate $\{V_{10}O_{28}\}^{6-}$, ten molecules of protonated 4-aminopyridine and one unit of zinc hexa aqua complex $[Zn(H_2O)_6]^{2+}$. In addition, ten lattice water molecules are crystallized in the crystal structure of the present compound. Thermal diagram of compound **8** is presented in Fig. 3.25. In the crystal structure, lattice water molecules (O36, O37, O40, O38) and coordinated water molecules (O16) are noncovalently interacted due to O–H···O interactions resulting in the generation of a cyclic water pentamer. As O16 is linked to zinc complex, two cyclic pentamers are formed both sides of Zn via Zn–O16 leading to the formation of the dumbbell like picture as shown in the Fig. 3.26 (O···H distances lie between 2.007 Å and 2.158 Å). Hydrogen bonding situation around {N1N2}, {N3N4}, {N5N6}, {N7N8}, {N9N10}, {Zn} and water due to C–H···O, N–H···O and O–H···O interactions in the crystal structure of **8** is shown in the Fig. 3.17 and hydrogen bond distances and angles are listed in the Table 3.9 with symmetry codes.

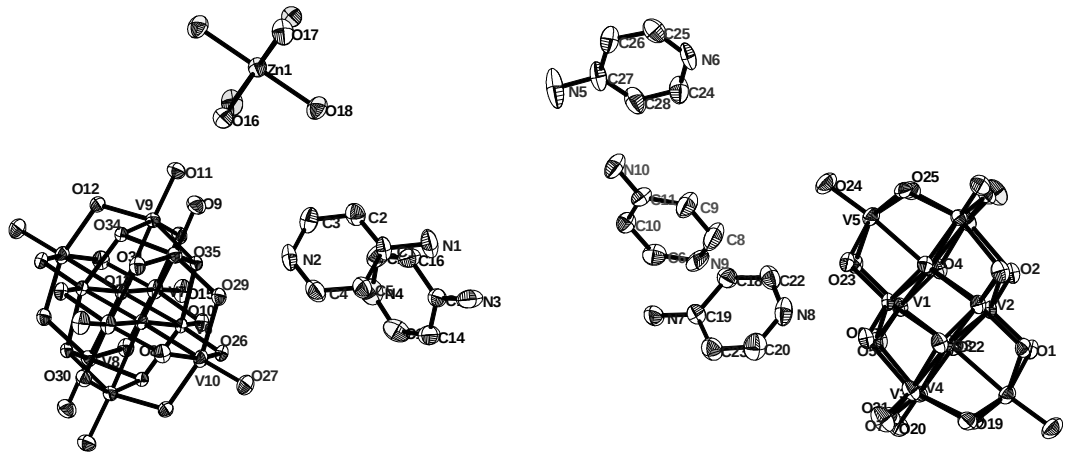


**Fig. 3.25** ORTEP diagram of the $[4\text{-ampH}]_{10}[Zn(H_2O)_6]\{V_{10}O_{28}\}_2\cdot 10H_2O$ (**8**) with 30% probability (Hydrogen atoms and solvent water molecules are omitted for clarity)

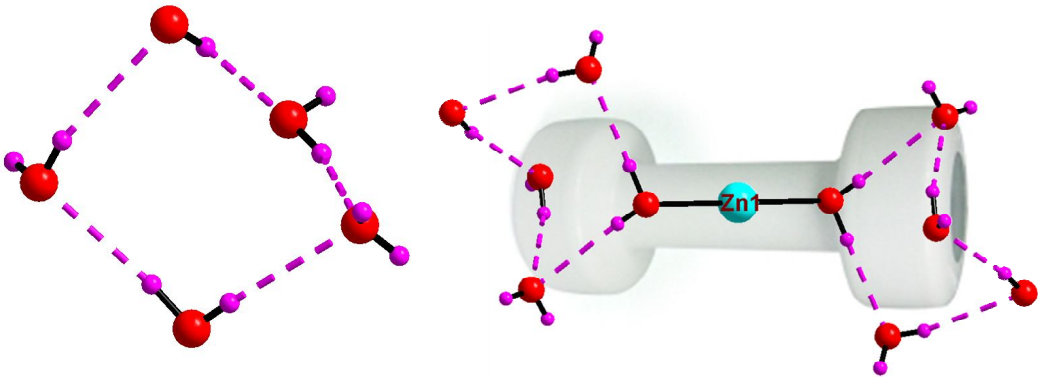


**Fig. 2.26** (Left) Cyclic water pentamer generated because of O–H···O interaction in $[4\text{-ampH}]_{10}[Zn(H_2O)_6]\{V_{10}O_{28}\}_2\cdot 10H_2O$ (**8**) (right) Two cyclic water pentamers are connected to Zn complex, dumbbell shape picture in $[4\text{-ampH}]_{10}[Zn(H_2O)_6]\{V_{10}O_{28}\}_2\cdot 10H_2O$ (**8**) Color codes: O, red; Zn, cyan; H, Purple.

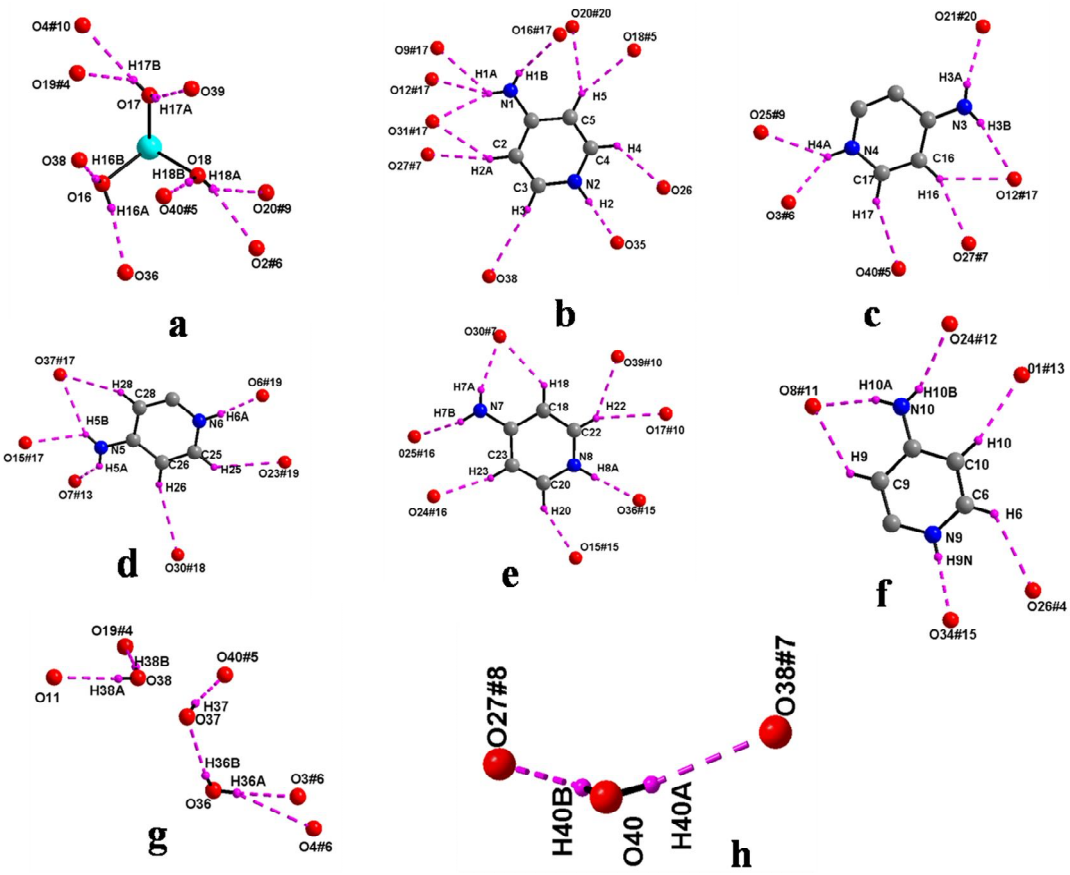


**Fig. 3.27** Hydrogen bonding environment around a) {Zn}; b){N1N2}, c){N3N4},d) {N5N6}, e){N7N8}, f){N9N10}, g-h) water moieties for [4-ampH]$_{10}$[Zn(H$_2$O)$_6$]{V$_{10}$O$_{28}$}$_2$·10H$_2$O (**8**). Symmetry codes: #1, -x,-y,-z; #2,-x+1,-y+1,-z; #3, -x,-y+1,-z; #4,x,-y+3/2,z-1/2; #5, x+1,y+1,z; #6, -x+1,y+1/2,-z+1/2; #7, -x+1,y+1/2,-z+3/2; #8, -x,y+1/2,-z+1/2; #9, x,y+1,z; #10, x,-y+3/2,z+1/2; #11, -x+1,y-1/2,-z+1/2; #12, x,-y+1/2,z+1/2; #13, x+1,y,z; #14, x-1,y,z; #15, -x+1,-y+1,-z+1; #16, x,y,z-1; #17, x,y,z+1; #18, x+1,-y+1/2,z+1/2; Color codes: O, red; C, grey; H, Purple.

**Table 3.9** Hydrogen bonds and anlges for compound **8** [Å and º ].

| D–H···A | d(D–H) | d(H···A) | d(D···A) | <(DHA) |
|---|---|---|---|---|
| O(38)-H(38B)...O(19)#4 | 0.69(6) | 2.01(6) | 2.683(5) | 168(7) |
| O(38)-H(38A)...O(11) | 0.69(5) | 2.21(6) | 2.902(5) | 176(6) |
| O(37)-H(37)...O(40)#5 | 0.74(7) | 2.12(7) | 2.853(6) | 171(8) |
| O(36)-H(36B)...O(37) | 0.70(5) | 2.16(5) | 2.837(6) | 163(6) |
| O(36)-H(36A)...O(3)#6 | 0.74(5) | 2.11(5) | 2.828(5) | 165(5) |
| O(36)-H(36A)...O(4)#6 | 0.74(5) | 2.79(5) | 3.235(5) | 121(4) |
| O(40)-H(40A)...O(38)#7 | 0.74(6) | 2.11(6) | 2.788(6) | 151(6) |
| O(40)-H(40B)...O(27)#8 | 0.73(6) | 2.02(6) | 2.746(5) | 171(6) |
| O(18)-H(18B)...O(40)#5 | 0.81(6) | 2.00(6) | 2.804(6) | 176(6) |
| O(18)-H(18A)...O(20)#9 | 0.65(5) | 2.59(6) | 3.113(6) | 139(6) |
| O(18)-H(18A)...O(2)#6 | 0.65(5) | 2.30(6) | 2.852(5) | 144(6) |
| O(16)-H(16A)...O(36) | 0.79(5) | 2.01(5) | 2.793(5) | 171(5) |
| O(16)-H(16B)...O(38) | 0.66(5) | 2.13(5) | 2.795(6) | 175(6) |
| O(17)-H(17B)...O(19)#4 | 0.68(6) | 2.53(7) | 2.981(5) | 127(7) |
| O(17)-H(17B)...O(4)#10 | 0.68(6) | 2.30(7) | 2.963(5) | 165(7) |
| O(17)-H(17A)...O(39) | 0.73(6) | 2.12(6) | 2.806(6) | 158(6) |
| C(9)-H(9)...O(8)#11 | 0.95 | 2.61 | 3.328(6) | 132.6 |
| N(10)-H(10A)...O(8)#11 | 0.83(7) | 2.13(7) | 2.910(6) | 157(6) |
| N(10)-H(10B)...O(24)#12 | 0.76(5) | 2.28(5) | 2.976(6) | 152(5) |
| C(10)-H(10)...O(1)#13 | 0.95 | 2.40 | 3.327(5) | 166.3 |
| C(6)-H(6)...O(26)#14 | 0.95 | 2.63 | 3.344(5) | 132.2 |
| N(9)-H(9N)...O(34)#15 | 0.73(5) | 1.96(5) | 2.684(5) | 176(5) |
| C(22)-H(22)...O(39)#10 | 0.95 | 2.56 | 3.332(7) | 138.3 |
| C(22)-H(22)...O(17)#10 | 0.95 | 2.76 | 3.645(6) | 154.6 |
| N(8)-H(8A)...O(36)#15 | 0.88 | 1.93 | 2.795(5) | 169.4 |
| C(20)-H(20)...O(15)#15 | 0.95 | 2.31 | 3.107(6) | 141.4 |
| C(23)-H(23)...O(24)#16 | 0.95 | 2.25 | 3.159(6) | 158.6 |
| N(7)-H(7B)...O(25)#16 | 0.87(6) | 2.17(6) | 3.002(5) | 161(5) |
| N(7)-H(7A)...O(30)#7 | 0.78(5) | 2.14(5) | 2.892(5) | 163(5) |
| C(18)-H(18)...O(30)#7 | 0.95 | 2.47 | 3.223(5) | 135.9 |
| C(28)-H(28)...O(37)#17 | 0.95 | 2.82 | 3.523(7) | 131.3 |
| N(5)-H(5B)...O(37)#17 | 0.78(8) | 2.47(8) | 3.176(10) | 150(8) |
| N(5)-H(5B)...O(15)#17 | 0.78(8) | 2.34(8) | 2.924(6) | 132(8) |

| | | | | |
|---|---|---|---|---|
| N(5)-H(5A)...O(7)#13 | 0.81(6) | 2.33(6) | 2.935(6) | 133(5) |
| C(26)-H(26)...O(30)#18 | 0.95 | 2.82 | 3.700(6) | 154.3 |
| C(25)-H(25)...O(23)#19 | 0.95 | 2.83 | 3.532(5) | 131.2 |
| N(6)-H(6A)...O(6)#19 | 0.88 | 1.79 | 2.670(4) | 173.8 |
| N(4)-H(4A)...O(25)#9 | 0.88 | 2.63 | 3.331(5) | 137.4 |
| N(4)-H(4A)...O(3)#6 | 0.88 | 2.04 | 2.846(5) | 151.3 |
| C(17)-H(17)...O(40)#5 | 0.95 | 2.65 | 3.466(7) | 143.7 |
| C(16)-H(16)...O(27)#7 | 0.95 | 2.39 | 3.263(5) | 153.1 |
| N(3)-H(3B)...O(12)#17 | 0.76(5) | 2.36(5) | 3.020(5) | 146(5) |
| N(3)-H(3A)...O(21)#20 | 0.77(5) | 2.10(5) | 2.833(5) | 161(5) |
| C(5)-H(5)...O(20)#20 | 0.95 | 2.77 | 3.474(5) | 131.3 |
| C(5)-H(5)...O(18)#5 | 0.95 | 2.54 | 3.428(6) | 155.2 |
| C(4)-H(4)...O(26) | 0.95 | 2.56 | 3.248(5) | 129.2 |
| N(2)-H(2)...O(35) | 0.88 | 1.82 | 2.697(4) | 174.6 |
| C(3)-H(3)...O(38) | 0.95 | 2.81 | 3.756(6) | 173.5 |
| C(2)-H(2A)...O(27)#7 | 0.95 | 2.50 | 3.348(5) | 148.4 |
| C(2)-H(2A)...O(31)#17 | 0.95 | 2.81 | 3.535(5) | 134.1 |
| N(1)-H(1A)...O(31)#17 | 0.79(5) | 2.42(5) | 3.158(6) | 156(4) |
| N(1)-H(1A)...O(12)#17 | 0.79(5) | 2.48(5) | 3.111(5) | 138(4) |
| N(1)-H(1A)...O(9)#17 | 0.79(5) | 2.74(5) | 3.287(5) | 128(4) |
| N(1)-H(1B)...O(16)#17 | 0.73(6) | 2.45(6) | 3.128(6) | 154(6) |

Symmetry transformations used to generate equivalent atoms:
#1, -x+1,-y,-z+1; #2, -x,-y+2,-z+1; #3, -x+1,-y,-z; #4, x+1,y-1,z; #5, x,-y+1/2,z-1/2; #6, x,y-1,z;#7, x,-y+1/2,z+1/2; #8, x,y,z+1; #9, -x,-y+1,-z+1; #10, -x+1,-y+1,-z+1; #11, x+1,y+1,z; #12, x+1,-y+3/2,z-1/2; #13, -x+1,y-1/2,-z+1/2; #14, -x+1,-y+1,-z; #15, x,y+1,z; #16, x,-y+3/2,z-1/2; #17, -x+1,y+1/2,-z+1/2; #18, x+1,-y+1/2,z+1/2; #19, x+1,y,z; #20, -x,y-1/2,-z+1/2.

**Crystal structure description of $[3\text{-ampH}]_6[V_{10}O_{28}]\cdot 2H_2O$ (9):**

The crystal structure of $[3\text{-ampH}]_6[V_{10}O_{28}]\cdot 2H_2O$ (**9**) shows the abundance of $[V_{10}O_{28}]^{6-}$, six protonated 3-aminopyridine and two lattice water molecules per formula unit. The thermal ellipsoidal plot of compound **9** is shown in Fig. 3.28. The isopolyanion $[V_{10}O_{28}]^{6-}$ is formed by ten $\{VO_6\}$ octahedra connected with each other *via* edge sharing oxygen atoms. The oxygen atoms present in this POV cluster anion are of three kinds: terminal oxygen (Ot), bridging oxygen (Ob) and central oxygen (Oc). There is an extensive hydrogen bonding interactions between the cluster anion and surrounding 3-

aminopyridinium cation. There are three crystallographically independent organic cations (3-aminopyridinium) in the asymmetric unit and each of them are involved in hydrogen bonding interactions as shown in Fig. 3.29. Corresponding hydrogen bond distances and angles are provided in Table 3.11. The selected bond distances and angles in the crystal structure of compound **9** is presented in Table 2. There is one lattice water molecule in the asymmetric unit (thereby two water molecules per formula unit of compound **9**. This water molecule is also involved in an extensive hydrogen bonding intraction as shown in Fig. 3.30. In the crystal, the lattice water molecule is hydrogen bonded to two adjacent isopolyanions and one 3-aminopyridinium cation. The combination of these C–H···O/ O–H···O/ N–H···O hydrogen bonds leads to an intricate three-dimensional hydrogen bonding supramolecular network as shown in Fig. 3.31. It is worth mentioning that 2-aminopyridinium salt analogue of the same decavanadate cluster $[2\text{-ampH}]_6[V_{10}O_{28}]\cdot 2H_2O$ is reported,[15] that was characterized by a different supramolecular structure and a different space group. The crystallographic details of compound **9** are summarized in Table 3.10.

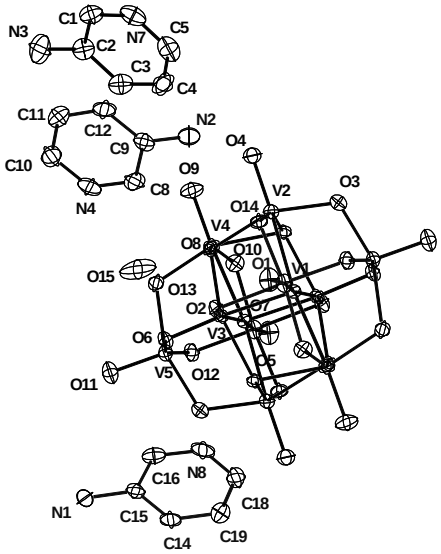


**Fig. 3.28** The thermal ellipsoidal plot (50% probability) of compound $[3\text{-ampH}]_6[V_{10}O_{28}]\cdot 2H_2O$ (**8**). Three (instead of six) aminopyridinium cations are shown.

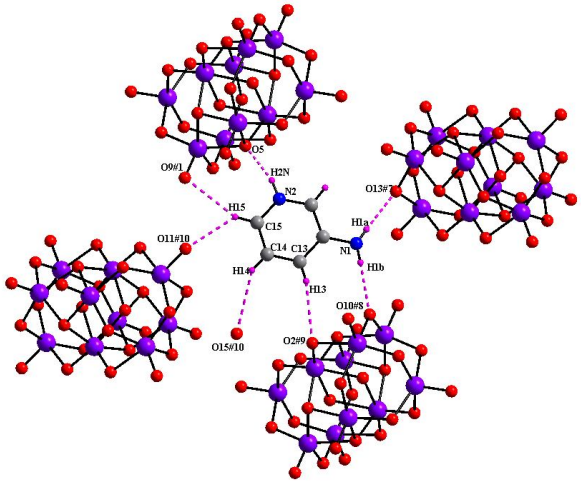


**Fig. 3.29a** The hydrogen bonding environment around the cation {N1N2} compound $[3ampH]_6[V_{10}O_{28}]\cdot 2H_2O$ (**9**).

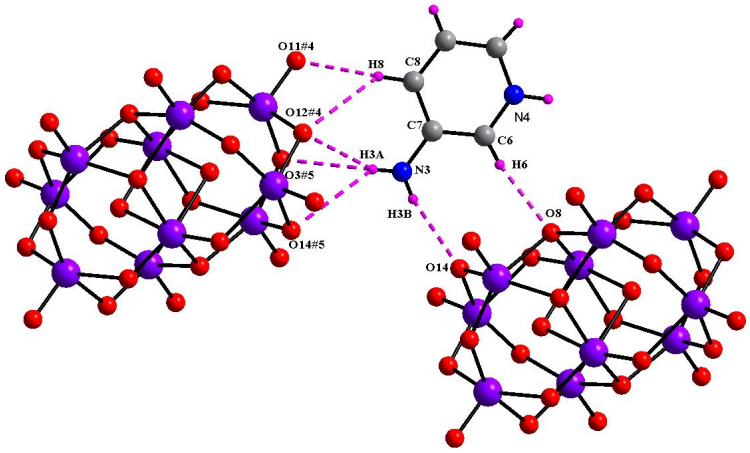


**Fig. 3.29b** The hydrogen bonding environment around the cation {N3N4} compound [3-$ampH]_6[V_{10}O_{28}]\cdot 2H_2O$ (**9**).

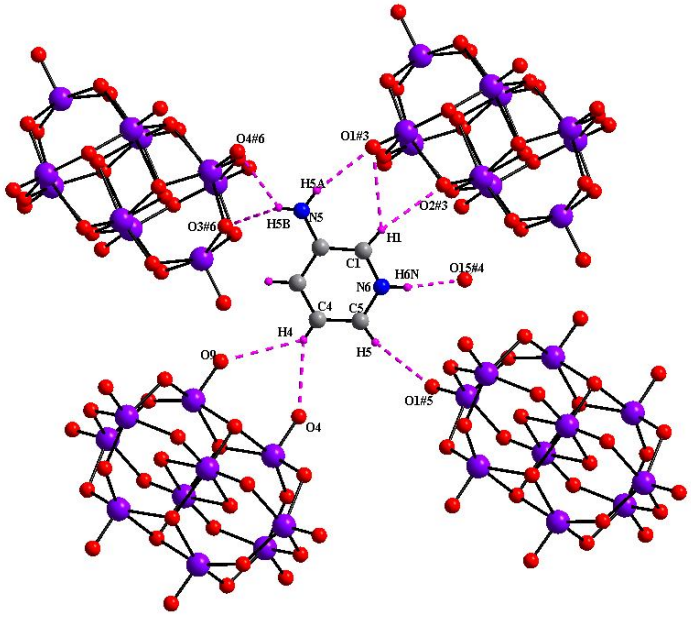


**Fig. 3.29c** The hydrogen bonding environment around the cation {N5N6} compound [3-ampH]$_6$[$V_{10}O_{28}$]·2$H_2O$ (**9**). Color codes: Color code: V, blue violet; O, red; C, gray; N, blue; hydrogen bonds are shown in purple dotted lines. #1, -x+1,-y+1,-z; #2, -x+1,y+1/2,-z+1/2; #3, -x+2,y+1/2,-z+1/2; #4, x+1,y,z; #5, -x+2,-y+1,-z; #6, x,-y+3/2,z+1/2; #7, -x+1,y-1/2,-z+1/2; #8, x,y-1,z; #9, -x+1,-y,-z; #10, x,-y+1/2,z-1/2.

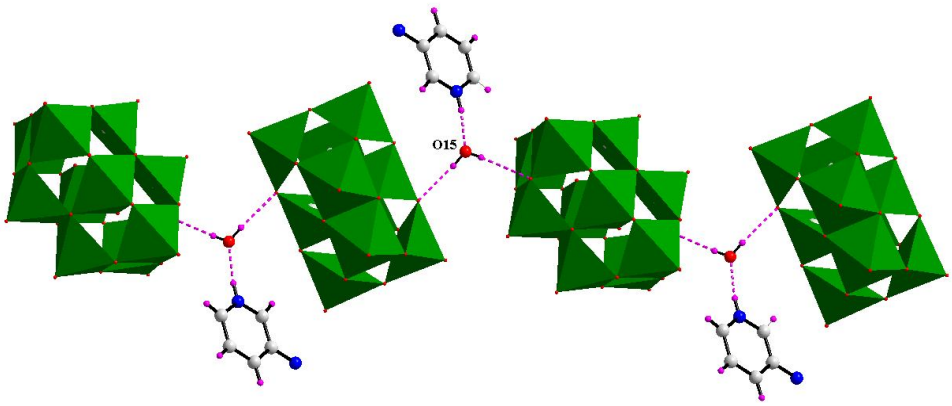


**Fig.3.30** Hydrogen bonding situation around lattice water molecule of compound **9**. The isopolyanion is shown in green polyhedral representation. Color code: V, blue violet; O, red; C, gray; N, blue; H, Purple.

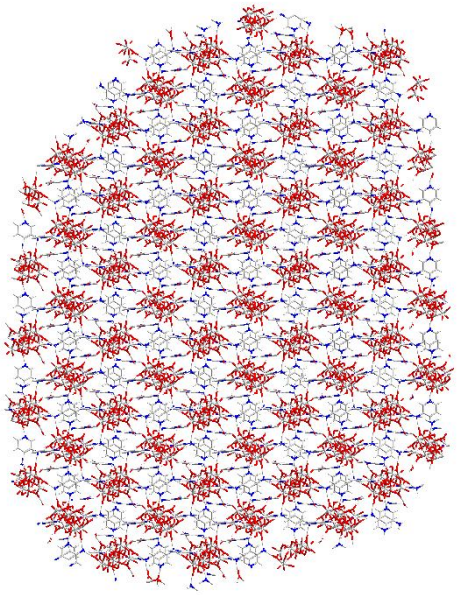

**Fig. 3.31** An intricate hydrogen bonding network observed in the crystal structure of compound **9**. Color code: V, blue violet; O, red; C, gray; N, blue.

**Table 3.10** Crystal data and structure refinement for compound **7, 8** and **9**

| Entry | **7** | **8** | **9** |
|---|---|---|---|
| Molecular formula | $C_{30}H_{88}Co_2N_{12}O_{88}V_{20}$ | $C_{50}H_{96}N_{20}O_{72}V_{20}Zn$ | $C_{30}H_{46}N_{12}O_{30}V_{10}$ |
| Formula weight | 3161.78 | 3213.64 | 1564.19 |
| Temperature (K) | 100(2) | 100(2) | 298(2) |
| Wavelength (Å) | 0.71073 | 0.71073 | 0.71073 |
| Crystal system | Triclinic | Monoclinic | Monoclinic |
| Space group | *P*-1 | *P*2 (1)/c | *P*2 (1)/c |
| a (Å) | 10.5396(12) | 13.087(3) | 11.6246(17) |
| b (Å) | 11.4041(13) | 19.997(4) | 12.9657(19) |
| c (Å) | 21.068(2) | 20.005(4) | 16.492(2) |
| α(º) | 99.843(2) | 90.000 | 90.000 |
| β (º) | 96.625(2) | 95.680(3) | 96.625(2) |
| γ(º) | 91.547(2) | 90.000 | 90.000 |
| Volume ($Å^3$) | 2493.5(5) | 5209.6(18) | 2469.0(6) |
| Z | 2 | 2 | 2 |
| ρ (g $cm^{-3}$) | 2.106 | 2.049 | 2.104 |
| μ ($mm^{-1}$) | 2.226 | 2.043 | 1.910 |
| F (000) | 1570 | 3204 | 1560 |
| Crystal size ($mm^3$) | 0.34x0.18x0.16 | 0.26x0.20x0.18 | 0.36x0.22x0.12 |
| θ range (º) | 1.81 to 26.00 | 1.44 to 26.02 | 1.76 to 25.96 |
| Reflections collected | 25672 | 50931 | 24629 |
| Unique reflections | 9682 | 10234 | 4822 |
| R(int) | 0.0230 | 0.0215 | 0.0215 |
| Parameters | 9682 / 0 / 898 | 10234 / 0 / 832 | 4822 / 0 / 462 |
| GOF on $F^2$ | 1.188 | 1.147 | 1.119 |
| $R_1$, $wR_2[I > 2\sigma(I)]$ | 0.0465, 0.1044 | 0.0468, 0.1020 | 0.0259, 0.0664 |
| $R_1$, $wR_2$ (all data) | 0.0500, 0.1060 | 0.0549, 0.1056 | 0.0284, 0.0678 |
| Largest diff. Peak and hole (e.$Å^{-3}$) | 2.084 and -1.072 | 0.551, -0.345 | 0.346,-0.322 |

**Table 3.11** Geometrical parameters of the C–H···O/ O–H···O/ N–H···O hydrogen bonds (Å, °) involved in supramolecular network of compound **9**. D = donor; A = acceptor.

| D-H···A | d(D-H) | d(H···A) | d(D···A) | <(DHA) |
|---|---|---|---|---|
| O(15)-H(15A)...O(10) | 0.69(3) | 2.48(3) | 3.019(3) | 137(3) |
| O(15)-H(15A)...O(13) | 0.69(3) | 2.46(3) | 3.097(3) | 155(3) |
| O(15)-H(15A)...O(12) | 0.69(3) | 2.52(3) | 3.014(3) | 130(3) |
| O(15)-H(15B)...O(6)#2 | 0.78(5) | 2.08(5) | 2.824(3) | 160(5) |
| C(1)-H(1)...O(1)#3 | 0.90(3) | 2.69(3) | 3.371(3) | 134(2) |
| C(1)-H(1)...O(2)#3 | 0.90(3) | 2.58(3) | 3.393(3) | 150(2) |
| N(6)-H(6N)...O(15)#4 | 0.83(3) | 1.86(3) | 2.682(3) | 171(3) |
| C(5)-H(5)...O(1)#5 | 0.85(3) | 2.55(3) | 3.366(3) | 161(3) |
| C(4)-H(4)...O(4) | 0.81(3) | 2.46(3) | 3.171(3) | 147(3) |
| C(4)-H(4)...O(9) | 0.81(3) | 2.75(3) | 3.390(3) | 137(3) |
| N(5)-H(5B)...O(3)#6 | 0.78(4) | 2.64(4) | 3.305(4) | 144(4) |
| N(5)-H(5B)...O(4)#6 | 0.78(4) | 2.37(4) | 2.984(3) | 137(4) |
| N(5)-H(5A)...O(1)#3 | 0.81(4) | 2.29(4) | 3.070(4) | 162(4) |
| C(6)-H(6)...O(8) | 0.87(3) | 2.29(3) | 3.118(3) | 160(2) |
| N(3)-H(3A)...O(14)#5 | 0.80(3) | 2.76(3) | 3.411(3) | 139(2) |
| N(3)-H(3A)...O(3)#5 | 0.80(3) | 2.74(3) | 3.416(3) | 144(3) |
| N(3)-H(3A)...O(12)#4 | 0.80(3) | 2.42(3) | 3.138(3) | 150(3) |
| C(8)-H(8)...O(12)#4 | 0.95(3) | 2.72(3) | 3.440(3) | 133(2) |
| C(8)-H(8)...O(11)#4 | 0.95(3) | 2.37(3) | 3.250(3) | 153(2) |
| N(1)-H(1A)...O(13)#7 | 0.80(3) | 2.09(3) | 2.883(3) | 173(3) |
| N(1)-H(1B)...O(10)#8 | 0.84(3) | 2.21(3) | 3.042(3) | 171(3) |
| C(13)-H(13)...O(2)#9 | 0.84(3) | 2.58(3) | 3.402(3) | 167(2) |
| C(14)-H(14)...O(15)#10 | 0.90(3) | 2.76(3) | 3.556(4) | 149(2) |
| C(15)-H(15)...O(11)#10 | 0.93(3) | 2.42(3) | 3.128(3) | 133(2) |
| C(15)-H(15)...O(9)#1 | 0.93(3) | 2.62(3) | 3.492(3) | 156(2) |
| N(2)-H(2N)...O(5) | 0.83(4) | 1.81(4) | 2.618(2) | 165(4) |

Symmetry transformations used to generate equivalent atoms:

#1, -x+1,-y+1,-z; #2, -x+1,y+1/2,-z+1/2; #3, -x+2,y+1/2,-z+1/2; #4, x+1,y,z; #5, -x+2,-y+1,-z; #6, x,-y+3/2,z+1/2; #7, -x+1,y-1/2,-z+1/2; #8, x,y-1,z; #9, -x+1,-y,-z; #10, x,-y+1/2,z-1/2.

**Table 3.12** Selected bond lengths [Å] and angles [°] for decavanadate anion of compound **1**

| | | | |
|---|---|---|---|
| V(7)-O(16) | 1.617(3) | V(7)-O(9) | 1.800(3) |
| V(7)-O(11) | 1.845(3) | V(7)-O(14) | 1.965(3) |
| V(7)-O(17) | 2.009(3) | V(7)-O(10) | 2.238(3) |
| V(7)-V(11) | 3.0844(10) | V(7)-V(10) | 3.1024(11) |
| V(7)-V(9) | 3.1533(10) | V(8)-O(18) | 1.618(3) |
| V(8)-O(20) | 1.791(3) | V(8)-O(19) | 1.846(3) |
| V(8)-O(10) | 2.237(3) | V(8)-V(11) | 3.1094(11) |
| V(8)-V(10) | 3.1128(11) | V(8)-V(9) | 3.1481(10) |
| V(9)-O(15) | 1.685(3) | V(9)-O(13) | 1.687(3) |
| V(9)-O(14) | 1.951(3) | V(9)-O(10) | 2.098(3) |
| V(9)-V(10) | 3.0431(11) | V(10)-O(8) | 1.594(3) |
| V(10)-O(7) | 1.827(3) | V(10)-O(19) | 1.862(3) |
| V(10)-O(9) | 1.890(3) | V(10)-O(13) | 2.039(3) |
| V(10)-O(10) | 2.296(3) | V(10)-V(11) | 3.0442(12) |
| V(11)-O(12) | 1.614(3) | V(11)-O(7) | 1.822(3) |
| V(11)-O(11) | 1.836(3) | V(11)-O(20) | 1.899(3) |
| V(11)-O(10) | 2.291(3) | | |
| O(16)-V(7)-O(9) | 103.89(15) | O(16)-V(7)-O(11) | 101.89(14) |
| O(9)-V(7)-O(11) | 94.39(14) | O(16)-V(7)-O(14) | 100.54(14) |
| O(9)-V(7)-O(14) | 91.39(13) | O(11)-V(7)-O(14) | 154.73(12) |
| O(16)-V(7)-O(17) | 99.41(14) | O(9)-V(7)-O(17) | 155.36(13) |
| O(11)-V(7)-O(17) | 88.53(13) | O(14)-V(7)-O(17) | 76.42(12) |
| O(16)-V(7)-O(10) | 174.48(14) | O(9)-V(7)-O(10) | 80.91(12) |
| O(11)-V(7)-O(10) | 80.24(12) | O(14)-V(7)-O(10) | 76.41(11) |
| O(17)-V(7)-O(10) | 75.48(11) | O(16)-V(7)-V(11) | 134.78(11) |
| O(9)-V(7)-V(11) | 83.36(10) | O(11)-V(7)-V(11) | 33.00(9) |
| O(14)-V(7)-V(11) | 124.14(8) | O(17)-V(7)-V(11) | 85.96(8) |
| O(10)-V(7)-V(11) | 47.79(7) | O(16)-V(7)-V(10) | 137.40(12) |
| O(9)-V(7)-V(10) | 33.69(9) | O(11)-V(7)-V(10) | 83.62(10) |
| O(14)-V(7)-V(10) | 87.72(8) | O(17)-V(7)-V(10) | 123.08(8) |
| O(10)-V(7)-V(10) | 47.62(7) | V(11)-V(7)-V(10) | 58.95(3) |
| O(16)-V(7)-V(9) | 136.17(11) | O(9)-V(7)-V(9) | 77.57(10) |
| O(11)-V(7)-V(9) | 121.82(10) | O(14)-V(7)-V(9) | 36.23(8) |
| O(17)-V(7)-V(9) | 80.12(8) | O(10)-V(7)-V(9) | 41.62(7) |
| V(11)-V(7)-V(9) | 89.04(3) | V(10)-V(7)-V(9) | 58.21(3) |
| O(18)-V(8)-O(20) | 104.09(15) | O(18)-V(8)-O(19) | 102.59(14) |
| O(20)-V(8)-O(19) | 95.01(14) | O(18)-V(8)-O(10) | 174.39(13) |
| O(20)-V(8)-O(10) | 80.61(12) | O(19)-V(8)-O(10) | 79.83(12) |
| O(18)-V(8)-V(11) | 137.60(11) | O(20)-V(8)-V(11) | 33.67(9) |
| O(19)-V(8)-V(11) | 83.80(10) | O(10)-V(8)-V(11) | 47.34(7) |
| O(18)-V(8)-V(10) | 135.48(11) | O(20)-V(8)-V(10) | 83.13(10) |
| O(19)-V(8)-V(10) | 33.07(9) | O(10)-V(8)-V(10) | 47.43(7) |
| V(11)-V(8)-V(10) | 58.58(3) | O(18)-V(8)-V(9) | 133.66(11) |
| O(20)-V(8)-V(9) | 122.25(10) | O(19)-V(8)-V(9) | 75.63(9) |
| O(10)-V(8)-V(9) | 41.72(7) | V(11)-V(8)-V(9) | 88.69(3) |
| O(13)-V(9)-O(14) | 95.86(13) | | |

### 3.4. Catalysis

The catalysis mediated by decavanadate is relatively differed from the other polyoxometalates, because of the more reactivity of V and the availability of mixed oxidation states (IV and V) of vanadium atoms in the metal-oxo clusters. So it offers the catalytic activity in oxidation of simple organic molecules with industrial importance.

Generally, the oxidation of styrene will give initially styrene epoxide, which is oxidized to benzaldehyde, which again leads to further oxidized product, benzoic acid.[17] In other hand, due to attack of the proton on epoxide, it leads to another product acetophenone.[18] Thus, if styrene is oxidized by using $H_2O_2$/ catalyst, the expected products in the reaction mixture are styrene epoxide, benzaldehyde, benzoic acid and acetophenone. Currently our aim is to get the benzaldehyde as a selective product by using the decavanadate based compounds. And the reactions are monitored by varying the time of reaction.

In the present chapter, we described catalytic activities of all the compounds (**1–9**) in the reaction of oxidation of styrene, which gives the selective product as benzaldehyde. We have succeeded to get the >99% conversion of styrene at room temperature. (% of conversions are determined by GC-MS*). The optimized condition for the conversion of styrene to benzaldehyde is 1:3 molar ratio of styrene and $H_2O_2$ with 0.25 mg of the catalyst for 24 h at room temperature.[19] The full details for the reaction is provided in the Table 3.13

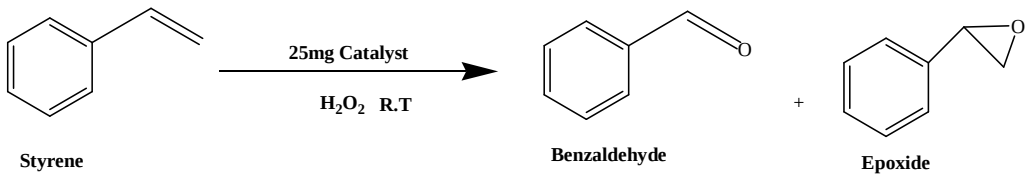


Even there is a possibility for the formation of epoxide, benzoic acid and acetophenone, benzaldehyde is the major product in all the reactions by using our title compounds as catalysts; the reason might be the fact that decavanadate is the common cluster involved in the reaction, which leads to over oxidation up to benzaldehyde.

**Table 3.13** Tabular form of the results for reaction of styrene oxidation.

| Time (h) | conversion (%) | Selectivity (%) | |
|---|---|---|---|
| | | Benzaldehyde | Epoxide |
| 1 | 99.5 | 99.5 | 0.5 |
| 2 | >99 | 100 | 0 |
| 3 | 99 | 97 | 3 |
| 4 | >99 | 100 | 0 |
| 5 | >99 | 100 | 0 |
| 6 | >99 | 100 | 0 |
| 7 | 99 | 99.5 | 0.5 |
| 8 | 99.9 | 96 | 4 |
| 9 | 99 | 99 | 1 |

Note: Room Temperature (30 ºC) and amount of the catalyst taken as 0.25 mg and 1:3 ratio of styrene and $H_2O_2$ for 24 h.

Catalysts are reused for at least three times for the same reaction with similar percentage of conversion. It is confirmed that catalyst doesn't lose the catalytic activity after using in the reaction once which was characterized by I.R spectroscopy, powder X-ray diffractormeter and diffused reflectance spectroscopy.

We have examined compounds **1**, **7, 8** and **9** as catalyst by changing the time of the reactions with 8 h, 12 h, 16 h, 20 h and 24 h. As expected, as time of the reaction increases, % of conversion increases and selectivity of benzaldehyde varies, which is shown in the Table 3.14 for compound **1**. (As the yields of remaining compounds (catalysts) are poor, we could not go for the reactions by changing the time.). From Table 3.14, it is clearly understood that in all the cases, the formation of benzaldehyde is the major. Another point is to be noted that with increasing the time, the generated epoxide is

oxidized to benzaldehyde so that formation of epoxide decreases with time. (Total information is listed in Table 3.14)

**Table 3.14** The variation of the time with percentage of conversion by using compound **1** as catalyst.

| Time | Percentage of the conversion | Selectivity | |
|---|---|---|---|
| | | Benzaldehyde | Epoxide |
| 8 | 91 | 99 | 1 |
| 12 | 97 | 98 | 2 |
| 16 | 98 | 96 | 4 |
| 20† | 98.5 | 97.6 | 1.3 |
| 24 | 99 | 99.5 | 0.5 |

† 1.1 % of selectivity of acetophenone. Note: Room Temperature (30 ºC) and 1:3 ratio of styrene and $H_2O_2$ for 24 h. (Time is expressed in hours)

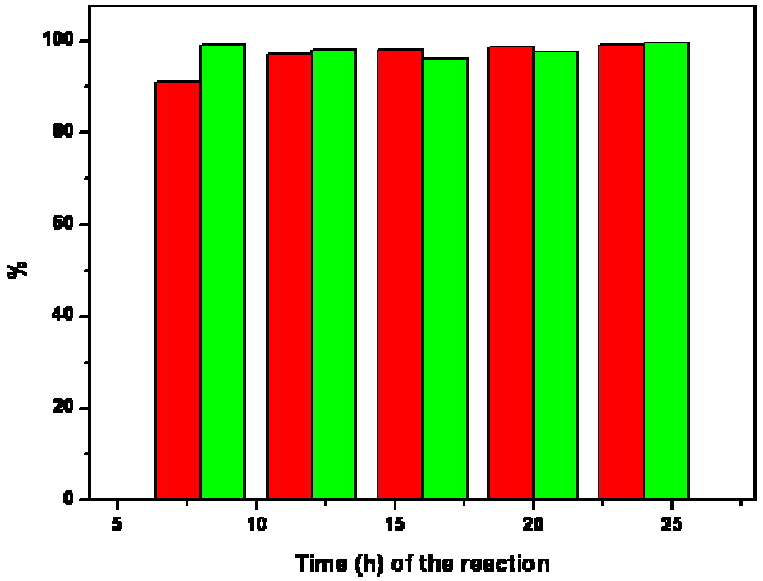


**Fig. 3.32** A graphical view of the results concerning to percentage of conversion and selectivity of benzaldehyde in oxidation of styrene by using the catalyst **1** with increasing the time. Colors: red= % of conversion of styrene and green = % of selectivity.

**Table 3.15** The variation of the time with percentage of conversion by using compound 7 as catalyst.

| Time (h) | conversion (%) | Selectivity (%) | |
|---|---|---|---|
| | | Benzaldehyde | Epoxide |
| 8 | 72 | 77 | 23 |
| 12 | 86 | 85 | 15 |
| 16 | 90 | 98.6 | 1.4 |
| 20 | 98.8 | 99 | 1 |
| 24 | 99 | 99.5 | 0.5 |

Note: Room Temperature (30 ºC) and 1:3 ratio of styrene and $H_2O_2$ for 24 h.

From the Table 3.15, the reaction with 8 h, gives the moderate percentage of epoxide, and it decreases to 15 % when we performed 12 h reaction. In a similar manner, epoxide completely oxidized to benzaldehyde when time is improved for the reaction. So finally, the percentage of benzaldehyde is more for 24 h reaction, which is the optimized condition for compound 7 as a catalyst in the reaction.

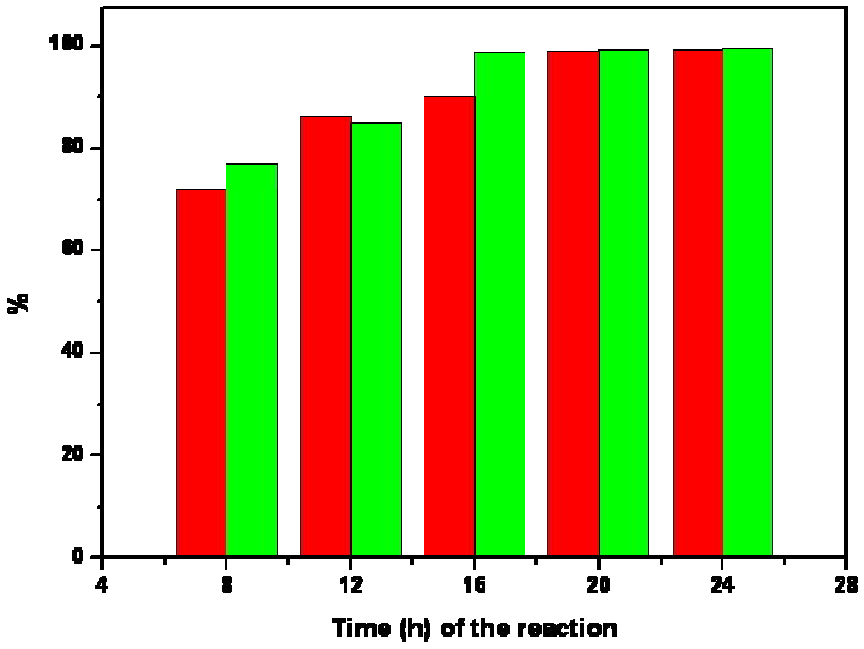


**Fig. 3.33** A graphical view of the results concerning to percentage of conversion and selectivity of benzaldehyde in oxidation of styrene by using the catalyst **7** with increasing

the time. Colors: red= % of conversion of styrene and green = % of selectivity of benzaldehyde.

**Table 3.16** The variation of the time with percentage of conversion with compound **8** as catalyst.

| Time | Percentage of the conversion | Selectivity | |
|---|---|---|---|
| | | Benzaldehyde | Epoxide |
| 8 | 70 | 99 | 1 |
| 12 | 83 | 84 | 16 |
| 16 | 90 | 95 | 5 |
| 20 | 95 | 98 | 2 |
| 24 | 99.9 | 96 | 4 |

Note: Room Temperature (30 ºC) and 1:3 ratio of styrene and $H_2O_2$ for 24 h. Time is expressed in hours.

As shown in Table 3.16, initially the selectivity of epoxide is less (8 h), but for 12 h reaction, 16 % of product is observed along with 84 % of benzaldehyde. But as time increases, formation of epoxide decreases as well as benzaldehyde formation is slightly changed. But the optimization condition (24 h) gives the maximum percentage of conversion of styrene to maximum selective product, benzaldehyde (with compound **8**).

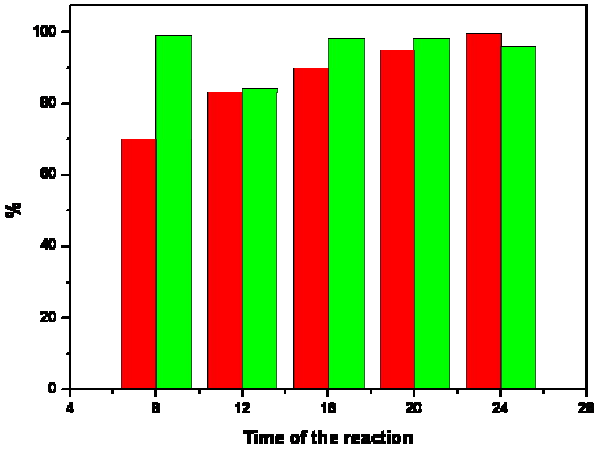


**Fig. 3.34** A graphical view of the results concerning to percentage of conversion and selectivity of benzaldehyde in oxidation of styrene by using the catalyst **8** with increasing the time. Colors: red= % of conversion of styrene and green = % of selectivity of benzaldehyde.

**Table 3.17** The variation of the time with percentage of conversion with compound **9** as catalyst. (Time is expressed in hours)

| Time | Percentage of the conversion | Selectivity | |
|---|---|---|---|
| | | Benzaldehyde | Epoxide |
| 8 | 88 | 90 | 10 |
| 12 | 93 | 99.9 | 1 |
| 16 | 97 | 99 | 1 |
| 20 | 98.5 | 98.7 | 1.3 |
| 24 | 99 | 99 | 1 |

Note: Room Temperature (30 ºC) and 1:3 ratio of styrene and $H_2O_2$ for 24 h.

However, in the case of compound **9,** percentage of conversion increased with time (h) and completely converted to benzaldehyde for 12 h, 16 h, 20 h and 24 h, but in the case of 8 h, we have identified 10 % of epoxide in the product. Few amount of epoxide is also observed (with 20 h and 24 h) in the reaction which was determined by GC-MS (see Table 3.17).

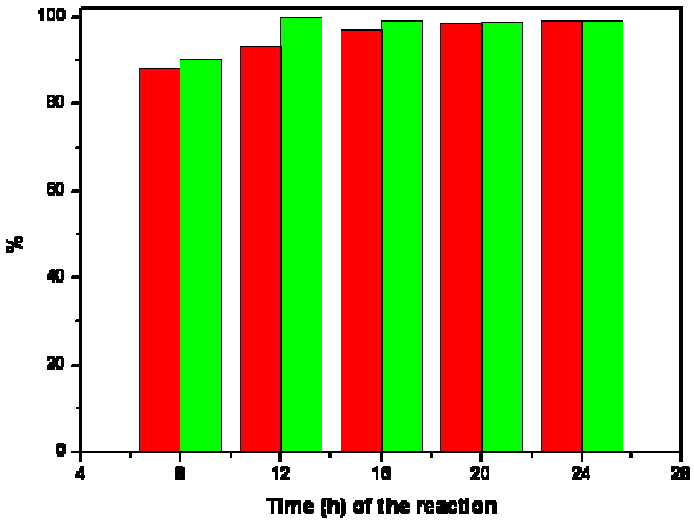


**Fig. 3.35** A graphical view of the results concerning to percentage of conversion and selectivity of benzaldehyde in oxidation of styrene by using the catalyst **8** with increasing the time. Colors: red= % of conversion of styrene and green = % of selectivity of benzaldehyde.

Therefore, the oxidation of styrene with lower time duration (8 h – 12 h), leads to the formation of moderate percentage of epoxide in the reaction mixture. So we can optimize the condition to get the epoxide by reducing the period of the reaction (still less than 8 h) with similar conditions as above mentioned reactions.

**3.5 Conclusions**

We have described in the present chapter, the synthesis and characterization of inorganic-organic hybrid materials (**1–9**) based on decavanadate $\{V_{10}O_{28}\}^{6-}$ anionic cluster. The synthesis has been achieved from the corresponding aqueous sodium-vanadate solution, by varying the pH condition and amino pyridine/hexamine derivatives in an aqueous medium at an ambient temperature. Synthesized compounds are characterized by X-ray crystallography and additionally characterized by elemental analyses, infrared spectroscopy. In compounds **1**–**9**, the POV cluster is $[V_{10}O_{28}]^{6-}$, which is the common cluster isolated. It is worth mentioning that in compound **1**, it is supported to alkali metal (sodium), which is extended coordination polymer and in compound **2,** total moiety is discrete and the residual negative charges have been compensated by the Zinc hexa aqua complex $[Zn(H_2O)_6]^{2+}$ and sodium aqua complex $[Na_4(H_2O)_{14}]^{4+}$ acting as cations. So that compounds **1** and **2** are totally organic free compounds. In compound **3**, charge is compensated by two molecules of $[HMATAH]^{1+}$ and rest of the charge was balanced by protonating itself $\{H_4V_{10}O_{28}\}$. In its crystal structure, lattice water molecules generated cyclic water tetramer. In compound **4**, POV cluster anion supports the zinc coordination complexes, $\{Zn(H_2O)_4\}^{2+}$, in total it is a coordination polymer. The overall negative charges of the resulting POV supported transition metal complexes in compounds **4** has been counter-balanced by the $[HMATAH]^{+}$ molecules. Compound **5** is also**,** the anionic cluster unit $[V_{10}O_{28}]^{6-}$ that exists as discrete moiety, where the species $\{Co(H_2O)_6\}^{2+}$ and 4-amp$H^{1+}$ respectively act as mere counter cation. Compound **6** is constructed by $[V_{10}O_{28}]^{6-}$ anion and $[Na(H_2O)_6]^{1+}$ and protonated 4-aminopyridine [4-amp$H^{1+}$] cation moieties. Cyclic pentamer is found among the lattice water molecules in the crystal structure of compound **8** because of O–H···O interaction. Compounds **7** and **8** are isomorphous, where decavanadate cluster exists as anion and it is counter balanced by $\{Co(H_2O)_6\}^{2+}$ and $\{Zn(H_2O)_6\}^{2+}$ respectively. Compound **9** is simple salt of decavandate anionic cluster with protonated 3-aminopyridine. All the compounds exhibit

catalytic behavior in the reaction of styrene oxidation with good percentage of conversion. Interestingly, these compounds are suitable catalysta to get the product, benzaldehyde as a selective product. For four compounds (**1**, **7**, **8**, **9**) as catalyst, the catalysis is analyzed by varying the time of the reaction.

### 3.6 References:


1. a) Yamase, T. *Mol. Eng.***1993**, *3*, 241 b) Craig, L. H. *Mol. Eng*. **1993**, *3*, 263.
2. a) Pope, M. T. 1983 *Heteropoly and Isopoly Oxometalates*, (Berlin: Springer−Verlag); Izumi, Y.; Urabe, K.; Onaka, M. 1992 *Zeolites,Clay and Heteropoly Acid in Organic Reactions*, Tokyo; b) Pope, M. T.; Müller, A.; *Angew. Chem., Int. Ed. Engl.* **1991**, *30*, 34 c) Okumara, T.; Mizuno, N.; Misono, M.; *Adv. Catal*. **1996**, *41*, 113 d) Hill, C. L.; Prosser-McCartha, C. M.; *Coord. Chem. Rev*. 1995 **143**, 407 e) Hill, C. L .; Chem. Rev. **1998**, *98*, 1, special edition on polyoxometalates.

3. a) Day, V. W.; Klemperer, W. G.; Yagasaki, A. *Chem. Lett.* **1990**, 1267. b) Day, V. W.; Klemperer, W. G.; Yaghi, O. M. *J. Am. Chem. Soc.* **1989**, *111*, 4518. c) Day, V. W.; Klemperer, W. G.; Yaghi, O. M. *J. Am. Chem. Soc.* **1989**, *111*, 5959. d) Hou, D.; Hagen, K. S.; Hill, C. L. *J. Am. Chem. Soc.* **1992**, *114*, 5864. e) Müller, A.; Penk, M.; Rohlfing, R.; Krickemeyer, E.; Döring, J. *Angew. Chem., Int. Ed. Engl.* **1990**, *29*, 926. f) Hou, D.; Hagen, K. S.; Hill, C. L. *J. Chem. Soc., Chem. Commun.* **1993**, 426. g) Chen, Y.; Gu, X.; Peng, J.; Shi, Z.; Yu, H.; Wang, E.; Hu, N. *Inorg. Chem. Commun*. **2004**, *7*, 705. h) Hayashi, Y.; Fukuyama, K.; Takatera, T.; Uehara, A. *Chem. Lett.* **2000**, *29*, 770. i) Johnson, G. K.; Schlemper, E. O. *J. Am. Chem. Soc*. **1978**, *100*, 3645. j) Müller, A.; Penk, M.; Krickemeyer, E.; Bögge, H.; Walberg, H.-J. *Angew. Chem., Int. Ed. Engl.* **1988**, *27*, 1719. k) Müller, A.; Rohlfing, R.; Döring, J.; Penk, M. *Angew. Chem., Int. Ed. Engl.* **1991**, *30*, 588. l) Khenkin, A. M.; Weiner, L.; Neumann, R. *J. Am. Chem. Soc*. **2005**, *127*, 9988. m) Khenkin, A. M.; Neumann, R. *Angew. Chem., Int. Ed. Engl.* **2000**, *39*, 4088. n) Khenkin, A. M.; Weiner, L.; Wang, Y.; Neumann, R. *J. Am. Chem. Soc.* 2001, 123, 8531. o) Haimov, A.; Neumann, R. Chem. Commun. 2002, 876. p) Maayan, G.; Ganchegui, B.; Leitner, W.; Neumann, R. *Chem. Commun.* 2006, 2230. q) Gaspar, A. R.; Evtuguin, D. V.; Neto, C. P. *Ind. Eng. Chem. Res.* **2004**,

*43*, 7754. r) Bose, A.; He, P.; Liu, C.; Ellman, B. D.; Twieg, R. J.; Huang, S. D. *J. Am. Chem. Soc*. **2002**, *124*,4.

4. a) Arumuganathan, T.; Rao. A. S.; Das. S. K.; *Cryst. Growth Des.* **2010**,*10*, 4272. ( b) Arumuganathan, T.; Rao, A. S.; Kumar, T. V.; Das, S. K. *J. Chem. Sci*., **2008**, *120*, 95. c) Arumuganathan, T.; Rao, A. S.; Das, S. K. *J. Chem. Sci., 120*, **2008**, *3*, 297.

5. a) Gong, Y.; Hu, C.; Li, H.; Tang, W.; Huang, K.; Hou, W. *J. Mol. Struct.* **2006**, *784*, 228. b) Correia, I.; Avecilla, F.; Marcão, S.; Pessoa, J. C. *Inorg. Chem. Acta,* **2004,** *357*, 4476. c) Li, Y- T.; Zhu, C- Y.; Wu, Z- Y.; Jiang, M.; Yan, C-W. *Transition Met Chem,* **2010**, *35*, 597. d) Liana, C.; Zheng-Zhonga, L.; Fei-Longa, F.; Da-Qianga, Y.; Mao-Chuna, H.; *Chinese J. Struct. Chem,* **2005**, 10, *24*, 1186. e) Kasuga, N. C.; Umeda, M .; Kidokoro, H.; Ueda, K.; Hattori, K.; Yamaguchi, K. *Cryst. growth Des.* 2009, 9, 1494. f) Liu, J. T.; Wang, X. H.; Liu, J. F. *Chinese Chem. Lett.* **2004**, 15, *7*, 859. g) Duaisamy, T.; Ramanan, A.; Vittal, J. J. *Cryst. Eng*. **2000**, *3*, 237.

6. a) Wang, J.; Zhang, G.; Ma, P. ; Niu, J. *Inorg. Chem. Commun.* **2008**, *11*, 825. b) laronze, N.; Marrot, J.; Herve, G. *Inorg. Chem.* **2003**, *42*, 5857. c) Reinoso, S.; Vitoria, P.; Felices, L. S.; Lezama, L. Gutiérrez-Zorrilla, J. M. *Inorg. Chem.* **2006**, *45*, 108. d) Wang, R. –Z.; Xu, J.-Q.; Yang, G. –Y. ; Bu, W. –M.; Xing, Y. –H.; Li, D. –M.; Liu, S. –Q.; Ye, L.; Fan, Y. –G. *Polyhedron* **1999**, *18*, 2971. e) Hayashi, K.; Takahashi, M.; Nomiya, K. *J. Chem. Soc., Dalton Trans.* **2005**, 3751. f) Chen, L.; Wang, Y.; Hu, C.; Feng, L.; Wang, E.; Hu, N.; Jia, H. *J. Solid State Chem.* **2001**, *161*, 173. g) Li, F.; Xu, L.; Wei, Y.; Wang, X.; Wang, W.; Wang, E. *J. Mol. Struct.* **2005**, 753, 61. h) Zhang, Z.; Wang, E.; Li, Y.; An, H.; Qi, Y. ; Xu, L. *J. Mol. Struct.* **2008**, *872*, 176. j) Tian, C. –H.; Sun, Z. –G.; Li, J.; Zheng, X. –F.; Liang, H.-D.; Zhang, L. –C.; You, W. –S.; Zhu, Z. –M. *Inorg. Chem. .Commun*. **2007**, *10*, 757. k) Wang, J. ; Li, S.; Zhao, J.; Niu, J.; *Inorg. Chem. Commun*. **2006**, *9*, 599. l) Wei, X.; Dickman, M. H.; Pope, M. T. *Inorg. Chem.* **1997**, *36*, 130. m) Lu, Y.; Lu, J.; Wang, E.; Guo, Y.; Xu, X. ; Xu, L. *J. Mol. Struct.* **2005**, *740*, 159. n) Niu, J.; Shen, Y. ; Wang, J.; *J. Mol. Struct.* **2005**, *733*, 19. o) Long, D. –L.; Kögerler, P. ; Farrugia, L. J.; Cronin, L. *J. Chem. Soc., Dalton Trans.* **2005**, 1372. p) Xiao, D.; Hou, Y.; Wang, E.; Wang, S.; Li, Y.; Xu. L.; Hu, C. *Inorg. Chim. Acta*. **2004**, *357*, 2525. q) Laurencin, D.; Villanneau, R.; Herson, P.; Thouvenot, R.; Jeannin, Y.; Proust, A. *Chem. Commun.* **2005**, 5524. r) Cui, J. –W.; Cui, X. –B.; Yu, H. –H.; Xu, J. –Q.; Yi, Z. –H.; Duan, W.

–J.; *Inorg. Chim. Acta*. **2008**, *361*, 2641−2647; s) Gili, P.; Lorenzo-Luis, P.; Mederos, A.; Arrieta, J. M.; Germain, G.; Castinñeiras, A.; Carballo, R.; *Inorg. Chim. Acta* **1999**, *295*, 106. t) Tian, C.-H.; Sun, Z.-G.; Li, J.; Zheng, X.-F.; Liang, H.-D.; Zhang, L.-C.; You, W.-S.; Zhu, Z.-M. *Inorg. Chem. Commun*. **2007**, *10*, 757. u) Han, Z.; Ma, H.; Peng, J.; Chen, Y.; Wang, E.; Hu, N. *Inorg. Chem. Commun*. **2004**, *7*, 182. v) Rarig, R. S.; Bewley, L.; Golub, V.; O'Connor, C. J.; Zubieta, J. *Inorg. Chem. Commun*. **2003**, *6*, 539.

7. a) Khenkin, A. M.; Shimon, L. J. W.; Neumann, R. *Inorg. Chem.* **2003**, *42*, 3331. b) Arumuganathan, T.; Srinivasarao, A.; Kumar, T. V.; Das, S. K. *J. Chem. Sci.*, **2008**, *120*, 95. c) Sidle, A. R.; Markell, C. G.; Lyon, A.; Hodgson, K. O.; Roe, A. L. *Inorg. Chem.* **1987**, *26*, 219. d) Lyon, D. K.; Finke, R. G. *Inorg. Chem.* **1990**, *29*, 1787. e) Lin. Y.; Finke, R. G. *J. Am. Chem. Soc.* **1994**, *116*, 8335. f) Pohl, M.; Lyon, D. K.; Mizuno, N.; Nomiya, K.; Finke, R. G. *Inorg. Chem.* **1995**, *34*, 1413.

8. a) Bar-Nahum, I.; Ettedgui, J.; Konstantinovski, L.; Kogan, V.; Neumann, R. *Inorg. Chem.* **2007**, *46*, 5798. b) Bar-Nahum, I.; Cohen, H.; Neumann, R. *Inorg. Chem.* **2003**, *42*, 3677. c) Khenkin, A. M.; Neumann, R. *Inorg. Chem.* **2000**, *39*, 3455; d) Derat, E.; Kumar, E.; Neumann, R.; Shaik, S. *Inorg. Chem.* **2006**, *45*, 8655. e) Neumann, R.; Khenkin, A. M. *Inorg. Chem.* **1995**, *34*, 5753.

9. a) Long, D. –L.; Song, Y. –F.; Wilson, E. F. ; Kögerler, P. ; Guo, S. –X.; Bond, A. M.; Hargreaves, J. S. J. ; Cronin, L. *Angew. Chem.* **2008**, *120*, 4456. b) Long, D. –L.; Song, Y. –F.; Wilson, E. F.; Kögerler, P.; Guo, S. –X.; Bond, A. M.; Hargreaves, J. S. J.; Cronin, L. ; *Angew. Chem. Int. Ed.*, **2008**, *47*.
10. Pybus, D. H.; Sell, C. S. *The chemistry of Frangrances* (Eds.; RSC Paperbacks), Cambridge, **1999**. b) Singh, R. P.; Subbarao, H. N.; Sukh, D. *Tetrahedron* **1979**, *35* 1789−1793. c) Fey, T.; Fischer, H.; Bachmann, S.; Albert, K.; Bolm, C. *J. Org. Chem.* **2001**, *66*, 8154.
11. Dess, D. B.; Martin, J. C. *J. Org. Chem.* **1983**, *48*, 4155.
12. a) Marko, I. E.; Giles, P. R.; Tsukazaki, M.; Chelle-Regnaut, I.; Gautier, A.; Brown, S. M.; Urch, C. *J. Org. Chem.* **1999**, *64*, 2433. b) Haimov, A.; Neumann, R. *Chem.*

*Commun.* **2002**, 876. c) Khenkin, A. M.; Neumann, R. *J. Org. Chem.* **2002**, *67*, 7075. d) Khenkin, A. M.; Shimon, L. J. W.; Neumann, R. *Eur. J. Inorg. Chem.* **2001**, 789. e) Peterson, K. P.; Larock, R. C. *J. Org. Chem.* **1998**, *63*, 3185. f) Stahl, S. S.; Thorman, J. L.; Nelson, R. C.; Kozee, M. A. *J. Am. Chem. Soc.* **2001**, *123*, 7188. g) Steinhoff, B. A.; Fix, S. R.; Stahl, S. S. *J. Am. Chem. Soc.* **2002**, *124*, 766. h) Betzemeier, B.; Cavazzini, M.; Quici, S.; Knochel, P.; *Tetrahedron Lett.* **2000**, *41*, 4343−4346; i) Dijksman, A. ; Marino-Gonzalez, A. ; Payeras, A. M. I.; Arends, I. W. C. E.; Sheldon, R. A. *J. Am. Chem. Soc.* **2001**, *123*, 6826. j) Lorber, Y.; Smidt, S. P.; Osborn, J. A. *Eur. J. Inorg. Chem.* **2000**, 655. k) Muldoon, J.; Brown, S. N. *Org. Lett.* **2002**, *4*, 1043. l) Csjernyik, G.; Éll, A. H.; Fadini, L.; Pugin, B.; Backvall, J. –E. *J. Org. Chem.* **2002**, *67*, 1657. n) Yamaguchi, K.; Mori, K.; Mizugaki, T.; Ebitani, K.; Kaneda, K. *J. Am. Chem. Soc.* **2000**, *122*, 7144. o) Lee, M.; Chang, S. *Tetrahedron Lett.*. **2000**, *41*, 7507. p) Ciriminna, R.; Pagliaro, M. *Chem. Eur. J.* **2003**, *9*, 5067. q) Zhan, B.-Z.; White, M. A.; Sham, T.-K.; Pincock, J. A.; Doucet, R. J.; Rao, K. V. R.; Robertson,; Cameron, T. S. *J. Am. Chem. Soc.* **2003**, *125*, 2195. r) Kluytmans, J. H. J.; Markusse, A. P.; Kuster, B. F. M.; Marin, G. B.; Schouten, J. C. *Catal. Today* **2000**, *57*, 127. s) Besson, M.; Gallezot, P. *Catal. Today* **2000**, *57*, 143. t) Mallat, T.; Baiker, A. *Chem. Rev.* **2004**, *104*, 3037. u) Son, Y.-C.; Makwana, V. D.; Howell, A. R.; Suib, S. L.; *Angew.Chem.* **2001**, *113*, 4410. *Angew. Chem. Int. Ed.* **2001**, *40*, 4280. v) Velusamy, S.; Punniyamurthy, T. *Org. Lett.* **2004**, *6*, 217.

13. Sheldon, R. A.; Arends, I. W. C. E.; Dijksman, A. *Catal. Today* **2000**, *57*, 157.
14. a) Software for the CCD Detector System, Bruker Analytical X-ray Systems Inc., Madison, WI, 1998. b) Bruker SADABS, SMART, SAINTPLUS and SHELXTL, Bruker AXS Inc., Madison, WI, USA, 2003. c) Sheldrick, G.M. SHELX-97, Program for Crystal Structure Solution and Refinement, University of Göttingen, Germany, 1997. d) Sheldrick, G. M. *Acta Cryst.* **2008**, *A64*, 112.
15. a) Cram, D. C.; Mahroof-Tahir, M.; Anderson, O. P.; Miller, M. M. *Inorg. Chem.* **1994**, *33*, 5586. b) Nilsson, J.; Nordlander, E.; Behrens, U.; Rehde, D. Acta. Cryst. **2010,** *E66*, i30. c) Crans, D. C. *Comments Inorg. Chem.* **1994**, *16*. 33. d) Ferreira D. Silva, J. L.; Minas da Piedade, M. F.; Duarte, M. T. *Inorg. Chim. Acta*, **2003**, 356, 222.

16. a) Kumagai, H.; Arishima, M.; Kitagawa, S.; Ymada, K.; Kawata, S.; Kaizaki, S. *Inorg.Chem*. **2002**, *41*, 1989. B) Zavalij, P.Y.; Whittingham, M.S.; Boylan, E.A.; Pecharsky, V.K.; Jacobson, R.A. *Z. Kristallogr*.**1996**, *211*, 464. c) Zhang, Y.; O'Connor, C.J.; Clear"eld, A.; Haushalter, R.C. *Chem. Mater.* **1996**, *8*, 595. d) Riou, D.; Roubeau, O.; Ferey, G. *Z. Anorg.Allg. Chem*. **1998**, 624, 1021. e) Wang, X.; Liu, H-X.; Xu, X-X.; You, X-Z. *polyhedron,* **1993,** *12*, 1, 77.

17. Takao, K.; Wayaku, M.; Fujiwara, Y.; Imanaka, T.; Teranishi, S. *Bull. Chem.Soc.Jpn.* **1972,** *45***,** 1505.

18. Rao, S. N.; Munshi, K.N.; Rao, N.N. *J. Mol. Catal*. **2000**, *A56*,205.

19. For standard optimized catalytic reaction: 1 mmol of styrene and 3 mmol of $H_2O_2$ are taken into the 25 ml of round bottom flask, to which was already added 25 mg of catalyst and stirred for 24 h ( desired time) at 80 ºC, the reaction was quenched with DCM after time period. When the mixture came to room temperature organic layer was extracted in DCM and catalyst was completely dissolved in water layer. Small amount of the organic layer was diluted with DCM and used for GC-MS analysis as discussed in chapter 2.

# Synthesis and Structural Characterization of Inorganic-Organic Hybrid Materials Based on Anderson-Type Heteropolyanion and Their Catalytic Applications

**ABSTRACT** This chapter describes the syntheses, structural characterization of inorganic-organic hybrid materials based on Anderson anionic cluster including their non-covalent supramolecular hydrogen bonding interactions, and their catalytic activities. The crystal structures of an inorganic–organic hybrid materials, $[2\text{-AmpH}]_2[\{Na(H_2O)_2\}\{AlMo_6(OH)_6O_{18}\}]\cdot 4H_2O$ (**1**), $[3\text{-AmpH}]_2[HAlMo_6(OH)_6O_{18}]\cdot 4H_2O$(**2**), $[4\text{-AmpH}]_6[AlMo_6(OH)_6O_{18}]_2\cdot 18H_2O$(**3**) and $[2\text{-AmpH}]_5[IMo_6O_{24}]\cdot H_2O$(**4**) (where 2-ampH = protonated 2-aminopyridine, 3-ampH = protonated 3-aminopyridine and 4-ampH = protonated 4-aminopyridine) have been demonstrated in the present chapter. Compounds **1**, **2** and **3** are composed of the common anionic cluster; Anderson anion with aluminum as a central metal ion and compound **4** is generated with iodine based Anderson anion, isolated as a salt of corresponding protonated aminopyridine derivatives. Catalytic studies of all these compounds / materials toward the oxidation of styrene leading to benzaldehyde as a selective product with good percentage of conversions are also described in this chapter.

## 4.1. Introduction

Anderson type heteropolyanion is generated at lower pH (~3) in aqueous solution. It is constructed by one central atom ( $Al^{3+}$, $Te^{6+}$, $Cr^{3+}$ etc…) and it is surrounded with six tri bridged ($\mu^3$) oxygen atoms with another two molybdenum atoms. Six more oxygen atoms are doubly bridged ($\mu^2$) between each of the two molybdenum atoms. And each of molybdenum atoms is again linked with two terminal oxygen atoms. Finally, each molybdenum is connected with two terminal oxygen atoms and two triply bridged oxides and one triply bridged oxygenation. A representative example of an Anderson type cluster is shown in Fig. 4.1.

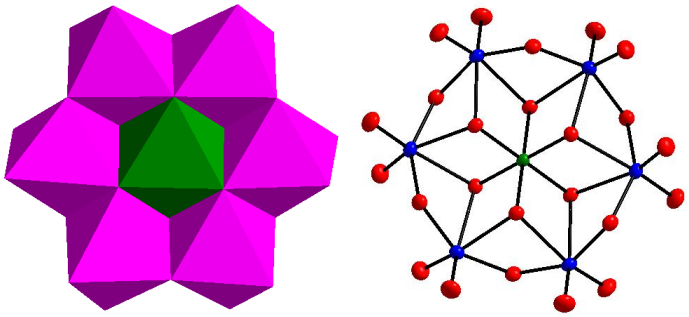

**Fig. 4.1** Anderson anion $\{AlMo_6(OH)_6O_{18}\}^{3-}$, Ball and stick, and polyhedral representation.

Other examples for Anderson anion are $[IMo_6O_{24}]^{5-}$ and $[TeMo_6O_{24}]^{6-}$ having iodine and tellurium as the central ion respectively and their syntheses and crystal structures are discussed in several reports.[1] One main feature of polyoxometalates or anionic molecular oxides is that they provide structurally well-characterized surfaces, formed by approximately coplanar, closest-packed oxygen atoms. Such materials have received considerable attention due to their fascinating solid state properties and because of their potential applications in many fields such as catalysis, materials science, medicinal chemistry, and magnetochemistry.[2] For the past century, the literature survey revealed that Anderson anion plays a key role in constructing 1-D to 3- dimensional networks.[3] The cluster consists of negative charge, so a proper cation is the basic requirement for its isolation. By changing / tuning the cation concerned supramolecular chemistry would be changed. The supramolecular chemistry of such system generally depends on both cation and anion.

In the recent era, other properties like catalytic and biological properties are also described in the context of a poly anion with proper cation.[4] Wide-range of physical and thermal properties are also demonstrated of polyoxometalate anion with various organic cations or transition metal ions.[5] Heteropolyoxometalates have attracted interest over the last few years as oxidiation catalysts because their inorganic nature bodes well for potentially long-lived catalysts.[6] Even though, the reports on synthesis and crystal structures of inorganic-organic hybrid materials, based on polyoxometalate anions are numerous, the catalytic activities of these toward organic oxidations of industrial importance (for example, the oxidation of alcohols, epoxidation of alkenes and

sulfoxidation reactions) are less explored. In particular, applications of heteropolyanion based inorganic-organic hybrid materials in oxidation of olefin are of great importance. This is because the oxidation of olefin can be described into three categories (i) breaking of C=C bond over the surface of the material such as osmium tetra oxide and ruthenium tetra oxide in stoichiometry amount [7], (ii) the attack of ozone on olefins leads to ozonides and the sub-sequent conversion to aldehydes or ketones in reductive work up conditions [7d],and (iii) the oxidation of olefins by hydrogen peroxide [8]. Due to waste problem and chemical cost, the practice of using normal metal salts as oxidants is not desirable [9]. By taking into account all these for environmental protection, oxidation, carried by means of hydrogen peroxide, appears to be a better alternative.[8] It contains 47.1% of active oxygen (wt %) which is significantly higher than the other common oxidizing agents[10] such as $HNO_3$ (25.0%), tBuOOH (17.8%), and $NaIO_4$ (29.9%) etc. and furthermore, it is prominently easy to handle and gives only water as the by-product. As we have discussed nicely in the chapter 2 for the reason to prefer the $H_2O_2$ as an oxidant in our oxidation reaction. The current field the catalysis of metal-oxo clusters have received much importance because metal-oxo clusters are efficient catalysts in several reactions, e.g., oxidation of alcohol and styrene towards the selective products.[11] We are interested to study the catalytic activities of some of the Anderson anion based materials toward styrene oxidation. In this chapter, we describe the syntheses and structural characterization of $[2\text{-AmpH}]_2[\{Na(H_2O)_2\}\{AlMo_6(OH)_6O_{18}\}]\cdot 4H_2O$ (**1**), $[3\text{-AmpH}]_2[HAlMo_6(OH)_6O_{18}]\cdot 4H_2O$(**2**), $[4\text{-AmpH}]_6[AlMo_6(OH)_6O_{18}]_2\cdot 18H_2O$ (**3**) and $[2\text{-AmpH}]_5[IMo_6O_{24}]\cdot 2H_2O$ (**4**) including their supramolecular chemistry. Lastly, we have described the catalysis aspect of these compounds towards the oxidation of styrene.

## 4.2. Experimental Section

### 4.2.1. Materials

Sodium molybdate ($Na_2MoO_4\cdot 2H_2O$) is received from FINAR Reagents. The distilled water was used throughout the experiments. 2-aminopyridine, 3-aminopyridine, 4-aminopyridine are received from CHEMLABS. $AlCl_3\cdot 6H_2O$ and $HIO_4\cdot 6H_2O$ are used as received from S.D Fine and FINAR respectively. Styrene and 30% $H_2O_2$ are received from HiChem and used without further purification.

### 4.2.2. Physical Measurements

Micro analytical (C, H, N) data were obtained with a FLASH EA 1112 Series CHNS Analyzer. Infrared (IR) spectra were recorded on KBr pellets with a JASCO FT/IR-5300 spectrometer in the region of 400–4000 $cm^{-1}$. G.C. analysis was performed on GCMS equipped with ZB-1column (30 m x 0.25mm, pressure= 20.0 kPa, detector= EI, 300 $^oC$) with helium gas as carrier.

### 4.2.3. Experimental section

**Synthesis of $[2\text{-AmpH}]_2[\{Na(H_2O)_2\}\{AlMo_6(OH)_6O_{18}\}]\cdot 4H_2O$ (1):**

Sodium molybdate (1g, 4.13 mmol) was dissolved in 35 mL of water and 10 ml of glacial acetic acid was added followed by the addition of 0.5 g of $AlCl_3\cdot 6H_2O$ (2 mmol) and 0.20 g of 2-aminopyridine ( 2 mmol). The pH of the reaction mixture was adjusted to 3.0 by dil. HCl. The resulting mixture was then stirred for 10 min (during stirring, the formation of precipitate / turbidity was dissolved by heating the reaction mixture at 70–80$^oC$ in three to four slots). The reaction mixture was then filtered and kept in open beaker for crystallization without any disturbance at room temperature. After 24hrs, colorless crystals formed, were filtered, washed with plenty of water and finally dried at room temperature. One of the single crystals, suitable for X-ray diffraction study, was selected and characterized structurally. The product obtained with Yield: 1.45 g. Anal. Calcd (%) for $AlMo_6O_{30}N_4C_{10}NaH_{32}$: C, 9.14; H, 2.45; N, 4.26. Found: C, 9.36; H, 2.49; N, 4.56. IR (KBr pellet): ($\nu/cm^{-1}$): 3329, 3171, 1658, 1622, 1541,1475, 1383, 1327, 1244, 1168, 991, 889, 829, 765, 617.

**Synthesis of $[3\text{-AmpH}]_2[HAlMo_6(OH)_6O_{18}]\cdot 4H_2O$(2)**

Sodium molybdate (1g, 4.13 mmol) was dissolved in 35mL of water and added 10 ml of glacial acetic acid followed by 0.5 g of $AlCl_3\cdot 6H_2O$ (2 mmol) and 0.20 g of 3-aminopyridine (2 mmol) were added and pH of the reaction mixture was adjusted to 3.0 by dil. HCl. The resulting mixture was then stirred for 10 min (during stirring, the formation of precipitate / turbidity was dissolved by heating the reaction mixture at 70–80 $^oC$ in three to four slots). The reaction mixture was then filtered and kept in open beaker for crystallization without any disturbance at room temperature. After 24hrs, colorless crystals formed, were filtered, washed with plenty of water and finally dried at room temperature. One of the single crystals, suitable for X-ray diffraction study, was selected and characterized structurally. The product obtained with yield: 1.15 g. Anal. Calcd (%) for $AlMo_6O_{28}N_4C_{10}NaH_{29}$: C, 9.39; H, 2.28; N, 4.38. Found: C, 9.36; H, 2.49;

N, 4.56. IR (KBr pellet): (ν/cm$^{-1}$): 3345, 3124, 1676, 1629, 1535,1478, 1389, 1322, 1248, 1176, 995, 883, 838, 762, 615.

**Synthesis of [4-AmpH]$_6$[AlMo$_6$(OH)$_6$O$_{18}$]$_2$·18H$_2$O(3)**

Sodium molybdate (1 g, 4.13 mmol) was dissolved in 35mL of water and added 10 mL of glacial acetic acid followed by 0.5g of $AlCl_3·6H_2O$ (2 mmol) and 0.20 g of 4-aminopyridine (2 mmol) were added and pH was adjusted to 3.0 by dil. HCl. The resulting mixture was stirred for 10 min (during stirring, the formation of precipitate / turbidity was dissolved by heating the reaction mixture at 70–80$^o$C in three to four slots). The reaction mixture was then filtered and kept in open beaker for crystallization without any disturbance at room temperature. After 24 h, colorless crystals formed, were filtered, washed with plenty of water and finally dried at room temperature. One of the single crystals, suitable for X-ray diffraction study, was selected and characterized structurally. The product obtained with yield: 1.73 g. Anal. Calcd (%) for $Al_2Mo_{12}O_{66}N_{12}C_{30}H_{90}$: C, 12.51; H, 3.14; N, 5.83. Found: C, 12.41; H, 3.54; N, 5.56. IR (KBr pellet): (ν/cm$^{-1}$): 3405, 3228, 1666, 1688, 1535,1463, 1335, 1338, 1217, 1189, 985, 888, 832, 768, 619.

**Synthesis of [2-AmpH]$_5$[IMo$_6$O$_{24}$]·2H$_2$O(4)**

Periodic acid (1 g, 4.13 mmol) was dissolved in 35 mL of water and added 10 mL of glacial acetic acid followed by 0.5 g of $HIO_4·6H_2O$ (2 mmol) and 0.20 g of 2-aminopyridine(2 mmol) were added and pH was adjusted to 3.0 by dil. HCl. The resulting mixture was stirred for 10 min (during stirring, the formation of precipitate / turbidity was dissolved by heating the reaction mixture at 50–60$^o$C in three to four slots). The reaction mixture was then filtered and kept in open beaker for crystallization without any disturbance at room temperature. After 24 h, colorless crystals formed, were filtered, washed with plenty of water and finally dried at room temperature. One of the single crystals from each, suitable for X-ray diffraction study, was selected and characterized structurally. The product obtained with The product obtained with yield: 1.73 g. Anal. Calcd (%) for $IMo_6O_{26}N_{10}C_{25}H_{39}$: C, 18.78; H, 2.45; N, 8.76. Found: C, 12.51; H, 2.24; N, 8.56. IR (KBr pellet): (ν/cm$^{-1}$): 3415, 3288, 1676, 1658, 1595,1453, 1355, 1398, 1277, 1149, 965, 848, 764, 615.

### 4.2.4. X-ray Data Collection and Structure Determination

Data were measured on a Bruker SMART APEX CCD area detector system [λ(Mo Kα) = 0.71073 Å], graphite monochromator, 2400 frames were recorded with an ω scan width of 0.3º, each for 5 second, a crystal detector distance of 60 mm, and a collimator of 0.5mm. The data were reduced using SAINTPLUS,[12a] the structures were solved using SHELXS-97,[12b] and refined using SHELXL-97.[12c-d] All non hydrogen atoms were refined anisotropically. We tried to locate the hydrogen atom of solvent water molecules through differential Fourier maps, but couldn't succeed. A summary of the crystallographic data and structure determination parameters for **1**–**2** are provided in Table 4.2, and Table 4.5 describes the data for compounds **3–4**; selected bond lengths and angles for common Anderson anion of **1** and **4** are listed in Tables 4.6 and 4.7.

## 4.3. Results and discussion

### 4.3.1 Synthesis of the materials

The synthesis of all the materials are possible at a particular pH (~3) and it is a simple one pot wet synthesis at room temperature, where pH of the solution is adjusted by adding dil. HCl. Here, we have isolated four ion pair compounds with Anderson based materials by altering the various cations , e.g., different amino pyridine derivatives. The generation of Anderson anion can be explained by protonation of molybdate anion followed by the series of condensation reactions and by inserting the proper central metal ion, e.g., $Al^{3+}$ and $I^{7+}$. The formation of the Anderson anion is shown in the Scheme 4.1.

$$Al^{3+} + 6MoO_4^{2-} + 6H^+ \longrightarrow [AlMo_6(OH)_6O_{18}]^{3-}$$

**Scheme 4.1** Formation of the Anderson anionic cluster $[AlMo_6(OH)_6O_{18}]^{3-}$

We have described the isolation of Anderson anion with three isomers of amino pyridine.

Infrared spectra of all the compounds (**1-4**), the presence of the broad peak at 1000-900 $cm^{-1}$ suggested that Anderson hetero poly anion unit is common in all the materials. The symmetric and asymmetric stretching of the different modes of Mo–O bonds are observed at 950-440 $cm^{-1}$. The $\nu_{sym}$ (Mo–Ot) stretching frequency is observed in the range of 947- 951 $cm^{-1}$. The broad peaks at 3460- 3100 $cm^{-1}$ are the characteristic peaks for water molecules.

### 4.3.2 X-ray crystallographic studies

**Crystal structure of $[2\text{-AmpH}]_2[\{Na(H_2O)_2\}\{AlMo_6(OH)_6O_{18}\}]\cdot 4H_2O$ (1)**

Compound **1** crystallizes in centrosymmteric triclinic *P-1* space group and the asymmetric unit of the crystal structure of $[2\text{-AmpH}]_2[\{Na(H_2O)_2\}\{AlMo_6(OH)_6O_{18}\}]\cdot 4H_2O$ (**1**) reveals the presence of half of the Anderson cluster , which supports the sodium aqua complex; two molecules of protonated 2-aminopyridine exist for charge compensation. The relevant thermal ellipsoidal plot is shown in Fig. 4.2. In the full molecule of **1**, the sodium ion of complex $[Na(H_2O)_2]^+$ , is coordinated with oxo group of the Anderson anion so that the total cluster moiety consists of –2 charge, which is counter balanced by two protonated 2-aminopyridine molecules as presented in Fig. 4.3. The observed C–C and C–N bond lengths and angles of the compound **1** are in good agreement with those reported in the literature.[13] As well as the observed Mo–O bond lengths and angles of the compound **1** also in good agreement with those reported in the literature for similar compounds.[5] The geometry around each sodium ion in sodium-aqua complex is a distorted octahedron as shown in Fig.4.3. In the crystal structure, 1-D coordination polymer is formed, that involves sodium aqua complex and the $[AlMo_6(OH)_6O_{18}]^{3-}$ heteropolyanion as shown in Fig.4.4. The non-covalent interactions between lattice water molecules and coordinated water molecules leads to supramolecular chainlike arrangement as shown in Fig. 4.5, in which Na coordinated water molecule (O13) and solvent water molecule (O14) are involved in O···H–O interactions with O11 and O2 of Anderson anion with distances of 2.342 Å and 1.867 Å respectively. The hydrogen bonding situations around the organic cation and Anderson moiety of $[2\text{-AmpH}]_2[\{Na(H_2O)_2\}\{AlMo_6(OH)_6O_{18}\}]\cdot 4H_2O$ (1) are shown in the Figs. 4.6 (a-c). The relevant hydrogen bonding distances and angles are shown in Table 4.1. The crystallographic data is available at Table 4.2.

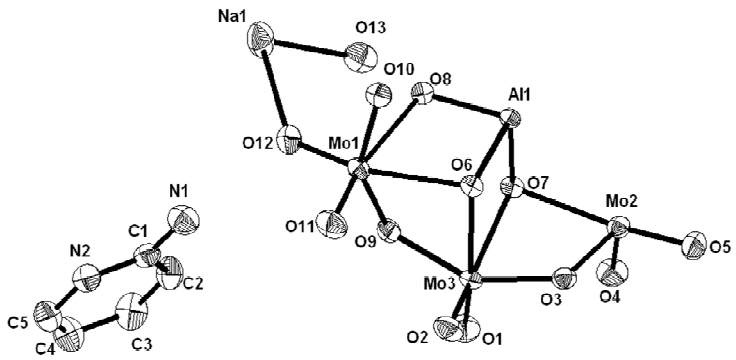


**Fig. 4.2** ORTEP diagram of the asymmetric unit of [2-AmpH]$_2$[{Na(H$_2$O)$_2$}{AlMo$_6$(OH)$_6$O$_{18}$}]·4H$_2$O (**1**) with 30% probability (hydrogen atoms and solvent water molecules are omitted for clarity).

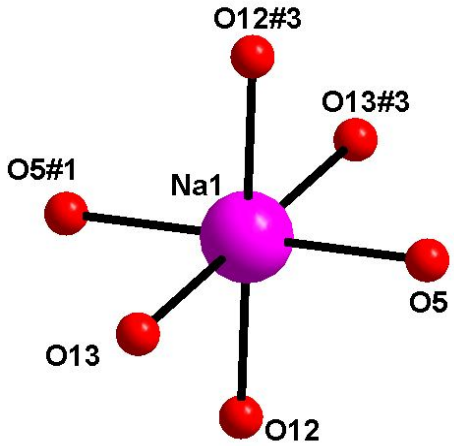


**Fig. 4.3** Octahedral geometry of sodium complex in which two of the sights are occupied by oxygen atom of the Anderson anion in compound **1.** Color code: Na, Purple, O, red;

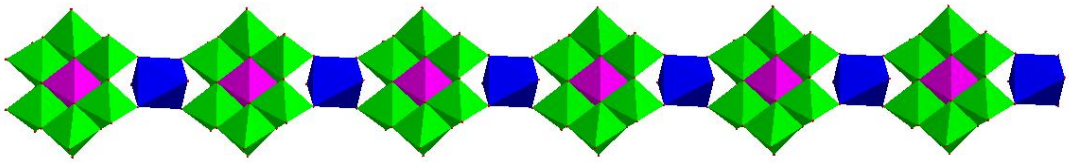

**Fig. 4.4** Picture of 2-dimensional coordination polymer of [2-AmpH]$_2$[{Na(H$_2$O)$_2$}{AlMo$_6$(OH)$_6$O$_{18}$}]·4H$_2$O (1), Na polyhedra, blue; aluminium, Purple and Molybdenum, green.

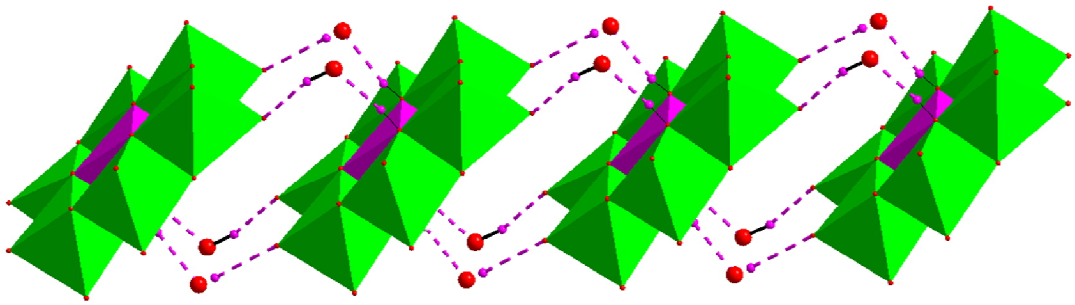

**Fig. 4.5** 1-Dimensional chain produced because of the O···H–O interaction between lattice water molecules and the Anderson anionic cluster in compound **1.** Al polyhedra, purple; Mo polyhedra, green; O, red; H, purple;

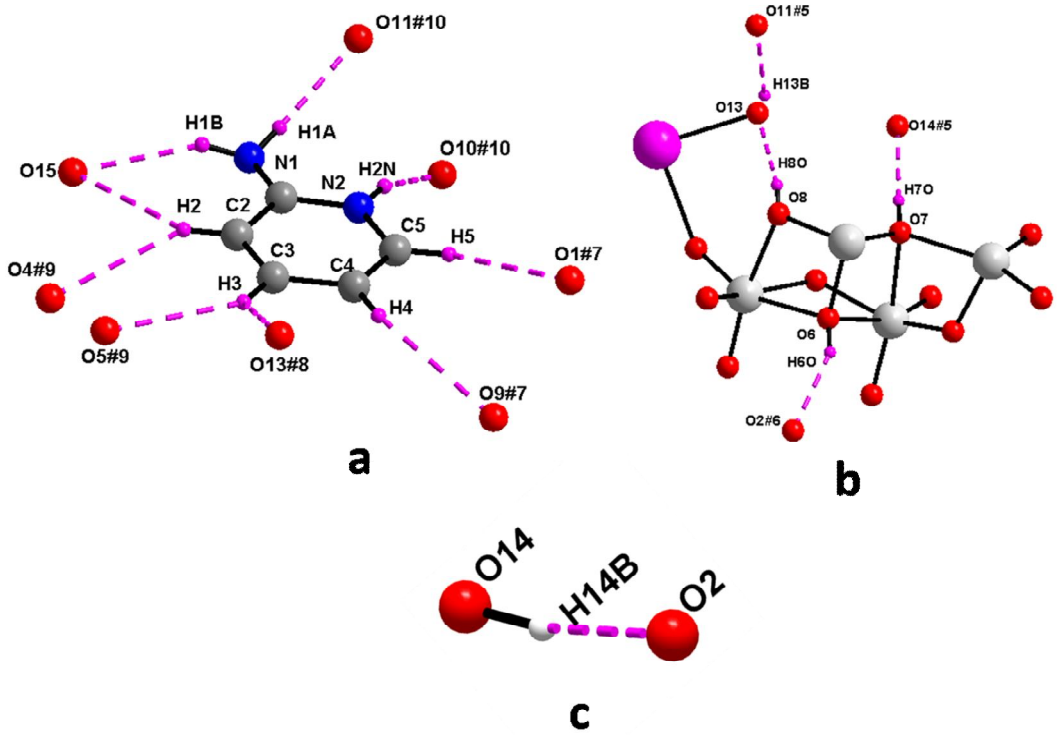


**Fig.4.6** Hydrogen bonding situation around a) {N1N2}, b){And} and c) water motifs in $[2\text{-AmpH}]_2[\{Na(H_2O)_2\}\{AlMo_6(OH)_6O_{18}\}]\cdot 4H_2O$ (1), Color codes: Na, magenta, Al, gray; Mo, grey, C, medium grey; O, red, H, purple. Symmetry codes: #1, -x,-y+1,-z ; #2, x,y,z-1; #3, -x,-y+1,-z+1; #4, x,y,z+1; #5, x-1,y,z ; #6, -x+1,-y+1,-z ; #7, -x+1,-y,-z+1; #8, -x,-y,-z+1; #9, -x,-y,-z; #10, -x+1,-y+1,-z+1;

**Table 4.1** Hydrogen bond distances and angles for compound **1** [Å and °].

| D–H···A | d(D–H) | d(H···A) | d(D···A) | <(DHA) |
|---|---|---|---|---|
| O(13)-H(13B)...O(11)#5 | 0.52(3) | 2.34(3) | 2.826(4) | 156(5) |
| O(7)-H(7O)...O(14)#5 | 0.83 | 1.84 | 2.670(3) | 173.2 |
| O(6)-H(6O)...O(2)#6 | 0.87 | 2.13 | 2.936(3) | 154.6 |
| C(4)-H(4)...O(9)#7 | 0.93 | 2.67 | 3.451(4) | 142.1 |
| C(3)-H(3)...O(13)#8 | 0.93 | 2.80 | 3.470(4) | 130.0 |
| C(3)-H(3)...O(5)#9 | 0.93 | 2.63 | 3.454(4) | 147.8 |
| C(2)-H(2)...O(4)#9 | 0.93 | 2.58 | 3.401(3) | 147.2 |
| C(5)-H(5)...O(1)#7 | 0.93 | 2.72 | 3.489(4) | 140.4 |
| C(2)-H(2)...O(15) | 0.93 | 2.81 | 3.527(4) | 134.6 |
| N(1)-H(1B)...O(15) | 0.85 | 2.28 | 3.063(3) | 152.8 |
| N(1)-H(1A)...O(11)#10 | 0.84 | 2.24 | 3.074(3) | 172.9 |
| N(2)-H(2N)...O(10)#10 | 0.85(4) | 1.91(4) | 2.724(3) | 160(4) |
| O(14)-H(14B)...O(2) | 0.93 | 1.87 | 2.775(3) | 164.3 |

Symmetry transformations used to generate equivalent atoms:

#1, -x,-y+1,-z; #2, x,y,z-1; #3, -x,-y+1,-z+1; #4, x,y,z+1; #5, x-1,y,z; #6, -x+1,-y+1,-z; #7, -x+1,-y,-z+1; #8, -x,-y,-z+1; #9, -x,-y,-z; #10, -x+1,-y+1,-z+1;

**Table 4.2** Crystal data and structure refinement for compounds **1** and **2**

| Entry | **1** | **2** |
|---|---|---|
| Molecular formula | $C_{10}H_{24}AlMo_6N_4NaO_{30}$ | $C_{10}H_{28}Al\ Mo_6N_4O_{28}$ |
| Formula weight | 1305.94 | 1254.98 |
| T (K) | 298(2) | 298(2) |
| λ (Å) | 0.71073 | 0.71073 |
| Crystal system | Triclinic | Triclinic |
| Space group, | P-1 | P-1 |
| Z | 1 | 1 |
| a (Å) | 7.9443(16) | 7.8799(16) |
| b (Å) | 10.250(2) | 10.135(2) |
| c (Å) | 10.869(2) | 10.353(2) |
| α (deg) | 98.88(3) | 88.20(3) |
| β (deg) | 99.28(3) | 78.74(3) |
| γ (deg) | 90.65(3) | 88.05(3) |
| Volume ($Å^3$) | 862.4(3) | 810.2(3) |
| ρ ($g\ cm^{-3}$) | 2.515 | 2.572 |
| μ ($mm^{-1}$) | 2.264 | 2.388 |
| F (000) | 628 | 605 |
| Crystal size ($mm^3$) | 0.38 x 0.24 x 0.14 | 0.36x0.22x0.16 |
| Θ for data collection (º) | 1.92 to 26.11 | 2.01 to 25.88 |
| Reflections collected/unique | 8924/3365 | 8094 / 3079 |
| R(int) | 0.0205 | 0.0146 |
| Data/restraints/parameters | 3365 / 0 / 251 | 3079 / 0 / 239 |
| Goodness of fit on $F^2$ | 1.134 | 1.032 |
| $R_1$,$wR_2$ [ I > 2 sigma(I)] | 0.0220,0.0592 | 0.0351 ,0.0912 |
| R indices (all data) | 0.0227, 0.0596 | 0.0242, 0.0647 |
| Largest diff. Peak and hole ($e.Å^{-3}$) | 0.519/-0.822 | 0.721 , -0.639 |

**Crystal structure of $[3\text{-AmpH}]_2[HAlMo_6(OH)_6O_{18}]\cdot 4H_2O$(2)**

Compound **2** also crystallizes in centrosymmteric, and space group *P-1*. The crystal structure consist of half of the Anderson anion and one molecule of the protonated 3-aminopyridine and two lattice water molecules. Thermal ellipsoidal diagram is shown in Fig.4.7. In the present molecule, Anderson anion is itself mono-protonated so that the total charge of the molecule is counter balanced by two molecules of protonated 3-aminopyridine. In the crystal structure, the C–C, C–N and Mo–O bond lengths are in good agreement with those reported for similar compounds in literature.[13,5] The full crystallographic information is described in Table 4.2.

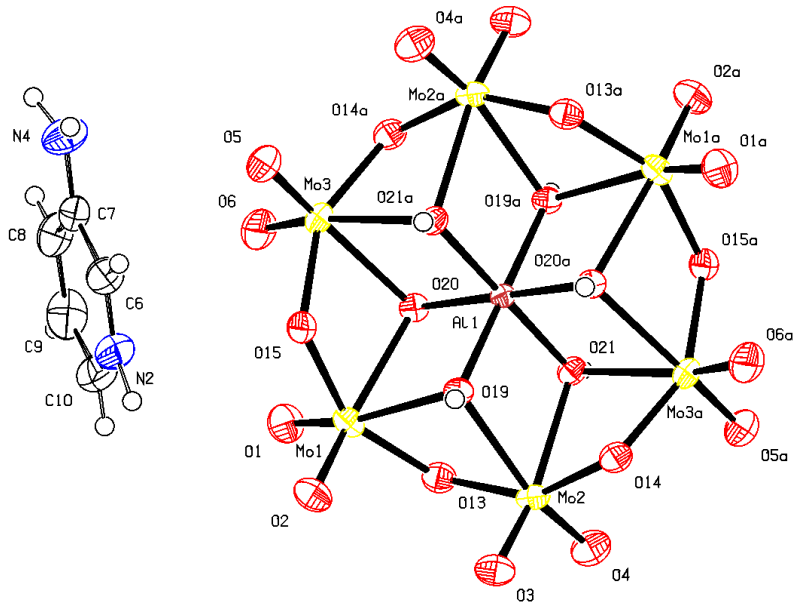


**Fig. 4.7** ORTEP diagram of the asymmetric part of $[3\text{-AmpH}]_2[HAlMo_6(OH)_6O_{18}]\cdot 4H_2O$ (**2**) with 50% probability (solvent water molecules are omitted for clarity).

In this compound, two lattice water molecules (O25 and O28) interact with surrounding clusters resulting in the formation of 2-dimensional network as shown in Fig 4.8 because of O···H–O supramolecular interaction with the range of hydrogen bond distances lie between 2.2 Å and 2.6 Å. Hydrogen bonding distances and angles are provided in Table 4.3. The hydrogen bonding situation around the cation, Anderson anionic cluster and water are shown in Fig. 4.8.

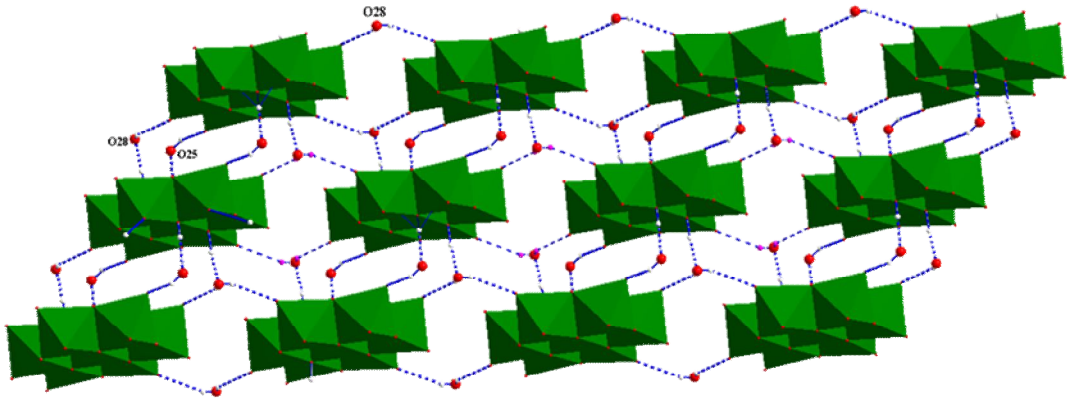


**Fig. 4.8** 2-Dimensional framework because of O···H–O interaction among the lattice water molecules and Anderson cluster. Green polyhedra are shown for Anderson anion and oxygen in red color.

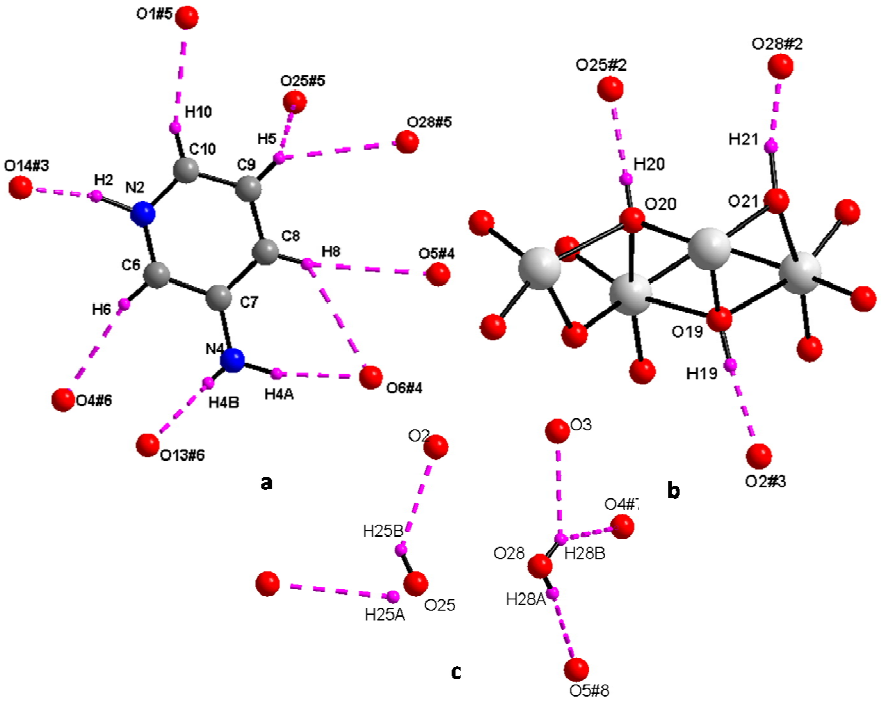


**Fig. 4.9** Hydrogen bonding environment around a) {N2N4}, c){Anderson},c) water moieties for $[3\text{-AmpH}]_2[HAlMo_6(OH)_6O_{18}]\cdot 4H_2O$ (**2**) . Symmetry codes: #1,-x,-y+1,-z+1; #2, x-1, y, z; #3 -x+1,-y+1,-z+1; #4, -x,-y,-z+2; #5, -x+1,-y,-z+1; #6, x, y, z+1; #7, -x+1,-y+1,-z; #8, x+1, y, z-1 ; Color codes: O, red; C, grey; H, Purple;

**Table 4.3** Hydrogen bonding distances and angles for compound **2** [Å and º].

| D-H···A | d(D–H) | d(H···A) | d(D···A) | <(DHA) |
|---|---|---|---|---|
| O(21)-H(21)...O(28)#2 | 1.08 | 1.61 | 2.667(4) | 167.0 |
| O(20)-H(20)...O(25)#2 | 0.81 | 1.82 | 2.638(4) | 178.5 |
| O(19)-H(19)...O(2)#3 | 0.94 | 1.85 | 2.783(3) | 174.2 |
| C(8)-H(8)...O(5)#4 | 0.93 | 2.78 | 3.685(5) | 165.7 |
| C(8)-H(8)...O(6)#4 | 0.93 | 2.85 | 3.520(5) | 129.5 |
| C(9)-H(5)...O(25)#5 | 0.93 | 2.89 | 3.465(5) | 121.4 |
| C(9)-H(5)...O(28)#5 | 0.93 | 2.76 | 3.550(5) | 143.0 |
| C(10)-H(10)...O(1)#5 | 0.93 | 2.35 | 3.231(5) | 158.9 |
| N(2)-H(2)...O(14)#3 | 1.08 | 1.73 | 2.784(4) | 164.4 |
| C(6)-H(6)...O(4)#6 | 0.93 | 2.46 | 3.316(4) | 152.7 |
| N(4)-H(4B)...O(13)#6 | 0.74(4) | 2.29(4) | 2.992(4) | 159(4) |
| N(4)-H(4A)...O(6)#4 | 0.97 | 2.03 | 2.974(4) | 163.5 |
| O(25)-H(25B)...O(2) | 0.80(8) | 2.27(8) | 2.918(5) | 138(7) |
| O(25)-H(25A)...O(1)#5 | 0.55(6) | 2.58(6) | 3.032(5) | 142(8) |
| O(28)-H(28B)...O(3) | 0.77 | 2.24 | 2.868(4) | 139.1 |
| O(28)-H(28B)...O(4)#7 | 0.77 | 2.76 | 3.350(4) | 135.4 |
| O(28)-H(28A)...O(5)#8 | 0.66(6) | 2.30(6) | 2.925(4) | 158(7) |

Symmetry transformations used to generate equivalent atoms:
#1, -x,-y+1,-z+1; #2, x-1,y,z; #3, -x+1,-y+1,-z+1; #4, -x,-y,-z+2; #5, -x+1,-y,-z+1; #6, x,y,z+1; #7, -x+1,-y+1,-z; #8 x+1,y,z-1.

**Crystal structure of $[4\text{-AmpH}]_6[AlMo_6(OH)_6O_{18}]_2 \cdot 18H_2O$ (3)**

Compound **3** crystallizes in the non-centrosymmteric orthorombic space group Pna2(1). The asymmetric unit of the crystal structure of **3** is composed of two molecules of Anderson anion, six protonated 4–aminopyridine molecules and eighteen lattice water molecules. Oak Ridge Thermal Ellipsoidal Plot of the compound **4** is presented in the Fig. 4.10. The total crystallographic information is presented in the Table 4.4. As a result of the O···O weak interactions among the water molecules and Anderson anionic cluster, a 2- dimenaional frame work is formed; it can be described as Anderson cluster in the water pool as shown in Fig. 4.11.

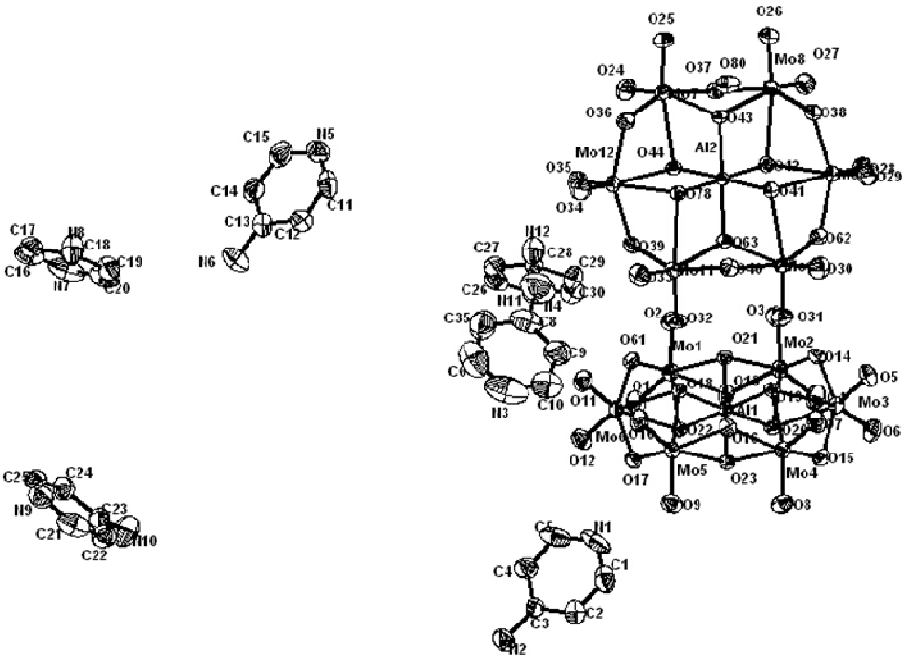


**Fig.4.10** Thermal Diagram of the compound **4** with 30 % probability (Hydrogen atoms and solvent molecules are not shown for clarity)

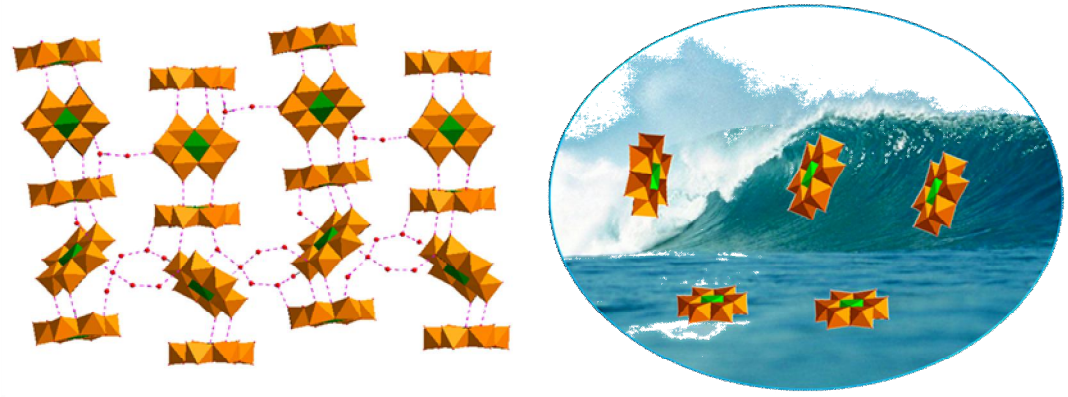

**Fig. 4.11 (**Left) 2-dimensional network due to O···O interaction among the Anderson anionic cluster and lattice water molecules, (right); Anderson cluster is shown as brown polyhedral.

Eighteen lattice water molecules are non covalently interacted with each other through O···O interactions resulting in the formation of a 2-dimensional network with

O···O separation range of 2.45 to 2.78 Å (Fig. 4.12.), in which layers arrange in a helical manner.

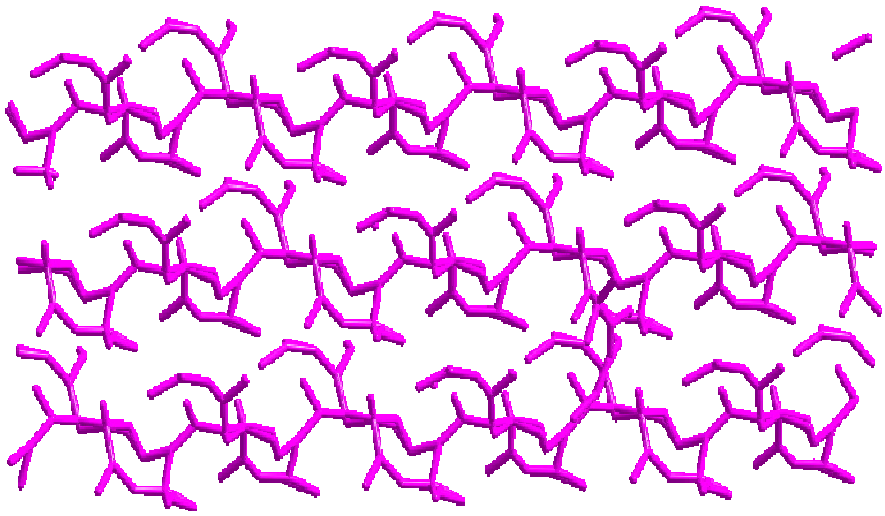

**Fig 4.12** 2-Dimensional network due to O···O interaction among the lattice water molecules (wire frame representation.)

**Crystal structure of $[2\text{-AmpH}]_5[IMo_6O_{24}]\cdot H_2O$ (4)**

$[2\text{-AmpH}]_5[IMo_6O_{24}]\cdot H_2O$ **(4)** crystallizes in centrosymmteric triclinic space group *P-1*. In the present case, Anderson anion is isolated with iodine as a central atom, which has a +7 oxidation state resulting in overall charge of -5 for the cluster anion. This is counter balanced by five molecules of protonated 2-aminopyridine (2-ampH). The cluster unit of the crystal structure of **4** is shown in Fig. 4.13 (cations and water molecule are omitted for clarity).

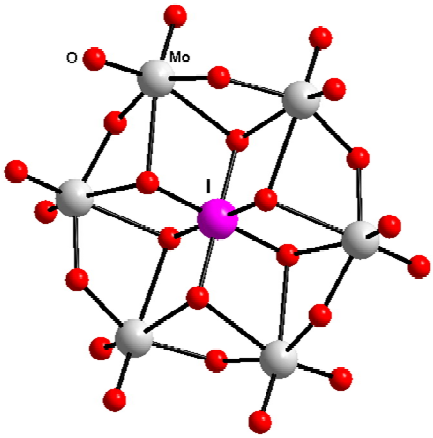


**Fig. 4.13** The Anderson anion unit of the compound **5** with ball and stick representation. (Iodine is the central atom)

In the crystal structure, lattice water molecule (O35) interacts with both Anderson anion and 2-ampH by non covalent interactions (O···O, C–H···O and N–H···O) leading to 2-dimensional network as shown in the Fig.4.14. Hydrogen bonds and angles corresponding to this network are available in Table 4.4 The possible C–H···O hydrogen bonding situation around the each cation, labeled as {N1N6}, {N2N7}, {N3N8}, {N4N9} and {N5N10} are shown in the Fig. 4.15 and their distances and angles are tabulated in Table 4.4. The bond lengths and angles of the Anderson anionic cluster are in good agreement with reported literature.[14]

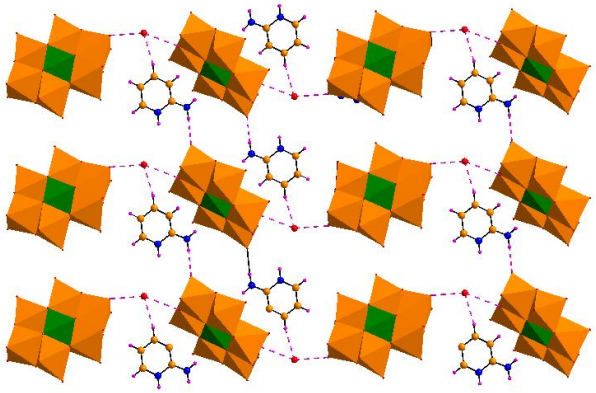

**Fig.4.14** Supramolecular interaction of lattice water molecule with surrounding Anderson cluster and counter cation (2-ampH) due to O···O, C–H···O and N–H···O interactions. Color codes: Anderson cluster is shown as brown polyhedra, C, orange, N, blue, O, red, H, Purple.

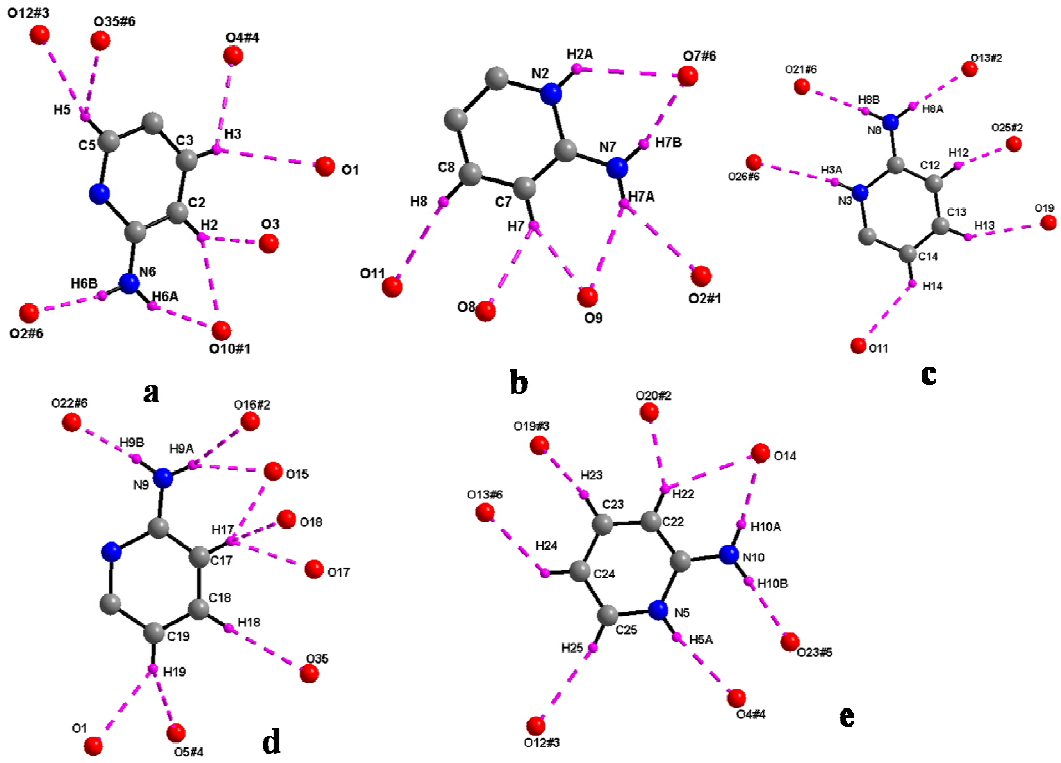


**Fig. 4.15** The hydrogen bonding environment around the each cation a) {N1N6}, b) {N2N7}, c) {N3N8}, d) {N4N9} and e) {N5N10} of the compound **4.** Color code: C, medium grey; N, blue; O, red, H, purple. Symmetry transformations used to generate equivalent atoms: #1, -x+1,-y,-z; #2, -x+1,-y+1,-z+1; #3, x-1, y+1, z; #4, -x+1,-y+1,-z; #5, x, y+1, z; #6, x-1, y, z.

**Table 4.4** Hydrogen bond distances and angles for compound **4** [Å and º].

| D–H···A | d(D–H) | d(H···A) | d(D···A) | <(DHA) |
|---|---|---|---|---|
| C(25)-H(25)...O(12)#3 | 0.93 | 2.54 | 3.452(12) | 166.6 |
| N(5)-H(5A)...O(4)#4 | 0.86 | 2.36 | 3.153(11) | 154.0 |
| N(10)-H(10B)...O(23)#5 | 0.86 | 2.09 | 2.924(9) | 165.0 |
| N(10)-H(10A)...O(14) | 0.86 | 1.98 | 2.812(10) | 161.2 |
| C(22)-H(22)...O(14) | 0.93 | 2.70 | 3.412(12) | 133.9 |
| C(22)-H(22)...O(20)#2 | 0.93 | 2.06 | 2.856(10) | 143.1 |
| C(23)-H(23)...O(19)#3 | 0.93 | 2.39 | 3.045(13) | 127.4 |
| C(24)-H(24)...O(13)#6 | 0.93 | 2.44 | 3.134(12) | 131.4 |
| C(19)-H(19)...O(5)#4 | 0.93 | 2.62 | 3.355(13) | 136.9 |
| C(19)-H(19)...O(1) | 0.93 | 2.58 | 3.351(13) | 140.6 |
| C(18)-H(18)...O(35) | 0.93 | 2.61 | 3.47(2) | 154.7 |
| C(17)-H(17)...O(17) | 0.93 | 2.31 | 3.028(10) | 133.2 |
| C(17)-H(17)...O(18) | 0.93 | 2.67 | 3.388(10) | 134.5 |
| C(17)-H(17)...O(15) | 0.93 | 2.14 | 2.955(10) | 144.9 |
| N(9)-H(9A)...O(15) | 0.86 | 2.17 | 2.918(9) | 144.9 |
| N(9)-H(9A)...O(16)#2 | 0.86 | 2.66 | 3.386(10) | 143.6 |
| N(9)-H(9B)...O(22)#6 | 0.86 | 1.95 | 2.803(10) | 172.5 |
| N(3)-H(3A)...O(26)#6 | 0.86 | 2.72 | 3.518(12) | 155.5 |
| C(14)-H(14)...O(11) | 0.93 | 2.60 | 3.274(12) | 129.9 |
| C(13)-H(13)...O(19) | 0.93 | 2.57 | 3.385(11) | 147.1 |
| C(12)-H(12)...O(25)#2 | 0.93 | 1.91 | 2.811(9) | 164.0 |
| N(8)-H(8A)...O(13)#2 | 0.86 | 2.13 | 2.979(10) | 169.7 |
| N(8)-H(8B)...O(21)#6 | 0.86 | 2.16 | 3.005(10) | 166.9 |
| C(8)-H(8)...O(11) | 0.93 | 2.49 | 3.364(11) | 155.8 |
| C(7)-H(7)...O(8) | 0.93 | 2.63 | 3.308(8) | 130.4 |
| C(7)-H(7)...O(9) | 0.93 | 2.15 | 3.028(9) | 156.0 |
| N(7)-H(7A)...O(9) | 0.86 | 2.45 | 3.188(9) | 144.6 |
| N(7)-H(7A)...O(2)#1 | 0.86 | 2.58 | 3.319(10) | 144.1 |
| N(7)-H(7B)...O(7)#6 | 0.86 | 2.01 | 2.817(9) | 156.7 |
| N(2)-H(2A)...O(7)#6 | 0.86 | 2.71 | 3.340(11) | 131.4 |
| N(6)-H(6B)...O(2)#6 | 0.86 | 2.09 | 2.937(9) | 169.4 |
| N(6)-H(6A)...O(10)#1 | 0.86 | 2.05 | 2.862(9) | 158.2 |
| C(2)-H(2)...O(10)#1 | 0.93 | 2.39 | 3.167(9) | 141.3 |
| C(2)-H(2)...O(3) | 0.93 | 2.10 | 2.895(9) | 142.6 |
| C(3)-H(3)...O(1) | 0.93 | 2.81 | 3.505(11) | 132.5 |
| C(3)-H(3)...O(4)#4 | 0.93 | 2.58 | 3.214(11) | 125.9 |
| C(5)-H(5)...O(35)#6 | 0.93 | 2.66 | 3.344(19) | 130.4 |
| C(5)-H(5)...O(12)#3 | 0.93 | 2.49 | 3.224(11) | 135.4 |

Symmetry transformations used to generate equivalent atoms:
#1 -x+1,-y,-z; #2 -x+1,-y+1,-z+1; #3 x-1,y+1,z; #4, -x+1,-y+1,-z; #5, x,y+1,z; #6, x-1,y,z.

**Table 4.5** Crystal data and structure refinement for compounds **3** and **4**

| Entry | **3** | **4** |
|---|---|---|
| Molecular formula | $Al_2Mo_{12}O_{66}N_{12}C_{30}H_{90}$ | $C_{25}H_{35}IMo_6N_{10}O_{25}$ |
| Formula weight | 2880.3 | 1578.17 |
| Temperature (K) | 298(2) | 298(2) |
| Wavelength (Å) | 0.71073 | 0.71073 |
| Crystal system | Orthorhombic | Triclinic |
| Space group | Pna2(1) | P-1 |
| a (Å) | 29.508(2) | 9.934(2) |
| b (Å) | 12.6221(9) | 10.372(2) |
| c (Å) | 22.9265(16) | 23.293(5) |
| α (º) | 90 | 85.44(3) |
| β (º) | 90 | 79.99(3) |
| γ (º) | 90 | 68.78(3) |
| Volume ($Å^3$) | 8539.0(10) | 2201.5(8) |
| Z | 4 | 2 |
| ρ ($g\ cm^{-3}$) | 2.515 | 2.381 |
| μ ($mm^{-1}$) | 2.264 | 2.457 |
| F (000) | 628 | 1520 |
| Crystal size ($mm^3$) | 0.38 x 0.24 x 0.14 | 0.12x0.10x0.08 |
| Θ range for data collection (º) | 1.92 to 26.11 | 1.78 to 26.11 |
| Reflections collected/unique | 8924/3365 | 22929 / 8647 |
| R(int) | 0.0205 | 0.0424 |
| Data/restraints/parameters | 3365 / 0 / 251 | 8647 / 0 / 607 |
| Goodness of fit on $F^2$ | 1.134 | 1.105 |
| Final R indices [ I > 2 sigma(I)] | 0.0220,0.0592 | 0.0599 ,0.1192 |
| R indices (all data) | 0.0227, 0.0596 | 0.0841, 0.1286 |
| Largest diff. Peak and hole ($e.Å^{-3}$) | 0.519/-0.822 | 1.346 , -1.046 |

Table 4.6 Selected bond lengths for alkali complex of Anderson anionic cluster [Å] and angles [º] for 1

| | | | |
|---|---|---|---|
| Mo(1)-O(12) | 1.7085(18) | Mo(1)-O(11) | 1.7115(18) |
| Mo(1)-O(9) | 1.9153(18) | Mo(1)-O(10) | 1.9423(17) |
| Mo(1)-O(8) | 2.2806(17) | Mo(1)-O(6) | 2.3323(17) |
| Mo(2)-O(4) | 1.7023(18) | Mo(2)-O(5) | 1.7095(18) |
| Mo(2)-O(3) | 1.9257(17) | Mo(2)-O(7) | 2.2874(17) |
| Mo(3)-O(1) | 1.7006(18) | Mo(3)-O(2) | 1.7207(18) |
| Mo(3)-O(3) | 1.8985(17) | Mo(3)-O(9) | 1.9520(17) |
| Mo(3)-O(7) | 2.2936(16) | Mo(3)-O(6) | 2.3049(16) |
| Al(1)-O(8) | 1.8749(17) | Al(1)-O(7) | 1.8993(16) |
| Al(1)-O(6) | 2.2874(17) | O(12)-Na(1) | 2.4596(19) |
| Na(1)-O(13) | 2.379(3) | | |
| Bond angles (º) | | | |
| O(12)-Mo(1)-O(11) | 106.04(10) | O(12)-Mo(1)-O(9) | 99.09(9) |
| O(11)-Mo(1)-O(9) | 100.11(9) | O(12)-Mo(1)-O(10) | 101.52(9) |
| O(11)-Mo(1)-O(10) | 96.89(9) | O(9)-Mo(1)-O(10) | 48.41(7) |
| O(12)-Mo(1)-O(8) | 90.55(8) | O(11)-Mo(1)-O(8) | 161.86(8) |
| O(9)-Mo(1)-O(8) | 84.05(7) | O(10)-Mo(1)-O(8) | 72.12(7) |
| O(12)-Mo(1)-O(6) | 156.24(7) | O(11)-Mo(1)-O(6) | 97.29(8) |
| O(9)-Mo(1)-O(6) | 71.90(7) | O(10)-Mo(1)-O(6) | 79.71(7) |
| O(8)-Mo(1)-O(6) | 67.02(6) | O(4)-Mo(2)-O(5) | 106.98(10) |
| O(4)-Mo(2)-O(3) | 101.45(9) | O(5)-Mo(2)-O(3) | 97.93(8) |
| O(4)-Mo(2)-O(7) | 93.84(8) | O(5)-Mo(2)-O(7) | 158.39(8) |
| O(3)-Mo(2)-O(7) | 71.68(7) | O(1)-Mo(3)-O(2) | 106.31(10) |
| O(1)-Mo(3)-O(3) | 101.32(9) | O(2)-Mo(3)-O(3) | 99.87(9) |
| O(1)-Mo(3)-O(9) | 95.37(9) | O(2)-Mo(3)-O(9) | 100.14(9) |
| O(3)-Mo(3)-O(9) | 149.08(7) | O(1)-Mo(3)-O(7) | 96.23(9) |
| O(2)-Mo(3)-O(7) | 157.23(8) | O(3)-Mo(3)-O(7) | 71.98(7) |
| O(9)-Mo(3)-O(7) | 80.53(7) | O(1)-Mo(3)-O(6) | 160.72(8) |
| O(2)-Mo(3)-O(6) | 90.50(8) | O(3)-Mo(3)-O(6) | 84.58(7) |
| O(9)-Mo(3)-O(6) | 71.93(7) | O(7)-Mo(3)-O(6) | 67.90(6) |
| O(8)-Al(1)-O(7) | 95.30(8) | O(8)-Al(1)-O(6) | 84.49(8) |
| O(7)-Al(1)-O(6) | 84.68(7) | Al(1)-O(8)-Mo(1) | 105.80(8) |
| Al(1)-O(7)-Mo(2) | 103.46(7) | Al(1)-O(7)-Mo(3) | 104.13(7) |
| Mo(2)-O(7)-Mo(3) | 92.14(6) | Mo(3)-O(3)-Mo(2) | 119.24(9) |
| Mo(1)-O(12)-Na(1) | 135.67(10) | Mo(1)-O(9)-Mo(3) | 118.97(8) |
| Al(1)-O(6)-Mo(3) | 103.24(7) | Al(1)-O(6)-Mo(1) | 102.58(7) |
| Mo(3)-O(6)-Mo(1) | 91.85(6) | | |

**Table 4.7** Selected bond lengths of Anderson anionic cluster with iodine central atom [Å] and angles [º] for 4

| | | | |
|---|---|---|---|
| I(1)-O(8) | 1.872(5) | I(1)-O(9) | 1.880(5) |
| I(1)-O(10) | 1.891(5) | Mo(3)-O(1) | 1.672(6) |
| Mo(3)-O(2) | 1.705(6) | Mo(3)-O(3) | 1.915(5) |
| Mo(3)-O(7) | 1.933(5) | Mo(3)-O(8) | 2.328(5) |
| Mo(4)-O(11) | 1.686(6) | Mo(4)-O(12) | 1.706(6) |
| Mo(4)-O(7) | 1.930(5) | Mo(4)-O(23) | 1.936(5) |
| Mo(4)-O(10) | 2.370(5) | Mo(4)-O(8) | 2.374(5) |
| Mo(5)-O(5) | 1.686(6) | Mo(5)-O(4) | 1.699(5) |
| Mo(5)-O(3) | 1.927(5) | I(2)-O(16) | 1.875(5) |
| I(2)-O(18) | 1.878(5) | I(2)-O(15) | 1.880(5) |
| Mo(6)-O(19) | 1.683(6) | Mo(6)-O(20) | 1.704(6) |
| Mo(6)-O(21) | 1.917(6) | Mo(6)-O(18) | 2.349(5) |
| Mo(7)-O(26) | 1.685(7) | Mo(7)-O(22) | 1.703(7) |
| Mo(7)-O(21) | 1.921(6) | Mo(7)-O(17) | 1.932(6) |
| Mo(7)-O(18) | 2.304(5) | Mo(7)-O(16) | 2.358(6) |
| Mo(8)-O(13) | 1.694(6) | Mo(8)-O(14) | 1.707(6) |
| Mo(8)-O(25) | 1.907(6) | Mo(8)-O(17) | 1.913(6) |
| Mo(8)-O(16) | 2.311(5) | Mo(8)-O(15) | 2.333(5) |
| Bond Angles (º) | | | |
| O(8)-I(1)-O(9) | 91.6(2) | O(8)-I(1)-O(10) | 87.6(2) |
| O(9)-I(1)-O(10) | 87.5(2) | O(1)-Mo(3)-O(2) | 107.0(3) |
| O(1)-Mo(3)-O(3) | 98.2(3) | O(2)-Mo(3)-O(3) | 102.8(3) |
| O(1)-Mo(3)-O(7) | 99.8(3) | O(2)-Mo(3)-O(7) | 95.2(3) |
| O(3)-Mo(3)-O(7) | 149.5(2) | O(1)-Mo(3)-O(8) | 95.5(3) |
| O(2)-Mo(3)-O(8) | 156.4(3) | O(3)-Mo(3)-O(8) | 80.20(19) |
| O(7)-Mo(3)-O(8) | 73.72(19) | O(11)-Mo(4)-O(12) | 106.7(3) |
| O(11)-Mo(4)-O(7) | 101.3(3) | O(12)-Mo(4)-O(7) | 96.9(3) |
| O(11)-Mo(4)-O(23) | 97.7(2) | O(12)-Mo(4)-O(23) | 101.3(2) |
| O(7)-Mo(4)-O(23) | 148.5(2) | O(11)-Mo(4)-O(10) | 156.6(2) |
| O(12)-Mo(4)-O(10) | 96.1(2) | O(7)-Mo(4)-O(10) | 80.61(19) |
| O(23)-Mo(4)-O(10) | 72.15(19) | O(11)-Mo(4)-O(8) | 91.5(2) |
| O(12)-Mo(4)-O(8) | 160.8(3) | O(7)-Mo(4)-O(8) | 72.68(19) |
| O(23)-Mo(4)-O(8) | 82.04(19) | O(10)-Mo(4)-O(8) | 66.63(16) |
| O(5)-Mo(5)-O(4) | 107.2(3) | O(5)-Mo(5)-O(3) | 99.4(3) |
| O(4)-Mo(5)-O(3) | 100.5(2) | I(1)-O(8)-Mo(3) | 102.7(2) |
| I(1)-O(8)-Mo(4) | 103.1(2) | Mo(3)-O(8)-Mo(4) | 89.55(17) |
| Mo(3)-O(3)-Mo(5) | 119.0(3) | I(1)-O(10)-Mo(4) | 102.6(2) |
| Mo(4)-O(7)-Mo(3) | 118.0(3) | O(16)-I(2)-O(18) | 87.4(2) |
| O(16)-I(2)-O(15) | 87.9(2) | O(18)-I(2)-O(15) | 92.6(2) |
| O(19)-Mo(6)-O(20) | 107.1(3) | O(19)-Mo(6)-O(21) | 101.1(3) |
| O(20)-Mo(6)-O(21) | 99.6(3) | O(19)-Mo(6)-O(18) | 95.4(3) |
| O(20)-Mo(6)-O(18) | 157.3(3) | O(21)-Mo(6)-O(18) | 73.1(2) |
| O(26)-Mo(7)-O(22) | 107.0(4) | O(26)-Mo(7)-O(21) | 100.6(3) |
| O(22)-Mo(7)-O(21) | 96.8(3) | O(26)-Mo(7)-O(17) | 97.9(3) |
| O(22)-Mo(7)-O(17) | 99.8(3) | O(21)-Mo(7)-O(17) | 150.3(2) |
| O(26)-Mo(7)-O(18) | 93.5(3) | O(22)-Mo(7)-O(18) | 159.0(3) |

**4.4. Catalysis**

Catalytic activities of all the compounds (1-4) have been performed in the reaction of oxidation of styrene to give the selective major product benzaldehyde. Styrene epoxide is another product formed in this reaction (as a minor product). We have succeeded to get 95-99% conversion of styrene at room temperature by using all the four catalysts. (% of conversions was determined by GC-MS*). The optimized condition for the conversion of styrene to benzaldehyde is 1:3 molar ratio of styrene and $H_2O_2$ with 0.25mg of the catalyst for 24hrs at room temperature. The full details of the reaction are provided in the caption of Table 4.8. The present reaction condition is environmentally benign because hydrogen peroxide is an oxidant so that the side product will be water, which is not harmful to environment and all the reactions are solvent free reactions. In green chemistry, it is being explored in several areas.[15]

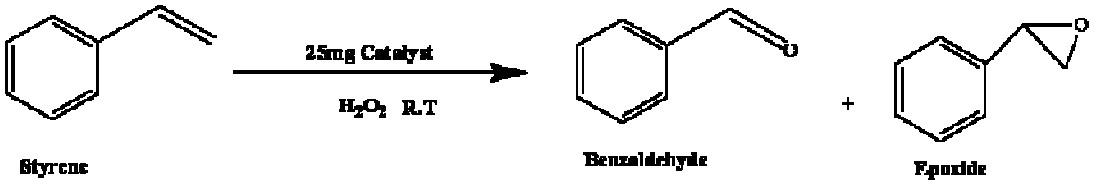


**Table 4.8** Tabular form for the results in the reaction of styrene oxidation

| Compound | Conversion ( %) | Selectivity (%) | |
|---|---|---|---|
| | | benzaldehyde | epoxide |
| 1 | 94 | 88 | 12 |
| 2† | 99 | 95.3 | 4.2 |
| 3 | 95 | 93 | 7 |
| 4 | 99.5 | 99 | 1 |

Note: R.T: Room Temperature (30 ºC) and amount of the catalyst taken as 0.25mg. Reaction time = 24 h († for 2nd catalyst, 0.5% selectivity of benzoic acid is observed.)

Condition: Temperature = Room Temperature; styrene: $H_2O_2$ = 1:3.(mmol)

All the compounds are reused at least for three times for the same reaction with similar yields. The catalysts are not destroyed after using in the reaction as confirmed by infrared spectroscopy, powder X-ray diffractormeter and diffused reflectance spectroscopy.

For all the compounds (**1–4),** reactions are monitored by changing the time of the reactions with 8 h, 12 h, 16 h, 20 h and 24 h. Corresponding results are shown in the Table 4.9 to Table 4.12. Typically, as we increase the time of the reaction, percentage of conversion increases and selectivity of benzaldehyde remains unchanged, which is shown in the Table 4.9. $H_2O_2$ is involved in the complete oxidation, till the formation of benzaldehyde. As shown from the Table 4.7, the formation of benzaldehyde is same with increasing the time under similar conditions of ratio of styrene and hydrogen peroxide, amount of the catalyst **1.** But at optimized condition, formation of epoxide was observed due to insufficient amount of hydrogen peroxide. Graphical representation for the variation of the time with percentage of conversion, catalyzed by compound **1** is shown in the Fig. 4.16.

**Table 4.9** The variation of the time with percentage of conversion of compound **1**

| Reaction Time (h) | Conversion ( %) | Selectivity (%) | |
|---|---|---|---|
| | | benzaldehyde | epoxide |
| 8 | 24 | 100 | 0 |
| 12 | 46 | 100 | 0 |
| 16 | 60 | 100 | 0 |
| 20 | 75 | 100 | 0 |
| 24 | 94 | 88 | 12 |

From the Table 4.8, it is clear that as the time (h) of the reaction increases, the percentage of conversion has increased drastically with compound **2** as a catalyst, but formation of both the benzaldehyde and epoxide are possible in the reaction medium. The reactions with 20 h and 24 h, benzoic acid also formed due to further oxidation of

benzaldehyde. But in the case of compound **3,** percentage of conversion increased with time (h) and completely converted to benzaldehyde for 8 h, 12 h, 16 h, but for 20 h and 24 h some amount of epoxide is also observed (with 20 h and 24 h) in the reaction which was determined by GC-MS (Table 4.11). When we use compound **4** as catalyst, almost 100 % of selectivity was found for 8 – 20 h but with 24 h reaction 1% of epoxide is formed due unavailability of $H_2O_2$,which is shown in Fig.4.12.

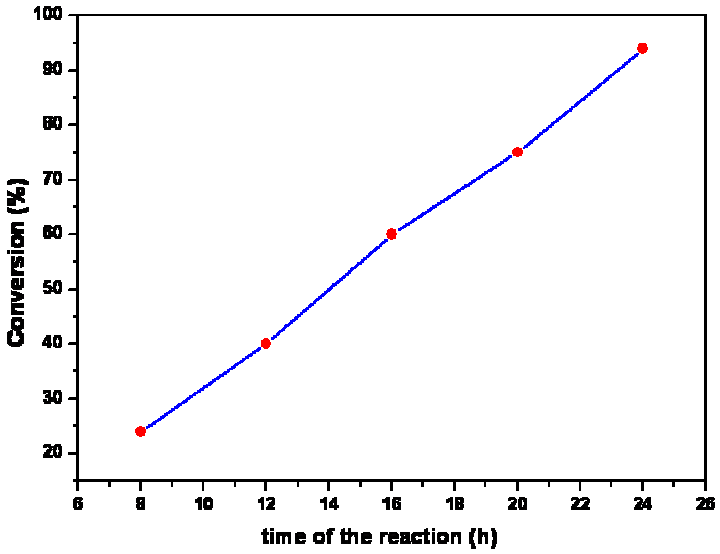


**Fig 4.16** Graphical representation of percentage of conversion with duration of the reaction for **1.**

**Table 4.10** The variation of the time with percentage of conversion of compound **2**

| Reaction Time (h) | Conversion ( %) | Selectivity (%) | |
|---|---|---|---|
| | | Benzaldehyde | Epoxide |
| 8 | 63 | 95.5 | 4.5 |
| 12 | 92 | 98 | 2 |
| 16 | 98.9 | 95 | 5 |
| 20* | 99 | 95.3 | 4.2 |
| 24# | 99.9 | 86 | 13.3 |

Note: 25mg of the catalyst and 1:3 molar ratios of styrene and $H_2O_2$. *0.5 % and $^{\#}$0.7% selectivity for benzoic acid.

**Table 4.11** The variation of the time with percentage of conversion of compound **3**

| Reaction Time (h) | Conversion ( %) | Selectivity (%) | |
|---|---|---|---|
| | | Benzaldehyde | Epoxide |
| 8 | 25 | 100 | 0 |
| 12 | 45 | 100 | 0 |
| 16 | 55 | 100 | 0 |
| 20 | 75 | 98 | 2 |
| 24 | 95.5 | 93 | 7 |

**Table 4.12** The variation of the time with percentage of conversion of compound **4**

| Reaction Time (h) | Conversion ( %) | Selectivity (%) | |
|---|---|---|---|
| | | Benzaldehyde | Epoxide |
| 8 | 97 | 100 | 0 |
| 12 | 98 | 100 | 0 |
| 16 | 98.5 | 100 | 0 |
| 20 | 99 | 100 | 0 |
| 24 | 95.5 | 99 | 1 |

**4.5. Conclusion:**

We have described the synthesis and characterization of inorganic-organic hybrid materials based on Anderson anionic cluster with amino pyridine derivatives as cations. Compounds (**1**-**3**) are composed of common Anderson anion $[AlMo_6(OH)_6O_{18}]^{3-}$ and 2-amino pyridine, 3-amino pyridine and 4-amino pyridine respectively. Compound **4** is stabilized by iodine based Anderson anion $[IMo_6O_{24}]^{5-}$ with 2-amino pyridine. The supramolecular chemistry of all the compounds was described successfully in the present chapter. They give 2-dimensional networks due to hydrogen bonding interaction between lattice water molecules and cluster anion. All the materials are used as catalyst in the reaction of oxidation of styrene that gives benzaldehyde with recyclability of catalyst. Hydrogen peroxide has been used as an oxidant in the reaction which is benign to nature. Catalytic activities of all the materials are performed and described successfully.

**4.5. References:**


1. a) Honda, D.; ShusakuIkegami.; TomoakiInoue.; Ozeki, T.; Yagasaki, A. *Inorg.chem*. **2007**, *46*, 1464. b) Li, J.; Zhang, L-C.; Sun, Z-G.; Tian, C-H.; Zhu, Z-M.; Zhao, Y.; Zhua, Y-Y.; Zhang J.; Zhang, N.; Liu, L.; Lu, X. *Inorg.chem. Z.Anorg.Allg.Chem.* **2008**, *634*, 1173.
2. a) Pope, M. T. *Heteropoly and Isopoly Oxometalates;* Springer-Verlag: Berlin, 1983. b) Pope, M. T.; Müller, A. *Angew.Chem.* **1991**, *103*, 56; *Ang Chem.,Int.Ed.* **1991**, *30*, 34. c) Hagrman, P. J.; Hagrman, D.; Zubieta, J.; *Angew.Chem.* **1999,** *111*, 2798; *Angew.Chem. Int. Ed*. **1999**, *38*, 2638.
3. a) Manikumari, S.; Shivaiah, V.; Das. S. K. *Inorg.chem.* **2002**, *4*,1464. b) Golhen,S.; Ouahab, L.; Grandjean, D.; Molinié, P. *Inorg.Chem*. 1998, *37*, 1499. c) Shivaiah, V.; Nagaraju, M.; Das. S. K. *Inorg.chem*. **2003**, *42*,6604. d) Shivaiah, V.; Das. S. K. *Inorg.chem*. **2005**, *44*, 8846. e) Shivaiah, V.; Das. S. K. *J. Chem. Sci.,* **2005**, *117*, 227.
4. a) Craig, L. H. *Mol. Eng*. **1993**, *3*, 263. b) Yamase, T. *Mol. Eng*. **1993**, *3*, 241.
5. a) Arumuganthan, T.; Srinivasa Rao, A.; Das, S. K. *J. Chem. Sci.,* **2008**, *120*, 297. b) Arumuganthan, T.; Srinivasa Rao, A.; Das, S. K. *J. Chem. Sci.,* **2008**, *120*, 208. c) Arumuganthan, T.; Srinivasa Rao, A.; Das, S. K. *J. Chem. Sci.*,

**2008**, *120*, 297. e) Arumuganthan, T.; Srinivasa Rao, A.; Das, S. K. *Cryst. Growth Des.* **2010,** *10*, 4272.

6. Neumann, R.; Levin, M. *Dioxygen Activation and Homogeneous Catalytic Oxidation,* **1991**, 121.
7. a) Pappo, R.; Allen Jr, D.S.; Lemieux, R. U.; Johnson, W. S. *J. Org. Chem.* **1956**, *21*, 478. b) Carlsen, P. H. J.; Katsuki, T.; Martin, V. S.; Sharpless, K. B. *J. Org. Chem*. 1981, *46,* 3936. c) Michael, B. S. *Organic Synthesis*, secondEd., McGraw-Hill, New York, 2002. d) Bailey, P. S. *Chem. Rev*. **1958**, *58*, 925.
8. a) Sheldon, R. A.; ochi, J. K.K. *Metal- Catalyzed Oxidations of Organic Compounds*, Academic Press, NewYork, 1981. b) Sawyer, D. T. *Oxygen Chemistry*, Oxford University Press, New York, 1991.
9. March, J. *Advanced Organic Chemistry*, fourth Ed., Wiley Interscience, 1992, 1177.
10. Noyori, R.; Aokib, M,; Satoc, K. *Chem.Commun*. **2003**, 1977.
11. a)Tangestaninejad, S.; Yadollahi, B. *Chem. Lett.* **1998**, 511. b) Zhao, Zhang, Y.; Ma, B.; Ding, Y.; Qiu, W. *Catal.Commun.* **2010**, *11*, 527. c) Hill, C. L.; Kim, G-S.; Prosser-Mccartha, C. M.; Judd, C. M. *Mol. Engin*. **1993**, *3*, 263. d) Hayashi, T.; Kishida, A.; Mizuno, N. *Chem. Commun*., **2000**, 381. e) Li,G.; Ding , Y.; Wang. J.; Wang. X.; Suo. J. *J. Mol. Catal. A*: Chemical. **2007**, *262* 67. f) Ishikawa, E.; Yamase. T. *J. Mol. Catal. A*: Chemical. **1999**, *142*, 61. g) Wang. J, Yan. L, Li. G, Wang. X, Dinga. Y, Suoa. J, *Tetrahedron Lett*. **2005**, *46,* 7023.
12. a) Software for the CCD Detector System, Bruker Analytical X-ray Systems Inc., Madison, WI, 1998.b)Bruker SADABS, SMART, SAINTPLUS and SHELXTL, Bruker AXS Inc., Madison, WI, USA, 2003.c) Sheldrick, G. M. SHELX-97, Program for Crystal Structure Solution, University of Göttingen, Germany, 1997.d) Sheldrick, G. M. SHELX-97, Program for Crystal Structure refinement, University of Göttingen, Germany, 1997. e) d) Sheldrick, G. M. *Acta Cryst*. **2008**, *A64*, 112.
13. a) Gong, Y.; Hu, C.; Li, H.; Tang, W.; Huang, K.; Hou, W, *Inorg. Chem.Commun*. **2005**, *784*, 228. b) Upreti, S,; Ramanan, A. *Cryst. Growth and Des.* **2005,** 5, 1837. c) Upreti, S,; Ramanan, A. *Cryst. Growth and Des* **2006**, *6*, 2066.
14. Wang, H. A. E.; Xiao, D.; Li, Y.; Xu, L. *Inorg. Chem. Commun.* **2005,** *8*, 267.

15. a) Neumann, R.; Gara, M. *J. Am. Chem. Soc*. **1995**, *117*, 5066. b) Noyori, R.; Aoki, M.; Satoc, K. *Chem. Commun*. **2003**, 1977. c) Jones, C. W. *Applications of Hydrogen Peroxide and Derivatives,* Royal Society of Chemistry, Cambridge, 1999. d) *Catalytic Oxidations with Hydrogen Peroxide as Oxidant*, ed. G. Strukul, Kluwer Academic, Dordrecht, The Netherlands, 1992. e) *Kirk–Othmer Encyclopedia of Chemical Technology*, ed. Kroschwitz, J. I.; Howe-Grant, M. John Wiley & Sons, Inc., New York, 4th edn. **1995**, *13*, 961.(f) *Ullmann's Encyclopedia of Industrial Chemistry*, ed. Elvers, B.; Hawkins, S.; Ravenscroft, M.; Schulz, G. VCH, New York, 5th edn. **1989**, *A13*, 443. g) Sumitomo Chemical News Release, 2000, Oct. 11; http://www.sumitomo-chem.co.jp/english/e1newsrelease/pdf/20001011e.pdf. h) Dow Products and Businesses News, 2002, Aug. 1; http://www.dow.com/dow_news/prodbus/2002/20020801a.htm.

# Isolation of Bismuth-Chloroderivatives $Bi_2Cl_9^{3-}$, $BiCl_6^{3-}$ and $Bi_2Cl_{10}^{4-}$ by Using Variuos Organic Precursors and Physical Properties of Their Respective Inorganic – Organic Hybrid materials.

**ABSTRACT:** Syntheses, crystal structures and physical properties of ion pair compounds $[C_5H_7N_2]_3[BiCl_6]$ (**1**), $[C_5H_7N_2][C_5H_8N_2][BiCl_6]$ (**2**), $[C_{10}H_{10}N_2]_2[Bi_2Cl_{10}]$ (**3**), $[C_{12}H_{17}N_2]_3[Bi_2Cl_9]\cdot 2EtOH$ (**4**) and $[C_{12}H_{17}N_2]_3[Bi_2Cl_9]\cdot 2(2\text{-}PrOH)$ (**5**) have been described. Compounds **1**, **2, 4** and **5** crystallize in triclinic system (space group, *P-1*), whereas compound **3** crystallizes in monoclinic (space group, $P2_1/c$). In their crystal structures, supramolecular hydrogen bonding interactions between bismuth-chloro anion and organic cation play an important role in the stabilization of $[BiCl_6]^{3-}$, $[Bi_2Cl_{10}]^{4-}$ and $[Bi_2Cl_9]^{3-}$ anions in the title ion pair compounds. All the compounds are characterized by routine spectral analysis and elemental analyses, besides crystal structure determinations. Compounds **1, 2** and **3** are additionally characterized by thermogravimetric analysis. Interestingly, compounds $[C_5H_7N_2][C_5H_8N_2][BiCl_6]$ (**2**), $[C_{12}H_{17}N_2]_3[Bi_2Cl_9]\cdot 2EtOH$ (**4**) and $[C_{12}H_{17}N_2]_3[Bi_2Cl_9]\cdot 2(2\text{-}PrOH)$ (**5**) exhibit emission spectra at room temperature in the visible region.

## 5.1. Introduction:

Investigations of compounds possessing organic cations and inorganic anions are of considerable interest because of their supramolecular networks. The supramolecular networks become more fascinating when the relevant cation and the anion can take part in hydrogen bonding interactions. The hydrogen bond is usually recognized as the most powerful tool for generating supramolecular assemblies of molecules. Halogenobismuthates(III) of general formula $R_aM_bX_{(3b+a)}$ (R = alkyl ammonium cations; M = Bi; X = Cl,) are examples of such systems exhibiting diverse properties like ferroic (ferroelastic, ferroelectric) behaviour in commensurate modulated phases.[1] Some representative examples of such species that are characterized in various anionic forms, belong to $R_2Bi_2X_{10}$ and $R^1{}_3BiCl_6$ classes (where R is doubly protonated cation and $R^1$ is mono-protonated cation). Another class of halogenobismuthates(III) is represented by anionic $[M_2X_9]^{3-}$ sub-lattice. Compounds containing $[M_2X_9]^{3-}$ anion exhibit versatile

supramolecular structures, such as (i) one-dimensional zigzag chains,[2] (ii) two-dimensional layers,[3] and (iii) discrete bioctahedra[4] based on $[M_2X_9]^{3-}$ unit, in respective crystal structures. Another important class of the molecules to be known is about benzodiazepine derivatives, introduced by Sternbach et al. in 1971,[5] constitute an important class molecules that are not only used as drugs[6] (anti-anxiety, anti-depressive, sedative, analgesic and hypnotic) but also play an important role in photography and dye industry.[7] The biological interest of 1,5-benzodiazepines has also been extended to important diseases such as cancer, viral infection and cardiovascular disorders.[8] In addition to such practical utility, these molecules have been used as appropriate precursors for other fused ring systems such as oxadiazolo-, oxazino- and furano-benzodiazepines.[9] Thus because of diverse applications, an easy synthetic approach for 1,5-benzodiazepines is a subject of research / a challenge to synthetic chemists. In view of this, numerous methods for the synthesis of benzodiazepines have been reported in literature.[10] The main theme of all these synthetic efforts is the condensation reaction between 1,2-diamines and various enolizable ketones in the presence of a suitable reagent/ catalyst as shown in scheme 5.1.

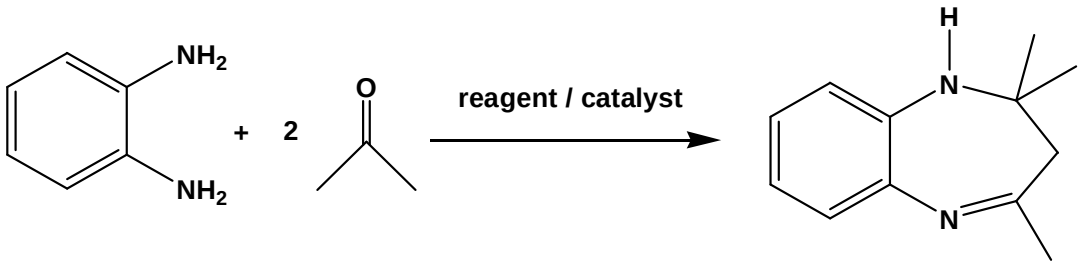


**Scheme 5.1** The formation of 1,5- benzodiazepine cation from opda and acetone in the presence of suitable catalyst.

We report here a simple approach for the synthesis of 1, 5-benzodiazepine ring system that can be achieved by the reaction between ethanol (as the source of ketone) and *o*-phenylenediamine (opda) in the presence of bismuth trichloride at ambient conditions. This work is a part of our efforts on the metal based drugs initiative. Although our original aim was to begin investigations on multinuclear bismuth coordination compounds as an extension of earlier studies on antimony,[11] the present study led to an interesting chemistry leading to benzodiazepines and amino pyridine salts of bismuth chloro derivatives.

## 5.2 Experimental Section:

### 5.2.1. Materials:

All reactions were performed in an open atmosphere. O-phenylenediamine (opda, Loba Chem.), $BiCl_3$ (Hi Chem, 99%) and amino pyridines (CHEMLABS) were used as received. Ethanol (Merck, 99.9%) and 2-propanol (Merck) were used without further purification.

### 5.2.2 Physical Measurements

Micro analytical (C, H, N) data were obtained with a FLASH EA 1112 Series CHNS Analyzer. Infrared (IR) spectra were recorded on KBr pellets with a JASCO FT/IR-5300 spectrometer in the region of 400–4000 $cm^{-1}$. Electronic absorption spectra were recorded on a Cary 100 Bio UV–Vis spectrophotometer. The emission spectra for the samples in solutions were recorded at room temperature on a Horiba Jobin Yvon Fluoromax-4 spectrofluorometer. In the measurements of emission and excitation spectra, the pass width was 5 nm. All the measurements were carried out under the same experimental conditions.

### 5.2.3 Synthetic Method:

**Synthesis of $[C_5H_7N_2]_3[BiCl_6]$ (1)**

Bismuth trichloride (1.00 g, 3.12 mmol) was dissolved in 35 mL of water by adding dil HCl. Its pH was noticed as 2.00; subsequently 2-aminopyridine (0.23 g, 2.44 mmol) was added. The resulting solution was stirred for 5 h; then it was filtered and the filtrate was kept for crystallization at room temperature for 7 days. The resulting colorless block-shaped crystals, suitable for X-ray structure determination, were separated by filtration and washed with chloroform. Yield 0.90 g (41% based on $BiCl_3$). IR ($\nu/cm^{-1}$): 3398, 3306, 3182, 3088, 1662, 1543, 1473, 1377, 1323, 1242, 1159, 995, 858,754, 711, 503. Calcd. anal (%) for $C_{15}H_{21}BiCl_6N_6$ : C, 25.48; H, 2.99; N, 11.88; found (%): C, 25.25; H, 2.64; N, 11.99.

**Synthesis of $[C_5H_7N_2][C_5H_8N_2][BiCl_6]$ (2)**

Bismuth trichloride (1.00 g, 3.12 mmol) was dissolved in 35 mL of water by adding dil HCl (pH 2.00). It was then treated with 3-aminopyridine (0.23 g, 2.44 mmol). The resulting solution was stirred for 5 h; Then it was filtered and the filtrate was kept for crystallization at room temperature for 10 days. The resulting light-yellowish block-shaped crystals, suitable for X-ray structure determination, were separated by filtration and washed with chloroform. Yield: 1.45 g (75% based on $BiCl_3$). IR ($\nu/cm^{-1}$): 3408, 1626, 1601, 1552, 1483, 1375, 1323, 1269, 1180, 1114, 941, 773, 667, 520, 461. Calcd anal (%) for $C_{10}H_{15}BiCl_6N_4$ : C, 19.59; H, 2.46; N, 9.14; found (%): C, 19.07; H, 2.63; N, 9.21.

**Synthesis of $[C_{10}H_{10}N_2]_2[Bi_2Cl_{10}]$ (3)**

Bismuth trichloride (1.00 g, 3.12 mmol) was dissolved in 35 mL of water by adding dil. HCl. In this case, pH was noticed as 1.00. It was reacted with 4, 4'-bipyridine (0.23 g, 1.5 mmol). The reaction mixture was then stirred for 5 h, filtered and kept for crystallization at room temperature for one week. The colorless block shaped crystals, obtained during this time, were separated by filtration and washed with water. Yield 1.90 g (52% based on $BiCl_3$). IR ($\nu/cm^{-1}$): 3437, 2492, 1950, 1633, 835, 636, 580, 538. Calcd anal. (%) For $C_{20}H_{20}Bi_2Cl_{10}N_4$ : C, 22.06; H, 1.85; N, 5.14; found (%): C, 22.07; H, 1.63; N, 5.21.

**Synthesis of $[C_{12}H_{17}N_2]_3[Bi_2Cl_9]\cdot 2EtOH$ (4)**

Bismuth trichloride (0.32 g, 1 mmol) and opda (0.22 g, 2 mmol) were dissolved in ethanol (35 mL) and the reaction mixture was stirred for 12 h in open atmosphere in a beaker. The little white turbid solution, formed during this time, was filtered and the filtrate was kept at 4 $^oC$ for crystallization for 4 days. The resulting yellowish needle-shaped crystals, suitable for X-ray structure determination, were separated by filtration and washed with ethanol. Yield 0.125 g (25% based on $BiCl_3$). IR ($cm^{-1}$): 3489, 3354, 3298, 3209, 3107, 3055, 2966, 2924, 1963, 1919, 1799, 1666, 1610, 1491, 1369, 1269, 1163, 1043, 877, 758, 646. Calcd anal. For $C_{40}H_{59}Bi_2Cl_9N_6O_2$ ($M_r$=1392.98): C, 34.49; H, 4.27; N, 6.03; found: C, 34.07; H, 4.19; N, 6.21.

**Synthesis of $[C_{12}H_{17}N_2]_3[Bi_2Cl_9]\cdot 2(2\text{-PrOH})$ (5)**

The procedure was similar to that for **4** using bismuth trichloride (0.32 g, 1 mmol), opda (0.22 g, 2 mmol) and 2-propanol (35 mL). The resulting yellowish needle-shaped crystals were washed with 2-propanol. Yield 0.12 g (24% based on $BiCl_3$). IR ($\nu/cm^{-1}$): 3327, 2972, 1652, 1608, 1487, 1456, 1371, 1263, 1197, 1026, 910, 837, 750, 646, 542,482. Calcd anal. For $C_{42}H_{67}Bi_2Cl_9N_6O_2$ ($M_r$ = 1425.07): C, 35.39; H, 4.74; N, 5.89; found: C, 35.56; H, 4.38; N, 6.02.

### 5.2.4. Single crystal X-ray structure determination:

Data were measured at room temperature for all the compounds on a Bruker SMART APEX CCD, are a detector system [λ(Mo Kα) 0.7103 Å], graphite monochromator, 2400 frames were recorded with an ω scan width of 0.3°, each for 8s, crystal-detector distance 60mm, collimator 0.5mm. Data reduction by SAINTPLUS, (Software for the CCD Detector System, Bruker Analytical X-Ray Systems Inc., Madison., WI, 1998), absorption correction using an empirical method SADABS[12a] structure solution using SHELXS-97[12b] (G. M. Sheldrick, program for structure solution, University of Göttingen, Germany 1997) and refined using SHELXL-97[12c,d] (G. M Sheldrick, Program for crystal structure analysis, University of Göttingen, Germany 1997). A brief summary of the crystallographic data for compounds **1-3** is provided in the Table 5.1 and 4-5 is provided in Table 5.6.

## 5.3. Results and discussion:

### 5.3.1. Synthesis of 1, 2 and 3

One pot wet synthesis from $BiCl_3$ and 2-aminopyridine / 3-aminopyridine / 4, 4′-bipyidine affords inorganic-organic hybrid material $[C_5H_7N_2]_3[BiCl_6]$ (**1**) / $[C_5H_7N_2][C_5H_8N_2][BiCl_6]$ (**2**) / $[C_{10}H_{10}N_2]_2[Bi_2Cl_{10}]$ (**3**). In the present synthesis, bismuth chloro anionic species are generated *in situ* in the solution, and organic precursors, that get protonated, act as cations in the isolation of compounds **1-3**. Both compounds **1** and **2** include $[BiCl_6]^{3-}$ as an anion and in the case of compound **3**, $[Bi_2Cl_{10}]^{4-}$ species acts as the anion. Formation of the title compounds is shown schematically in Scheme 5.2.

**Table 5. 1** Crystallographic data for compounds **1, 2** and **3.**

| **Entry** | **1** | **2** | **3** |
|---|---|---|---|
| Formula | $C_{15}$ $H_{21}$ Bi $Cl_6$ $N_6$ | $C_{10}$ $H_{11}$ Bi $Cl_6$ $N_4$ | $C_{20}$ $H_{20}$ $Bi_2$ $Cl_{10}$ $N_4$ |
| FW | 707.06 | 612.94 | 1088.86 |
| Crystal system | Monoclinic | Triclinic | Triclinic |
| Space group | *P*2(1)/c | *P*-1 | *P*-1 |
| a/A˚ | 8.3759(7) | 7.401(3) | 8.3670(17) |
| b/A˚ | 16.1703(14) | 11.203(4) | 9.809(2) |
| c/A˚ | 17.5383(16) | 11.734(5) | 11.035(2) |
| α/º | 90 | 92.013(6) | 112.90(3) |
| β/º | 93.6340(10) | 105.496(6) | 101.52(3) |
| γ/º | 90 | 98.714(6) | 98.60(3) |
| Z | 4 | 2 | 1 |
| μ/$mm^{-1}$ | 8.128 | 10.407 | 11.970 |
| $\rho_{cal}$/ Mg $m^{-3}$ | 1.981 | 2.204 | 2.285 |
| $R_1(F^2_0)$ [ I > 2 σ(I)] | 0.0212 | 0.0223 | 0.0182 |
| $wR_2$ $(F^2_0)$ [ I > 2 σ(I)] | 1.039 | 0.0541 | 0.0346 |
| $R_1(F^2_0)$ (all data) | 0.0250 | 0.0256 | 0.0220 |
| $wR_2$ $(F^2_0)$ (all data) | 0.0543 | 0.0554 | 0.0349 |
| Largest diff peak and hole ( e $A^{-3}$) | 1.421, -0.992 | 0.567, -0.869 | 0.556, -0.485 |

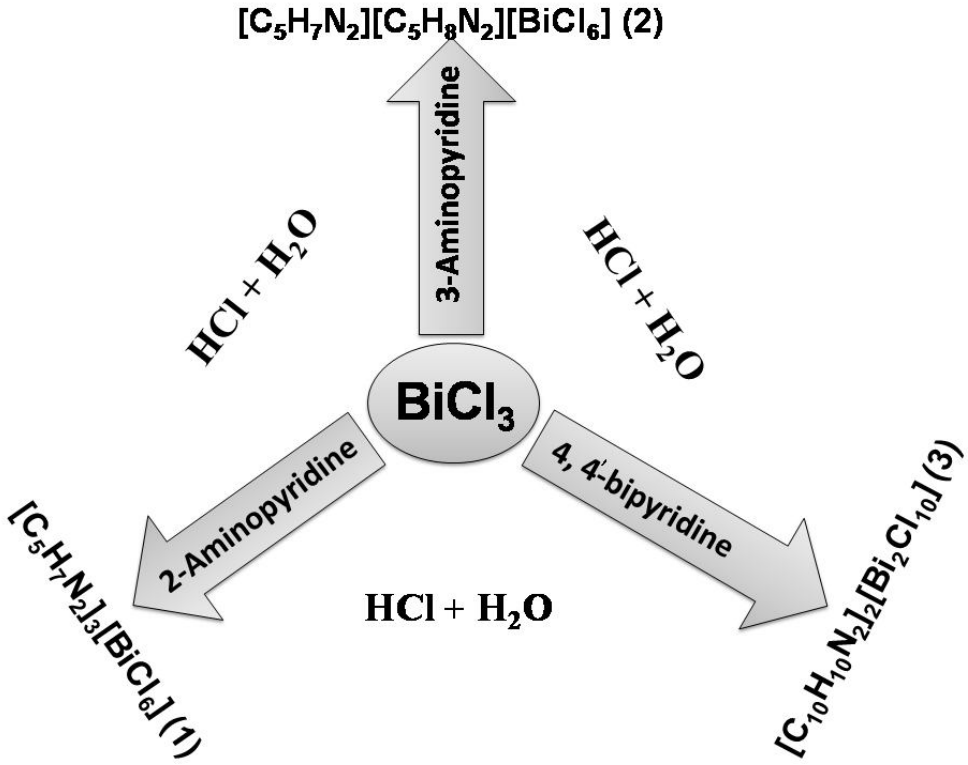


**Scheme 5.2**: Schematic representation of the generation of title compounds in a one pot wet synthesis.

Both the species, $[BiCl_6]^{3-}$ and $[Bi_2Cl_{10}]^{4-}$ are speculated to be formed as shown in the following series of stoichometrically balanced reactions. As our syntheses are carried in acidic medium, besides the formation of $[BiCl_6]^{3-}$ and $[Bi_2Cl_{10}]^{4-}$ species, the respective organic precursor gets protonated so that they can act as cations while isolating the chlorobismuthates.

$$BiCl_3 + 3HCl \longrightarrow H_3[BiCl_6]$$

$$2BiCl_3 + 4HCl \longrightarrow H_4[Bi_2Cl_{10}]$$

$$C_5H_6N_2 + HCl \longrightarrow [C_5H_7N_2]Cl$$

2-Aminopyridine

$$H_3[BiCl_6] + 3[C_5H_7N_2]Cl \longrightarrow [C_5H_7N_2]_3[BiCl_6]\,(1) + 3HCl$$

$$2C_5H_6N_2 + 3HCl \longrightarrow [C_5H_7N_2]Cl + [C_5H_8N_2]Cl_2$$

3-Aminopyridine

$$H_3[BiCl_6] + [C_5H_7N_2]Cl + [C_5H_8N_2]Cl_2 \longrightarrow [C_5H_7N_2][C_5H_8N_2][BiCl_6]\,(2) + 3HCl$$

$$C_{10}H_8N_2 + 2HCl \longrightarrow [C_{10}H_{10}N_2]Cl_2$$

4,4'-bipyridine

$$H_4[Bi_2Cl_{10}] + 2[C_{10}H_{10}N_2]Cl_2 \longrightarrow [C_{10}H_{10}N_2]_2[Bi_2Cl_{10}]\ (3) + 4HCl$$

**5.3.2. Synthesis of 4 and 5.**

Synthesis from $BiCl_3$ and opda in ethanol/2-propanol affords inorganic-organic hybrid material $[C_{12}H_{17}N_2]_3[Bi_2Cl_9]\cdot 2EtOH$ (**4**)/$[C_{12}H_{17}N_2]_3[Bi_2Cl_9]\cdot 2(2\text{-}PrOH)$ (**5**). Earlier reports have shown that condensation reaction between a 1,2-diamine (e.g., opda) and a ketone (e.g., acetone) in the presence of a suitable reagent/catalyst, as shown in scheme 5.1, affords 1,5-benzodiazepine.[13] In the present synthesis, we have used ethanol instead of acetone (ketone). It is worth mentioning that various gas phase catalytic transformations of ethanol to acetone are known. [14] The extensive literature search on the synthesis of 1, 5-benzodiazepine shows that a ketone is a mandatory reactant that reacts with 1,2-diamine (Scheme 1). Thus, we believe that acetone, formed *in situ* in our synthesis, reacts with opda (1,2-diamine) leading to 1,5-benzodiazepine (Scheme 1). In the present study, the only evidence that acetone "may" have been formed is the formation of the benzodiazepine. The blank reaction performed in the absence of the diamine to see if $BiCl_3$ forms some acetone in the presence of alcohol does not yield acetone (checked by GC-Mass). The amount of acetone required to form the compound **4** is not much (*ca.* 0.25 mmol or so), so may be hard to detect in blank reactions.

**5.3.3. Crystal Structure:**

The compound $[C_5H_7N_2]_3[BiCl_6]$ (**1**) crystallizes in monoclinic system with space group *P2 (1)/c*. The asymmetric unit in the relevant crystal structure contains one $[BiCl_6]^{3-}$ anion, which has been explored earlier[15] and three units of protonated 2-amynopyridine (2-ampH) for charge compensation. The thermal ellipsoidal plot of compound **1** is presented in Fig. 5.1.

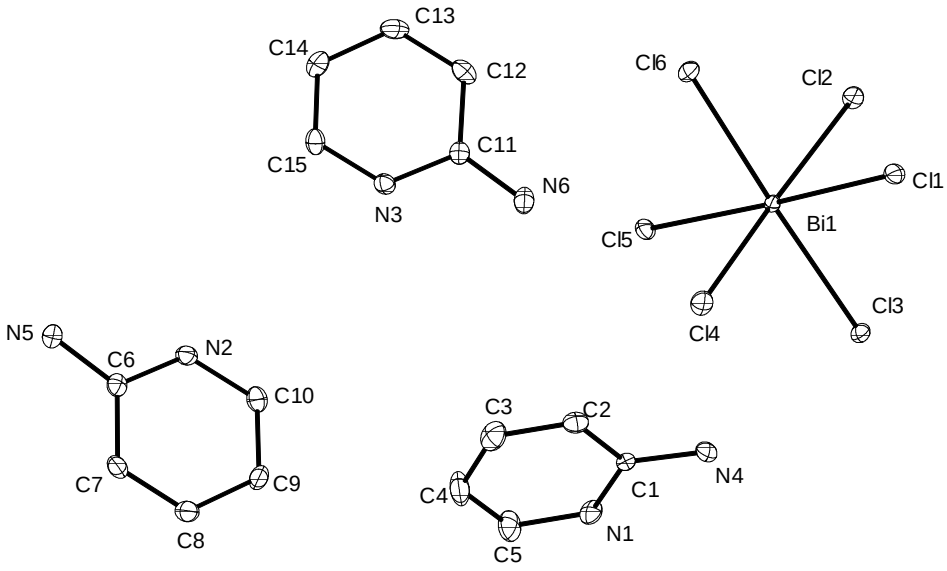


**Fig. 5. 1**. Thermal ellipsoidal plot for $[C_5H_7N_2]_3[BiCl_6]$ (**1**) with 30% probability (hydrogen atoms are not shown for clarity).

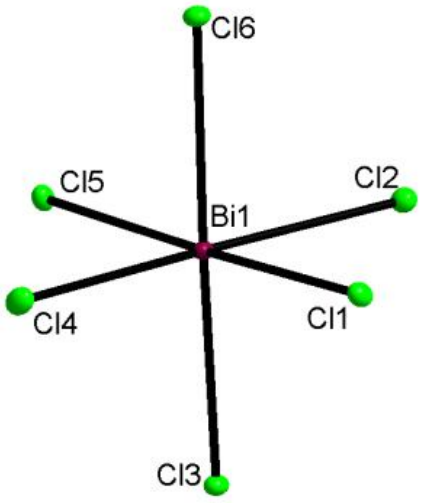


**Fig. 5.2.** Ball and stick representations of bismuth monomer $[BiCl_6]^{3-}$.

The basic crystallographic data for the title compounds are listed in Table 5.1. The relevant bond distances and angles are listed in Table 5.2. The $[BiCl_6]^{3-}$ moiety acquires octahedral geometry with bond lengths Bi(1)–Cl(2) : 2.7696(7) Å and Bi(1)–Cl(4) : 2.6416(7) Å as maximum and minimum bond lengths respectively. Their ∠Cl–Bi–Cl bond angles also support the octahedral arrangement, which is shown in Fig. 5.2.

2-Aminopyridine molecules are arranged in a stacking manner due to π–π interactions with alternative distances of 3.997Å and 4.390 Å as presented in Fig. 5. 3.

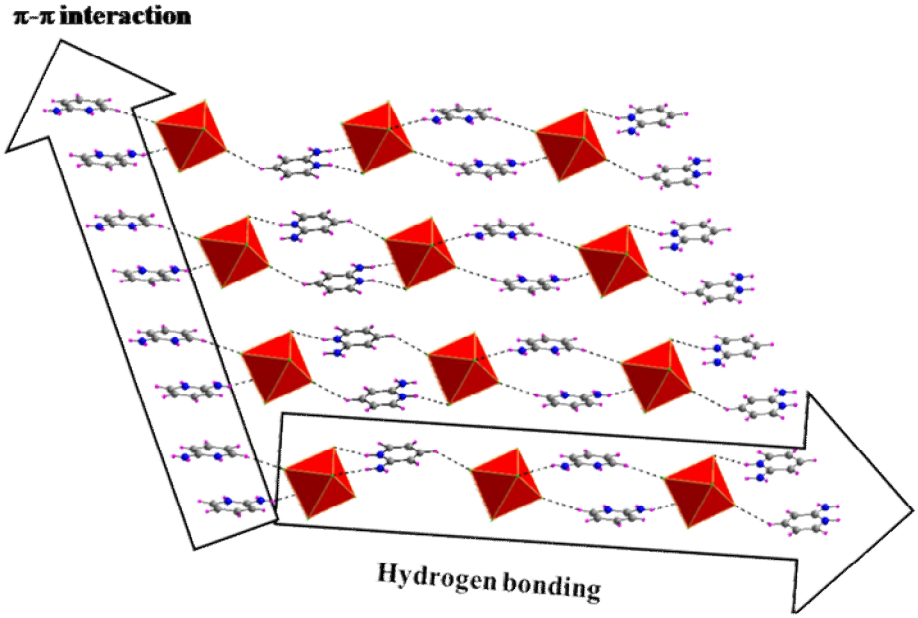


**Fig. 5. 3.** Two dimensional network due to C–H•••Cl interactions and π···π interactions in the crystal of compound $[C_5H_7N_2]_3[BiCl_6]$ **(1).**

Even though these are weak π–π interactions[16], the compound **1** gives a 2-dimensional supramolecular network due to the existence of further strong C–H•••Cl hydrogen bonds (Fig. 5.3). Thus the formation of the layer can be described by the assemblage of staircase type of chains by π–π interactions, whereby the chain is formed by C–H•••Cl hydrogen bonding interactions among cations and bismuth chloro anions. The hydrogen bonding environment around the three cations, namely, {N1N4}, {N2N5} and {N3N6} are shown in the Fig. 5.4. The relevant hydrogen bonding parameters (compound **1**) are presented in Table 5.3.

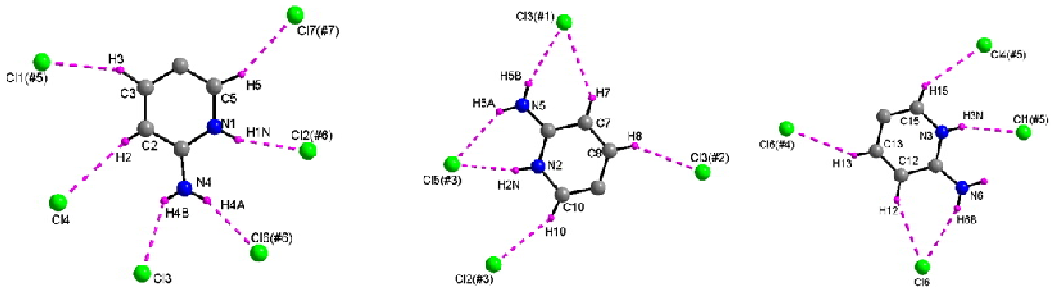

**(5.4a)** **(5.4b)** **(5.4c)**

**Fig.5.4.** Hydrogen bonding situation around the 2-aminopyridinium cation in $[C_5H_7N_2]_3[BiCl_6]$ (**1**) a){N1N4} b) {N2N5} c) {N3N6}; symmetry operations: #1) x,y+1,z; #2) -x+1,-y+1,-z+1; #3) -x,y+1/2,-z+1/2; #4) -x,-y+1,-z; #5) -x+1,y+1/2,-z+1/2; #6 x,-y+1/2,z+1/2; #7) -x,-y+1,-z+1;

**Table 5.2** Selected bond lengths (Å) and angles (º) for $[C_5H_7N_2]_3[BiCl_6]$ (**1**).

| | | | |
|---|---|---|---|
| Bi(1)-Cl(4) | 2.6416(7) | Bi(1)-Cl(1) | 2.6813(7) |
| Bi(1)-Cl(3) | 2.6952(7) | Bi(1)-Cl(6) | 2.6992(7) |
| Bi(1)-Cl(5) | 2.7337(7) | Bi(1)-Cl(2) | 2.7696(7) |
| Bond angles (º) | | | |
| Cl(4)-Bi(1)-Cl(1) | 90.82(2) | Cl(4)-Bi(1)-Cl(3) | 87.81(2) |
| Cl(1)-Bi(1)-Cl(3) | 86.80(2) | Cl(4)-Bi(1)-Cl(6) | 92.75(2) |
| Cl(1)-Bi(1)-Cl(6) | 91.31(2) | Cl(3)-Bi(1)-Cl(6) | 178.038(19) |
| Cl(4)-Bi(1)-Cl(5) | 89.22(2) | Cl(1)-Bi(1)-Cl(5) | 178.080(19) |
| Cl(3)-Bi(1)-Cl(5) | 95.12(2) | Cl(6)-Bi(1)-Cl(5) | 86.77(2) |
| Cl(4)-Bi(1)-Cl(2) | 176.87(2) | Cl(1)-Bi(1)-Cl(2) | 86.05(2) |
| Cl(3)-Bi(1)-Cl(2) | 92.00(2) | Cl(6)-Bi(1)-Cl(2) | 87.35(2) |
| Cl(5)-Bi(1)-Cl(2) | 93.91(2) | | |

**Table 5.3.** Hydrogen bond distances and angles for $[C_5H_7N_2]_3[BiCl_6]$ (**1)** [Å and º].

| D-H···A | d(D-H) | d(H···A) | d(D···A) | <(DHA) |
|---|---|---|---|---|
| C(7)-H(7)...Cl(3)#1 | 0.94(3) | 2.92(3) | 3.725(3) | 145(2) |
| C(8)-H(8)...Cl(3)#2 | 0.94(3) | 2.77(3) | 3.601(3) | 148(2) |
| C(10)-H(10)...Cl(2)#3 | 0.94(3) | 2.69(3) | 3.564(3) | 155(3) |
| N(2)-H(2N)...Cl(5)#3 | 0.86(3) | 2.38(3) | 3.218(3) | 165(3) |
| N(5)-H(5A)...Cl(5)#3 | 0.88(3) | 2.62(4) | 3.392(3) | 148(3) |
| N(5)-H(5B)...Cl(3)#1 | 0.81(3) | 2.61(3) | 3.400(3) | 164(3) |
| C(13)-H(13)...Cl(6)#4 | 0.86(3) | 2.95(3) | 3.695(3) | 146(2) |
| C(12)-H(12)...Cl(6) | 0.96(3) | 2.84(3) | 3.689(3) | 149(2) |
| N(6)-H(6B)...Cl(6) | 0.83(3) | 2.72(3) | 3.509(3) | 161(3) |
| N(3)-H(3N)...Cl(1)#5 | 0.81(3) | 2.46(3) | 3.240(3) | 160(3) |
| C(15)-H(15)...Cl(4)#5 | 0.92(3) | 2.83(3) | 3.580(3) | 139(3) |
| C(3)-H(3)...Cl(1)#5 | 1.04(4) | 2.70(4) | 3.586(3) | 144(3) |
| C(2)-H(2)...Cl(4) | 0.82(3) | 3.02(3) | 3.827(3) | 168(3) |
| N(4)-H(4B)...Cl(3) | 0.81(3) | 2.66(3) | 3.313(3) | 139(3) |
| N(4)-H(4A)...Cl(6)#6 | 0.86(4) | 2.49(4) | 3.319(3) | 162(4) |
| N(1)-H(1N)...Cl(2)#6 | 0.90(3) | 2.38(3) | 3.225(3) | 158(3) |
| C(5)-H(5)...Cl(5)#7 | 1.02(5) | 2.69(5) | 3.606(4) | 150(3) |

Symmetry transformations used to generate equivalent atoms:
#1 x, y+1, z; #2 -x+1, -y+1, -z+1; #3 -x, y+1/2 -z+1/2; #4 -x, -y+1, -z; #5, -x+1, y+1/2, -z+1/2; #6, x, -y+1/2, z+1/2; #7 -x, -y+1, -z+1;

In the case of compound $[C_5H_7N_2][C_5H_8N_2][BiCl_6]$ (**2**), the anionic species $[BiCl_6]^{3-}$ is identical to the anion for compound **1**; however, in the crystal structure of compound **2**, each chloro anion $[BiCl_6]^{3-}$ is stabilized by two molecules of 3-aminopyridine (one is mono-protonated and the other one is di-protonated). The thermal ellipsoidal plot for compound **2** is shown in Fig. 5.5. The packing of the organic cations shows an head-to-head pattern, in which every two organic moieties are very close to each other (3.170Å) due to π–π interaction (see Fig. 5.6). Hydrogen bonding situation in

the relevant crystal structure is shown in Fig. 5.7. We have labeled both cations as {N1N2} cation and {N3N4} cation. We found eight hydrogen bonding interactions around the {N1N2} cation and six hydrogen bonding interactions around the {N3N4} cation. The relevant hydrogen bonding parameters are presented in Table 5.4.

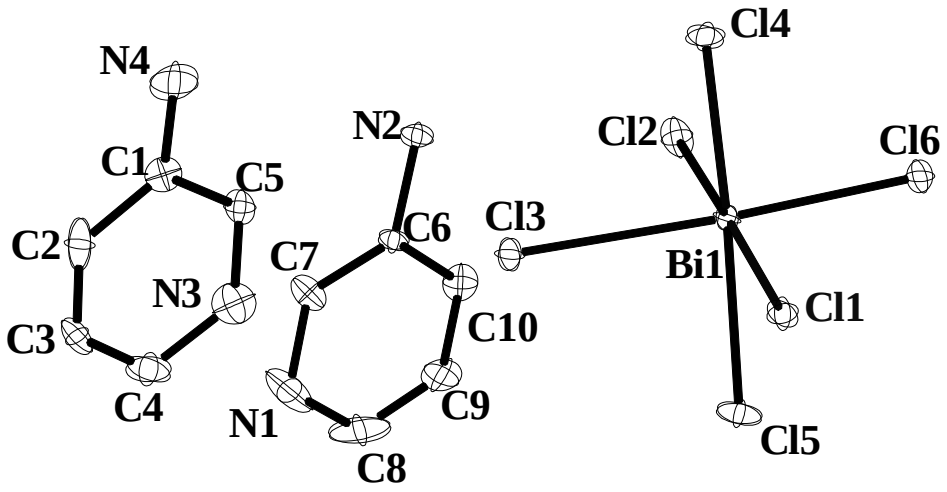


**Fig. 5.5.** The thermal ellipsoidal plot of $[C_5H_7N_2][C_5H_8N_2][BiCl_6]$ (**2**) with 30% probability(hydrogen atoms are not shown for clarity).

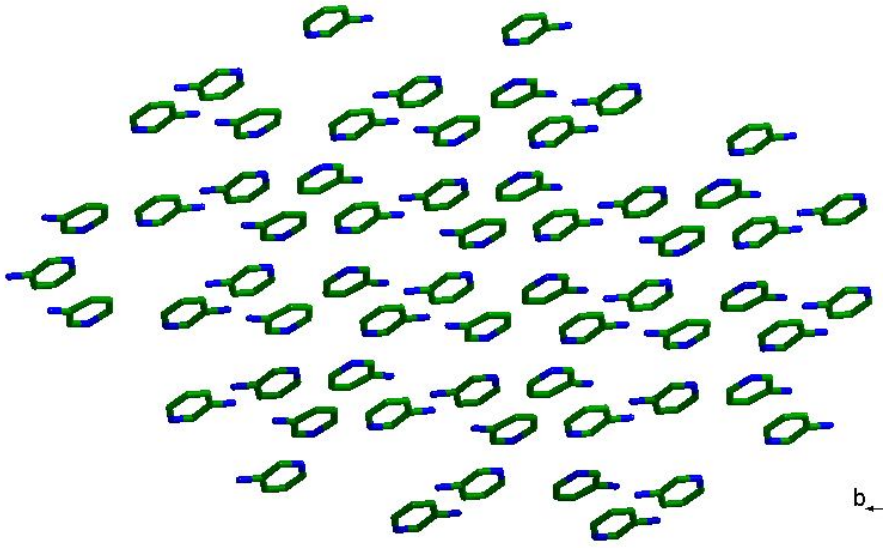


**Fig.5.6.** 3-Aminopyridine (3-Amp) molecules are arranged in parallel directions in $[C_5H_7N_2][C_5H_8N_2][BiCl_6]$ (**2**) which are viewed through C-axis.

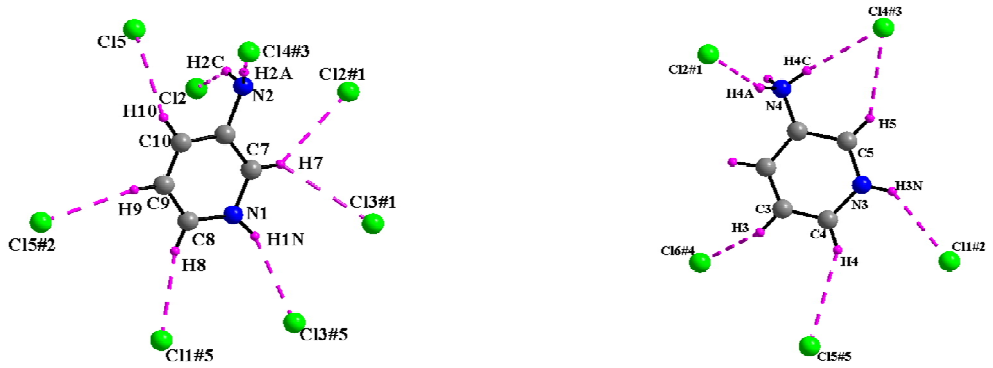


**(a)** **(b)**

**Fig.5.7** Hydrogen bonding environment around the cation (a) {N1N2}, (b) {N3N4} in $[C_5H_7N_2][C_5H_8N_2][BiCl_6]$ (**2**); symmetry operations: #1) -x+1,-y+1,-z; #2) -x+1,-y+1,-z+1; #3) x+1,y,z; #4) x+1,y-1,z; #5) x,y-1,z.

**Table 5.4** Hydrogen bonds for $[C_5H_7N_2][C_5H_8N_2][BiCl_6]$ (**2**) [Å and º.].

| D-H···A | d(D–H) | d(H···A) | d(D···A) | <(DHA) |
|---|---|---|---|---|
| N(4)-H(4A)...Cl(2)#1 | 0.89 | 3.04 | 3.889(6) | 159.4 |
| N(3)-H(3N)...Cl(1)#2 | 0.86 | 2.75 | 3.434(6) | 137.9 |
| N(4)-H(4C)...Cl(4)#3 | 0.89 | 2.68 | 3.554(7) | 167.3 |
| C(5)-H(5)...Cl(4)#3 | 0.93 | 2.97 | 3.750(5) | 141.9 |
| C(3)-H(3)...Cl(6)#4 | 0.93 | 2.45 | 3.248(6) | 144.5 |
| C(4)-H(4)...Cl(5)#5 | 0.93 | 2.95 | 3.770(6) | 147.9 |
| C(7)-H(7)...Cl(2)#1 | 0.93 | 2.79 | 3.548(6) | 138.9 |
| C(7)-H(7)...Cl(3)#1 | 0.93 | 3.01 | 3.682(6) | 130.5 |
| N(1)-H(1N)...Cl(3)#5 | 0.91 | 2.68 | 3.491(6) | 149.8 |
| C(8)-H(8)...Cl(1)#5 | 0.93 | 2.54 | 3.445(7) | 163.6 |
| C(9)-H(9)...Cl(5)#2 | 0.93 | 2.66 | 3.518(6) | 154.3 |
| C(10)-H(10)...Cl(5) | 0.93 | 2.87 | 3.543(6) | 130.4 |
| N(2)-H(2C)...Cl(2) | 0.81 | 2.57 | 3.173(4) | 132.5 |
| N(2)-H(2A)...Cl(4)#3 | 0.87 | 2.26 | 3.121(4) | 167.4 |

Symmetry transformations used to generate equivalent atoms:

#1, -x+1,-y+1,-z; #2, -x+1,-y+1,-z+1; #3, x+1, y, z; #4, x+1, y-1, z; #5, x,y-1,z;

The compound $[C_{10}H_{10}N_2]_2[Bi_2Cl_{10}]$ (**3**) crystallizes in triclinic with space group *P-1*. The crystal structure of compound **3** consists of a dimeric bismuth-chloro-anion $[Bi_2Cl_{10}]^{4-}$ and two doubly protonated 4, 4′-bipyridine organic moieties (cationic form of 4, 4′- bipyridine) per formula unit. The molecular structure of **3** is shown in Fig. 5.8. In the dimeric anion, two $Bi^{3+}$ ions are bridged by two $Cl^-$ ions and each $Bi^{3+}$ ion is additionally coordinated by four terminal $Cl^-$ ions. This dimeric bismuth-chloro-anion is a rare example of this kind; there are only two reports known that have described this anion.[17] The hydrogen bonding situation in the crystal structure of compound **3** is shown in Fig. 5.9. These C–H•••Cl hydrogen bonds, observed between $[Bi_2Cl_{10}]^{4-}$ anion and [4, 4′-bipyH$_2$]$^{2+}$ cation led to the 2-dimensional supramolecular network as shown in Fig. 5.10. The relevant hydrogen bonds are described in Table 5.5.

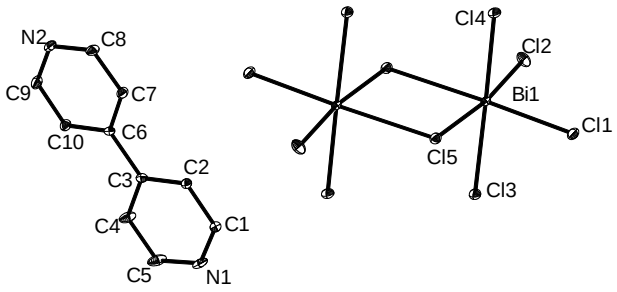


**Fig.5.8.** Thermal ellipsoidal plot of $[C_{10}H_{10}N_2]_2[Bi_2Cl_{10}]$ (3) with 30% probability (hydrogen atoms are not shown for clarity)

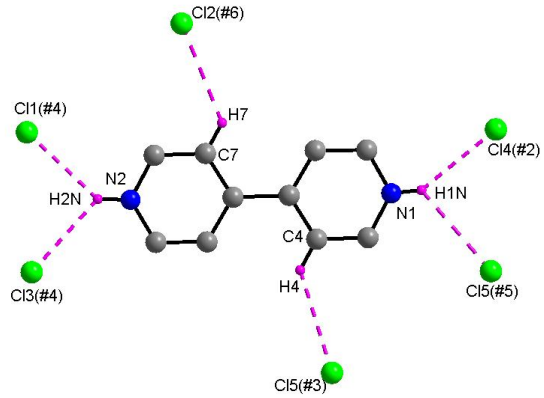


**Fig.5.9.** Hydrogen bonding situation around the 4, 4′-bipyridinium cation in $[C_{10}H_{10}N_2]_2[Bi_2Cl_{10}]$ (**3**); symmetry operations: #1) -x+1,-y+1,-z+1; #2) x,y-1,z; #3) x-1,y-1,z; #4) x-1,y,z+1; #5) -x+1,-y,-z+1; #6) x,y,z+1;

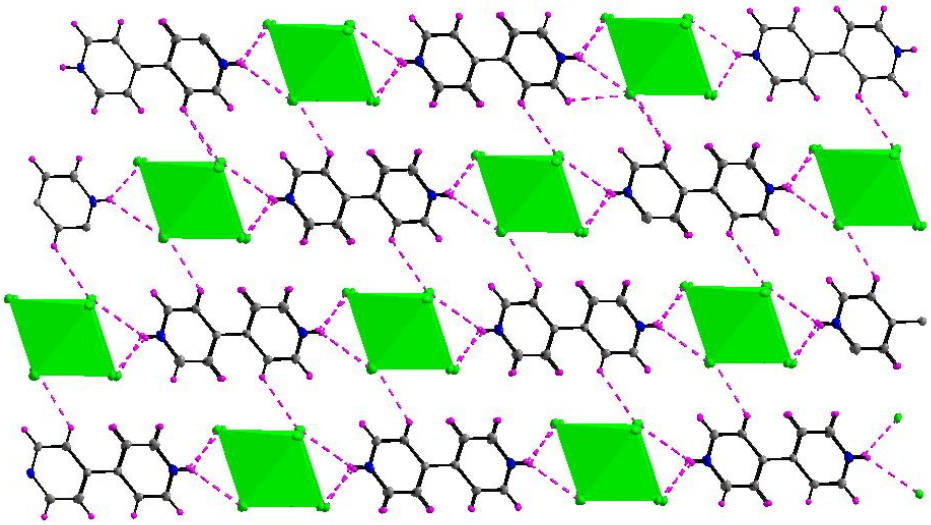

**Fig. 5.10.**Two dimensional network because of C–H•••Cl interaction between bipyridinium salt and $[Bi_2Cl_{10}]^{4-}$ in $[C_{10}H_{10}N_2]_2[Bi_2Cl_{10}]$ (**3**)

**Table 5. 5** Hydrogen bonds for $[C_{10}H_{10}N_2]_2[Bi_2Cl_{10}]$ **(3)** [Å and º.]

| D-H···A | d(D–H) | d(H···A) | d(D···A) | <(DHA) |
|---|---|---|---|---|
| N(1)-H(1N)...Cl(4)#2 | 0.81(5) | 2.56(5) | 3.266(4) | 146(4) |
| C(4)-H(4)...Cl(5)#3 | 0.93 | 2.87 | 3.582(5) | 133.8 |
| N(2)-H(2N)...Cl(1)#4 | 0.88(5) | 2.59(5) | 3.292(4) | 138(4) |
| N(2)-H(2N)...Cl(3)#4 | 0.88(5) | 2.62(5) | 3.261(4) | 131(4) |
| N(1)-H(1N)...Cl(5)#5 | 0.81(5) | 2.87(5) | 3.387(4) | 124(4) |
| C(7)-H(7)...Cl(2)#6 | 0.93 | 2.87 | 3.535(5) | 129.7 |

Symmetry transformations used to generate equivalent atoms:

#1, -x+1,-y+1,-z+1 #2, x,y-1,z #3, x-1,y-1,z

#4, x-1,y,z+1 #5, -x+1,-y,-z+1 #6, x,y,z+1

The compound $[C_{12}H_{17}N_2]_3[Bi_2Cl_9]\cdot 2EtOH$ (**4**) crystallizes in triclinic space group *P*-1. The asymmetric unit in the relevant crystal structure contains one $[Bi_2Cl_9]^{3-}$ anion, three 2,3-dihydro-1H-1,5-benzodiazepinium cations $[C_{12}H_{17}N_2]^+$ and two solvent molecules (EtOH). The thermal ellipsoidal plot of compound **4** is presented in Fig. 5.11. The basic crystallographic data for compound **4** and **5** are presented in Table 5.6. As shown in Figure 5.11, the anion $[Bi_2Cl_9]^{3-}$ is a bismuth dimer, in which two $Bi^{3+}$ ions are bridged by three $Cl^-$ ions and each $Bi^{3+}$ ion is additionally coordinated by three terminal $Cl^-$ ions. This anion is known in the literature.[37] There are three organic moieties (cationic forms of 2,3-dihydro-1H-1,5-benzodiazepine) per formula unit of compound **1**. Examination of these organic cations shows that each of them has different conformation as far as seven-membered rings are concerned (Fig. 5.12). We name these three organic moieties as "N1N2", "N3N4" and "N5N6" cations. In all the three moieties, the six-membered rings (essentially benzene rings) have planar conformations with average deviations of 0.0071 Å, 0.0045 Å and 0.0044 Å respectively (see Fig.5.12 and Table 5.7).

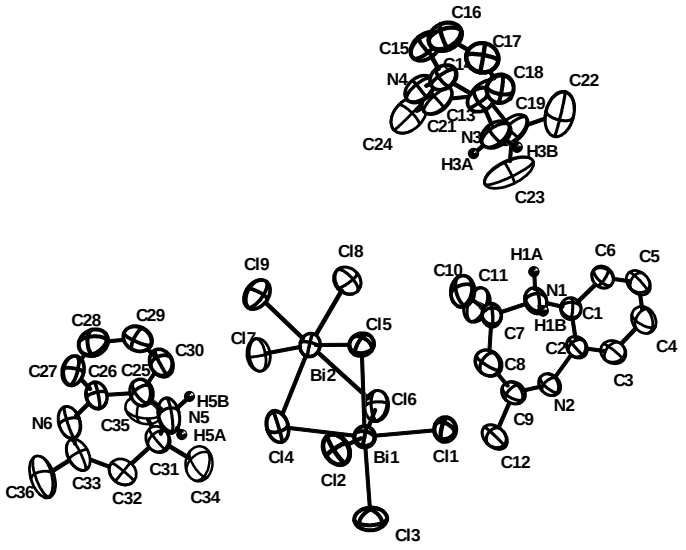


**Fig.5. 11** The thermal ellipsoidal plot of compound $[C_{12}H_{17}N_2]_3[Bi_2Cl_9]\cdot 2EtOH$ (**4**). The hydrogen atoms and solvent molecules are not shown for clarity.(The located hydrogen atoms on nitrogen are shown).

**Table 5.6** Crystallographic data for $[C_{12}H_{17}N_2]_3[Bi_2Cl_9] \cdot 2EtOH$ (**4**) and **5** (2PrOH)

| **Entry** | **4** | **5** |
|---|---|---|
| Formula | $C_{40}H_{63}Bi_2Cl_9N_6O_2$ | $C_{42}H_{67}Bi_2Cl_9N_6O_2$ |
| FW | 1396.97 | 1425.03 |
| Crystal system | Triclinic | Triclinic |
| Space group | P-1 | P-1 |
| a/A˚ | 9.6119(13) | 9.6622(16) |
| b/A˚ | 14.5182(19) | 14.589(2) |
| c/A˚ | 20.564(3) | 21.015(4) |
| α/º | 74.207(3) | 74.003(3) |
| β/º | 83.678(2) | 82.210(3) |
| γ/º | 87.280(2) | 85.965 |
| U/A ˚ | 2744.1(6) | 2819.6(8) |
| Z | 2 | 2 |
| $\rho_{cal}$/ Mg $m^{-3}$ | 5.157 | 1.678 |
| μ/$mm^{-1}$ | 48.537 | 6.697 |
| $R_1(F^2_0)$ [ I > 2 σ(I)] | 0.0250 | 0.0979 |
| $wR_2$ ($F^2_0$) [ I > 2 σ(I)] | 0.0594 | 0.1718 |
| $R_1(F^2_0)$ (all data) | 0.0337 | 0.1215 |
| $wR_2$ ($F^2_0$) (all data) | 0.0624 | 0.1792 |

On the other hand, the seven-membered rings (that are non-aromatic rings), as expected, have non-planar conformations with average deviations of 0.2048 Å, 0.6277 Å and 0.2161 Å respectively (Table 3). Interestingly, the deviations from planarity for the seven-membered ring found in three organic moieties did not occur in the same fashion (Fig. 5.12 and Table 5.7). We believe that this inadequacy in comparable trend is due to different hydrogen bonding environments around each of these "N1N2", "N3N4" and "N5N6" organic moieties found in the crystal structure of compound **4.** In the present study, the crystal structure of $[C_{12}H_{17}N_2]_3[Bi_2Cl_9]\cdot 2EtOH$ (**4**) witnessed 15 C–H···Cl and

3 N–H···Cl hydrogen bonds (taking H···Cl distance as 3.1 Å ) among $[C_{12}H_{17}N_2]^+$ cations and $[Bi_2Cl_9]^{3-}$ anions (Table 5.8).

The hydrogen bonding situations around each of these organic moieties are shown in Fig. 5.13. The hydrogen bonds, observed around $[Bi_2Cl_9]^{3-}$ anion, are shown in Fig.5.14. The Bi(III) ion is in a distorted octahedral environment composed of six chloride anions. As shown in Fig. 5.14, the $[Bi_2Cl_9]^{3-}$ anion is hydrogen bonded to its adjacent / surrounding organic cations by fourteen C–H···Cl bonds and two N–H···Cl bonds.The relevant hydrogen bonds are described in Table 5.8. These hydrogen bonds include C–H···Cl, N–H···Cl and O–H···Cl type interactions. The combination of all these hydrogen bonding interactions leads to an intricate supramolecular network as shown in Fig. 5.15. Compound $[C_{12}H_{17}N_2]_3[Bi_2Cl_9]\cdot 2$(2-PrOH) (**5**), that has been isolated using 2-propanol, is isostructural with compound **4**. The structural details of compound **4** & **5** are provided in Table 5.6.

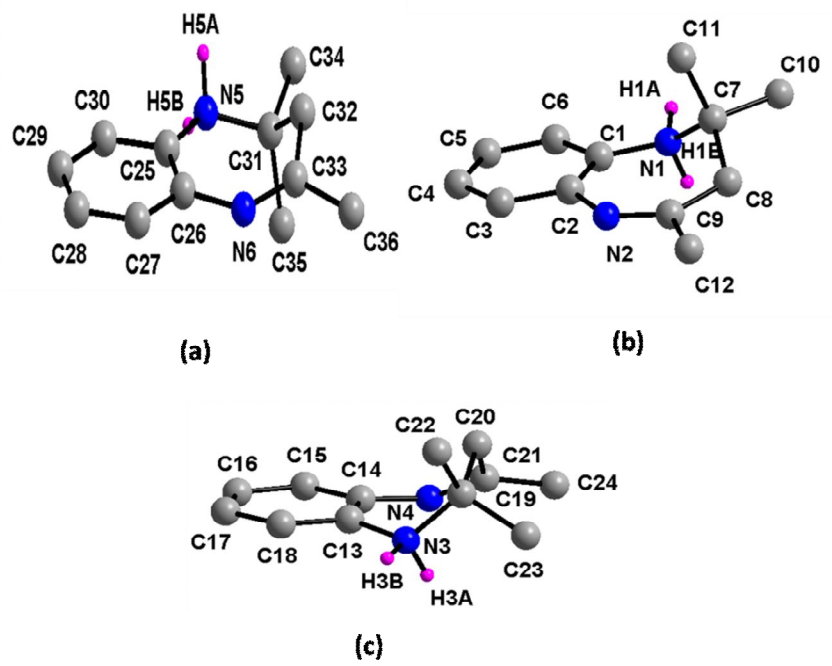


**Fig.5. 12** Conformations of organic moieties in compound $[C_{12}H_{17}N_2]_3[Bi_2Cl_9]\cdot 2EtOH$ (**4**): (a) "N1N2" moiety, (b) "N3N4" moiety and (c) "N5N6" moiety.

**Table 5.7.** Least-square planes for the three organic moieties in $[C_{12}H_{17}N_2]_3[Bi_2Cl_9] \cdot 2EtOH$ (**4**)

| "N1N2" moiety | | | "N3N4" moiety | | "N5N6" moiety | |
|---|---|---|---|---|---|---|
| | 6-memb.ring | 7-memb. ring | 6-memb. ring | 7-memb. ring | 6-memb. ring | 7-memb. ring |
| P | - 0.5425 | 0.7785 | 3.8240 | 0.3509 | 0.5978 | 0.8996 |
| Q | 14.4062<br>13.5902 | 14.4095 | 6.5179 | 3.2327 | 12.9589 | |
| R | 4.0063<br>12.1948 | 3.3134 | 19.2160 | 20.4835 | 13.9026 | |
| S | 3.2398 | 4.0410 | 16.6323 | 16.0062 | 8.5181 | 8.8438 |

Deviations from planes (Å)

| "N1N2" moiety | | | | "N3N4" moiety | | | | "N5N6" moiety | | | |
|---|---|---|---|---|---|---|---|---|---|---|---|
| 6-membered ring | | 7-membered ring | | 6-membered ring | | 7-membered ring | | 6-membered ring | | 7-membered ring | |
| C1 | 0.0028 | C1 | 0.0029 | C13 | 0.0032 | C13 | 0.0036 | C25 | 0.0031 | C25 | 0.0035 |
| C2 | 0.0029 | C2 | 0.0029 | C14 | 0.0034 | C14 | 0.0037 | C26 | 0.0031 | C26 | 0.0032 |
| C3 | 0.0034 | N1 | 0.0031 | C15 | 0.0037 | N3 | 0.0038 | C27 | 0.0034 | N5 | 0.0038 |
| C4 | 0.0035 | C7 | 0.0031 | C16 | 0.0039 | C19 | 0.0040 | C28 | 0.0035 | C31 | 0.0039 |
| C5 | 0.0032 | C8 | 0.0034 | C17 | 0.0037 | C20 | 0.0045 | C29 | 0.0034 | C32 | 0.0038 |
| C6 | 0.0030 | C9 | 0.0031 | C18 | 0.0034 | C21 | 0.0041 | C30 | 0.0034 | C33 | 0.0037 |
| | | N2 | 0.0027 | | | N4 | 0.0037 | | | N6 | 0.0035 |

Plane equation: Px + Qy + Rz = S. In the "N1N2' moiety, 6-membered ring: C1, C2, C3, C4, C5, C6; 7-membered ring:C1, C2, N1, C7, C8, C9, N2. In the "N3N4' moiety, 6-membered ring: C13, C14, C15, C16, C17, C18; 7-membered ring: C13, C14, N3, C19, C20, C21, N4. In the "N5N6' moiety, 6-membered ring: C25, C26, C27, C28, C29, C30; 7-membered ring: C25, C26, N5, C31, C32, C33, N6 (see also Figure 5.12).

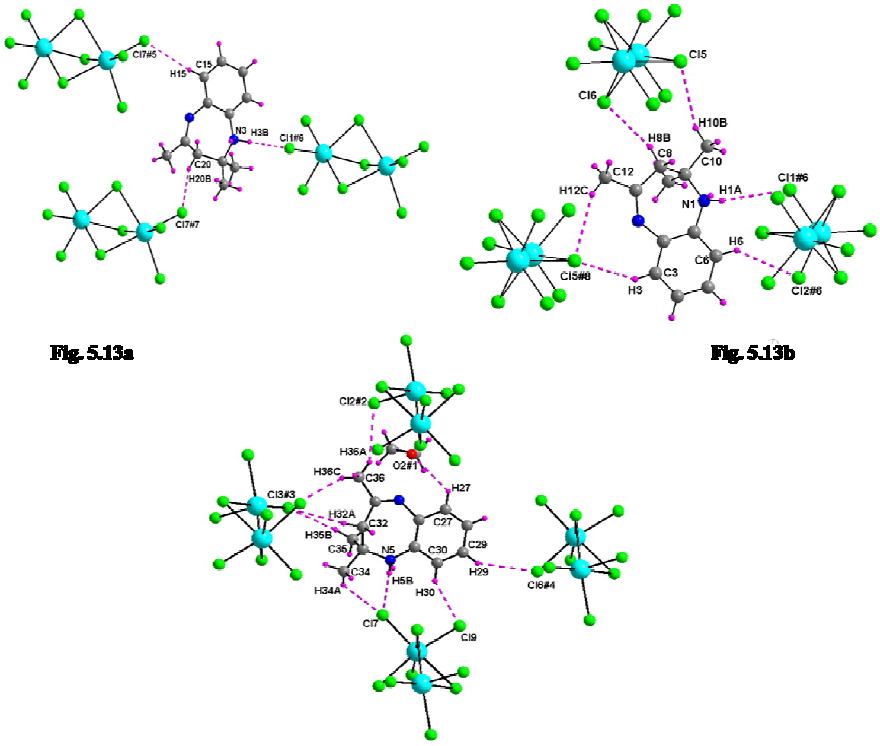


**Fig. 5.13b**

**Fig.5.13.** Hydrogen bonding environments around organic moieties in compound $[C_{12}H_{17}N_2]_3[Bi_2Cl_9]\cdot 2EtOH$ (**1**): (a) "N1N2" moiety, (b) "N3N4" moiety and (c) "N5N6" moiety. #1, x-1, y, z-1; #2, -x, -y+1, -z; #3, -x+1, -y+1, -z; #4, x-1, y, z; #5, -x, -y+1, -z+1; #6, -x+1, -y, -z+1; #7, -x+1, -y+1, -z+1; #8, x+1, y, z. color codes: C, grey, N, blue, Cl, green, H, purple.

**Table 5.8** Hydrogen bonds and angles observed in the crystal structure of **4**

| D-H...A | d(D-H) | d(H•••A) | d(D•••A) | <(DHA) |
|---|---|---|---|---|
| C(27)-H(27)...O(2)#1 | 0.93 | 2.74 | 3.347(7) | 123.7 |
| C(34)-H(34A)...Cl(7) | 0.96 | 3.10 | 3.880(6) | 139.5 |
| C(36)-H(36A)...Cl(2)#2 | 0.96 | 3.03 | 3.897(6) | 150.6 |
| C(36)-H(36C)...Cl(3)#3 | 0.96 | 3.02 | 3.833(6) | 143.7 |
| C(32)-H(32A)...Cl(3)#3 | 0.97 | 3.05 | 3.842(5) | 139.9 |
| C(29)-H(29)...Cl(6)#4 | 0.93 | 2.96 | 3.730(5) | 141.2 |
| C(30)-H(30)...Cl(9) | 0.93 | 2.92 | 3.675(5) | 138.7 |
| N(5)-H(5B)...Cl(7) | 0.90 | 2.57 | 3.454(4) | 169.2 |
| C(35)-H(35B)...Cl(3)#3 | 0.96 | 2.81 | 3.728(6) | 160.6 |
| C(15)-H(15)...Cl(7)#5 | 0.93 | 3.01 | 3.928(5) | 170.8 |
| N(3)-H(3B)...Cl(1)#6 | 0.90 | 2.52 | 3.344(4) | 152.6 |
| C(20)-H(20B)...Cl(7)#7 | 0.97 | 2.85 | 3.729(5) | 151.4 |
| C(10)-H(10B)...Cl(5) | 0.96 | 3.05 | 3.818(5) | 138.2 |
| C(8)-H(8B)...Cl(6) | 0.97 | 2.86 | 3.800(5) | 163.5 |
| C(12)-H(12C)...Cl(5)#8 | 0.96 | 2.91 | 3.751(4) | 147.5 |
| N(1)-H(1A)...Cl(1)#6 | 0.90 | 2.91 | 3.623(3) | 137.7 |
| C(6)-H(6)...Cl(2)#6 | 0.93 | 2.87 | 3.596(4) | 136.4 |
| C(3)-H(3)...Cl(5)#8 | 0.93 | 2.79 | 3.612(4) | 147.9 |

Symmetry transformations used to generate equivalent atoms:
#1, x-1, y, z-1; #2, -x, -y+1, -z; #3, -x+1, -y+1, -z; #4, x-1, y, z; #5, -x, -y+1, -z+1; #6, -x+1, -y, -z+1; #7, -x+1, -y+1, -z+1; #8, x+1, y, z;

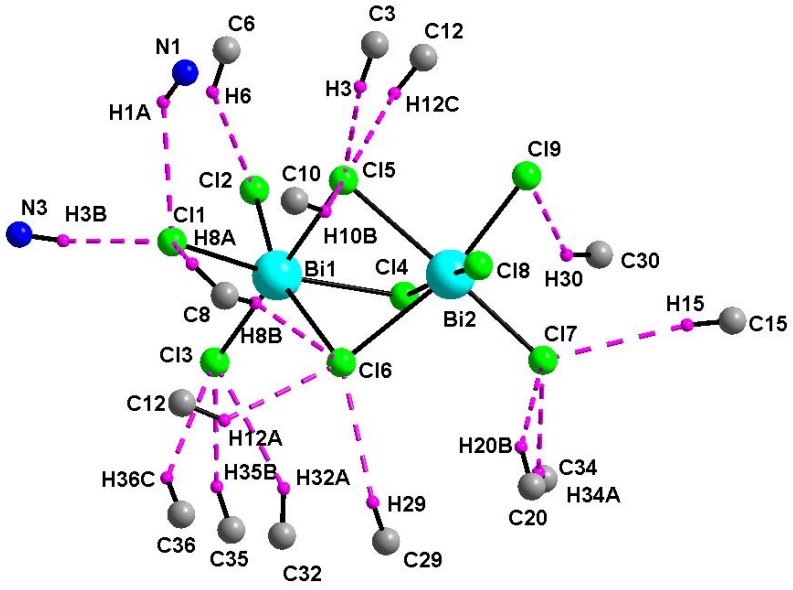


**Fig. 5.14** Hydrogen bonding environments around inorganic dimer anion $[Bi_2Cl_9]^{3-}$ in compound **4**.

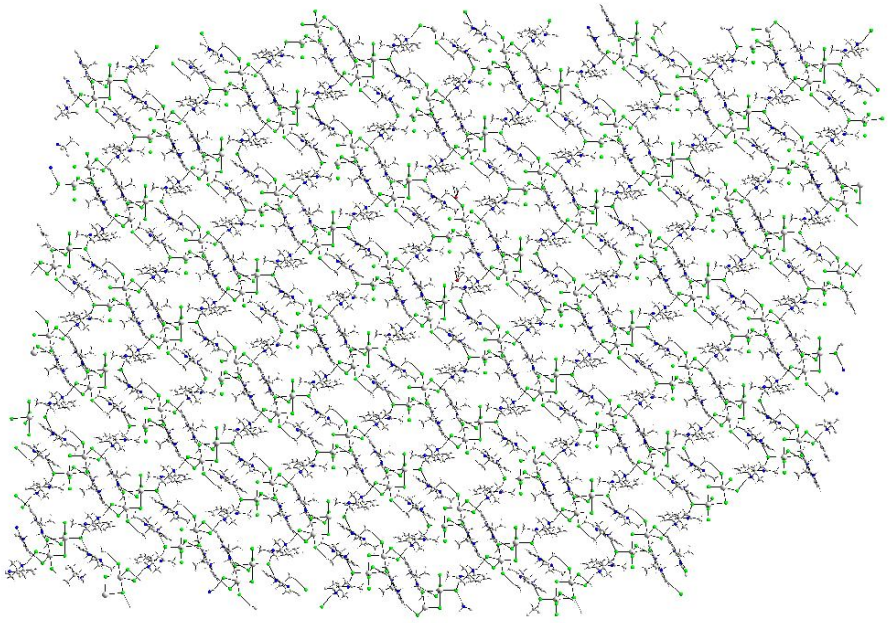

**Fig. 5.15** Three-dimensional supramolecular network in compound **4**.

### 5.3.4. Spectroscopy of compounds 1, 2 and 3.

Solid state diffuse reflectance (electronic absorption) spectra for compounds **1**, **2** and **3** are presented as Figs. 5.15, 5.16 and 5.17 respectively. The absorption peaks at 230 nm and 309 nm (compound **1**), 252 nm and 342 nm (compound **2**) and 214 nm, 250 nm and 326 (compound **3**) reveal that organic cation dominates the electronic absorption spectra for all three compounds.

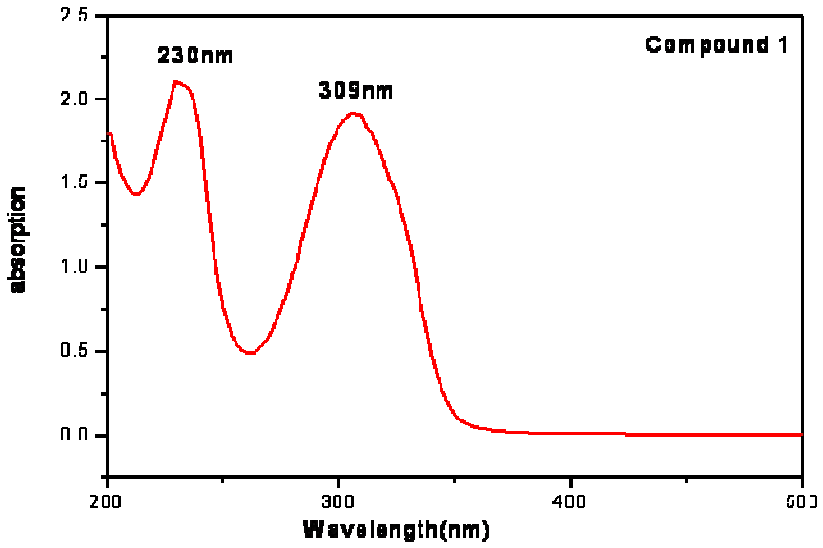


**Fig. 5.15** Solid state UV-Visible spectroscopy of $[C_5H_7N_2]_3[BiCl_6]$ (**1**)

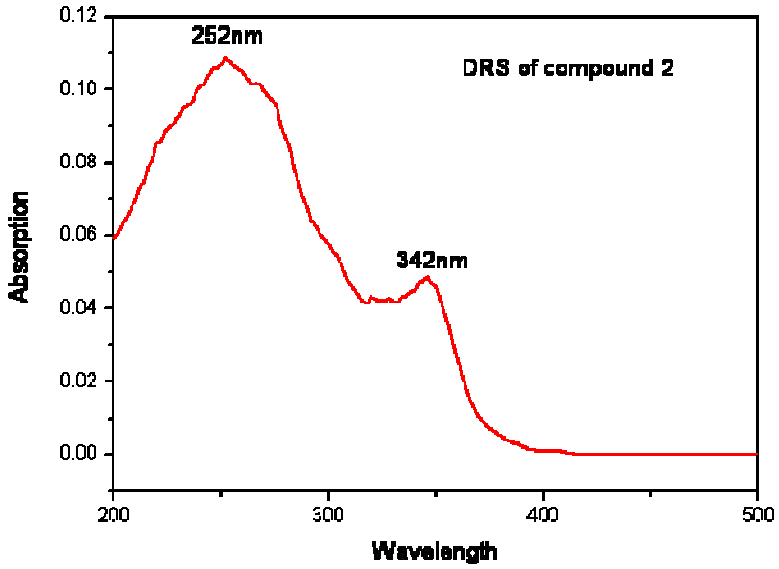


**Fig.5.16** Diffused reflectance spectroscopy of $[C_5H_7N_2][C_5H_8N_2][BiCl_6]$ (**2**).

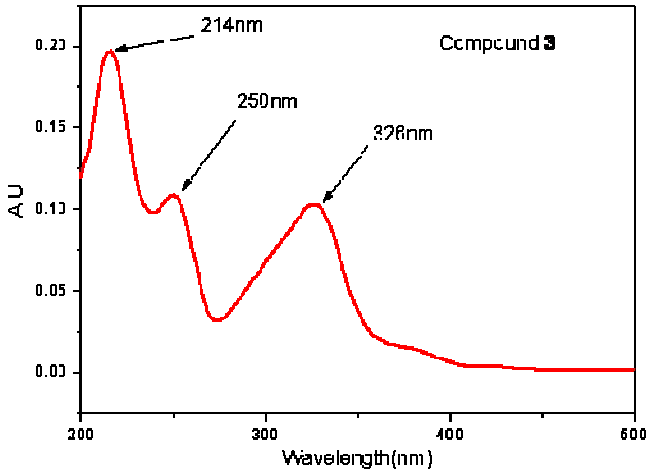


**Fig. 5.17** Diffuse reflectance spectrum of $[C_{10}H_{10}N_2]_3[Bi_2Cl_{10}]$ (**3**).

The solution state UV-Visible spectral studies of all three materials were performed in DMSO solvent (see Fig. 5.18). The absorptions at 225 nm, 258 nm and 260 nm for compounds **1**, **2** and **3** respectively are due to nπ* transition and the peaks at 300 nm, 327 nm and 315 nm for compounds **1**, **2** and **3** respectively seem to originate from ππ* transition based on bathochromic shift in non-polar solvents [19] The solution electronic absorption spectrum for compound **2** in DMSO (Fig. 5.19) is significantly different from that in solid state (Fig. 5.16). It reveals that there are significant cation–anion interactions in the solid state in the case of compound **2** and these interactions are not in same in its solution. One extra weak shoulder is observed at 398 nm (in the solution state of compound **2**) apart from strong peaks at 258 nm and 327 nm in its solution state.

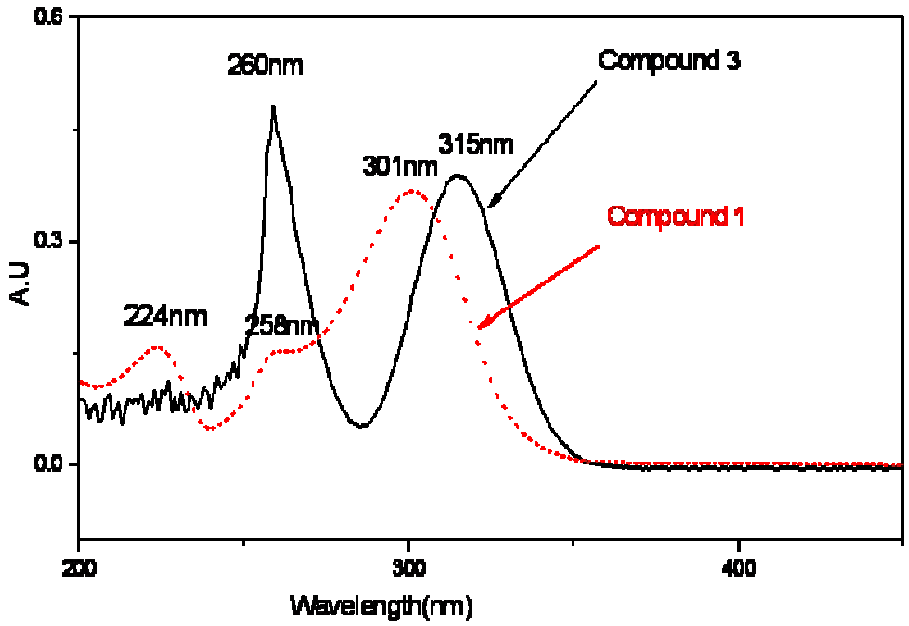


**Fig. 5.18** Solution state UV-Visible spectra of $[C_5H_7N_2]_3[BiCl_6]$ (**1**) with $0.33X10^{-3}$M in DMSO ( dotted lines) and $[C_{10}H_{10}N_2]_3[Bi_2Cl_{10}]$ (**3**) in $1.1X10^{-5}$M in DMSO (solid line) respectively.

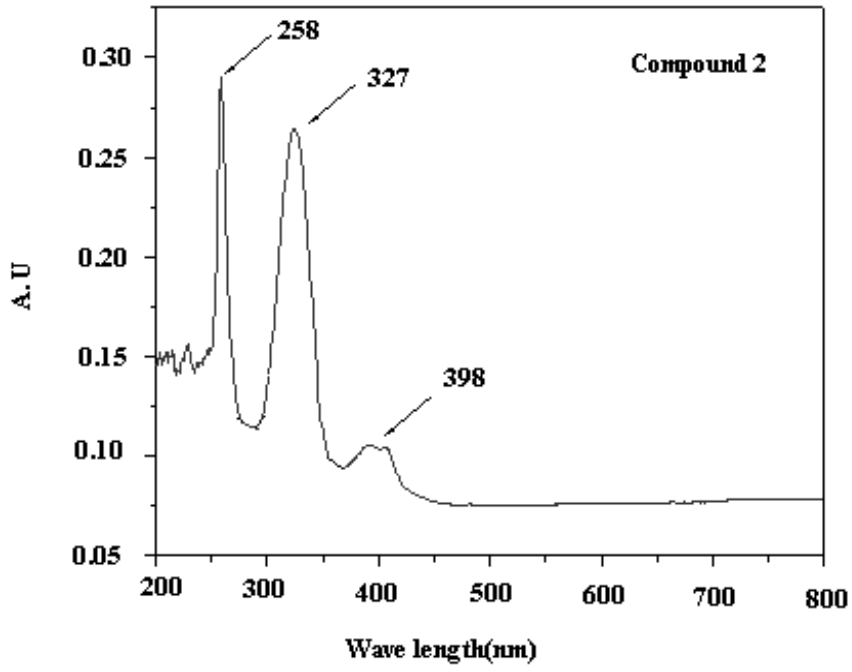


**Fig. 5.19** Electronic absorption spectrum of $[C_5H_7N_2][C_5H_8N_2][BiCl_6]$ (**2**) in DMSO ($0.25X10^{-4}$M).

Compound **2** exhibits emission signal at room temperature in the visible region as shown in Fig. 5.20. It shows emission at 358 nm (when it was excited at 327 nm) and 437 nm (when it was excited at 398 nm). It prompted us to investigate the emission behavior of 3-aminopyridine itself and it indeed exhibits emission signal in the visible region at room temperature. Since its protonated form is present in compound **2**, we intended to check its emission behavior in its protonated form by adding $HClO_4$ / HCl to its solution. The emission signal was found to be quenched after adding $HClO_4$ / HCl to its solution. Surprisingly, the emission feature of compound **2** (even it contains protonated form of 3-aminopyridine) is not much quenched (Fig. 5.21 for related emission behavior comparison). Quantum yield calculations have been performed in following the equation

$$\frac{\Phi_{sample}}{\Phi_{std.}} = \frac{A_{sample}}{A_{std.}} \times \frac{OD_{std.}}{OD_{sample}} \times \frac{\eta^{2}_{sample}}{\eta^{2}_{std.}}$$

where std. abbreviates for the standard (here quinine sulfate), A is the integrated emission intensity, O.D. stands for the optical density at the excited wavelength and $\eta$ is the refractive index (for dimethyl sulfoxide, $\eta$ = 1.4793 and for water, $\eta$ = 1.333). The excitations have been performed at similar optical density for all the samples, where the absorption curve of the sample intersects the absorption curve of quinine sulfate. The quantum yield calculations, shown in the Table 5.9, shows that the quantum yield value (0.15) for compound **2** is considerably larger than that (0.04) for protonated 3-aminopyridine species (by adding HCl / $HClO_4$), even though protonated 3-aminopyridine is present in compound **2**. We believe that in the present system (compound **2**), the cation-anion interactions are someway responsible to reduce this quenching of the protonated 3-aminopyridine in compound **2**.

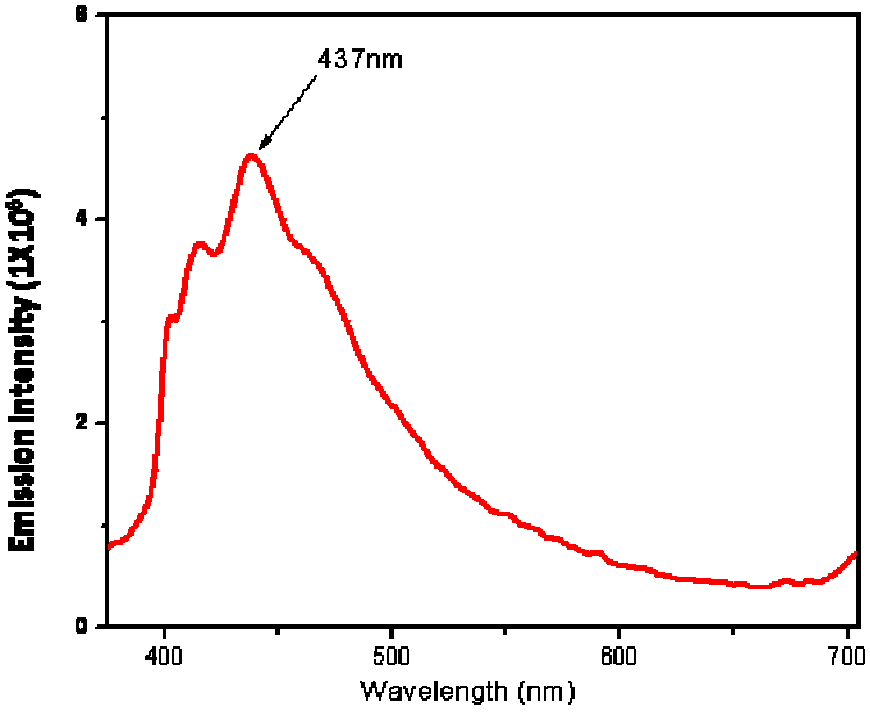


**Fig. 5.20a** Emission spectra when excited at 327nm

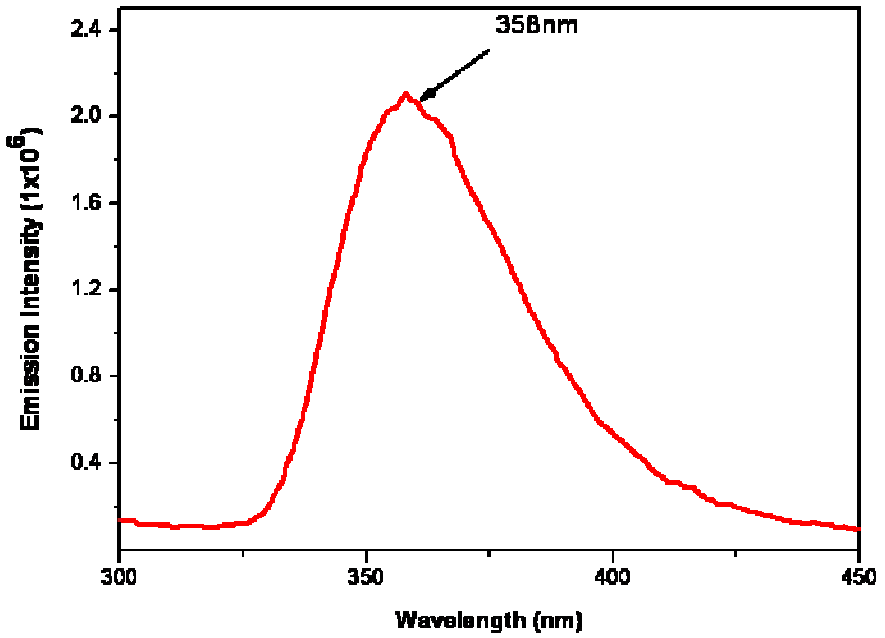


**Fig. 5.20b** emission spectra when excited at 398nm for $[C_5H_7N_2][C_5H_8N_2][BiCl_6]$ (**2**) in DMSO with $0.25X10^{-4}$M.

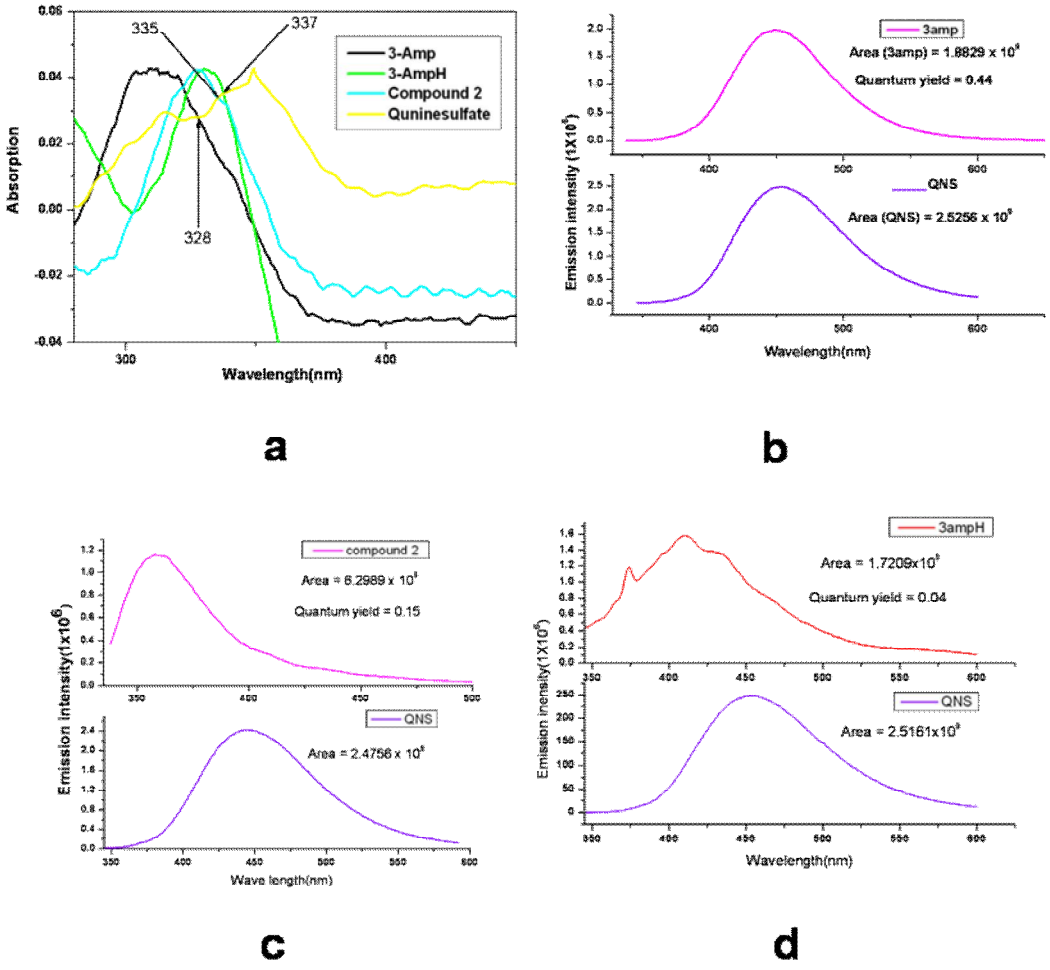


**Fig. 5.21** (**a**) UV-visible spectra of 3-aminopyridine, protonated 3-aminopyridine and compound **2**, note that OD has been matched with QNS. Numbers inside the figure denote the excitation points. (**b**) Emission spectrum of 3-aminopyridine(3-amp) w.r.t. QS at 328 nm. (**c**) Emission spectrum of protonated 3-aminopyridine(3-ampH) w.r.t. QS at 337 nm. (**d**) Emission spectrum of compound 2 w.r.t. QS at 335 nm

**Table 5.9** Observed quantum yield of following entries ($\lambda_{abs}$ and $\lambda_{em}$ = Absorption and emission maxima)

| Entry | $\lambda_{abs}$ [nm] | $\lambda_{em}$ [nm] | $\Phi_F$ |
|---|---|---|---|
| 3-Amp | 309 | 450 | 0.44 |
| 3-AmpH | 330 | 410 | 0.04 |
| Compound **2** | 327 | 360 | 0.15 |

### 5.3.5 Spectroscopic discussion of compounds 4 & 5

The solid state electronic absorption spectrum (Fig. 5.22) of compound **4** is characterized by strong bands at 230, 338 and 390 nm and a weak shoulder at 505 nm. The spectral features are mainly dominated by the monoprotonated form of 1,5-benzodiazepine. The electronic absorption spectra of benzodiazepines were reported in the solvents ethanol and cyclohexane depending on their solubility. [20] Typically, a short wavelength band is observed below 250 nm and other two bands of lower intensity are observed in the region of 300 nm and 350 nm respectively. These peaks were described to originate from ππ* transition based on bathochromic shift in non-polar solvents.[21] The corresponding spectra have also been described in acidic media that provides mono-protonation on benzodiazepines resulting in extended conjugation in the seven-membered ring. [21, 22] However, the possible extended conjugation in benzodiazepines does not substantially modify the electronic spectral features characteristic of the monoprotonated benzodiazepines. Based on this knowledge, we assign the peaks at 230, 338 and 390 nm for compound **4** to ππ* transitions and the shoulder at 505 nm is probably due to the anion (which is $[Bi_2Cl_9]^{3-}$ here) to cation ($[C_{12}H_{17}N_2]^+$) charge-transfer transition. The solution electronic absorption spectrum of compound **1** in acetone (Fig. 5.22b) is significantly different from that in solid state (Fig. 5.22a). This reflects the importance of cation–anion interactions in the solid state and these interactions do not remain same in the solution state.

To understand the nature of the first excited singlet state in 1,5-benzodiazepines, emission studies had been attempted earlier and it was found that 1,5-benzodiazepines are not emissive at room temperature[21] A benzodiazepine has a seven membered ring

containing two ring nitrogen atoms. In this context, it is worth mentioning that in six-membered aromatic heterocycles that contain two ring nitrogen atoms (for example, pyrazines, pyrimidines, pyridazines etc.) the lowest lying excited ππ* singlet state lies close in energy to the lowest excited nπ* singlet state.[21] This results in vibronic interaction between the concerned states that permits unusually rapid radiationless decay and hence these heterocycles are characterized by very weak fluorescence, a phenomenon known as "proximity effect" [20] The intervention of the "proximity effect" (found with six-membered ring) was also suggested in the case of 1,5-benzodiazepines, that do not exhibit emission at room temperature.[21]

To our surprise, the compound $[C_{12}H_{17}N_2]_3[Bi_2Cl_9]\cdot 2EtOH$ (**4**) exhibits emission at 400 nm (when it was excited at 328 nm) and 475 nm (when it was excited at 385 nm) at room temperature as shown in Fig. 5.23. We believe that in the present system, the cation-anion interactions play an important role to reduce the "proximity effect" and thereby to rise the lowest lying excited ππ* singlet state considerably from the lowest excited nπ* singlet state.

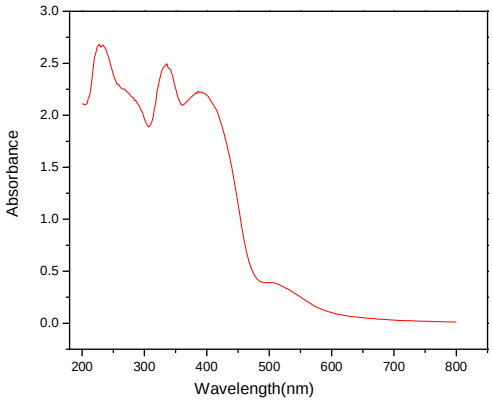


**Fig.22a**

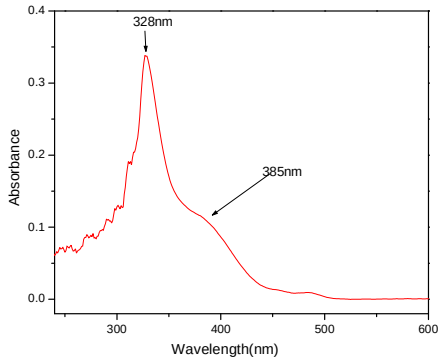


**Fig.22b**

**Fig. 5.22 (a)** Diffuse reflectance electronic spectrum for compound **4**. (**b**) Electronic absorption spectrum in acetone for compound **4**.

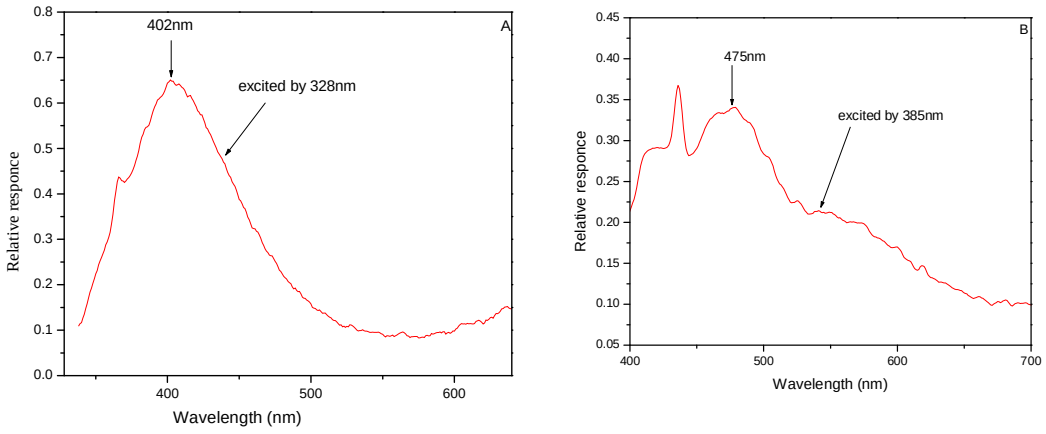


**a** **b**

**Fig. 5.23:** Room temperature emission spectra for compound **4** in acetone: (**a**) excited at 328 nm, (**b**) excited at 385 nm

Thermo gravimetric analyses for all compounds were performed in flowing $N_2$ with a heating rate of 5 $^{\circ}C\ min^{-1}$ in the temperature range of 30–800 $^{\circ}C$. TG curves for compounds **1**, **2** and **3** show that all the compounds are stable up to around 200 $^{\circ}C$; subsequently decomposition started at 235, 195 and 190 $^{o}C$ for compounds **1**, **2** and **3** respectively. TG curve for compound **1** (Fig. 5.24) shows the loss of 70 % in the temperature range of 235–430 $^{\circ}C$. This weight loss corresponds to the decomposition of organic moieties and expelling of six chlorine moieties present in compound **1** (calculated value is 70.44 %). TG curves for compounds **2** and **3**, that reveal the loss of 64.5% and 61.6% in the temperature ranges of 195–300 $^{o}C$ and 190–295 $^{\circ}C$ respectively, are shown in Fig. 5.25 and Fig. 5.26. These weight losses correspond to the loss of organic cations and decomposition of the corresponding chloro species (calculated mass loss 64.25 % and 61.55 % for compound **2** and **3** respectively).

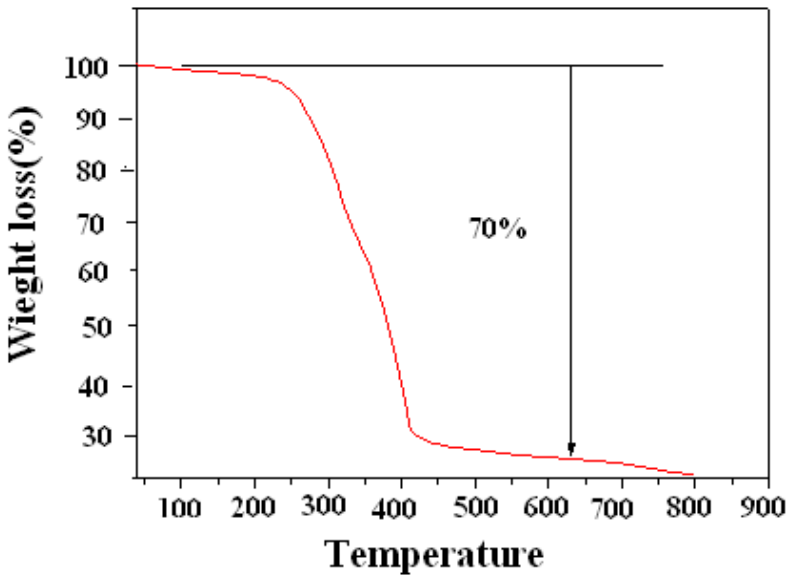


**Fig. 5.24** Thermo gravimetric plot for $[C_5H_7N_2]_3[BiCl_6]$ (**1**)

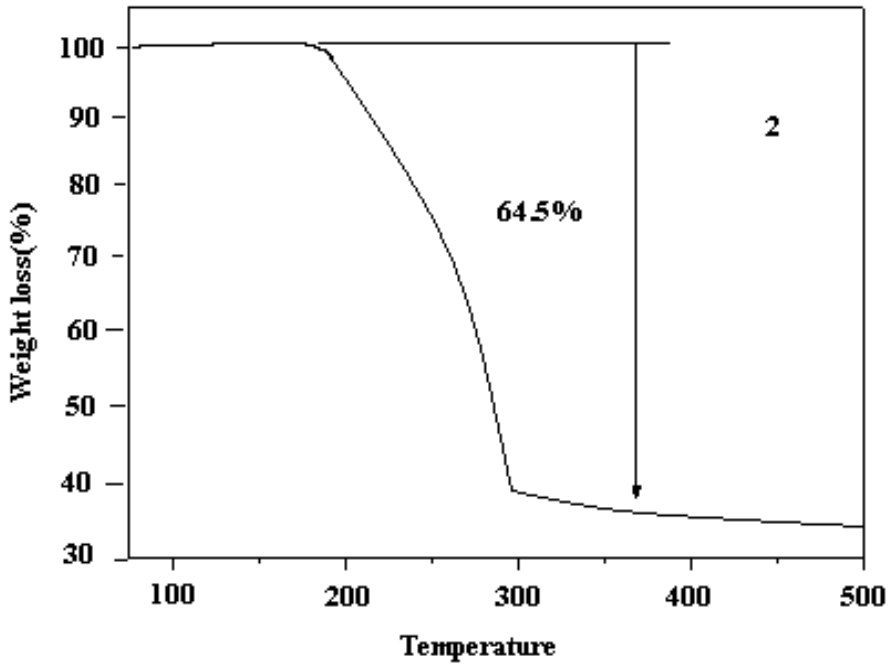


**Fig.5.25** Thermogravimetric plot of $[C_5H_7N_2][C_5H_8N_2][BiCl_6]$ (**2**).

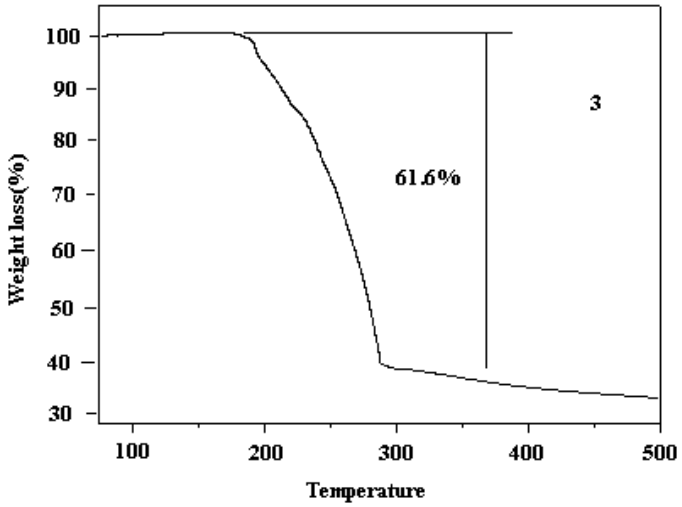


**Fig.5.26** Thermogravimetric plot of $[C_{10}H_{10}N_2]_2[Bi_2Cl_{10}]$ (**3**)**.**

## 5.4. Conclusion

One pot wet syntheses of $[C_5H_7N_2]_3[BiCl_6]$ (**1**), $[C_5H_7N_2][C_5H_8N_2][BiCl_6]$ (**2**), $[C_{10}H_{10}N_2]_2[Bi_2Cl_{10}]$ (**3**), $[C_{12}H_{17}N_2]_3[Bi_2Cl_9]$ · 2EtOH (**4**) and $[C_{12}H_{17}N_2]_3[Bi_2Cl_9]$·2(2-PrOH) (**5**) are described and the resulting compounds have been structurally characterized by single crystal X-ray crystallography. Diverse supramolecular networks were built due to C–H•••Cl interactions for all compounds. Their spectroscopic studies reveal that spectral features are dominated by organic precursors. In addition to this, the ion pair compound **2** exhibits emission signal at room temperature in the visible region. Quantum yield values are consistent with emission intensities. We are now working with biologically important organic amines, so that the resulting ion pair compounds can be used as potential models for bismuth metal containing drugs.

The synthesis of compound $[C_{12}H_{17}N_2]_3[Bi_2Cl_9]$ · 2EtOH (**4**) has many-fold importance: (i) a biologically important molecule, 2,3- dihydro-1H-1,5-benzodiazepine (in its cationic form) has been synthesized from an inexpensive solvent ethanol at ambient conditions; (ii) the present synthesis involves the conversion of *in situ* ethanol to acetone that reacts with *o*-phenylenediamine leading to the formation of compound **4**; as such the conversion of ethanol to acetone is a hectic process that is known to occur in gas phase at a high

temperature; [23] (iii) many bismuth (III) compounds are important as anti-ulcer drugs[44] thus the combination of 1,5-benzodiazepine (known anti-cancer agent) and bismuth(III) species $[Bi_2Cl_9]^{3-}$ results in a composite type compound **4** that should have potential biological properties. Compounds $[C_{12}H_{17}N_2]_3[Bi_2Cl_9]\cdot 2EtOH$ (**4**) and $[C_{12}H_{17}N_2]_3[Bi_2Cl_9]\cdot 2(2\text{-}PrOH)$ (**5**) represent a new class of organic-inorganic hybrid materials, in which organic cations and inorganic anions undergo an extensive supramolecular hydrogen bonding interactions resulting in an intricate hydrogen bonding network. Even though **4** and **5** crystallize in same space group, their supramolecular hydrogen bonding networks are considerably different. Thus solvents of crystallization play an important role in determining the solid state networks. The present system shows room temperature emission indicating the cationic form of 1,5-benzodiazepine is emissive when it is supramolecularly associated with an inorganic complex cation. The neutral molecule 1,5-benzodiazepine is as such is not emissive. We like to extend the work for bismuth coordination with oxo donors and sulfur donor, since they have much importance in drug industry.

## 5.5. References


1. a) Jakubas, R.; Sobczyk, L. *Phase Transit.* **1990**, *20*. 163. b) Sobczyk, L.; Jakubas, R.; Zaleski, J. *Pol. J. Chem.* **1997**, *71*, 265. c) Mróz, B.; Tuszyński, J. A.; Kiefte, H.; Clouter, M. J.; Jakubas, R.; Sept. D. *Phys.Rev.* 1997, *B58*, 14261. d) Kawai, T.; Takao, E.; Shimanuki, S.; Iwata, M.; Miyashita, A.; Ishibashi, Y.; *J. Phys. Soc. Japan*,**1999**, *68*, 2848. e) Hashimoto, M.; Hashimoto, S.; Terao, H.; Kuma, M.; Niki, H.; Ino, H.; *Z. Naturf.* **2002**, *a 55*, 167. f) Wojtaś, M.; Bator, G.; Jakubas, R.; Zaleski, J.; Kosturek, B.; Baran, J.; *J. Solid State Chem.* **2003**, *173*, 425. g) Gutbier, V. A.; Müller, M. *Z. Anorg. Allg. Chem.* **1923**, *128*, 137.
2. Jakubas, R.; Czapla, Z.; Galewski, Z.; Sobczyk, L.; Zogał, O. J.; Lis, T. *Phys. Status Solidi a*, **1986**, *93*, 449.
3. Kallel, A.; Bats, J. *Acta Crystallogr.* **1985**, *C 51*, 1022.
4. Lazarini, F. *Acta Crystallogr.* **1977**, *B 33*, 2686.
5. Sternbach, L. H. *Angew. Chem. Int. Ed.* **1971**, *10*, 34.
6. Fryer, R. I. in: E. C. Taylor (Ed.), *Bicyclic Diazepines, in Comprehensive Heterocyclic Chemistry*, vol. 50, Wiley, New York, 1991, chapter II.

7. a) Harris, R.C.; Straley, J.M. *US Patent*, **1968**, 1,537,757. b) Harris, R.C.; Straley, J. M. *Chem. Abstr.* **1970,** *73*, 100054w.

8. a) Merluzzi, V.; Hargrave, K. D.; Labadia, M.; Grozinger, K.; Skoog, M.; Wu, J. C.; Shih, C.-K.; Eckner, K.; Hattox, S.; Adams, J.; Rosenthal, A. S.; Faanes, R.; Eckner, R. J.; Koup, R. A.; Sullivan, J. L. *Science*, **1990**, *250* 1411. b) Braccio, M. D.; Grossi, G.; Romoa, G.; Vargiu, L.; Mura, M.; Marongiu, M. E.; *Eur. J. Med. Chem.* **2001**, *36*, 935.

9. a) Aversa, M. C.; Ferlazzo, A.; Giannetto, P.; Kohnke, F. H.; *Synthesis*, **1986**, 230**.** b) Chimirri, A. S.; Grasso, S.; Ottana, P.; Romeo, G.; Zappala, M.; *J. Heterocyclic Chem.* **1990**, *27*, 371. c) El-Sayed, A. M.; Abdel-Ghany, H.; El-Saghier, A. M. *Synth*.*Commun*.**1999**, *29* 3561.

10. a) Claramunt, R. M.; Sanz, D.; Aggarwal, S.; Kumar, A.; Prakash, O.; Singh, S. P.; Elgueroc, J. *Arkivoc,* **2006,** 35. b) Pinilla, E.; Torres, M. R.; Claramunt, R. M.; Sanz, D.; Prakash, R.; Singh, S. P.; Elguero, J.; Alkorta, I. *Arkivoc,* **2006**, *2*, 136. c) Prakash, O.; Kumar, A.; Sadana, A.; Prakash, R.; Singh, S. P.; Claramunt, R. M.; Sanz, D.; Alkorta, I.; Elguero, J. *Tetrahedron*, **2005**, *61*, 6642.d) Alcalde, E.; Pérez-García, L.; Dinarés, I.; Frigola, J. *J. Org. Chem.* **1991**, *56*, 6516. e) Boruah, R. C.; Skibo, E. B. *J. Org. Chem.* **1993**, *58*, 7797.

11 a) Said, M. A.; Kumara Swamy, K. C.; Poojary, D. M.; Clearfield, A.; Veith M.; Huch, V.; *Inorg. Chem.* **1996**, *35*, 3235. b) Said, M. A.; Swamy, K. C. K.; Babu, K.; Nethaji, M.; *J. Chem. Soc. Dalton Trans.* **1995,** 2151. c) Swamy, K. C. K.; Said, M. A.; Netaji, M. *J. Chem. Crystallogr.* **1999**, *29*, 1103.d) Anjaneyulu, O.; Prasad T. K.; Swamy, K. C. K. *Dalton Trans.* **2010,** *39*,1935.

12. a) Software for the CCD Detector System, Bruker Analytical X-ray Systems Inc., Madison, WI, 1998. b) Bruker SADABS, SMART, SAINTPLUS and SHELXTL, Bruker AXS Inc., Madison, WI, USA, 2003.c) G.M. Sheldrick, SHELX-97, Program for Crystal Structure Solution and Refinement, University of Göttingen, Germany, 1997.d) Sheldrick, G. M. *Acta Cryst.* **2008**, *A64*, 112.

13. Pasha, M. A.; Jayashankara, V. P. *J. Pharmcol. Toxicol.* **2006**, *1*, 573.

14. Bussi, J.; Parodi, S.; Irigaray, B.; Kieffer, R. *Appl. Catal. A*: *General*, **1998**, *172*, 117.

15. a) Podesta, T. J.; Orpen, A. G. *Cryst. Growth Des.* **2005**, *5*, 681. b) Jarraya, S.; Salah, A. B.; Daoud, A. *Acta Cryst.* **1993**, *C49*, 1594. c) Lazarini, F. *Acta Cryst.* **1987**, *C43*, 637. d) Herdtweck, E.; Kreusel, U. *Acta Cryst.* **1993**, *C49*, 318. e) Benetollo, F.; Bombieri, G.; Pra, A. D.; Alonzo, G.; Bertazzi, N. *Inorg. Chim. Acta,***2001**, *319*, 49.

16. Sarma, B.; Reddy, L.S.; Nangia, A. Cryst. Growth Des. **2008**, 4546.

17. a) Benetollo, F.; Bombieri, G.; Pra, A. D.; Alonzo, G.; Bertazzi, N. *Inorg. Chim. Acta,* **2001**, *319* , 49. b) Bigoli, F.; Lanfranchi, M.; Pellinghelli, M. A. *Inorg. Chim. Acta*, **1984**, *90* 215.

18. Jakubas, R.; Bator, G.; Medycki, W.; Pislewski, N.; Decressain, R.; Lefebvre, J.; Francois, P. *J. Mol. Str*. **1996**, *385,*145.

19. Barltrop, J. A.; Richards, C. G.; Russell, D. M.; Ryback, G. *J. Chem. Soc.* **1959**, 1132.

20. Mellor, J. M.; Pathirana, R. N.; Stibbard, J. H.A. *Spect. chim. Acta*. **1982**, *38A*, 389.

21. Barltrop, J. A.; Richards, C. G.; Russell, D. M.; Ryback, G. *J. Chem. Soc.* **1959**, 1132.

22. a) Lloyd, D.; Mcdougall, R. H.; Marshall, D. R. *J. Chem. Soc.* **1965**, 3785. b) Turner, D. W. *Molecular Photoelectron Spectroscopy*, Wiley, 1970.

23. Bussi, J.; Parodi, S.; Irigaray, B.; Kieffer, R. *Appl. Catal. General*, **1998**, *172*, 117.

24. Mccolm, A. A.; McLaren, A.; Klinkert, G.; Francis, M. R.; Connolly, P. C.; Grinham, C. J.; Campbell, C. J.; Selway, S.; Williamson, R. *Aliment Pharmacol Ther*. 10 (1996) 241.

# Future scope of the present thesis

## 6.1 Polyoxometalates

Polyoxometalates (POMs) have fascinating features / properties, such as, supramolecular interactions and catalysis. Supramolecular chemistry includes diverse architectures from 1-D to 3- D. Due to the presence of number of oxygen atoms, present in the POMs, they are extensively involved in hydrogen bonding interactions with counter cation (which is required to successful isolation of a POM). The oxo groups /oxides, which are from the four sides of a POM are involved in forming hydrogen bonds with surrounding organic cation leading to the 3-dimensional framework as shown in Fig 6.1. If the hydrogen bonding involvement proceeds from only three oxides of a POM, it generates 2-dimensional network as shown in Fig 6.2. If it happens from two sides of a POM, 1-dimensional chain has been generated (Fig. 6.3). In the present thesis, we have succeeded to generate from 1-D to 3-D networks in diverse POMs. Lattice water molecules also play a vital role to decide the dimensionality (compound **9** is generates 1-dimensional chain due to the involvement of lattice water molecules).

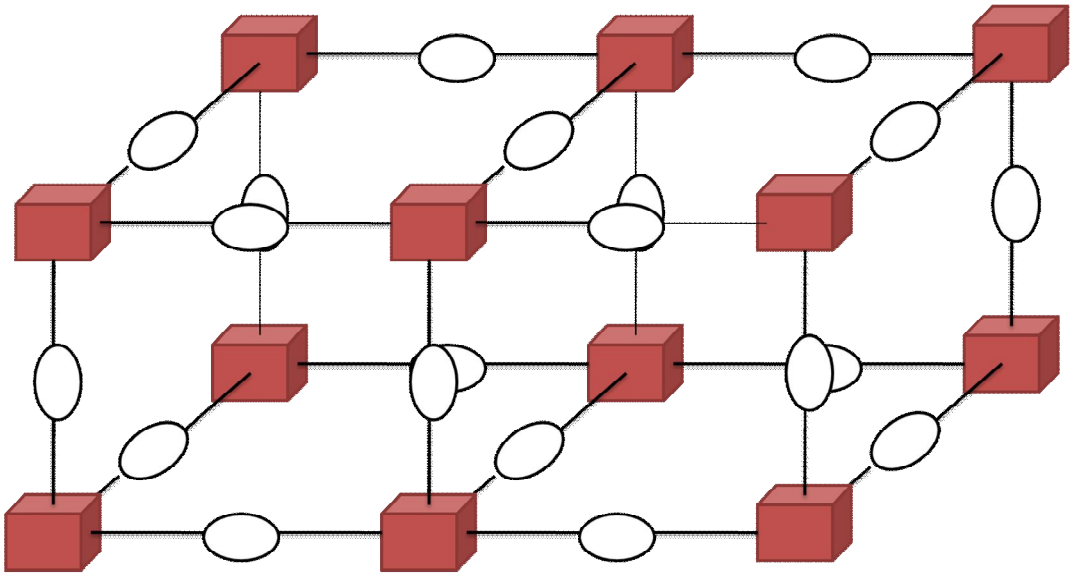

**Fig 6.1** 3-Dimensional framework established due to oxides of four sides involved in hydrogen bonding interactions with surrounding counter cations or lattice water

molecules. Red box corresponds to POM and white circle is counter cation or lattice water molecule.

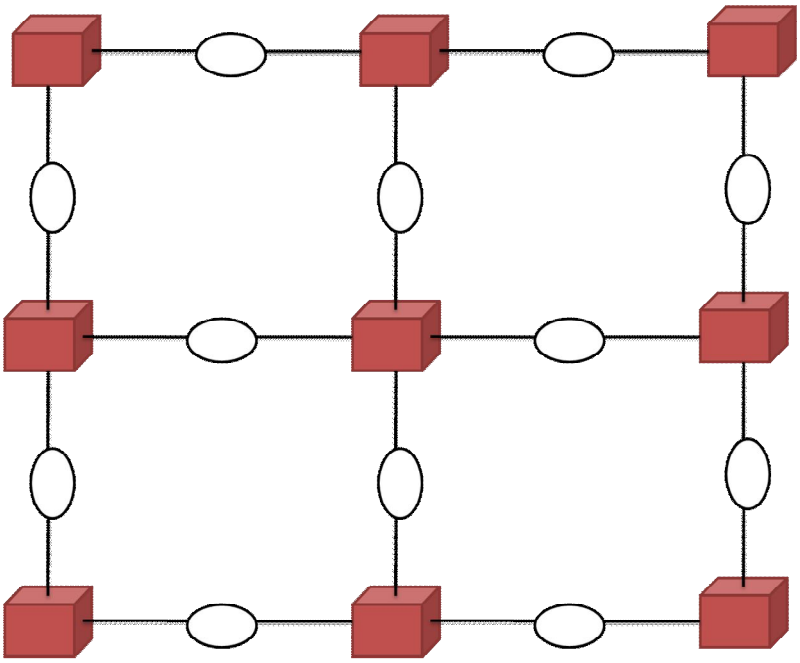

**Fig 6.2** 2-Dimensional network established due to oxides of four sides, involved in hydrogen bondings with counter cation or lattice water molecules. Red box corresponds to POM and white ellipsoid is counter cation or lattice water molecule.

**Fig 6.3** 1-Dimensional chain established due to oxides of two sides, involved in hydrogen bonding interactions with surrounding counter cation sor lattice water molecules. Red box corresponds to POM and white ellipsoid is counter cation or lattice water molecules.

Depending on the position of H accepter or donor , they can establish various kinds networks. If we isolate the Keggin or Lindquist or Well Dawson cluster with proper cation, we can make the 3-Dimensional framework which is useful in the gas absorption. Our aim is to synthesize such materials by using amino pyridines derivative.

We have demonstrated the styrene oxidation reactions catalyzed by POV-based materials in chapter 3. To continue this catalysis work, oxidation reactions of other olefins are to be extended; the catalysts to be chosen will be not only POVs, but also other POMs and even polyoxotungstates and other mixed valant vanadium clusters. The results are expected to be different from the catalysts described in this thesis. Our main observation from the catalysis part in the present thesis is that, if we reduce the time, the formation of epoxide will be favored. By optimizing further the conditions, the percentage can be improved largely.

The catalytic applications of $\{Mo_{132}\}$ and $\{Mo_{72}Fe_{32}\}$clusters in oxidations of alcohols and olefins are under progress in our laboratory; interestingly they show the good catalytic activity even with micro amount of the compounds in the concerned reaction. As the size of the cluster is big and the presence of more number of metal-oxo bridges, it has much surface area; thus micro amount of compound / catalyst is sufficient to get good percentage of conversion in the oxidation of olefin and alcohols.

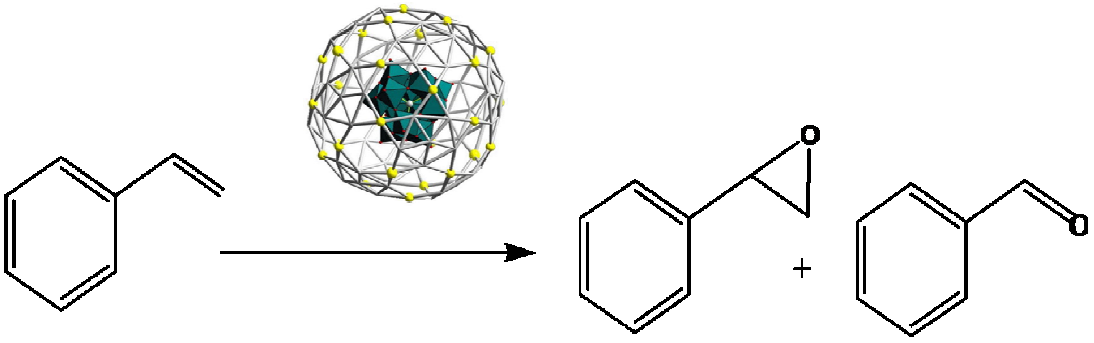

**Scheme 6.1** Oxidation of styrene by using the $Mo_{72}Fe_{30}$ with $H_2O_2$ as an oxidant.

Oxidation of styrene derivatives by using this cluster is our continuation of the current project. In addition to this, oxidation of alcohol to corresponding ketone is the future plan of this project by using our synthesized compounds as well as $\{Mo_{132}\}$ and $\{Mo_{72}Fe_{32}\}$.

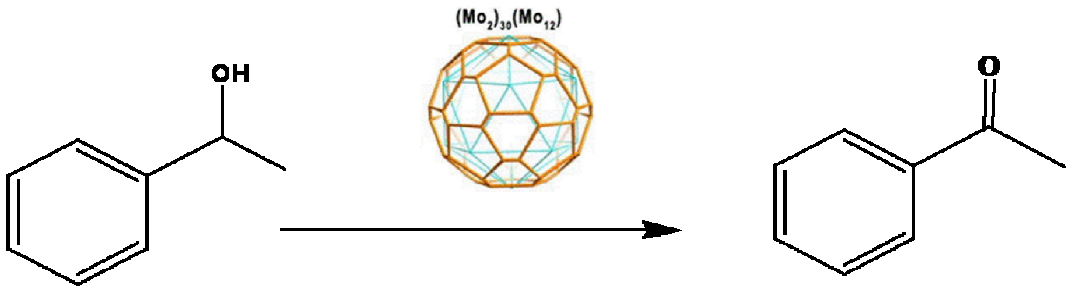


**Scheme 6.2** Oxidation of alcohol to corresponding ketone by using the $Mo_{132}$ cluster as catalyst with $H_2O_2$ as an oxidant.

We are also planning to synthesize the POM clusters by using chiral amines (as cations). Even though numerous reports have come in this area of POM synthesis, the catalysis in asymmetric synthesis has not much explored with these chiral amine associated POMs.

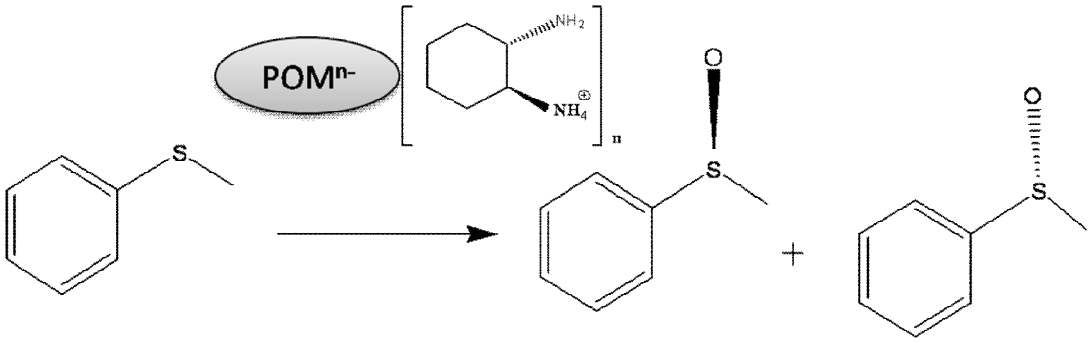


**Scheme 6.3** Oxidation of thioanisole leads to two enantiomers of sulfoxides with chiral POM molecule. ($H_2O_2$ as an oxidant)

If POMs are isolated with chiral amines e.g., 1, 2 cyclohexylamine and proline, then they are useful in asymmetric oxidation of sulfur analogues and in the reaction of Aldol with enantiomeric excess. Recently Aldol condensation reaction is reported with enantiomeric excess product by using the Keggin salt of the substituted proline as a chiral catalyst. We are interested to make other POMs like Standberg, decavanadate and Anderson anion with substituted proline and 1, 2 cyclohexylamine as counter cations. This type of catalysts will be useful in asymmetric aldol reactions and sulfoxidation reactions.

Another upcoming project is to synthesize these POMs with biological molecules, like cytosine, guanine thymine and uracil; they might be biologically active. Some of the model structures are shown in Fig 6.4.

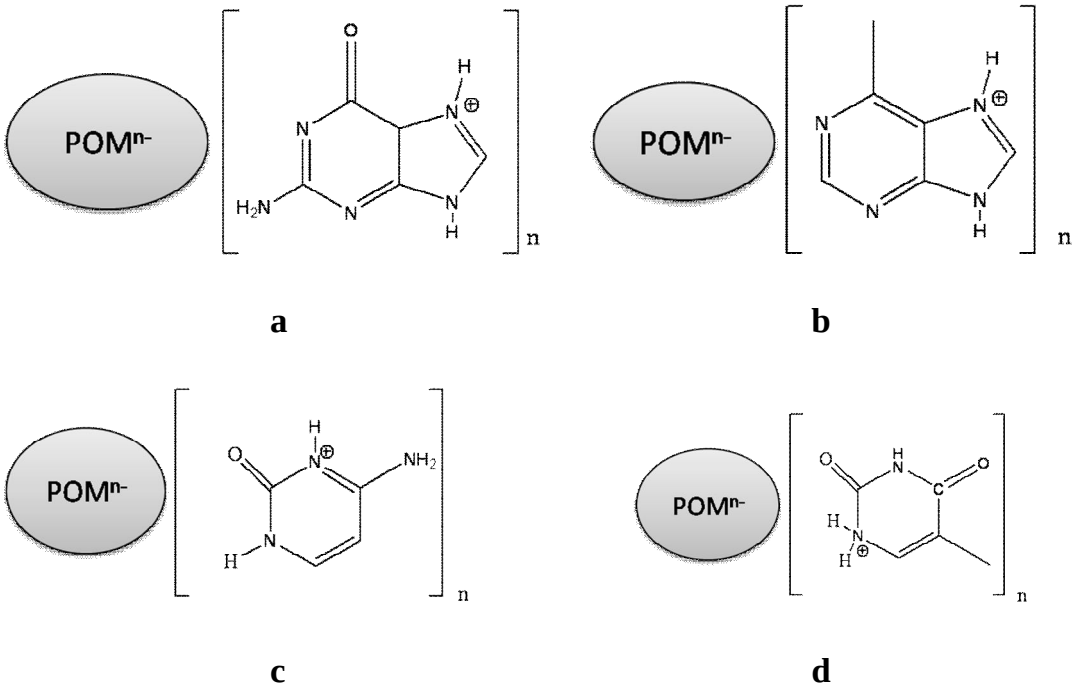


**Fig 6.4** Model POM salts of a) adenine, b) guanine, c) Cytosine d) thymine

### 6.2 Bismuth Derivatives

As bismuth coordination compounds are useful in drug industry, we would like to extend the synthesis of bismuth coordination materials with oxygen donar ligands and sulfur donor ligands, such as, mercaptomenzothiazole and amino acids (e.g., glycine, alanine and arginine). This work is under project in our laboratory. One model structure is shown in the following Fig 6.5.

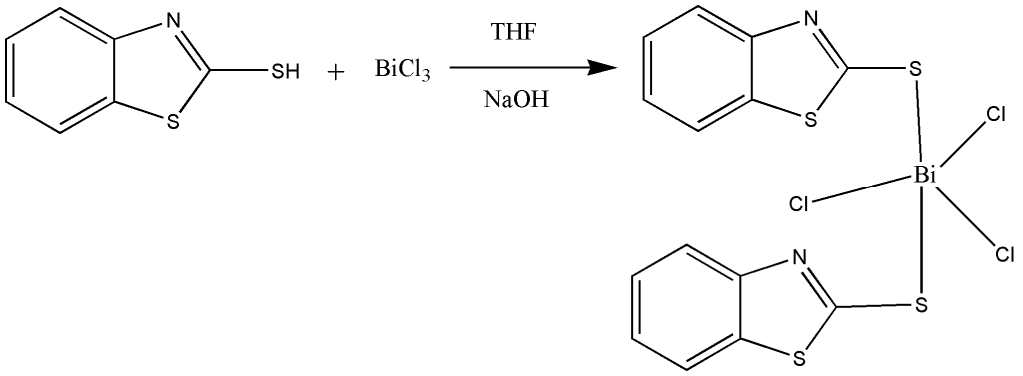


**Scheme 6.5** The model structure of bismuth coordination compound with mercaptobenzothiazole.

# List of Publications

1. Two different Zinc(II)-aqua complexes held up by a metal-oxide based support: Synthesis, crystal structure and catalytic activity of $[HMTAH]_2[\{Zn(H_2O)_5\}\{Zn(H_2O)_4\}\{Mo_7O_{24}\}]\cdot 2H_2O$ (HMTAH = protonated hexamethylenetetramine), *J. Chem. Sci*, 2008, **120**, 95-105.

   T. Arumuganathan, **A. Srinivasa Rao,** T. Vijay Kumar and Samar K Das*. *J. Chem. Sci*, 2008, **120**, 95-105.

2. Non-covalent O · · · O interactions among isopolyanions using a cis-{MoO2} moiety by the assistance of N–H···O hydrogen bonds.

   T. Arumuganathan, **A. Srinivasa Rao** and Samar K. Das*, *J. Chem. Sci*., 2008, ***120,*** 297–304.

3. Chiral synthesis of a mononuclear Nickel(II) complex from an Achiral Tripodal amine ligand: Spontaneous resolution.

   **A. Srinivasa Rao,** Abhijit Pal , Ghosh R and Samar K. Das*. *Inorg. Chem.* 2009, **48,** 1802-1804.

4. Isolation and structural characterization of 1, 5-benzodiazepinium cation in an Inorganic-organic hybrid compound $[C_{12}H_{17}N_2]_3[Bi_2Cl_9]\cdot 2EtOH$.

   **A. Srinivasa Rao,** Eadi Sunil Babu, K C Kumar Swamy* and Samar K. Das*. *polyhedron*, 2010, **29**, 1706-1714.

5. Orthophenylenium salt of chloro acetate.

   **A. Srinivasa Rao,** Bharat Kumar T, Kishore Ravada and Samar K. Das*. *Acta. Cryst.* 2010, ***E66***, o1945.

6. Polyoxometalates Supported Transition Metal Complexes: Synthesis, Crystal structures, and Supramolecular Structures

   T. Arumuganathan, **A. Srinivasa Rao** and Samar K. Das*. *Cryst. Growth Des.* 2010, **10**, 4272-4284.

7. Polyoxometalates: new materials and properties.

**A. Srinivasa Rao,** T Arumuganathan, V shivaiah and Samar K. Das*. *J. Chem. Sci*., 2011, **123**, 229-239. (**Cover page issue**)

8. Stabilization of $[BiCl_6]^{3-}$ and $[Bi_2Cl_{10}]^{4-}$ with Various Organic Precursors as Cations Leading to Inorganic-Organic Supramolecular Adducts: Syntheses, Crystal Structures and Properties of $[C_5H_7N_2]_3[BiCl_6]$, $[C_5H_7N_2][C_5H_8N_2][BiCl_6]$ and $[C_{10}H_{10}N_2]_2[Bi_2Cl_{10}]$.

**A. Srinivasa Rao,** Upama Baruah and Samar K. Das*. *Inorg.Chim.Acta.,* 2011, **372**, 206-212.

9. Uranyl ion lidded fluorescent supramolecular capsule with Cucurbit[5]uril.

S. Kushwaha, **A. Srinivasa Rao** and P. Padmaja**.** (Manuscript under revision)

10. Oxidation of styrene to benzaldehyde using transition metal complexes supported by heptamolybdate anion.

**A. Srinivasa Rao,** T.Arumuganathan, Anjali Patel and Samar K. Das*. (communicated)

11. Polyoxovanadate based materials: Synthesis, Structural characterization and catalytic properties

**A. Srinivasa Rao,** and Samar K. Das*. (To be communicated)

12. Synthesis and Structural characterization of Anderson based Inorganic-Organic Hybrid materials and their catalytic applications

**A. Srinivasa Rao,** T. Arumuganathan, and Samar K. Das*. (To be communicated)

## Posters and Presentations

1) **A. Srinivasa Rao** and Samar K. Das*, One Pot Wet Synthesis of Inorganic-Organic Hybrid Materials with Polyoxometalates: Synthesis, Characterization and catalytic activity towards the oxidation of alcohols and epoxidation of olefins, **poster presented** in "**X CRSI-2008**" and which was held in Febraury-**2008**, Indian Institute of Science, Bangalore, India.

2) **A. Srinivasa Rao** and Samar K. Das*, One Pot Wet Synthesis of Inorganic-Organic Hybrid Materials with Polyoxometalates: Synthesis, Characterization and catalytic activity towards the oxidation of alcohols and epoxidation of olefins, **poster presented** in "**Chemfest-2008**" and which was held in March-**2008**, School of Chemistry, University of Hyderabad, India.

3) **A. Srinivasa Rao** and Samar K. Das*, One Pot Wet Synthesis of Inorganic-Organic Hybrid Materials with Polyoxometalates: Synthesis, Characterization and catalytic activity towards the oxidation of alcohols and epoxidation of olefins. **Awarded as the best poster presentation**, which was held in July-**2008**, (**NCMC'08**)" held in GITAM University-Visakhapatnam, India, **2008**.

4) **A. Srinivasa Rao** and Samar K. Das*, Coordination polymers with unusual linkers: Synthesis. Characterization and Applications. **Poster presented** in "**Chemfest-2009**" and which was held in March-**2009**, School of Chemistry, University of Hyderabad, India

5) **A. Srinivasa Rao** and Samar K. Das*, Synthesis and Characterization of Inorganic-Organic Hybrid Materials and their Catalytic Activity Towards Organic Transformations of Industrial Importance. **Poster presented** in "**XIII-MTIC-2009**" and held in December-**2009**, Indian Institite of Science, Bangalore, India. (**Modern Trends in Inorganic Chemistry**)

6) **A. Srinivasa Rao** and Samar K. Das*, Synthesis and Characterization of Inorganic-Organic Hybrid Materials and their Catalytic Activities Towards Organic Transformations of Industrial Importance. **Lecture presented** in "**Chemfest-2010**" and which was held in January-**2010**, School of Chemistry, University of Hyderabad, India.

**7)** **A.Srinivasa Rao** and Samar K. Das*, Synthesis and Characterization of Inorganic-Organic Hybrid Materials and their Catalytic Activities Towards Organic Transformations of Industrial Importance. **Lecture presented** in "**KVR Presentation-2010**" and which was held in June-**2010**, KVR Building, Hyderabad, India.

## SYNOPSIS

This thesis work entitled with **"Diverse Polyoxometalate Clusters and Bismuth-chloro Derivatives: Synthesis, Characterization, Catalysis and Photo-physical Studies",** consists of five chapters: (**1**) Introduction, (**2**) Oxidation of Styrene to benzaldehyde using transition metal complexes supported by heptamolybdate anion, (**3**) Polyoxovanadete based materials: Synthesis, Structural characterization and catalytic properties, (**4**) Synthesis and Structural Characterization of Inorganic-Organic Hybrid Materials Based on Anderson Type Heteropolyanion Their Catalytic Applications, (**5**) Isolation of Bismuth-Chloroderivatives ($Bi_2Cl_9^{3-}$, $BiCl_6^{3-}$ and $Bi_2Cl_{10}^{4-}$ ) by Using Various Organic Precursors and Physical Properties of Their Respective Inorganic-Organic Hybrid Materials. The work described in this thesis, is in the direction of the synthesis and characterization of Inorganic-Organic hybrid materials based on Anderson anion $\{AlMo_6(OH)_6O_{18}\}^{3-}$ and decavanadate anion $\{V_{10}O_{28}\}^{6-}$ and their extensive application studies in the catalysis using these synthesized compounds in the reactions of oxidation of styrene. Chapter 5 describes the synthesis and characterization of chlorobismuthate salts of organic ammonium cations and finally their physical studies that include electronic and emission studies. This chapter also describes the isolation of 1, 5 benzodiazapine as a salt of $[Bi_2Cl_9]^{3-}$. Apart from the first chapter (introduction), all other chapters are sub-divided into Introduction, Experimental Section, Results and Discussion and Conclusions followed by References.

## Chapter 1

## Introduction to Polyoxometalates and Bismuth Based Materials

This chapter begins with more fundamental ideas about inner–transition metal (Mo, W and V) oxo clusters, known as polyoxometalate (POM) cluster anions, starting from its history. It also exposes the basic principles involved in POM clusters syntheses, structural characterization and properties. Some of the polyoxometalate cluster anions, that are more relevant to various chapters of this thesis, are picked up from the literature and their structural topologies, various properties, such as host–guest interactions, magnetism, catalysis, medicinal applications and supramolecular interactions are discussed briefly. The other part of Introduction is described by some literatures on bismuth-chloro derivatives that include structures, applications in diverse fields like semiconductor, ferroic and antiferroic materials and drug industry. Finally a brief note on the main objectives of this thesis work is conversed shortly.

## Chapter 2
## Oxidation of Styrene to Benzaldehyde Using Transition Metal Complexes Supported by Heptamolybdate Anion

This chapter describes the catalytic applications of polyoxometalate (POM) supported transition metal complexes (TMCs) in the reaction of oxidation of styrene that leads to selective product. A new series of polyoxometalate supported transition metal complexes namely, $[2\text{-ampH}]_4[Co(H_2O)_5Mo_7O_{24}]\cdot 9H_2O$ (**1**), $[3\text{-ampH}]_4[\{Co(H_2O)_5\}Mo_7O_{24}]\cdot 9H_2O$ (**2**), $[2\text{-ampH}]_4[\{Zn(2\text{-ampy})(H_2O)_4\}Mo_7O_{24}]\cdot 4H_2O$ (**3**), $[3\text{-ampH}]_4[\{Zn(3\text{-ampy})(H_2O)_4\}Mo_7O_{24}]\cdot 4H_2O$ (**4**) have been synthesized according to literature procedure.

Complete catalytic studies of all these compounds (**1**-**4**) are performed in oxidation reactions of styrene. As the catalysts are not destroyed after completion of the reactions, which has been confirmed by infrared, solid state UV-visible spectroscopy and powder X-ray crystallography, the catalyst has been used for three times more for the same conversion. Interestingly, when first two compounds (**1** and

**2**) are used as catalysts in the oxidation of styrene, the major product was benzaldehyde. On the other hand, the other two compounds (**3** and **4**) give benzoic acid as the major product. It is to be mentioned here that first two compounds are cobalt complexes supported on POM clusters and the last two compounds are POM supported zinc compounds.

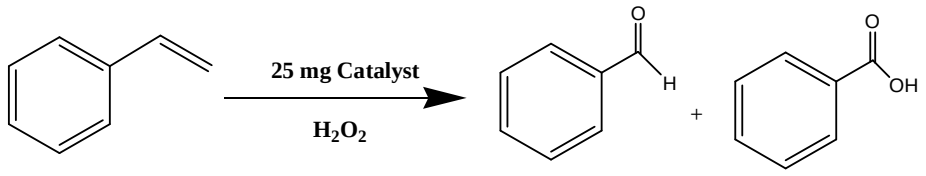


**Styrene** **Benzaldehyde** **Benzoic acid**

Apart from these two major products, some other products are also formed in these reactions, that are confirmed by GC-MS. Percentage of conversions are analyzed by gas chromatography associated with mass spectroscopy. A graphical study of percentage of conversion with time variation of reaction has been performed. Some relevant results are shown in the Table 1.1.

**Table 1.1** Oxidation of styrene by using all the catalysts (**1**–**4**).

| **Catalyst** | **Conversion (%)** | **Selectivity(%)** | | | | |
|---|---|---|---|---|---|---|
| | | **Benzaldehyde** | **Epoxide** | **Benzyl alcohol** | **Benzoic acid** | **Acetophenone** |
| **1*** | **99.3** | **76** | – | – | **24** | – |
| **2*** | **96** | **76** | **3** | **5** | **15** | **1** |
| **3†** | **100** | **16** | **0** | **6** | **58** | **20** |
| **4†** | **100** | **15** | **3.8** | **1.2** | **69** | **11** |

## Chapter 3
## Polyoxovanadate Based Materials: Synthesis, Structural Characterization and Catalytic Properties

A new series of polyoxovanadate (POV) compounds, based on decavanadate $\{V_{10}O_{28}\}^{6-}$ anionic cluster, formulated as $[Co(H_2O)_6][Na_4(H_2O)_{16}]\{V_{10}O_{28}\}\cdot 4H_2O$ (**1**), $[Zn(H_2O)_6][Na_4(H_2O)_{16}]\{V_{10}O_{28}\}\cdot 10H_2O$ (**2**), $[HMATAH]_2\{H_4V_{10}O_{28}\}\cdot 8H_2O$ **(3).**, $[HMTAH]_2\{(H_2O)_4Zn_2V_{10}O_{28}\}\cdot 2H_2O$ (**4**), $[Co(3\text{-amp})(H_2O)_5]_2[3\text{-ampH}]_2\{V_{10}O_{28}\}\cdot 6H_2O$ (**5**) $[4\text{-ampH}]_5[Na(H_2O)_6]\{V_{10}O_{28}\}\cdot 4H_2O$ (**6**), $[4\text{-ampH}]_{10}[Co(H_2O)_6]\{V_{10}O_{28}\}_2\cdot 10H_2O$ (**7**) and $[4\text{-ampH}]_{10}[Zn(H_2O)_6]\{V_{10}O_{28}\}_2\cdot 10H_2O$ (**8**) and $[3\text{-ampH}]_6[V_{10}O_{28}]\cdot 2H_2O$ (**9**) have been synthesized (where HMATAH = protonated hexamethylenetetramine, 3-ampH = protonated 3-aminopyridine and 4-ampH= protonated 4-aminopyridine) from the corresponding aqueous solutions of sodium-vanadate, by varying the pH condition and aminopyridine/Hexamine derivatives. In compounds **1**- **9**, the common POV cluster is $[V_{10}O_{28}]^{6-}$, which is presented in Fig. 3.1. In the crystal structure of compound **1**, this cluster supports alkali metal-aqua complexes that extend to coordination polymer. Conversely in the crystal structure of compound **2,** total moiety is discrete and the residual negative charges have been compensated by the Zinc hexa-aqua complex $[Zn(H_2O)_6]^{2+}$ and sodium-aqua complex $[Na_4(H_2O)_{14}]^{4+}$ acting as cations. Thus **1** and **2** are totally organic free compounds. In the case of compound **3**, the charges are compensated by [HMATAH] cation and protons. In its crystal structure, lattice water molecules generate cyclic water tetramers. In the crystal structure of compound **4**, POV cluster anion supports the zinc coordination complexes, $\{Zn(H_2O)_4\}^{2+}$, in total it is a coordination polymer. The overall negative charges of the resulting POV supported transition metal complexes, in compound **4**, have been counter-balanced by the [HMATAH] cationic form. In the case of compound **5,** the anionic cluster unit $[V_{10}O_{28}]^{6-}$ exists as a discrete moiety, where the species $[Co(3\text{-amp})(H_2O)_5]^{2+}$ and $[3\text{-ampH}]^{1+}$ respectively act as mere counter cations. The crystal structure of compound **6** is constructed by $[V_{10}O_{28}]^{6-}$ anion and $[Na(H_2O)_6]^{1+}$ and protonated 4-aminopyridine $[4\text{-ampH}]^{1+}$ cation moieties. Cyclic pentamer is found to be formed among the lattice water molecules in the crystal structure of compound **6** because of O–H···O interactions, as shown in Fig 3.2.

Compounds **7** and **8** are isomorpous where decavanadate cluster exists as anion and it is counter balanced by $\{Co(H_2O)_6\}^{2+}$ and $\{Zn(H_2O)_6\}^{2+}$ respectively. Compound **9** is simple salt of decavandate with protonated 3-aminopyridine. In compound **9,** lattice water molecules noncovalently interact with surrounding cluster, leading to one dimensional chain as shown in Fig. 3.3. All the compounds (**1**-**9**) are synthesized at an ambient temperature and are characterized by X-ray crystallography. Synthesized compounds are additionally characterized by elemental analyses, infra-red and diffuse reflectance spectropy including emission studies. All the compounds show good catalytic activity in the oxidation of styrene leading to the major product as benzaldehyde. These catalysts are reused in the same transformation as catalyst doesn't lose the activity. Due to the higher activity of vanadium, these reactions are successful even at room temperature. Percentage of conversion with respect to the duration of the reaction has been discussed in the present chapter.

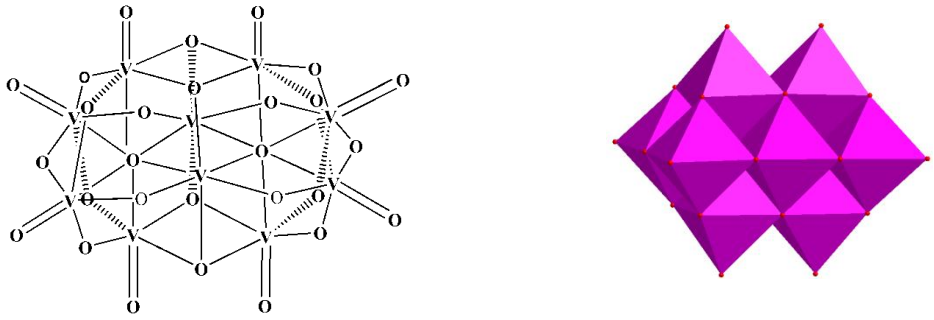

**Fig. 3. 1** Decavanadate $\{V_{10}O_{28}\}^{6-}$ anionic cluster as a ISIS Chem draw and polyhederal representation

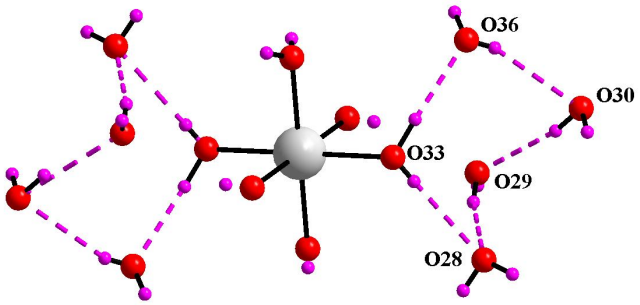


**Fig. 3.2** Generation of dumbell like network due to O–H···O interaction in compound **6**. Color codes: O, red; Na, grey; H, purple.

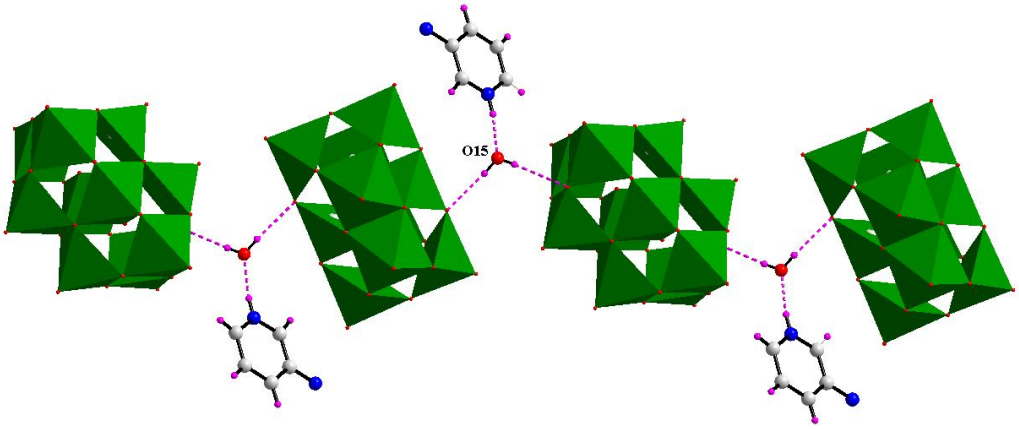


**Fig. 3.3** Hydrogen bonding situation around lattice water molecule of compound **9**. The isopolyanion is shown in green polyhedral representation. Color code: V, blue violet; O, red; C, gray; N, blue; H, Purple;

## Chapter 4

## Synthesis and Structural Characterization of Anderson Type Heteropolyanion based Inorganic-Organic Hybrid Materials and Their Catalytic Applications.

This chapter is mainly focused by the solid state characterization of inorganic-organic hybrid materials based on Anderson anionic cluster isolated. They are formulated as $[2\text{-AmpH}]_2[\{Na(H_2O)_2\}\{AlMo_6(OH)_6O_{18}\}]\cdot 4H_2O$(**1**), $[3\text{-AmpH}]_2[HAlMo_6(OH)_6O_{18}]\cdot 4H_2O$(**2**), $[4\text{-AmpH}_2]_6[AlMo_6(OH)_6O_{18}]_2\cdot 18H_2O$(**3**) and $[2\text{-AmpH}]_5[IMo_6O_{24}]\cdot 2H_2O$(**4**). Compounds **1**, **2** and **3** are synthesized starting from $AlCl_3\cdot 6H_2O$ and respective cation under wet condition at pH 3. Several reports have shown that Anderson anion plays key factor for making the building blocks for the formation of 1-D to 3- dimensional networks. Compound **1** is a coordination polymer of Anderson anion with sodium aqua complex which is shown in Fig. 4.1.

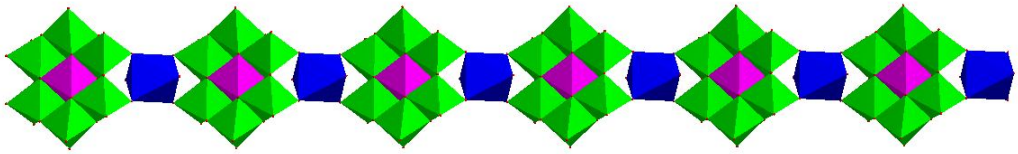

**Fig.4.1** 1- Dimensional coordination polymer in compound **1**. Color code: Na polyhedra, blue; Aluminium, megenta and Molybdenum, green**.**

Even though, compounds **1**, **2** and **3** contain the common Anderson anion; due to the variation of counter cation, their supramolecular structure is completely varied including their packing diagram.

Compound **4** is isolated under the same condition, which is based on Anderson anion with iodine as a central atom by using the 2-aminopyridine.This compound is formulated as $[2\text{-AmpH}]_5[IMo_6O_{24}]\cdot 2H_2O$(**4**). Structure of iodine based Anderson anion is represented in Fig. 4.2. Catalytic activities have been performed in the oxidation of styrene for selective conversion.

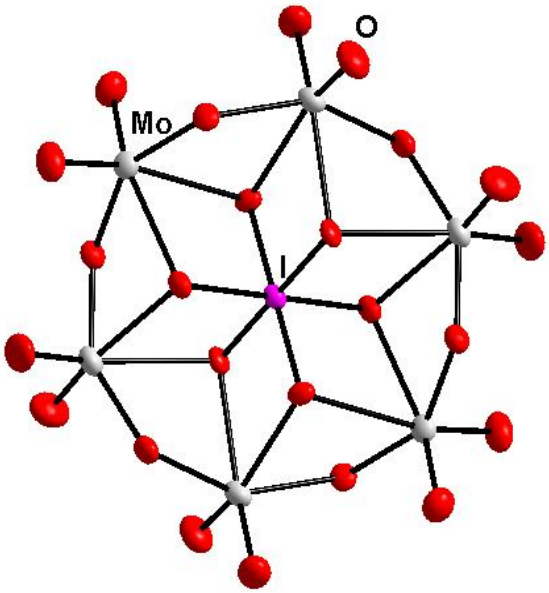


**Fig. 4.2** The picture of Anderson anion with iodine central atom. Color code: I, magenta; O, red; Mo, grey.

## Chapter 5
## Isolation of Bismuth-Chloroderivatives ($Bi_2Cl_9^{3-}$, $BiCl_6^{3-}$ and $Bi_2Cl_{10}^{4-}$) by using various organic precursors and physical properties of their respective Inorganic-Organic Hybrid materials

In the present chapter, we describe the syntheses, crystal structures and properties of ion pair compounds $[C_5H_7N_2]_3[BiCl_6]$ (**1**), $[C_5H_7N_2][C_5H_8N_2][BiCl_6]$ (**2**) $[C_{10}H_{10}N_2]_2[Bi_2Cl_{10}]$ (**3**), $[C_{12}H_{17}N_2]_3[Bi_2Cl_9]\cdot 2EtOH$ (**4**) and $[C_{12}H_{17}N_2]_3[Bi_2Cl_9]\cdot 2(2\text{-}PrOH)$ (**5**). Compounds **1**, **2, 4** and **5** crystallize in triclinic system (space group, *P-1*), whereas compound **3** crystallizes in monoclinic system (space group, $P2_1/c$). In their crystal structures, supramolecular hydrogen bonding interactions between bismuth-chloro anion and organic cation play an important role in the stabilization of $[BiCl_6]^{3-}$ , $[Bi_2Cl_{10}]^{4-}$ and $[Bi_2Cl_9]^{3-}$ anions. All the compounds are characterized by routine spectral analyses and elemental analyses, besides crystal structure determinations. Compounds **1, 2** and **3** are additionally characterized by thermogravimetric analyses. Interestingly, compounds $[C_5H_7N_2][C_5H_8N_2][BiCl_6]$ (**2**), $[C_{12}H_{17}N_2]_3[Bi_2Cl_9]\cdot 2EtOH$ (**4**) and

$[C_{12}H_{17}N_2]_3[Bi_2Cl_9]\cdot 2(2\text{-PrOH})$ (**5**) exhibit emission signal at room temperature in the visible region.

The crystal structure of compound **1** shows a 2-dimensional supramolecular network due to the existence of further strong C–H•••Cl hydrogen bonds and π–π interactions among the 2-aminopyridine, which is shown in Fig.5.1. In compound **2**, the packing of the organic cations shows an head-to-head pattern, in which every two organic moieties are very closed to each other (3.170Å) due to π–π interaction (see Fig. 5.2). On the other hand, compound **3** exhibits C–H•••Cl hydrogen bonds. The supramolecular interactions between $[Bi_2Cl_{10}]^{4-}$ anion and $[4, 4'\text{-bipyH}_2]^{2+}$ cation led to the 2-dimensional supramolecular network as shown in Fig. 5.3.

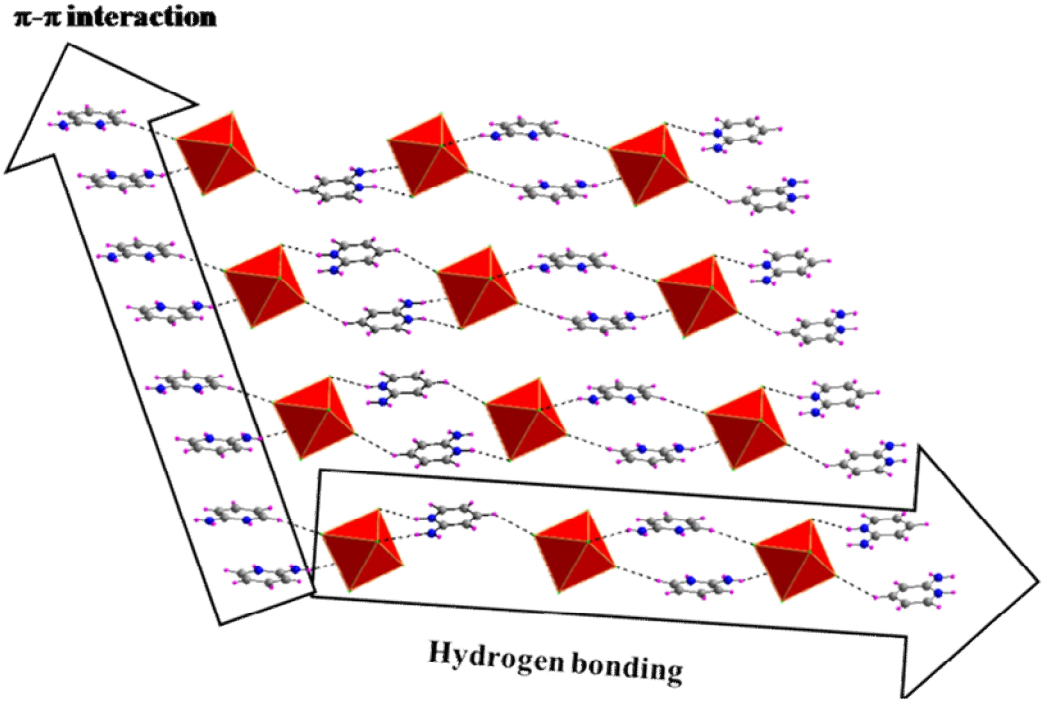


**Fig. 5.1** Two dimensional network due to C–H•••Cl interactions and π–π interactions in the crystal of compound $[C_5H_7N_2]_3[BiCl_6]$ **(1).**

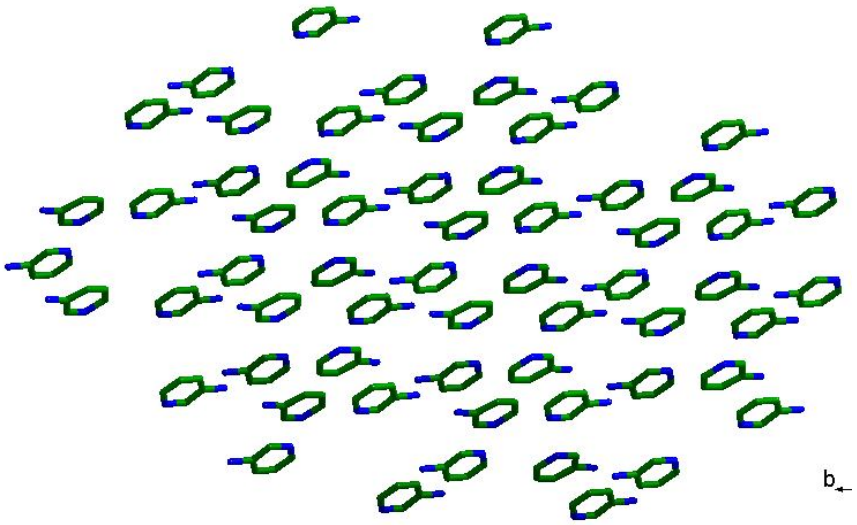


**Fig. 5.2** 3-Aminopyridine (3-Amp) molecules are arranged in parallel directions in $[C_5H_7N_2][C_5H_8N_2][BiCl_6]$ (**2**) which are viewed through C-axis.

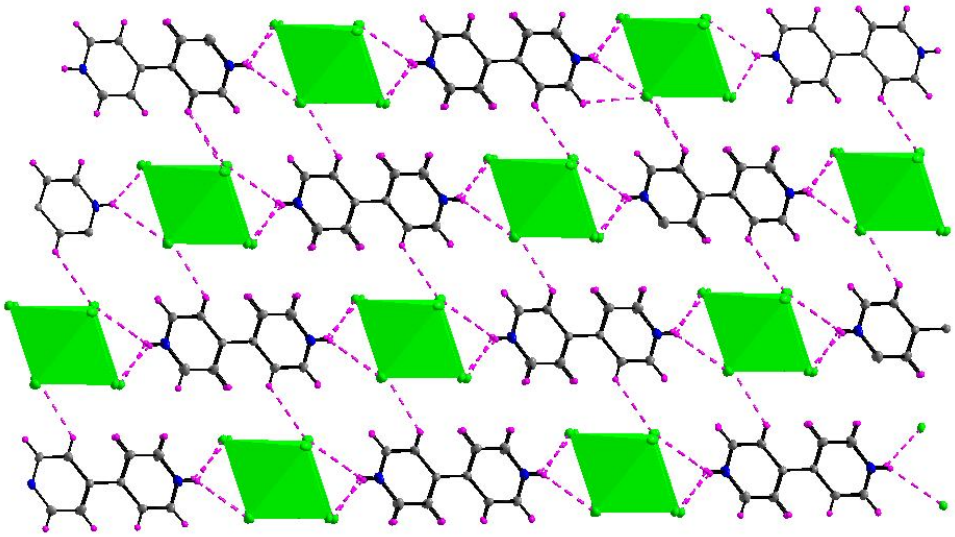

**Fig.5.3** Two dimensional network because of C–H•••Cl interaction between bipyridinium salt and $[Bi_2Cl_{10}]^{4-}$ in $[C_{10}H_{10}N_2]_2[Bi_2Cl_{10}]$ (**3**)

Survey of literature reveals that condensation reaction between a 1,2-diamine (e.g., opda) and a ketone (e.g., acetone) in the presence of a suitable reagent/catalyst, as

shown in scheme 5.1 [32], affords 1,5-benzodiazepine. In the present synthesis, we have used ethanol instead of acetone (ketone).

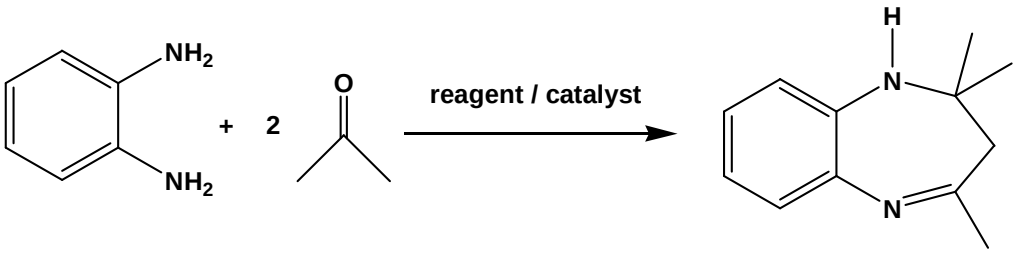


Thus, we believe that acetone, formed *in situ* in our synthesis, reacts with opda (1,2-diamine) leading to 1,5-benzodiazepine (Scheme 1). In the present study, the only evidence that acetone "may" have been formed is the formation of the benzodiazepine. The amount of acetone required to form the compound **4** is not much (*ca*. 0.25 mmol or so), so may be hard to detect in blank reactions. Thermal ellipsoidal diagram of the compound **4** is shown in the Fig. 5.4. Compound $[C_{12}H_{17}N_2]_3[Bi_2Cl_9]\cdot 2(2\text{-PrOH})$ (**5**), that has been isolated using 2-propanol, is isostructural with compound **4**.

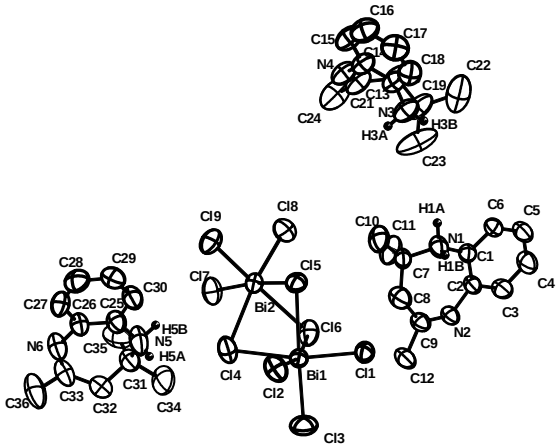


**Fig. 5.4** The thermal ellipsoidal plot of compound $[C_{12}H_{17}N_2]_3[Bi_2Cl_9]\cdot 2EtOH$ (**4**). The hydrogen atoms and solvent molecules are not shown for clarity.(The located hydrogen atoms on nitrogen are shown).

Compounds **2 & 4** exhibit emission property at room temperature. Compound **2** exhibits emission behavior at room temperature in the visible region as shown in Fig. 5.5. It shows emission at 358 nm (when it was excited at 327 nm) and 437 nm (when it was excited at 398 nm). It prompted us to investigate the emission behavior of 3-aminopyridine itself and it indeed exhibits emission property in the visible region at room temperature. Since its protonated form is present in compound **2**, we intended to check its emission behavior in its protonated form by adding $HClO_4$ / HCl to its solution. The emission behavior was found to be quenched after adding $HClO_4$ / HCl to its solution. Surprisingly, the emission feature of compound **2** (even it contains protonated form of 3-aminopyridine) is not much quenched (Fig. 5.6) It is described in terms of quantum yield calculations. Similarly compound **4** shows the emission behavior at room temperature.

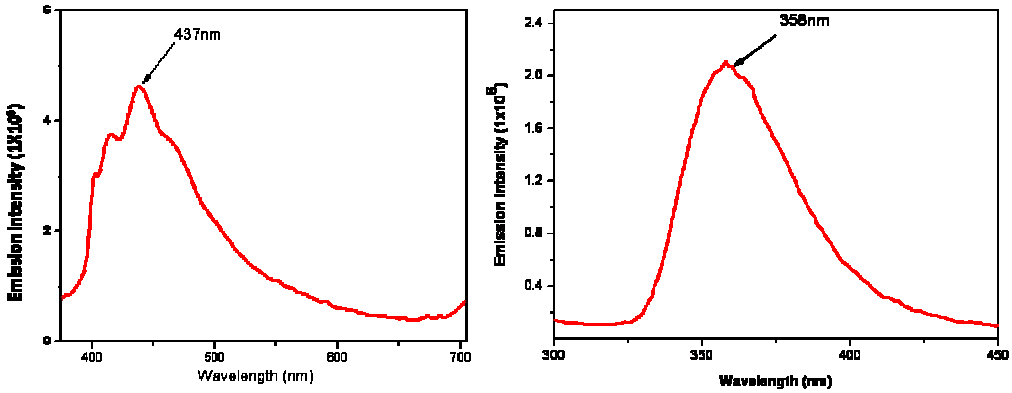


**Fig. 5.5** (left) Emission spectra when excited at 327nm and (right) emission spectra when excited at 398nm for $[C_5H_7N_2][C_5H_8N_2][BiCl_6]$ (**2**) in DMSO with $0.25X10^{4-}$ M.

## Summary: Future Scope

This chapter will demonstrate the future scope of this thesis work. In second chapter of the thesis, we have described catalytic studies of POM clusters in the oxidation of styrene. The crystal structures and properties of decavanadate based materials with organic cations have been demonstrated in the Chapter 3. Chapter 4 describes the isolation and supramolecular property of inorganic-organic hybrid

materials based on Anderson anion by changing the counter cations like aminopyridines. The final working chapter describes the isolation of bismuth-chloroderivatives by using aminopyridines and 4, 4-bipyridine as cations. Quenching of emission behavior by protonating the aminopyridine is described. Synthesis of 1,5-benzodiazepine in the presence of $BiCl_3$ is the new class of catalytic reactions. The catalytic applications of all the materials form chapter **2** to **4** have been demonstrated using oxidation of styrene. Oxidation of higher alcohols are being progressed in our laboratory. Synthesis of Anderson based materials with chiral amines and their catalytic studies of enantiomeric reactions is our future dream. We like to extend our work concerning bismuth chemistry. The synthesis of bismuth compound with sulfur donors can be attempted because sulfur donor containing bismuth compounds are important in drug industry. The relevant effort has already been undertaken in our laboratory and the results will be published in near future.

**********End of Synopsis**********